MASTER
MIT-18-T

ADA058017

(6) APPLICATION OF WELL-STIRRED REACTOR THEORY

TO THE PREDICTION OF COMBUSTOR PERFORMANCE

B.S.13

by

LEVEL

(10) Allan Hardy Bonnell

B. S. E. University of Michigan
(1953)

(12) 252 p.

(15) N6ori-105 (03)

Submitted in Partial Fulfillment of the

Requirements for the Degree of

Doctor of Science in Chemical Engineering

at the

Massachusetts Institute of Technology
(1958)

(14) SQUID-MIT-18-T

D D C
RECEIVED
AUG 15 1978
A

Signature of Author:

Department of Chemical Engineering
(11) May 1958

Signatures of Professors
in Charge of Research:

(9) Doctoral thesis,

Hoyt C. Hottel

Glenn C. Williams

Signature of Chairman,
Departmental Committee
on Graduate Students:

Glenn C. Williams

190 500

ACKNOWLEDGEMENTS

The author is indebted to Professor H. C. Hottel and Professor G. C. Williams for suggesting this problem and for their guidance throughout the course of the work. The author would also like to thank Mr. W. P. Jensen and the staff of the Fuels Research Laboratory for their many helpful suggestions in the design and construction of the apparatus.

Special thanks are due Mr. R. E. Rosensweig who was of invaluable aid during much of the experimental work and to Mr. A. C. Tobey for his suggestion and encouragement in many phases of this problem.

TABLE OF CONTENTS

LIST OF FIGURES

APPLICATION OF WELL-STIRRED REACTOR THEORY

TO THE PREDICTION OF COMBUSTOR PERFORMANCE

by

Allan Hardy Bonnell

B. S. E. University of Michigan
(1953)

Submitted in Partial Fulfillment of the

Requirements for the Degree of

Doctor of Science in Chemical Engineering

at the

Massachusetts Institute of Technology
(1958)

Signature of Author:

Department of Chemical Engineering
May 1958

Signatures of Professors
in Charge of Research:

Hoyt C. Hottel

Glenn C. Williams

Signature of Chairman,
Departmental Committee
on Graduate Students:

Glenn C. Williams

ABSTRACT

APPLICATION OF WELL-STIRRED REACTOR THEORY
TO THE PREDICTION OF COMBUSTOR PERFORMANCE

By

Allan Hardy Bonnell

Analysis and prediction of the performance characteristics of complex processes has often been successfully accomplished by use of single conceptual models. In the models such processes are visualized in terms of important basic mechanisms of the process which can interact in an idealized manner.

Exemplary in the field of combustion has been the use of wrinkled flame front models to analyze the behavior of low-intensity turbulent flames. In high-output combustion systems, however, substantial portions of the combustion chamber may be devoted to homogeneous combustion, and in such situations wrinkled flame front models break down.

In the work reported here conceptual models of high-output systems are considered in which the combustion chamber is visualized as consisting only of a small number of interacting elements composed of homogeneous reaction volumes. Pressure interaction and recirculation are considered. Performance curves developed for four typical models show qualitatively flow interactions and residual flame phenomena typically observed in real combustion chambers.

Predicted performance characteristics based on the above models were compared with experimental data obtained in a small combustion chamber burning premixed propane-air mixtures. Stability limits, combustion efficiency-loading rate data, and visual observation of flame and flow were typical measurements made on chamber performance.

The performance characteristics of combustion chambers predicted by these models, - including the existence of primary and secondary blowout, the effects of air-fuel ratio on blowout, the effects of recirculation and of non-uniform fuel-air ratio on combustion efficiency, the existence of conditions which can lead to pulsing combustion, the magnitude of the combustion rate, - all these are in encouraging agreement with measured performance of actual chambers.

Additional experimental work is required to establish more quantitatively the ability of simple conceptual models to predict actual combustor performance, but the experimental work discussed here provides reasonable assurance that such models have practical utility. It is recommended that reasons for the deviations between the model predictions and the experimental performance be investigated further.

Thesis Supervisor: Hoyt C. Hottel
Title: Professor of Fuel Engineering

Thesis Supervisor: Glenn C. Williams
Title: Professor of Chemical Eng'g

Department of Chemical Engineering
Massachusetts Institute of Technology
Cambridge 39, Massachusetts

May 19, 1958

Professor L. F. Hamilton
Secretary of the Faculty
Massachusetts Institute of Technology
Cambridge 39, Massachusetts

Dear Professor Hamilton:

In partial fulfillment of the requirements for the degree of Doctor of Science in Chemical Engineering, I hereby submit the thesis entitled "Application of Well-Stirred Reactor Theory to the Prediction of Combustor Performance".

Respectfully submitted,

Allan H. Bonnell

CHAPTER I

SUMMARY

The importance of mixing as a rate-limiting step in combustion processes has long been recognized. Prior to the development of high-output combustors for jet propulsion, however, mixing rates were sufficiently slow in most practical combustors to make chemical reaction rates appear infinitely fast by comparison.

The use of a simple conceptual model to aid in visualization of the processes involved in typical high-output combustion chambers could simplify the experimental development of new chamber designs. Since in the chambers under consideration both chemical reaction rates and mixing rates have important roles, it would be necessary to incorporate both phenomena into such a model. The model should predict behavior characteristics of combustion chambers (such as combustion efficiency, stability and tendency to resonate) resulting not only from limitations set by chemical reaction rate or mixing rates, but also from interactions of two or more phenomena. Although a sufficiently complex model could completely describe a chamber behavior pattern, the results of application of the model concepts to prediction of performance would be impressive only if the model were simple.

In the models discussed here, the combustion chamber
is considered to be divided into a small number of zones
each of which is assumed to be uniform in composition. Flow
between these zones is postulated as representing the fluid-
flow and mixing pattern. Within each zone, since the com-
position is uniform, it is postulated that the chemical reaction
rate is determined uniquely by the composition and temperature
of that zone. In the present discussion heat transfer is
neglected; however, adiabaticity is not a necessary assumption.
The relation between burning rate and composition is taken
from stirred reactor data on hydrocarbon combustion and is
limited to a burning rate-composition relation involving only
one composition variable. More complex reaction schemes could
be used, but the lengthy computations required for models
involving these severely limit the number of composition
variables which may be considered. Models similar in some
respects to those discussed here have appeared in the recent
literature (2, 6, 18, 24); however, little has been done to
relate their predicted performance quantitatively to the
performance of practical combustion chambers.

The purposes of this investigation were: (1) to consider
some possible conceptual models of combustion chambers which
allow for interaction between flow phenomena and reaction rate
phenomena, (2) to study the operation of a simple experi-
mental combustion chamber and (3) to examine the question

of whether the performance predicted by simple conceptual models can be quantitatively fitted to the measured performance of the experimental combustion chamber.

Data with which the predicted performance characteristics could be compared were obtained from a small experimental combustion chamber. The chamber design was chosen to be simple and yet to give characteristics typical of practical chambers. In the chamber used a small, rectangular two-dimensional combustion zone was fired with either one or three feed jets. Opposing the feed jets were corresponding exit flues. The combustion zone was formed by kaolin firebricks whose arrangement could be readily altered depending on the number of feed jets used. The front and back sides of the combustion zone were closed with Vycor windows which permitted direct observation of the flame. The feed jets were each 0.030" wide by 2" deep in the 2-dimensional direction, and mounted in the floor of the chamber with their axes accurately aligned. The opposing exit flues in the chamber roof were 1/2" wide. When three jets were used the chamber was 3" wide with 1" spacing between jet centerlines. With one feed jet a 2" chamber width was used. A pre-mixed propane-air mixture was prepared and metered individually to each jet to insure uniform operation.

Operating characteristics of these chambers demonstrated two general phenomena. In using the three-jet chamber it was

found that the three jets coalesced a short distance above the nozzles, and at low firing rates combustion proceeded on either side of the central core thus created. As the firing rate was increased one of these two zones became unstable. Consequent to this partial blowout there was a readjustment of the flow pattern in which the remaining active zone expanded in size. At a higher firing rate it was possible to blow out the remaining active zone.

In the one-jet chamber no symmetrical combustion pattern was observed. The jet from the centrally located feed bent over against one of the chamber walls, and combustion proceeded in a circulatory fashion in the large zone thus created. At low firing rates combustion appeared principally around the edges of the circulatory zone with the "eye" of the zone containing only completely burned gases. As the flow rate was increased the burned center shrank as the zone of most intense combustion moved inward, until at blowout only a small residual flame in the center of the vortex remained.

Four models were considered in this work. In the first of these, an interaction between the pressure effect of combustion and the chemical reaction rate was considered. The model, purporting to simulate a chamber with feed and discharge along lines located centrally on opposite walls, consisted of two well-stirred reactors of constant total volume separated from each other by an elastic barrier

capable of moving in response to pressure differences so that
the deflection was directly proportional to the pressure
difference between the reactors. The two reactors were
assumed to be fed equally with a pre-mixed fuel-air mixture
and when the pressure difference between the reactors was
zero, the two reactors had equal volumes.

When the firing rate to this model was changed, two
stability limits were predicted, the first corresponding
to an initial blowout of one of the two reactors followed
by a shift in the barrier position toward the colder side
and the second to blowout of the remaining active reactor
at a higher feed rate. These two blowout limits corresponded
to loading rates in the zones equivalent to stirred reactor
blowout rates. This was qualitatively the behavior observed
experimentally in the three-jet chamber studied. Although
a quantitative fitting of the predicted performance to all
of the data on the experimental chamber was not possible,
the relative firing rates between the two blowout limits
was predicted with some success.

The second combustor model considered allowed for re-
circulation of partially burned combustion products in a
pattern such as that typically produced by a jet firing
fuel-air mixture into a combustion zone. This model is
similar to one suggested by Spaulding (24) after the major
portion of this work had been completed; however, the

performance predicted by the model suggested here was
drastically different from that predicted by Spaulding. In
the recirculation model two zones are postulated, represent-
ing the central jet core and recirculation zone found in
actual combustors. Each of these zones is postulated to be
a well-stirred reactor. Fresh fuel-air mixture is mixed
instantaneously with partially burned recirculated gases
from the recirculation zone and the resulting mixture is
then fed into the initial stirred reactor representing the
jet core. Gases leaving the central core volume are divided
into two portions, one being recirculated through the
recirculation zone and the other leaving the model as burned
products. This model showed two interesting characteristics
at low recirculation ratios, residual flame phenomena and
potential flickering flame operation. At higher recircula-
tion ratios these phenomena disappeared. In a third model,
similar to the second, allowance was made for non-uniform
distribution of fuel. This was achieved by introducing
only a part of the fuel but all of the air into the central
core zone and the remainder of the fuel into the recirculation
zone along with the recirculated gases. The third model,
with the split-fuel-feed, showed essentially the same
behavior as that of the second model.

Study of the performance of the experimental one-jet
combustor indicated that a simple recirculation model was

inadequate to describe its performance. To fit the data a
fourth model was considered in which successive recirculation
zones were added. In this model a typical zone received
recirculated gases from its immediate successor and supplied
recirculated gases to its immediate predecessor. This
model predicted a performance similar to that of the simple
recirculation model, but the relative blowout limits for the
main flame and the residual flame were in better agreement
with experimental data on the one-jet chamber.

The performance characteristics of combustion chambers
predicted by these models, - including the existence of
primary and secondary blowout, the effects of air-fuel ratio
on blowout, the effects of recirculation and of non-uniform
fuel-air ratio on combustion efficiency, the existence of
conditions which can lead to pulsing combustion, the
magnitude of the combustion rate, -- all these are in
encouraging agreement with measured performance of actual
chambers.

Additional experimental work is required to establish
more quantitatively the ability of simple conceptual models
to predict actual combustor performance, but the experimental
work discussed here provides reasonable assurance that such
models have practical utility. It is recommended that reasons
for the deviations between the model predictions and the
experimental performance be investigated further.

CHAPTER II

INTRODUCTION

Scope of Thesis

Mixing has long been recognized as a dominant factor
in many industrial combustion processes. However, there
has been a growing realization that chemical reaction rates
place important limitations on the performance of high-
output combustors, especially those found in aviation
propulsion systems. This has led in recent years to the
study of the well-stirred reactor as a device which may
be used to relate burning rate to chemical kinetics as
affected by composition, temperature and pressure rather
than to mixing processes alone.

Practical combustors for high-output combustion
systems lie intermediate with respect to volumetric heat
release rates between purely mixing-controlled industrial
furnaces and the chemically rate-limited well-stirred
reactor. This suggests that mixing may be reduced in
importance as a rate limiting process in many practical
combustors. Furthermore, much experimental data obtained
on high-output combustors can only be explained by
postulating some chemical rate limitations. In principle,
therefore, to predict the behavior of high-output combustors
from fundamental data, one would have to account for the
simultaneous effects of both chemical reaction rates and

mixing rates in the combustion chamber. Both of these
phenomena are highly complex, and their interactions may
lead to unexpected results. Typical of these results are
the marked effects of different firing rates on combustion
efficiencies, and discontinuous shifts in flow patterns
and efficiency in certain firing rate ranges.

One might hope to divide the various phenomena occur-
ring in a combustion chamber, particularly of efficiency
and stability, into regions of operation where either
mixing rate or chemical reaction rate is the dominant
phenomenon. These could then be treated as independent
problems in terms of the present theories of mixing and
of chemical kinetics. This method has the deficiency,
however, of being unable to predict performance in the
transition regions where many interesting problems occur.

To study these regions the approach proposed here is
to use simplified models of both the mixing and combustion
rate phenomena, and to combine them to allow for inter-
action in the transition regions. The simplified conceptual
models of combustion chambers cannot be expected to include
all of the variables or effects; however, in principle a
sufficiently complex model should be able to completely
describe the performance of any combustion chamber.

In setting up the models to be presented here knowledge
of simple combustion chamber fluid dynamics and of well-

stirred reactor theory is required. The introductory material
is thus divided into three sections. The first section deals
with the fluid dynamics of combustion chambers, the second
discusses well-stirred reactor theory, and the third reviews
the literature on combustion chamber models.

Combustion Chamber Fluid Dynamics

The fluid-flow pattern of a modern can-type combustor,
typical of the combustors used in nearly all current gas-
turbines, is highly complex, and, as yet, has not received
adequate attention. A sectional view of a typical combustor
is shown in Figure II-1. Liquid fuel is sprayed into the
front end of the chamber, and combustion air enters through
a pattern of holes around the surface of the can.

Primary air and fuel   secondary air
spray injection nozzle   inlets
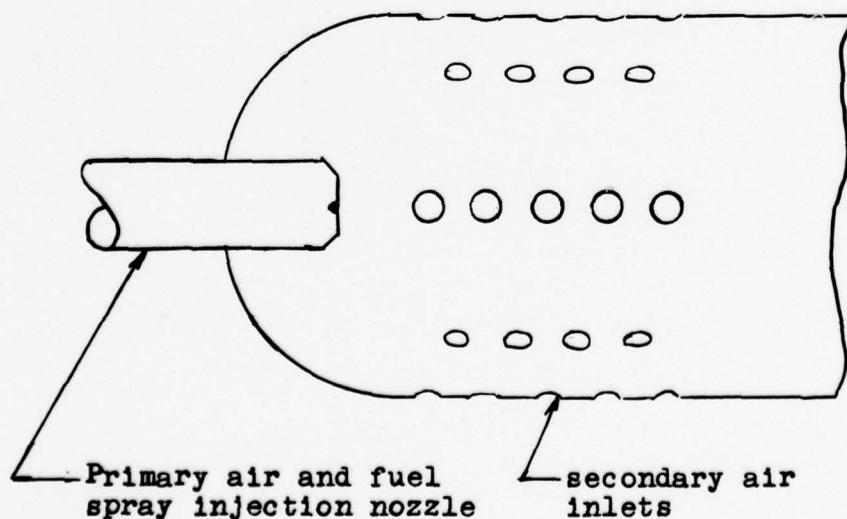
Figure II-1:   Typical can-type combustor

In a device such as this moderate mixing is achieved by the
"jet" effect of the air and fuel inlets. This mixing must
serve three purposes: (1) to contact the fuel and oxidant
so that combustion can occur, (2) to provide sufficient
recirculation of hot combustion products to the fuel inlet
so that the flame will stabilize, and (3) to create sufficient
turbulence to burn the fuel at the desired volumetric heat
release rate.

Little work has been done on the analysis of jet mixing
in chambers where there is mixing of recirculating fluid
with the jet. On the other hand, considerable work has been
done on jet mixing in pipes where the recirculation phenomenon
has been eliminated by the introduction of a secondary fluid
(11, 12, 29). The general conclusion is that so long as the
jet boundary does not reach the wall, the behavior of the
enclosed jet is identical to that of a free jet. It is
reasonable to expect that the same results would be found
in an enclosed system with recirculation.

In a practical chamber the problem is considerably
complicated by the interaction of two or more jets as well
as by deviations of the jet from idealized theory as the
confining walls are reached. In a multi-jet system, individual
jets tend to lose their identity and, instead, make their
contribution to the overall turbulence level in the chamber.
The arrangement of the jets may be such as to give flow
patterns ranging from no identifiable pattern to a well-

defined pattern.

In the combustion chambers considered here, the flow
pattern is imagined to be of this latter type. The jets
are arranged to give a well-developed circulatory pattern,
and flame is stabilized by the recirculation of hot burned
gases to the fresh feed inlets. Typically, fresh feed and
burned products counter-diffuse (turbulently) along a
portion of the circulatory pattern. This process provides
ignition for fresh gases in the mainstream of the flow
pattern as well as maintaining active combustion in the
sheltered recirculation zones.

The approach to well-stirredness in systems of this
type is influenced by two factors: (1) the portion of
the chamber devoted to recirculation and (2) the level
of turbulence in the chamber. If only a small portion of
the chamber is devoted to gross recirculation, the chamber
will approach well-stirredness only through extremely
intense turbulence in the chamber. Likewise, if the
gross recirculation pattern is of a large diameter, high
turbulence is required to couple the central portion of the
pattern with the outer regions. Spaulding (24) suggests
that gross circulation is a more efficient means of achieving
mixedness than is high turbulence. (Efficiency is in terms
of pressure drop required to achieve a given level of mixedness.)

Because of high reaction rates of combustion, incomplete mixing within a chamber leads to zones of high and low combustion rates. Consequently, completeness of mixing has been associated with high volumetric heat release rates. It has been postulated that it is possible to obtain even higher volumetric combustion rates by proper arrangement of combustor elements (6); however, these have not yet been achieved in practice. In visualizing models of combustion chambers such as these, the effects of recirculation which can be important in some regions must be recognized in the model.

Combustion Reaction Kinetics; Well-Stirred Reactor Behavior

The subject of combustion reaction kinetics has been treated by a large number of authors. General reviews of high temperature kinetics have been given by Shuler (21), Ubbelholde (27), and vonElbe (28). This subject will not be treated in detail here; only those aspects of the problem directly applicable to the present work will be discussed.

By far the largest proportion of chemical kinetics studies have been made in the region of low or moderate temperatures compared to the temperatures of normal combustion reaction (for example, extensive work on cool flames). These studies describe the combustion reactions in highly complex terms, and because of the relatively low temperatures involved, there is considerable doubt that these data can be extrapolated

to normal combustion temperatures. Furthermore, because of
the primary interest here in the interaction of combustion
and fluid flow, it is desirable to employ a much simpler
picture of the chemical kinetics.

Such a simple picture of combustion kinetics is one in
which it is hoped that a simple nth order reaction between
fuel and oxygen will adequately describe the combustion
kinetics. This assumption has been used by Longwell (13)
and Avery (2) in the analysis of a well-stirred reactor.
It is assumed that the reaction order is of α order in
fuel and n-α order in oxygen and that Arhennius form of
activation energy represents the effect of temperature on
the reaction rate.

Let the overall reaction between fuel and oxygen be:

$$F + a \ O_2 \longrightarrow p \ P \qquad\qquad II-1$$
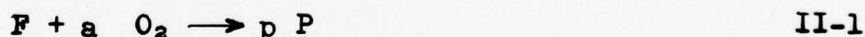
and let $\emptyset$ times the stoichiometrically required fuel be used.

If the identifiable components of the mixture at any
stage of completion of combustion are products of complete
combustion, fuel, and oxygen, specification of a single quan-
tity, for example β, the burned fraction of the fuel fed,
together with the stoichiometry, is sufficient to identify
the mixture. For each additional intermediate or competing
reaction involving a new specie (or species), one more
quantity, γ, δ, etc, must be specified to fix the composition;
and the choice of how best to define the new term will depend

on the postulated chemistry of the process. The mole fraction, f_X, of any component "X" is thus representable as f_X ($\emptyset$, β, γ, δ, ...), or for a fixed value of $\emptyset$, $\overline{f}_X$ (β, γ, δ, ...), and the single argument β is sufficient for the simplest possible picture of the combustion process.

The well-stirred reactor is by definition a chamber in which the composition, measured at the inlet by β_o, γ_o, δ_o, changes instantly to that measured by β, γ, δ ; and the composition is everywhere that of the outlet. In this system the temperature, T, is fixed by the exit composition and the inlet temperature T_o (i.e. an adiabatic reaction), and for a fixed $\emptyset$ can be represented as $\overline{f}_T$ (β, γ, δ, ..., T_o). For the simplest case in which the product composition and, consequently, T is assumed to be fixed by the single variable β, it is obvious that either β or T may be used as a measure of combustion progress or burnedness. Assumption of linearity between T and β, leading to the relation

$$\beta = \frac{T - T_o}{T_{af} - T_o}$$

(where T_{af} is the adiabatic flame temperature) simplifies numerical calculation, but is not necessary.

As many chemical rate equations are required as there are arguments β, γ, δ, ... necessary to fix the composition. Additional rate equations will be required if alternative routes between reactants and products exist. The present

treatment is restricted to the simplest description of the combustion process, requiring only one rate equation. This is most conveniently the rate of consumption of fuel, given by;

$$- \frac{dN_F}{Vdt} = \sqrt{T} k' e^{-E/RT} C_{O_2}^{(n-\alpha)} \quad C_F^{\alpha} \qquad \text{II-2}$$

on the assumption that the reaction is of overall nth order and of α order in fuel. Substituting $\bar{f}_F(\beta)(P/RT)$ for C_F and $\bar{f}_{O_2}(\beta)(P/RT)$ for C_{O_2}, one has;

$$- \frac{dN_F}{Vdt} = P^n \frac{k' e^{-E/RT}}{R^n T^{(n-1/2)}} \quad \bar{f}_F^{\alpha}(\beta) \quad \bar{f}_{O_2}^{(-\alpha)}(\beta) \quad \text{II-3}$$

Since T and β are uniquely related, Equation II-3 may be written:

$$- \frac{dN_F}{P^n V \, dt} = \psi_1(\beta) \qquad \text{II-3a}$$

In a well-stirred reactor fed at the molal fuel feed rate G with the burnedness changing from an inlet value β_0 to an outlet value β, the fuel consumption rate is $G(\beta - \beta_0)$; this replaces $- dN_F/dt$. Therefore, Equation II-3a becomes;

$$\frac{G}{VP^n} = \frac{\psi_1(\beta)}{\beta - \beta_0} \qquad \text{II-4}$$

and for a reactor being fed an unburned fuel-air mixture, this may be written:

$$\frac{G}{VP^n} = \frac{\psi_1(\beta)}{\beta} = \psi_2(\beta) \qquad \text{II-5}$$

A typical curve representing Equation II-5 appears as Fig. II-2.
The numerical magnitude of G/VP^n shown in Fig. II-2 is a
consequence of the normalization proceeding and is not
indicative of the actual values experimentally observed.
The normalization of this curve is discussed in Appendix A.

It will be noted that there are three solutions to
Equation II-5 for a given value of G/VP^n at low values of
this quantity. Of these, only two may be experimentally
found.   The uppermost (solid line) solution represents the
hot , stably-burning system, and the lowermost ($\beta=0$ axis)
the cold, "non-reacting" system. Solutions along the dotted
middle branch of Figure II-2 are thermally unstable, since
if a reactor were operating on this section of the curve, a
small perturbation in burnedness or flow rate would cause
the reactor efflux either to move up to the top-most branch
of the curve or to drop down to the lowest branch of the
curve. As the feed rate is increased, the burnedness
decreases, until a feed rate is reached where $d\beta/dG$ is
infinite. This point represents the blowout feed rate, since
beyond this feed rate the only solution to Equation II-5
corresponds to the "non-reacting" system. This blowout point
is a unique function of the fuel/air ratio, and has been a
basic measurement in the work which has been reported in
the literature on the well-stirred reactor.

In applying the well-stirred reactor theory to experi-
mental data, Longwell and Weiss (14) and Baker (3) have used
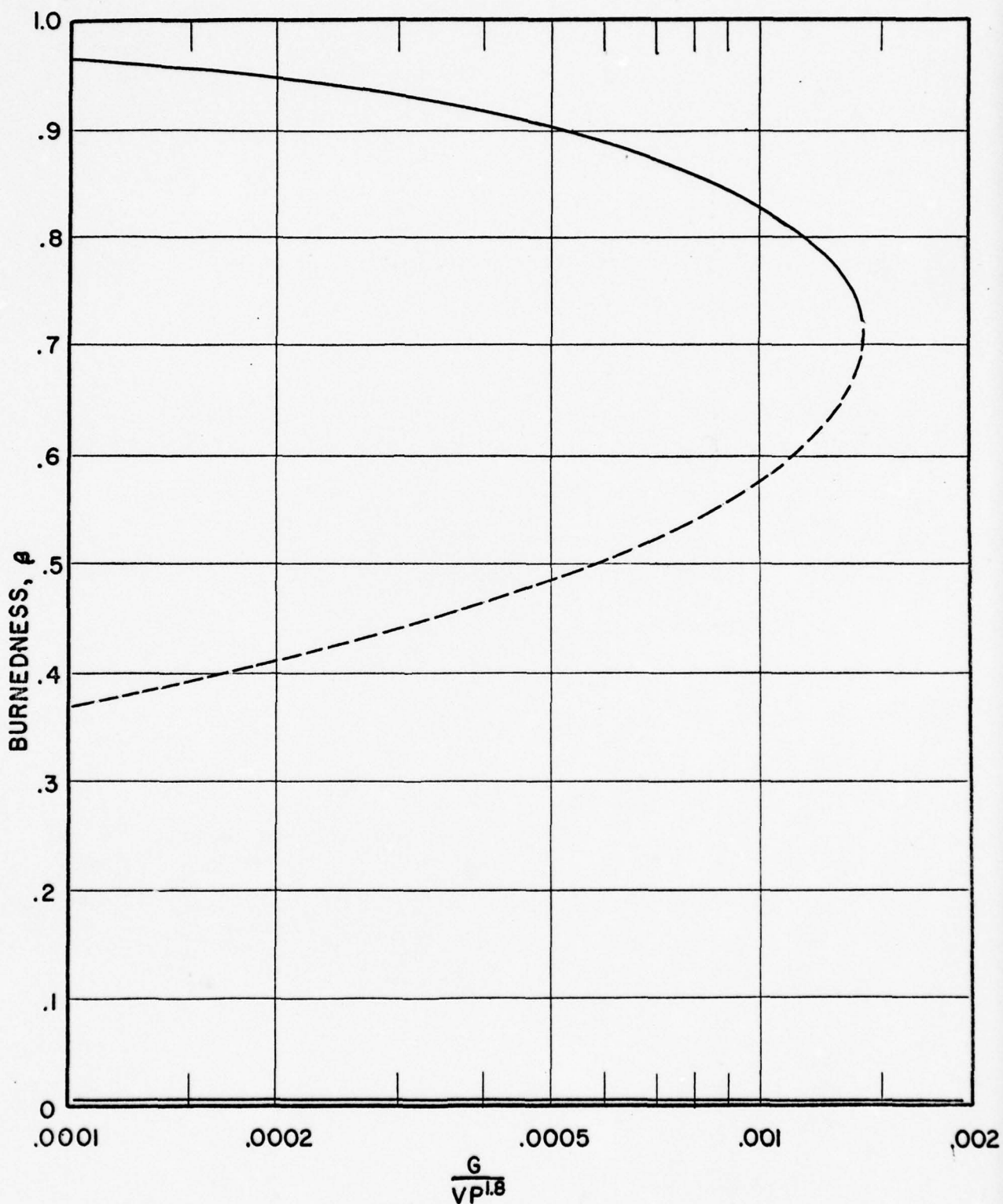
FIGURE II-2: WELL-STIRRED REACTOR PERFORMANCE

$\phi = 1.0$; $T_o = 500°R$; $T_{af} = 2772°R$

$C_3H_8 + 5O_2 + 18.8 N_2 \longrightarrow 3CO_2 + 4H_2O + 18.8N_2$
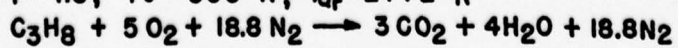
the simple (one rate equation) theory. In this approach no allowance is made for the existence of intermediate combustion products. Hence, any products of partial combustion are replaced by stoichiometrically equivalent quantities of unburned fuel and completely burned products such that the oxygen consumption efficiency remains unchanged. The burnedness, β, is defined in terms of this latter quantity in these experiments.

Since it is admittedly unrealistic to assume that there are no intermediate combustion products in the well-stirred combustor, both Longwell and Weiss and Baker have spent considerable effort in postulating stoichiometric and re-action schemes which will give a more realistic picture of the combustion products actually found. In the experimental work reported by Longwell and Weiss (14) gas analyses of samples drawn from the interior of the reactor were reported. These data show that very little unburned fuel appears in the reactor, and that only when the combustor is fed a rich fuel-air mixture do any appreciable quantities of hydrocarbons appear. In these samples the major unburned component reported is carbon monoxide, and hydrogen is the only other combustible reported in significant quantities for lean mixtures. Baker (3) in sampling data taken in another well-stirred reactor experiment confirms these observations.

Longwell suggested the following reaction equations to
explain the data:

$$\text{Fuel (hydrocarbon } C_xH_y) + aO_2 \rightarrow xCO + 1/2yH_2O \text{(instantaneous)}$$

II-6

$$CO + 1/2\ O_2 \rightarrow CO_2 \text{ (rate controlling)} \qquad \text{II-7}$$
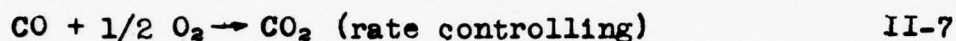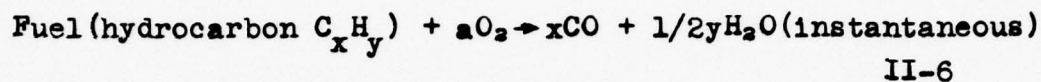
This scheme allowed Longwell to fit his fuel-lean data;
however, it is not adaptable to fuel-rich data since there is
insufficient oxygen to allow completion of the first step
beyond a certain fuel-air ratio (depending on the
carbon/hydrogen ratio of the fuel).

In fitting this reaction scheme to the simple well-
stirred reactor equations (Equation II-5), one must be
careful not to confuse the fractional oxygen consumption
with the fractional carbon monoxide consumption. Since
the rate-controlling reaction is equation II-7, the
substitutions into II-5 must be appropriate to this
stoichiometric equation. The fractional fuel consumption, β,
is now defined as the fraction of CO available from the fuel
which has been converted to CO_2. Temperatures, accounting
for the heat liberated by Equation II-6, and concentrations
are calculated as a function of this redefined β. It should
be noted that this definition of burnedness is different
from oxygen consumption efficiency, since at zero CO
consumption the oxygen consumption efficiency is that

required to react all of the fuel to CO and H_2O. Baker points out that proper substitution into Equation II-5 leads to the conclusion that for near-stoichiometric mixtures on the lean side, enough heat is liberated by reaction II-6 to prevent blowout of the reactor, no matter how fast it is fed. Longwell's correlation of his lean blowout data, unfortunately, confuses this distinction. Although his theoretical blowout curve extends to stoichiometric fuel-air ratio, close examination of this derivation reveals that an improper substitution was made for β in the denominator of Equation II-5.

Baker suggested two additional reaction schemes, one for the rich side and one for the lean side. Because of the anomolous behavior of the reaction scheme of Equations II-6 and II-7 (i.e. no blowout found near stoichiometric), Baker suggested an alternative scheme in which there was less heat liberated in the first stage of the reaction. This scheme is as follows:

$$C_xH_y + aO_2 \longrightarrow xCO + 1/2\ yH_2 \quad \text{(instantaneous)} \qquad \text{II-8}$$

$$CO + 1/2\ O_2 \longrightarrow CO_2$$
$$\text{(rate controlling)} \qquad \text{II-9}$$
$$H_2 + 1/2\ O_2 \longrightarrow H_2O$$
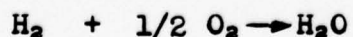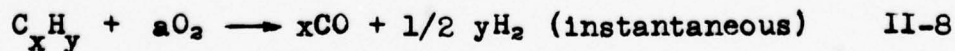
and the restriction is placed on II-9 that:

$$\frac{(CO)(H_2O)}{(CO_2)(H_2)} = k_{wg} \qquad\qquad \text{II-10}$$

where k_{wg} is the water-gas equilibrium constant at
the temperature of the reactor.

On the righ side it is postulated that fuel and oxygen
are consumed in the same ratio as the prevailing fuel/air
ratio to form the equilibrium mixture of carbon monoxide,
carbon dioxide, hydrogen and water. This scheme is the
same as that proposed by Longwell and Weiss for rich
mixtures.

In Baker's lean-side reaction scheme, II-8 to II-10,
there is a much lower temperature rise in the first step than
in the scheme proposed by Longwell and Weiss, and Baker was
able to calculate blowout rates from this mechanism for all
lean fuel/air mixtures. However, it was pointed out that
the ratios of CO, CO_2, H_2 and H_2O experimentally found in
the gas samples did not correspond to water-gas equilibrium.

Edgerton, Saunders, and Spaulding (8) have discussed
the well-stirred reactor theory in general, and they have
pointed out some of the implications of the simplified
theory dealt with thus far. The composition of a partially
burned mixture has been defined by a single quantity. This
definition was originally restricted to that case where the
rate-limiting step in the combustion of fuel was the initial
reaction between fuel and oxygen. However, in any reaction
scheme in which a single reaction is the rate-limiting

step, the composition of the mixture may be uniquely defined by a single argument such as β. Thus, a partially burned mixture whose composition is measured by β may be obtained either by partial combustion to this composition or by mixing unburned fuel/air mixture with completely burned gases. In this latter case, all instantaneous reactions must be allowed to occur (e.g. the conversion of hydrocarbon to CO and H_2O, Equation II-6) without any conversion of the reactants involved in the rate-limiting step. This postulation that the composition of a partially burned mixture is uniquely defined by a single parameter is of fundamental importance in calculating the behavior of combustion chamber models.

DeZubay (6) has called attention to an ambiguity in the meaning of "burnedness" which arises from Baker's and Longwell's assumption of stoichiometry for rich fuel-air mixtures (e.g. fuel and oxygen disappear in the same proportion as the prevailing fuel/air ratio). For this stoichiometry a burnedness of unity for a rich fuel-air mixture corresponds to a mixture in which there are no unreacted hydrocarbons, in conformity with the experimental facts. It is evident, however, that the result of mixing a completely burned rich and lean mixtures would be a mixture in which further combustion could occur. DeZubay has suggested that this ambiguity in the meaning of burnedness

can be clarified by the use of a "fuel availability factor" in addition to "burnedness" to specify the composition of the mixture. This composition variable permits one to account for the additional combustion which could occur if air or a lean fuel-air mixture is mixed with a burned or partially burned rich mixture.

The introduction of multi-step reactions with more than one rate constant and composition variable considerably complicates the stirred reactor problem. This possibility has not yet received adequate attention in the literature. Edgerton, Saunders and Spaulding (8) in their paper discuss this problem qualitatively. They point out that so long as one of the reaction rates is substantially slower than the others the simple formulation of the stirred-reactor problem is still valid. They further suggest that near the completion of the combustion process, a single reaction predominates, thus making valid the assumption that composition is independent of the path by which the burned-ness is reached. In the intermediate ranges of burnedness, however, it is postulated that the assumption of only one significant rate constant is unjustified. If more than one rate constant is required to describe the combustion reaction, then, in the general case, the composition and temperature are not uniquely defined by a single variable, but they depend on the path by which a given burnedness level is

reached. To allow for variation in the burning rate at a
given temperature, Edgerton, Saunders and Spaulding suggest
a "band of uncertainty", which includes all possible burning
rates corresponding to a given temperature level.

Behavior of Plug-flow and Staged Stirred Reactors

Because the performance of two-stage stirred reactors,
multi-stage stirred reactors, and plug-flow reactors are
all derivable from the same basic rate equation, (Equation
II-5), they are all derivable from one another. Consider
first the plug-flow reactor. Such a reactor may be
pictured as an infinite series of infinitesimal well-stirred
reactors. Since the flow rate through each of these is the
same, they are best considered as stirred reactors in which
volume is the independent variable. Equation II-5,
restricted to the case where only the single argument β is
required and for constant pressure operation, is inverted
to give:

$$\frac{VP^n}{G} = \frac{\beta - \beta_o}{\psi_1(\beta)} \qquad \text{II-11}$$

A typical slab of a plug-flow reactor, having a volume of
dV, being fed with reactants of composition β, and dis-
charging products of composition $\beta + d\beta$, is represented by
Equation II-11 with V replaced by dV and the accomplished

burnedness, $\beta - \beta_o$, by $d\beta$;

$$\frac{P^n}{G} \, dV = \frac{d\beta}{\psi_1(\beta)} \qquad \qquad \text{II-12}$$

If the reaction rate function, ψ_1, is available, as for
example from a postulated chemical mechanism of combustion,
Equation II-12 may be integrated directly to give the
performance of a plug-flow reactor. If, on the other hand,
data are available from a stirred reactor experiment in the
form of $\psi_2 (\beta)$ ($\psi_2 = \psi_1/\beta$), then the stirred
reactor relationship may be used to integrate II-12:
Equation II-12 may be written:

$$\frac{P^n}{G} \, dV = \frac{\beta}{\psi_1(\beta)} \frac{d\beta}{\beta} = \frac{1}{\psi_2(\beta)} \, d \ln \beta \qquad \text{II-13}$$

or, integrating between the limits $\beta = \beta_o$, $V = V_o$ and
$\beta = \beta$, $V = V$:

$$\frac{P^n}{G}(V - V_o) = \int_{\ln \beta_o}^{\ln \beta} \frac{d \ln \beta}{\psi_2(\beta)} \qquad \text{II-14}$$

If, one plots the stirred reactor performance curve in the
form $1/\psi_2 (\beta)$ vs β on a logarithmic scale, the area
under the curve from β_o to β (see Fig. II-3 with x and y
coordinates reversed to correspond to previous plots)
represents the generalized volume $(V-V_o)P^n/G$ necessary to
carry out that much reaction in plug-flow; and that area
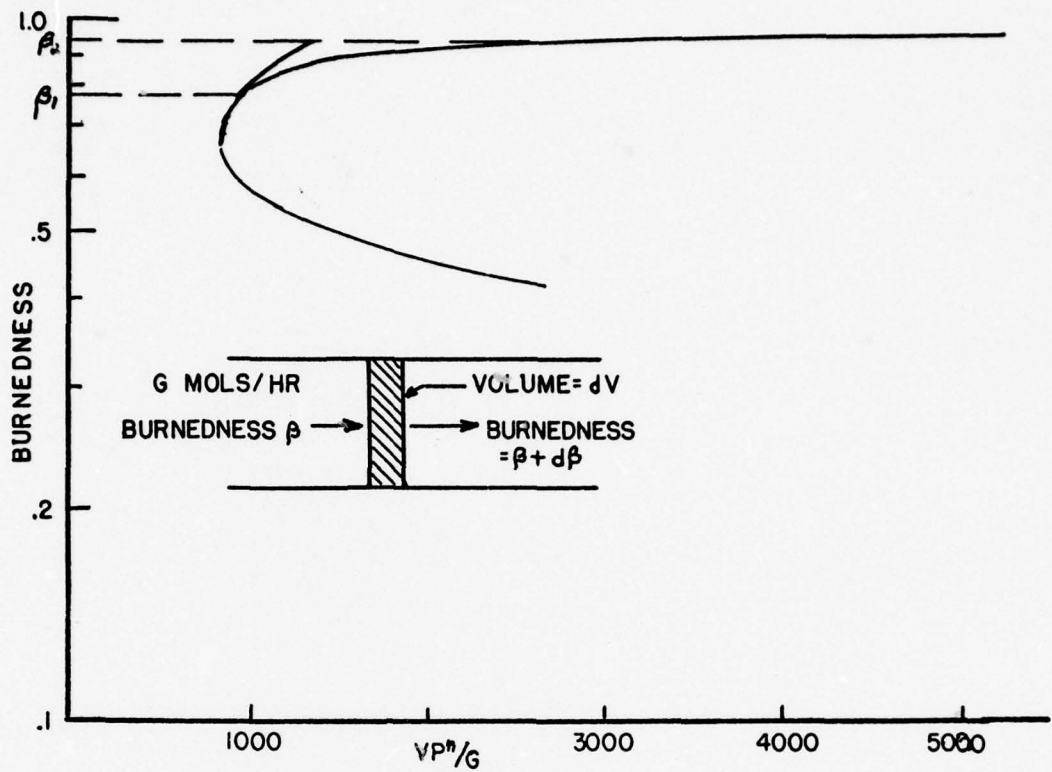
FIGURE II-3: INTEGRATION OF WELL-STIRRED REACTOR CURVE TO FIND PLUG-FLOW REACTOR PEFORMANCE
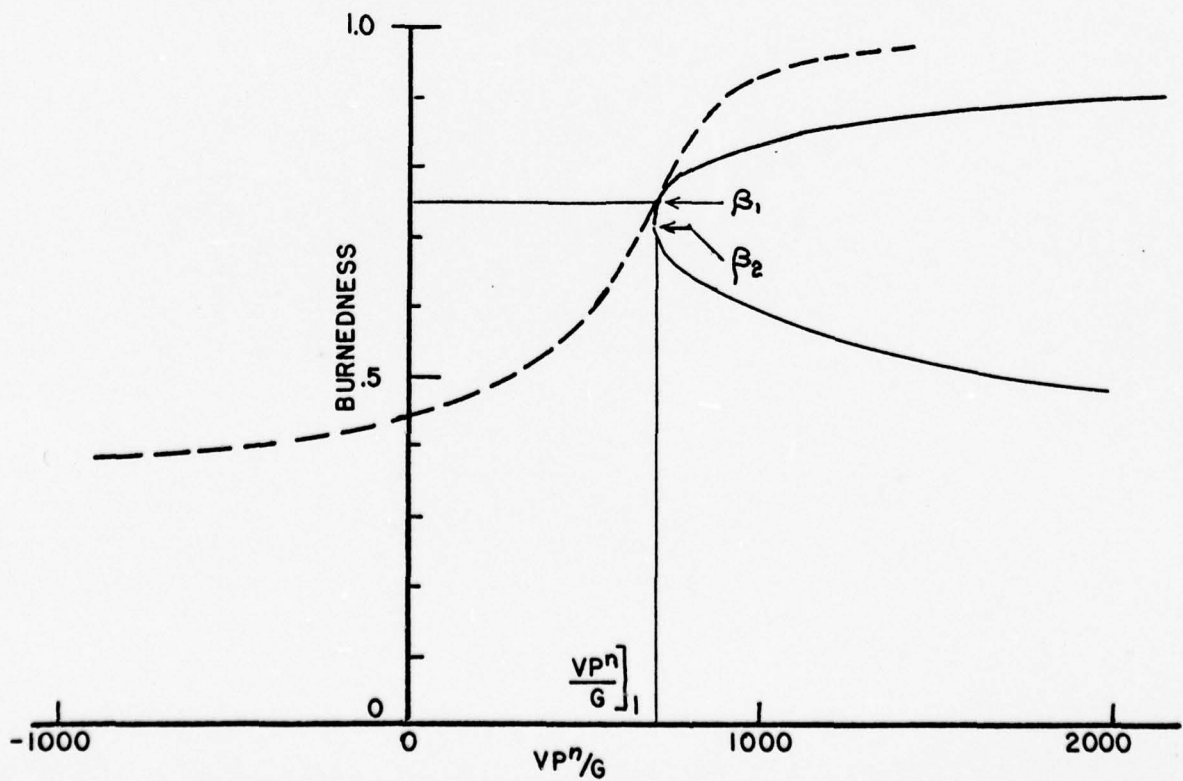
FIGURE II-4: PLUG-FLOW REACTOR CURVE (DOTTED)

can be plotted on the same plot (dotted line). In
Figure II-4 the results of integration over the full range
of β is shown on arithmetic coordinates (dotted line)
together with the basic stirred reactor curve. The plug-
flow curve has been displaced laterally to be tangent to
the stirred-reactor curve at a generalized volume of
VP^n/G_1, the significance of which requires comment: On a
plot of β vs VP^n/G on arithmetic coordinates, the point
of tangency to a line from the origin represents a stirred
reactor operating at the maximum possible rate per unit
volume, and the condition for this point is:

$$\frac{\beta}{1/\psi_2(\beta)} = \frac{d\beta}{d\left[1/\psi_2(\beta)\right]} \qquad \text{II-15}$$

Differentiating Equation II-5 and II-14 with respect to
volume (these are the curves represented on Figure II-4),
one obtains:

$$\frac{P^n}{G}\frac{dV}{d\beta}\bigg|_{WSR} = \frac{d[1/\psi_2(\beta)]}{d\beta} \qquad \frac{P^n}{G}\frac{dV}{d\beta}\bigg|_{PFR} = \frac{1}{\psi_2(\beta)}\frac{d\ln\beta}{d\beta}$$

Noting that the point where these two slopes are equal is
given by:

$$d(1/\psi_2(\beta)) = d\ln\beta/\psi_2(\beta) \qquad \text{II-16}$$

one sees that tangency occurs at the β, V combination
corresponding to the maximum burning rate in a stirred

reactor. Note that for any value of β above β_1 the
incremental volume in a plug-flow reactor is less than
in a well-stirred reactor, but to increase the burnedness
from any point lying between β_2, the stability limit of
the stirred reactor, and β_1 to the value β_1, a greater
volume is required in a plug flow reactor than in a well-
stirred reactor. For points below β_2 the well-stirred
reactor is unstable. The minimum total volume required to
accomplish any burnedness lying above β_1 is, therefore,
the sum of the volume of a well-stirred reactor operating
to give products at β_1 followed by a plug-flow reactor to
reach the burnedness β.

It is noticed that the plug-flow curve of Fig. II-4
looks very much like the profile of a laminar flame front
in which burnedness has been plotted against L/S_L, the
measure of time. However, in the calculation for Figure II-3
there is no allowance for diffusion of heat or mass such as
gives rise to a laminar flame propagation rate, and although
the abscissa has dimensions proportional to a length/flame
speed ratio, there is no definite distance associated with
the abscissa; consequently, there is no clear analogue to
flame propagation.

The performance of a well-stirred reactor being fed a
partly burned feed is readily obtained from the primary
stirred reactor curve such as Figure II-5, in which β is

plotted against $1/\psi_2$ (equal to VP^n/G). The slope of a line from the origin to a point on the curve represents the burning rate per unit volume in any system in which the burnedness is β. Since when the feed is partially burned, the burnedness to be accomplished is $\beta - \beta_0$ rather than β, the generalized volume necessary is (VP^n/G) $(\beta-\beta_0)/(\beta)$. This appears in Figure II-5 as $\Delta(VP^n/G)$. Figure II-5 can also be considered an example of operating two reactors in series. The first reactor, fed with the unburned fuel $(\beta_0 = 0)$, requires the volume $V_1 P^n/G$ to deliver products of composition β_1, and the second reactor, fed with products of burnedness β_1 and delivering products of burnedness β_2, requires the additional volume $\Delta(VP^n/G)$. Application of this principle leads directly to the following conclusions for a pair of stirred reactors: (Note the inset in Figure II-5. Two lines to the origin have been drawn, one tangent to the nose of the curve, and the other passing through the blowout point of the curve.) For cases where the burnedness leaving the second reactor lies above point "C", and all combinations of reactor pairs will require less volume than a single stirred reactor giving the same final burnedness. If the burnedness leaving the second reactor lies between points "B" and "C" it is always possible to have a pair of reactors operating more favorably than a single reactor, although not all reactor

INSET: ENLARGED DIAGRAM
OF NOSE REGION
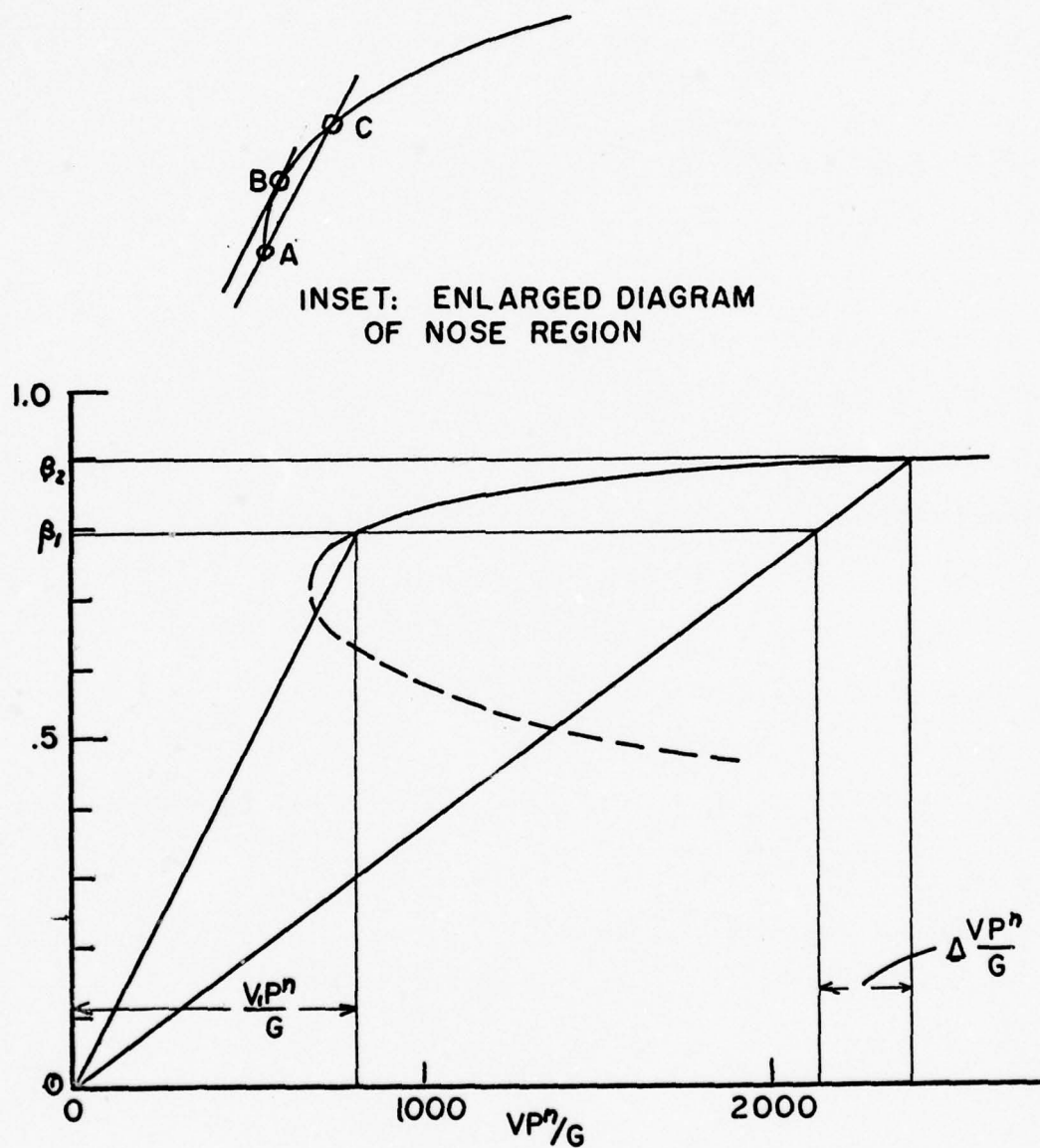
FIGURE II-5: STAGED WELL-STIRRED REACTOR
OPERATION

pairs in this range are better. If the final burnedness
leaving the second reactor lies between "A" and "B" there
is no possible combination of reactor pairs which requires
less total volume than a single reactor.

Staged Reactors with Intermediate Reactions

The discussion of reactor combination has been limited,
thus far to the case where only one composition variable is
required to describe the mixture. If two or more variables
are required, the treatment of staged reactors is considerably
complicated. The problems involved are best illustrated by
consideration of a simple case.

Consider a combustion process in which fuel is partially
oxidized in the first step to form "1" moles of an inter-
mediate "1" and "I" then reacts with additional oxygen to
form complete combustion products. For this reaction two
rate equations are required.

$$F \quad + \quad aO_2 \longrightarrow iI \quad \text{Step 1} \qquad \text{II-17}$$

$$iI \quad + \quad a_2O_2 \longrightarrow pP \quad \text{Step 2} \qquad \text{II-18}$$
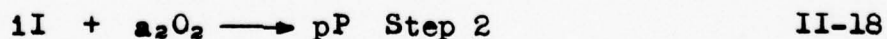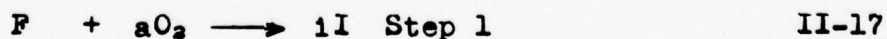
$$- \frac{dN_F}{Vdt} = \sqrt{T} \; k_1' \; e^{-E_1/RT} \; C_F^{\alpha_1} \; C_{O_2}^{n_1-\alpha_1} \qquad \text{II-19}$$

$$- \frac{dN_I}{dt} = 1 \left[\sqrt{T} \; k_2' \; e^{-E_2/RT} \; C_F^{\alpha_2} \; C_{O_2}^{n_2-\alpha_2} - T \; k_1' \; e^{-E_1/RT} C_F^{\alpha_1} \; C_{O_2}^{n_1-\alpha_1} \right]$$

$$\text{II-20}$$

In a manner similar to the previously discussed equation for the simple stirred reactor kinetics, these equations may be reduced to functions of two variables β and γ, representing the progress of reaction of steps 1 and 2 respectively:

$$\frac{G}{VP^n} (\beta - \beta_0) = f_1(\beta, \gamma) \qquad\qquad \text{II-21}$$

$$\frac{G}{VP^n} (\gamma - \gamma_0) = f_2(\beta, \gamma) \qquad\qquad \text{II-22}$$

Simultaneous solution of these equations is required to find the performance of a one-stage stirred reactor at any given feed rate. If it is desired to operate a two-stage reactor, the gas composition of the final stage, in general, will not be the same as the composition of a one-stage reactor whose exit temperature (or fractional oxygen consumption) is the same; and a second simultaneous solution is required for the β_0, γ_0 combination corresponding to the partially burned gases leaving the first stage.

To simplify calculations of these equations it is desirable to represent graphically the simultaneous solutions obtained from any given β_0, γ_0 starting combination (obtained in an unspecified manner). The composition of the exit gases from any reactor may be represented on a diagram of β vs γ for this two reaction postulated mechanism. On this same diagram lines of β γ combinations

having a constant ratio of the relative disappearance rates
of fuel and intermediate may also be mapped $(d\beta/d\gamma = C)$
(Figure II-6). Thus, in a stirred reactor whose outlet
composition is represented by β γ , the $d\beta/d\gamma$ in this reactor
may be read directly from this diagram, and this ratio must
be equal to the ratio of $(\beta - \beta_o)/(\gamma - \gamma_o)$ in that reactor.
Therefore, for any combination representing either outlet
or inlet conditions of a stirred reactor, lines representing
possible inlet or outlet β, γ combinations may be plotted.
Having found the inlet and outlet conditions from a diagram
such as Figure II-6, recourse to either Equation II-21 or
II-22 will give the volume required in that reactor. These
equations may be represented graphically to speed calcula-
tions (Figure II-7).

Using these two plots the performance of any desired
combination of plug-flow and stirred reactors in which a
two-step kinetic scheme is postulated may be calculated.
It is evident, however, that the addition of a third
variable would complicate the problem still further. Because
of the unwieldy calculation required for rigorously treating
the combination of stirred reactors with multi-step
reactions, one must hope that a simple one-step reaction
scheme will provide an accurate enough representation of the
gross kinetics to permit calculation of model performances.
This will be true, if, as suggested by Edgerton, Saunders
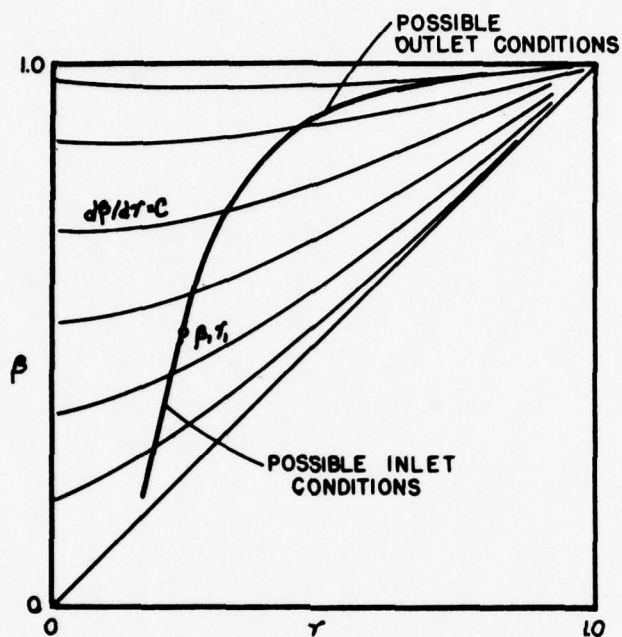
FIGURE II-6: LINES OF $d\beta/d\tau = C$, TYPICAL PATHS OF REACTOR COMPOSITION FOR A TERMINAL CONDITION (INLET OR OUTLET) OF β, τ_1 SHOWN
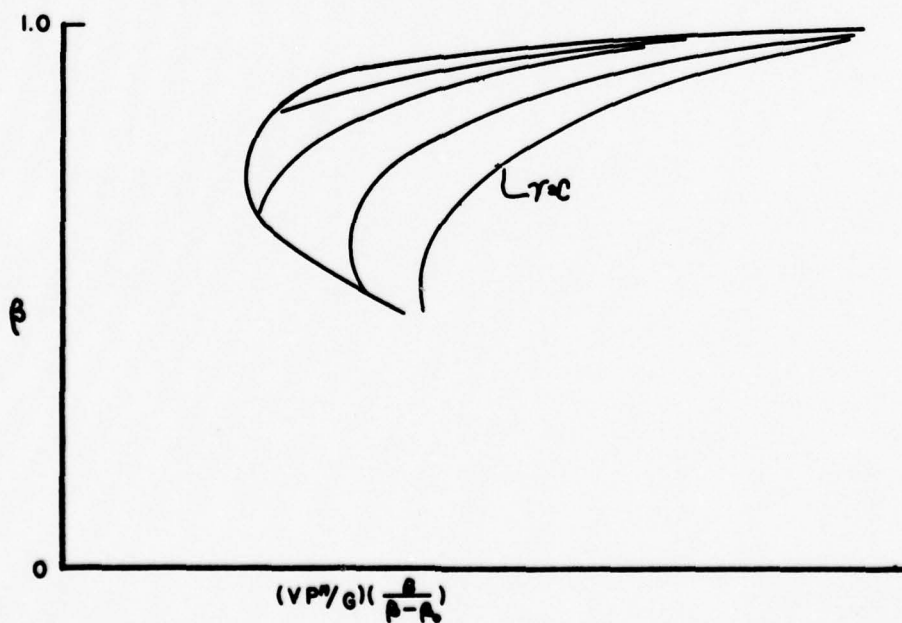
FIGURE II-7: VOLUME REQUIRED FOR GIVEN INLET & OUTLET CONDITIONS

and Spaulding, one reaction predominates over all others
in the range of practical interest.

Experimental Stirred Reactor Performance

Experimentally, the study of the stirred reactor in
combustion problems presents primarily the problem of
mixing fresh feed gases with the gases in the reactor at
an extremely high rate. This high mixing rate is required
to mix the gases before a significant amount of reaction
can occur. This obviously cannot be accomplished by simple
mechanical stirring. After some developmental work,
Longwell and Weiss (14) proposed the now familiar stirred
reactor in which a combination of intense turbulence and
gross recirculation, caused by a large number of small
jets issuing from a small concentric sphere into the
spherical reactor, mix the reacting gases moderately
well.

The data which have been published on this device
have been primarily blowout data. Three investigators
(3, 5, 14) have studied blowout loading factors as a
function of fuel-air ratio in reactors of this
design. Longwell and Weiss (14) were the first to
study this. They reported a pressure exponent of
1.8 as giving the best correlation

of their data, and they claimed that there was no significant
effect of hole size. Baker, in a somewhat later investiga-
tion, reported a trend of pressure exponent with fuel-air
ratio and recommended a pressure exponent of 1.3. He also
found a consistent effect of hole size. Because of the
differences in the results reported by Longwell and Weiss
and by Baker, Blichner (5) conducted a further investigation
on Baker's reactor. Blichner's results substantiated those
of Baker. He found an exponent lower than that reported by
Longwell and Weiss, and showed a significant effect of hole
size. A comparison of the blowout data reported in these
three investigations is shown in Figure 1I-8. Throughout
this thesis data of this type are reported on coordinates
of air loading rate, $N_A/V \ P^{1.8}$, and generalized fuel fraction
F. This latter quantity is given by $\emptyset/1 + \emptyset$, where $\emptyset$ is
the fraction of stoichiometric fuel. F is 0.5 for a
stoichiometric mixture, lean mixtures are less than F = 0.5,
and rich mixtures greater. In this comparison all three
sets of data are shown for a pressure exponent of 1.8, and
no distinction between hole size is made. All three sets
of data are corrected to an inlet temperature of 300°K using
the temperature correction factors suggested by Longwell
and Weiss.

Both Longwell and Weiss and Baker have reported
sampling data. Sampling traverses were made along a
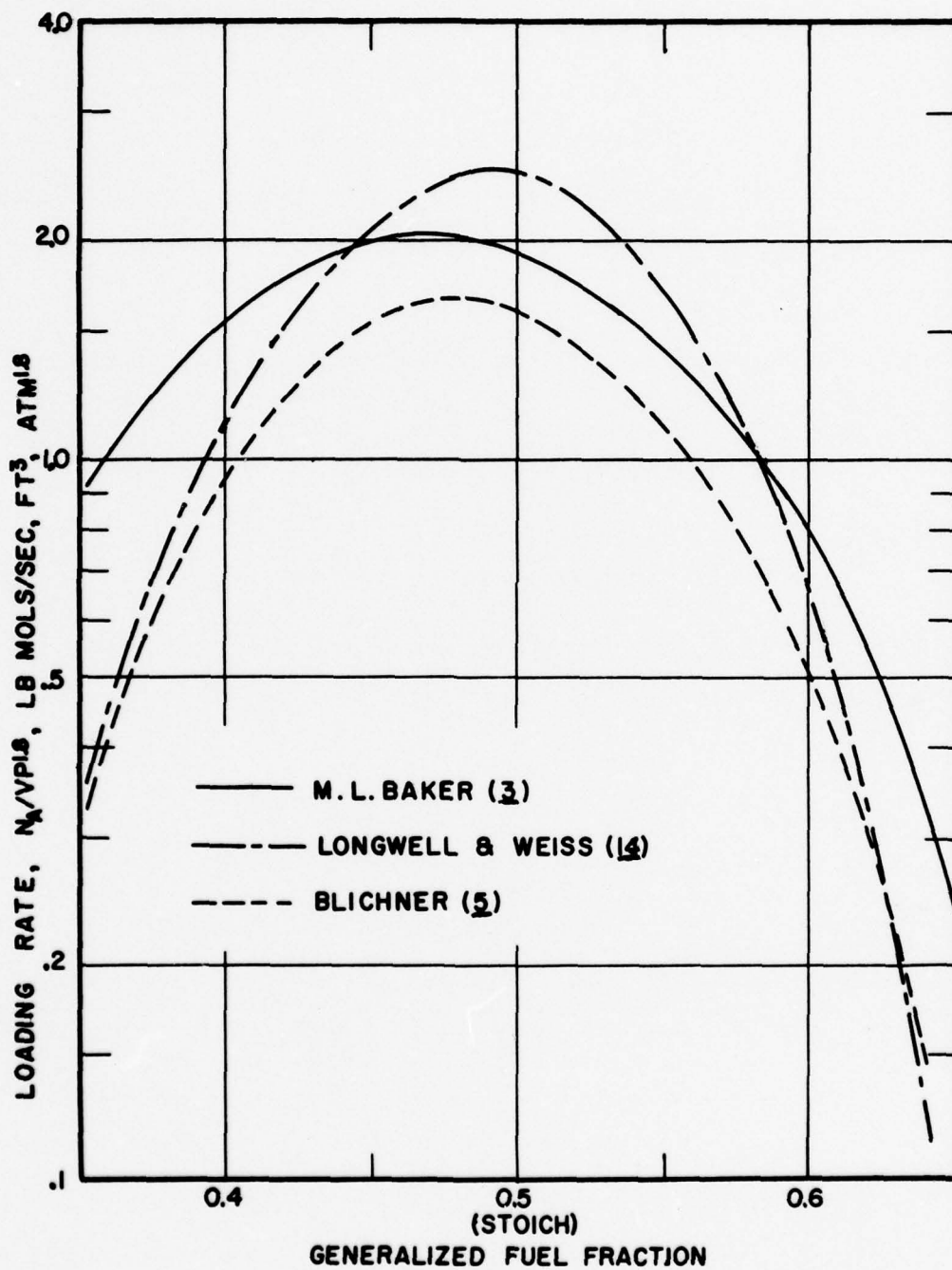
FIGURE II-8: STIRRED REACTOR STABILITY LIMIT
DATA. CORRECTED TO AN INLET TEMPERATURE
OF 300°K.

radius of the reactor to determine to what extent composition
varied within a reactor. Longwell and Weiss reported that
the composition was substantially constant over about 95%
of the volume. Baker points out, however that for their
sampling runs the burnedness level in the reactor was high
(over 90%), and consequently even if there were a composition
change it would not be great. Longwell and Weiss' data if
plotted on percent unburned basis show a much greater
relative change in composition within the reactor. Since
measurement of the variation in burnedness at high burned-
ness levels is not a very sensitive measure of the mixedness
of the reactor, Baker proposed to measure the variation of
burnedness within the reactor at a loading factor near
blowout. He found a greater variation of burnedness with
position as might be expected with this more stringent test,
but even so, the reactor still appears to be moderately
well-mixed.

Despite the evidence of the effect of hole size and of
sampling traverses that the reactor is not completely mixed,
the stirred reactor still remains a useful device for
studying the overall kinetic behavior of burning gases since
the evidence indicates that the mixing is rapid enough so
that chemical reaction rates are the predominant phenomena
controlling the reactor performance. Thus, using the blow-
out data of the stirred reactor, it is possible to

evaluate both a pseudo-collision constant and a pseudo-
activation energy for the reaction. These quantities, though
representing the gross reaction rather than the detail of the
individual stages of the combustion process are useful in
the evaluation of various fuels and in the prediction of
practical combustor performance.

In addition, Longwell and Weiss have reported sampling
runs in which combustion efficiency as a function of
loading factor for a constant fuel-air ratio was measured.
These data showed a poor agreement with the theoretical
curve for a simple bi-molecular collision process with
reaction rate constants predicted from blowout data.
However, other than this one bit of data, no work appears
to have been done on the operating characteristics of the
stirred reactor within the stable combustion region. In
the application of stirred reactor data to the prediction
of practical combustor performance, it is necessary to
have such information since combustion efficiency as well as
combustor stability is important in chamber operation and
design. Since the requisite data of feed rate vs efficiency
are not available, a calculated curve will be used here.
The curve is the one shown in Figure II-2. This curve was
calculated using combustion stoichiometry in which propane
is burned to CO_2 and H_2O in one step. A stoichiometric
mixture was postulated with an inlet temperature of 500°K,

a flame temperature at complete combustion of 2772°K, and
an activation energy of 40,000 cal/mol. The magnitude
obtained of the quantity G/VP^n is a consequence of the
normalizing procedure used in calculating this curve, and
these values must be multiplied by a constant factor to
make the blowout value correspond to the observed blowout
rate for a stirred reactor.

Combustion Chamber Models in the Literature

Based on the performance of the stirred reactor various
simple combinations of reactors can be postulated and their
behavior calculated. Some models of this type have already
been presented and discussed in the literature. Postulation
of such models may have as objectives: (1) In theoretical
studies one may attempt to find the ideal or optimum per-
formance which can be expected from combustion chambers, and
(2) In the study of real combustor performance one may
seek to find a simple combination of combustor elements
which will describe the performance of the chamber under
study with respect to changes in the various operating
or design variables. Several examples of the former type
have appeared in the recent literature.

Avery and Hart (2) considered a model of a can-type
combustor in which a pre-mixed fuel-air mixture was fed
into the can. The combustor was piloted in an unspecified
manner by a partly burned stream of the same fuel-air ratio

as the fresh feed to the can and of the same burnedness as the gases leaving the can. The rate of feed of the fresh fuel-air mixture along the length of the combustor was so adjusted that the composition within the can remained constant.

Since under these restrictions the composition of the gases in the combustor is the same throughout, the burning rate within the chamber was calculated directly from well-stirred reactor principles. In addition the pattern of fuel-air mixture injection required to maintain this optimum condition was calculated. Although no experimental work has been reported on this model it is of interest since it is the first such proposed used of basic stirred reactor information.

In this original model of Avery and Hart no allowance was made in the energy balance for the effects of directed-velocity kinetic energy. In a later paper Rosen and Hart (19) proposed a modification of this model to account for kinetic energy effects. These authors considered a straight, tubular combustor piloted by a partially burned gas in the same manner as in the Avery and Hart model and fed with fresh fuel-air mixture through the combustor walls in such a manner as to maintain a constant static temperature within the chamber. These authors then wrote differential equations of continuity, and momentum and energy balances. From these it is possible to derive:

(1) the maximum throughput of unburned gases permitted
by the assumption of constant static temperature (this
is not blowout, but analogous to "choking" in compressible
flow); (2) the relation required between kinetic energy,
temperature and combustion efficiency, and (3) the minimum
temperature (or maximum amount of enthalpy which may be put
into kinetic energy) allowing stable combustion for a con-
ventional nth order reaction.

The restriction of this model to a constant temperature
case and the restriction of the Avery and Hart model to a
constant efficiency case makes these models of relatively
small value in analyzing the behavior of real combustors.

DeZubay (6) suggested a different approach to the
modeling problem. He considered a combustor to which a
rich fuel-air mixture was fed, and after combustion was
partially completed, additional secondary air was added.

This problem was approached by considering the chamber
to be divided into two portions, each a well-stirred reactor.
The first portion was fed the rich fuel-air mixture, and the
second received the partly burned products from the first
chamber plus secondary air. In this model DeZubay demon-
strated that it was possible for two stirred reactors to give
a higher overall heat release rate than a single reactor
fed the same overall fuel-air mixture and operating under
the same conditions as the final reactor of the pair.

However, the force of this conclusion is somewhat clouded by the effects of the addition of secondary air.

The results which DeZubay presented also showed the quenching effect of adding air to the partly burned gases. It was shown that the addition of a large enough quantity of air would quench the reaction in the second reactor. Curves were given of heat release rate vs combustion efficiency leaving second reactor for various values of fuel-air ratio in the first of the two reactors. In all cases calculated by DeZubay the fuel-air ratio in the second stage and the relative volumes of the two stages were the same. For those cases where a large amount of secondary air was added more than one blowout point was found; i.e. as feed rate increased the second stage became unstable, and further increases in feed rate caused the first stage to blow out. It was also found, as might be expected, that the best operating conditions -- maximum heat release rates -- were found when the first stage had a fuel-air ratio of stoichiometric.

The models discussed thus far have treated the combustion chamber problem without cognizance of the effect of flow recirculation on combustion chamber performance. Since recirculation is generally postulated to have an important role, especially in combustor stability, any chamber model which is to be representative of combustor performance must

make allowance for the effect of recirculation. In a recent
paper Spaulding (24) has presented an analysis of combustion
chamber pressure drop requirements which does account for
the effect of recirculation.

Spaulding considered a combustion chamber in which the
gases flowed in a circulatory manner. Part of the chamber
was devoted to a mixing section in which fresh, unburned
gases mixed with recirculated gases; a portion of the
mixture was recycled and a portion left the chamber as
burned products. No combustion was postulated to occur in
the mixing section. The remainder of the chamber was
called the recirculation zone, and combustion occurred in
this region as the gases recirculated in a plug-flow fashion.

Using an assumed stirred reactor performance curve,
Spaulding could then calculate the performance of the model
in response to changes in either firing rate or recirculation
ratio. This model is very similar to the one proposed in
this work for modeling combustion chamber performance.
To facilitate comparison, Spaulding's model has been
recalculated using the stirred reactor curve which was used
through this work. The performance of Spaulding's model
is shown in Figure II-9.

Although no experimental work was done directly on
this model, Spaulding made some comparison of the model
performance with the performance of some combustor cor-
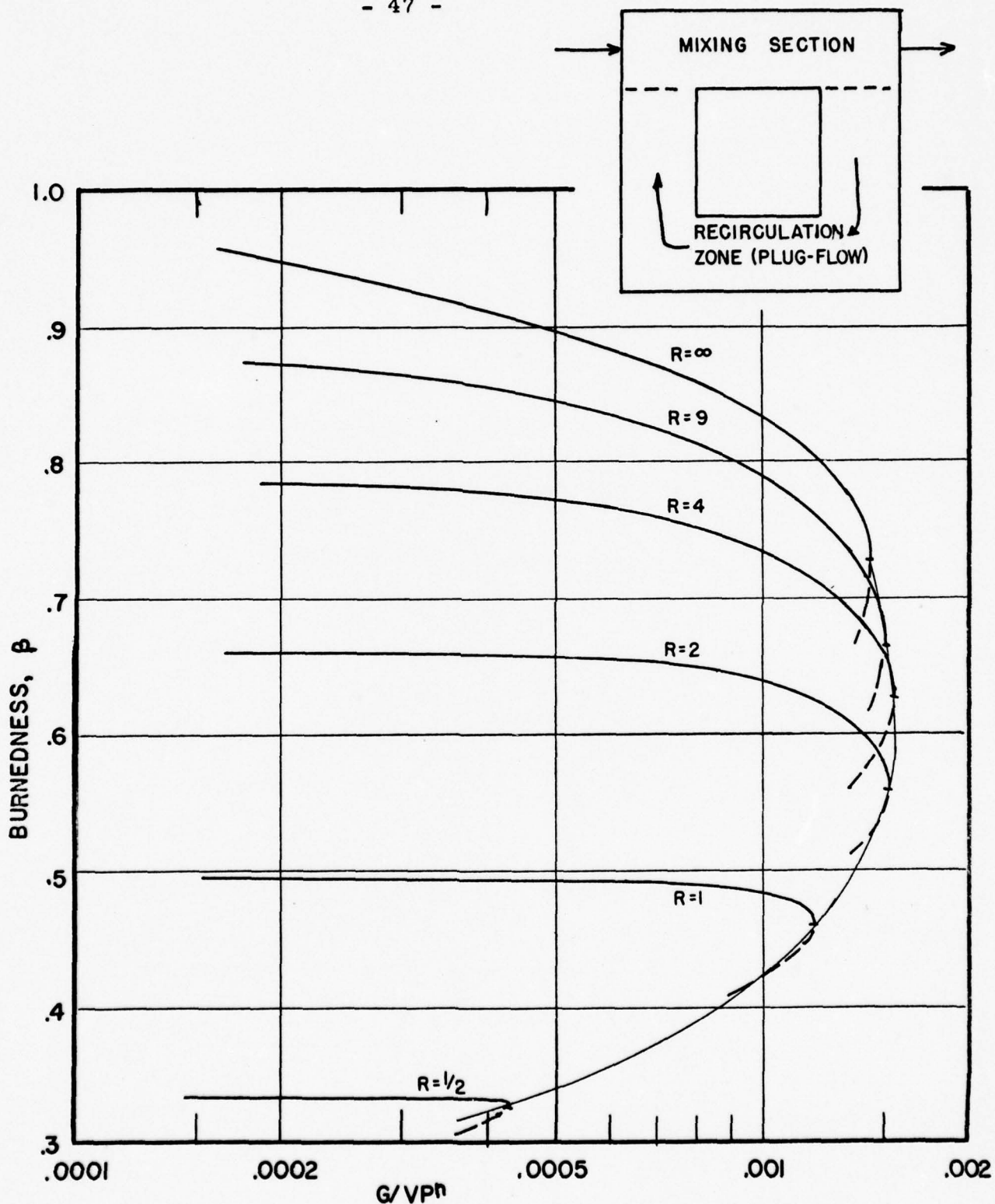
FIGURE II-9: RECALCULATED PERFORMANCE OF
SPAULDING'S SIMPLE MODEL (24)

$$R = \frac{\text{MOLS GAS RECIRCULATED}}{\text{MOL FRESH GAS FED}}$$

configurations in his electric analogue to combustion (23).
Because of differences between the model and combustor
configurations, it was not expected that a good correlation
would be obtained, however, the results of this comparison
were encouraging.

Spaulding also considered an application of this
model technique to the well-stirred reactor. From an
assumed flow pattern of the jet, a model was established in
which the outwardly-flowing cold gases received recirculated
gases from the reverse-flowing recirculating gases in a
continuous manner. The recirculation ratio was related
in this model to the down-stream distance from the jet
nozzle. Spaulding concluded from this analysis that the
well-stirred reactor design suggested by Longwell and Weiss
was, in fact, capable of producing moderately well-mixed
zones, although there was some departure from the ideally
well-mixed reactor performance.

One additional model of combustor performance has been
proposed by Berl, Rice and Rosen (4). They analyzed the
volume requirements for relatively low intensity combustion
in terms of an extended laminar flame front theory. This
model is not closely related to the models to be discussed
here and will not be considered further.

Summary

In recent years it has become evident that the analysis of high-output combustor performance must take into account the rate-limiting effect of chemical reaction as well as the effect of mixing. However, it was not until the concept of grossly simplified kinetics was applied to combustion problems that the required analysis became practical. The development of an experimental stirred reactor has permitted the gross kinetic constants in such a simple analysis to be estimated. The availability of stirred reactor performance data has tempted some investigators to devise conceptual models of practical combustor performance in terms of stirred reactor combinations. With one exception, however, no allowance has been made for the effect of recirculation, nor has much experimental work been done to test the validity of these models. In this thesis some new models of combustor performance are proposed and compared with experimental combustor performance.

CHAPTER III
MODELS OF COMBUSTION CHAMBERS

The classical analysis of combustion chambers has
been in terms of flame speeds. From the spreading angle
of a stabilized flame in a duct and a knowledge of the
stream velocity the velocity of the turbulent flame in
its normal direction is calculated. The classical analyst
then attempts to relate this turbulent flame speed to the
laminar flame speed of the combustible mixture and to the
turbulence level in the chamber which is assumed to cause
extension of the area available for flame propagation.

In more complex chambers it is difficult to extend
this analysis, since as the heat output rate of a chamber
increases it becomes more difficult to define a meaningful
boundary to represent a time-average flame front. As one
approaches the chemically limiting rates in a device such
as a well-stirred reactor it becomes difficult to justify
the use of an extended flame-front model since substantial
regions of the combustor are given over to homogeneous
combustion.

The analysis of this latter class of chambers can be
stated in terms of well-stirred reactor performance. Using
stirred reactor data to give the burning rate, or fuel
consumption rate per unit of volume, as a function of

temperature and a variety of composition variables, the
continuity equation for a differential segment of chamber
volume can be written. The time-rate of accumulation of
each chemical specie plus the rate of creation or destruction
of that specie by chemical reaction is equated to the
diffusive and convective fluxes of the specie into the
chosen control volume. An equation of this sort must be
written for each of the species present and the resulting
set must be solved either with an apriori knowledge of the
fluid-flow pattern or with the momentum balance differential
equations for the same control volume. Considerable
simplifications of these equations must be made for a
practical solution even in the   simplest of chambers.

As an alternative analysis, one may imagine that
relatively large regions of the combustor may be assigned
average compositions which will give the burning rate in
each region, and that these compositions may be related to
the feed rate and composition of gases entering each zone.
From a knowledge of the fluid-flow pattern the interchange
of materiel between zones may be evaluated and the per-
formance of the chamber synthesized.

A trivial model might consist in identifying the modest
performance of a practical combustor with that of a well-
stirred reactor operating at the same efficiency and firing
rate but of much smaller volume, and in making the

assumption that the departure of the practical chamber from
well-stirred reactor performance is due solely to incomplete
use of the volume available. One would not expect so simple
a model to fit over any extreme range of operating variables.
If, however, one were to postulate a combustor composed
not of just a single well-stirred volume and a single
inactive volume but of a small number of volumes character-
ized as well-stirred or plug-flow elements, representing
various regions of the real chamber connected in a
combination of series, parallel, and recirculating flow
patterns which is representative of the chamber flow pattern,
one could expect such a conceptual model to predict the
performance of a real chamber over a much wider range of
operating variables. Simplicity in these models is para-
mount, for only if the model consisted of a small number
of interacting elements would the results be impressive.

In any real combustor several types of zones are
expected. With a jet of fuel-air mixture feeding a chamber,
one expects the central core to be a relatively unburned
zone. Around the sides of the jet the more nearly burned
gases in the recirculation zones are in a well-mixed region
because of the intense turbulence created by the central
jet. In the corners of the chambers, regions of inactivity
are expected since these regions are relatively stagnant.
If the fuel and air are fed separately into a moderately

well-mixed chamber, similar zones are expected. In this
case one would also expect to find variations in the fuel/
air ratio in the various portions of the chamber.

In these models values must be assigned to the
relative rates of interchange between the various zones and
to their relative sizes. The magnitude of the variation
in the fuel/air ratio, if any, must also be chosen. These
values are associated with chamber design variables, and
to the extent that reasonable values may be associated with
the theoretical models, the models may be held to be
successful.

Three conceptual models have been developed which
predict some of the phenomena of practical combustors.
One of these phenomena is the abrupt change in flow pattern
observed in some combustors when the feed rate is increased.
When a certain feed rate is reached the flame in one portion
of the chamber disappears, and there is an accompanying
increase in the volume of the remaining active zones at
the expense of the zone which was extinguished. This
behavior has been observed in a two-dimensional chamber
fed by a mult-jet system of a premixed fuel/air mixture.
A simplified conceptual model of such a jet-chamber
combination will now be presented.

Figure III-1 shows such a chamber with the fuel/air
mixture entering a single jet and products leaving at the
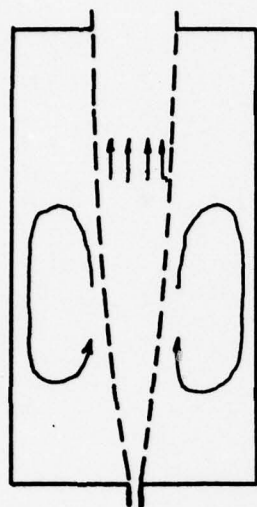
FIGURE III-1: PHYSICAL
PICTURE OF RECIRCULATION
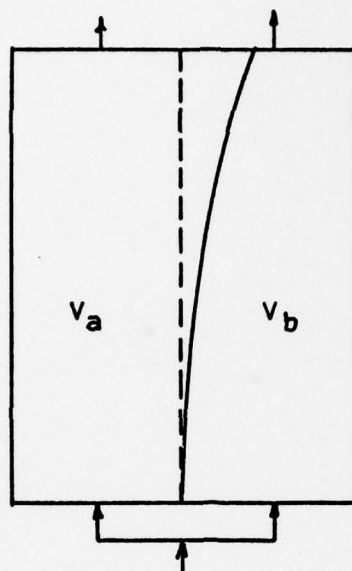
FIGURE III-2: MODEL
DIAGRAM

BURNEDNESS, β

$\dfrac{VP^n}{G}$
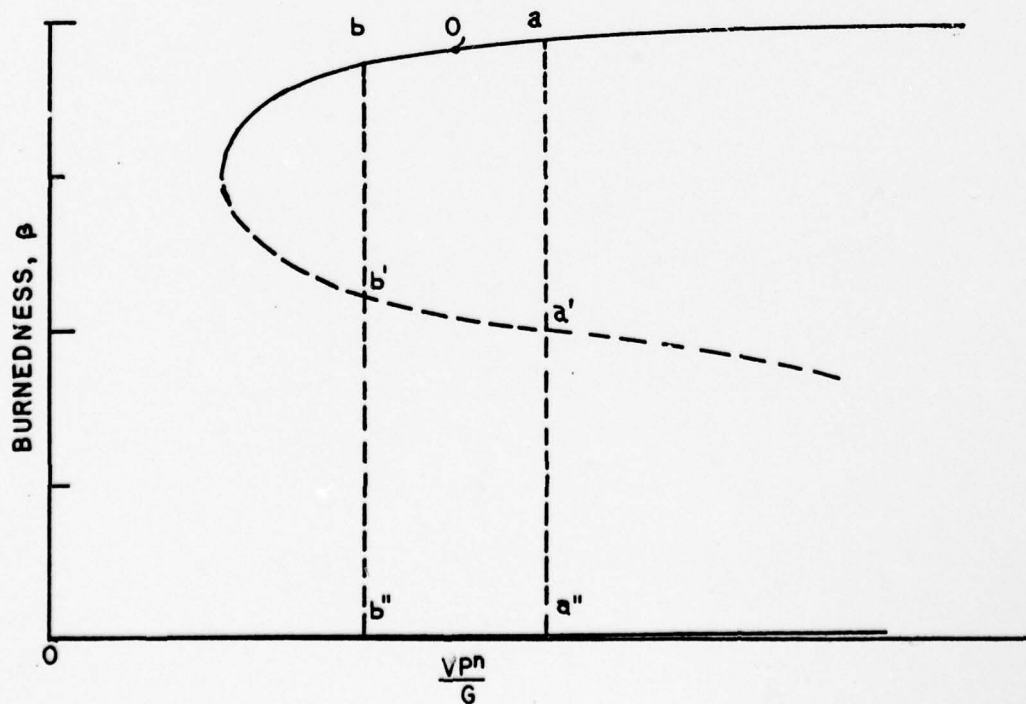
FIGURE III-3   WELL-STIRRED REACTOR CURVE FOR
TWO-STABILITY-LIMIT MODEL

top. Let the dotted lines bound the edges of those areas, taken normal to the axis of flow, through which the total upward gas flow is constant and equal to the feed rate. The volume thus bounded is called the "central core", and the region outside of this volume is called the "recirculation zone". It should be noted that the recirculation zone defined in this manner includes a complete vortex with gases flowing both upward and downward in contrast to a definition of the recirculation zone as that region where there is only downward gas flow. The dotted lines defining the boundary of the central core represent surfaces through any element of which there is no net mass flow, but there is equal and opposite turbulent diffusion through them. Because the feed to the zones external to the central core is on the average less burned than the gas which returns to the central core, the mean gas temperature in the outer zones is higher than that of the central core. Consequently the linear velocity of the outwardly moving gas is less than that of the inwardly moving, more completely burned gas; and the force producing this net inward momentum flux is a higher static pressure existing in the outer zones.

If both recirculation zones are equally active, the pressure effects on the two sides counter-balance. But if one zone is active and the other inactive, a pressure imbalance occurs, causing a deflection of the jet toward

the inactive side. This increases the volume of the active zone, thereby improving the opportunity for completion of combustion in it. The end effect is a bending of the jet, in response to the pressure exerted by the larger recirculation zone, to a position of equilibrium between the jet-momentum force and the pressure-area force of the hotter recirculation zone.

Since the system is two-dimensional the difference in the volumes of the recirculation zones may be assumed to be proportional to the pressure difference between them, and since the pressure effect is postulated to be the result of a tranverse momentum flux, the pressure difference between the two zones should be roughly proportional to their temperature difference. To simplify this treatment, the central core will be assumed to be a high-speed, non-reacting jet stream in which the gases reside for a relatively short time, serving to supply feed gases to the recirculation zones, and the latter zones will be considered well-stirred reactors.

The block diagram representing this model, Figure 111-2, consists of two well-stirred reactors of constant total volume, separated from each other by an elastic barrier zone, the jet, which has the property of bending in response to pressure differences so that the change in volume of either of the reactors is directly proportional

to the pressure difference between the two. In the absence
of a pressure difference the system is symmetrical. The
fuel-air mixture will be assumed to be fed equally to the
two reactors.

The deflection of the barrier is expressed in terms
of the difference in the volumes of the two reactors;

$$\frac{V_a - V_b}{2} = k_1 \ (P_a - P_b) \qquad\qquad III-1$$

and the pressure difference created by a difference in
burnedness in the two reactors is:

$$P_a - P_b = k_2 \ (\beta_a - \beta_b) \qquad\qquad III-2$$

Assume a well-stirred reactor performance curve is available
(e.g. Figure III-3), giving the relation between burnedness
and normalized volume.

In this model a series of stirred reactor pairs of
various volume differences may be considered at each firing
rate. For each volume difference considered the correspond-
ing pressure difference between the two reactors may be
found by combining Figure II-3 and Equation III-2. These
pressure differences found may then be compared with the
pressure difference required to maintain the postulated
volume difference from Equation III-1. For each new firing
rate considered a new series of volume differences and
pressure differences may be found.

This calculation may be represented graphically. Let the total volume/feed ratio, equal to the initial ratio for each reactor, be represented by point "0" of Figure III-3, and let the barrier be deflected by an amount $(V_a - V_b)/2$, causing zones a and b to increase and decrease respectively by this amount. These volume changes are accompanied by corresponding changes in burnedness which may be found from Figure III-3 where a and b represent the new volume/feed ratios of sides a and b. Solutions for the burnedness in the new volumes exist on the branches at a, a", and b and b" (a' and b' are thermally unstable reactor conditions). These burnedness differences, 4 of them (plus 5 involving unstable reactor conditions), can be evaluated and from Equation III-2 the corresponding $(P_a - P_b)$'s can be found. These points for a typical case are plotted on Figure III-4. (The designations ab, ab' etc. represent reactor conditions of Figure III-3.) Repitition of this calculation for a series of volume differences leads to branches I and II of Figure III-4. Those portions of the curves which involve thermally unstable reactor conditions, i.e. the dotted portions of Figure III-3, are included for completeness but are dotted. Figure III-3 shows rather inadequately that Branch II is symmetrical around the origin; no symmetry around either axis intended.

The ab solution occurs when both reactors are hot,
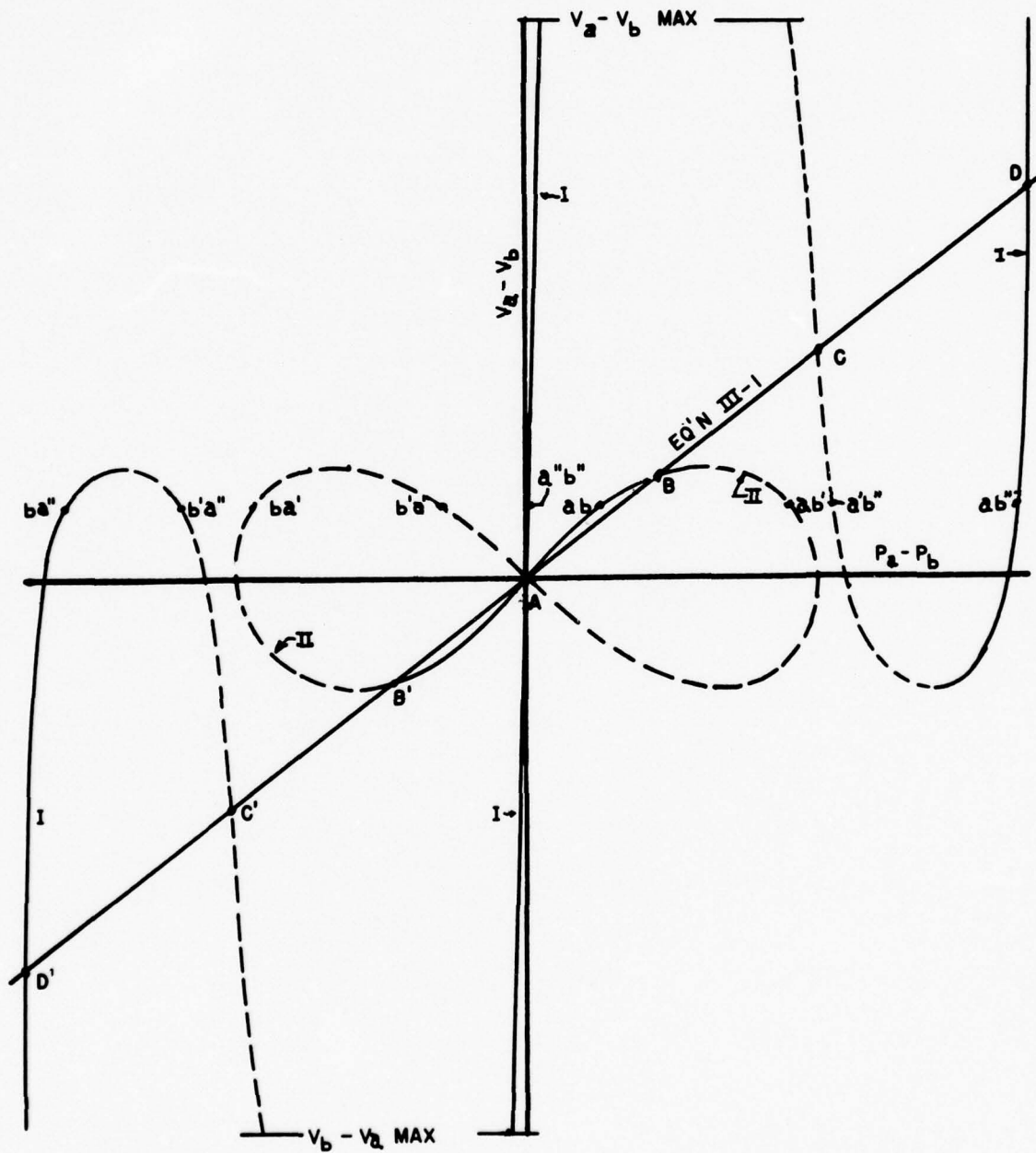
FIGURE III-4: PERFORMANCE OF A TWO-STABILITY-LIMIT
COMBUSTION CHAMBER MODEL. GROSS VOLUME-
FEED RATIO AND FEED COMPOSITION FIXED.

and a low P_a - P_b is developed, lying on Branch II in the first quadrant. If side b is blown out, a high P_a - P_b is developed at the point ab" on Branch I, also in the first quadrant. Similar reasoning leads to the remainder of the points.

For each new value firing rate chosen a new pair of branches I and II will be found. It will be noted that at a sufficiently high firing rate the reactor pair will just be able to operate with both sides active. This occurs when point "0" of Figure III-3 is just at the blowout point of the well-stirred reactor curve. If the feed rate to the same reactor paid is increased further, it may still be possible for one side of the model to operate on the stable "hot" branch of the reactor curve if the volume difference is large enough; however, since the maximum volume difference possible occurs when V_a is twice its initial value, the maximum feed rate which permits a possible "hot" reactor is twice the feed rate corresponding to the above blowout point.

To find the stable operating points on Figure III-4, the line representing Equation III-1 is superimposed on branches I and II for the specific "0" chosen. (A non-linear relation between V_a - V_b and P_a - P_b could be used equally well). The equilibrium values of V_a - V_b are found at the intersections of the line of Equation III-1 and either branch I or branch II. Branches I and II and the curve of

equation III-1 are symmetrical around the origin, i.e. it makes no difference which side becomes colder. Three stable solutions are found, the origin and the outermost intersections, $\underline{A}$, $\underline{D}$, and $\underline{D}'$. The remaining four intersections are all unstable; $\underline{C}$ and $\underline{C}'$ because one side of the reactor pair is operating on the unstable branch of the well-stirred reactor relation, and $\underline{B}$ and $\underline{B}'$ because the barrier is in a metastable position. A stable barrier position is one in which a momentary change in $V_a - V_b$ causes a change in $P_a - P_b$ such that a net restoring force results. This means that at a stable intersection of the branches I or II with the line of Equation III-1 both curves must have a positive slope and the slope of the former must be greater than the slope of the latter.

The physical significance of the constants in Equations III-1 and III-2 is of importance in relating the theory to experimental and design problems. The interpretation of these constants may be seen by reducing Equations III-1 and III-2 to dimensionless relations.

In any chamber which has a pressure difference transverse to the flow direction of a jet a deflection of the jet will be found. This deflection would be expected to be a function of the ratio of pressure-area forces to the jet-momentum force, and assuming dimensional similitude, this function may be expressed:

$$\Delta y_r = \varphi(\Delta P_r, x_r) \qquad\qquad III\text{-}3$$

where $\Delta y_r = \Delta y / y_N$, $x_r = x / x_N$, and $\Delta P_r = \Delta P / \rho_N U_N^2$.

y_N = nozzle width, U_N = nozzle velocity,

ρ_N = nozzle density.

ΔP = the difference in pressure on the two sides
of the jet averaged from the nozzle to the
distance x from the nozzle.

Δy = the deflection of the jet centerline at the
distance x from the nozzle.

The change in volume, $V - V_o$, for either side may be computed
by integration of the deflection of the jet over the length
L of the chamber:

$$V - V_o = w \int_o^L \Delta y \ dx = w y_N^2 \int_o^{L_r} \Delta y_r \ dx_r$$

$$= w y_N^2 \int_o^{L_r} (\Delta P_r, x_r) \ dx_r \qquad\qquad III\text{-}4$$

This reduces to:

$$\frac{V_a - V_b}{2} = w y_N^2 \ \bar{\Phi}(\Delta P_r^*, L_r) \qquad\qquad III\text{-}5$$

where ΔP_r is the reduced pressure difference averaged over
the entire chamber length and w is the width of the two-

dimensional jet. This may be compared with Equation III-1 directly, and to be in conformity with it, i.e. to make the displacement proportional to ΔP^*_r, Equation III-5 must be of the form:

$$\frac{V_a - V_b}{2} = wy_N^2 \quad (\Delta P^*_r) \; F \; (L_r) \qquad\qquad \text{III-6}$$

This equation may be rewritten in dimensionless form:

$$\frac{V_a - V_b}{V_a + V_b} = \frac{wy_N^2}{V_a + V_b} \quad \Delta P^*_r \; F \; (L_r) \qquad\qquad \text{III-7}$$

The "jet" will now be defined more precisely as that part of the flow pattern of constant axial mass flow rate (i.e. the same portion of the flow referred to in Figure III-1); and that part of the system external to the boundary surfaces of this special jet will be called the "recirculation zone". (Since that part of the zone in contact with the jet core has a large positive axial velocity component, this is not the conventional jet referred to in the literature on jet structure.)

Because of the definition of the recirculation zones, these zones must be fed with fresh combustible gases by an eddy diffusional process, and burned gases must leave them similarly. These diffusion terms may be assigned average velocities U_o outward and U_1 inward which are applicable

to the entire interface between the jet mainstream and
the recirculation zone, and by the similarity principle:

$$U_o = a U_N \qquad \text{III-8}$$

Using this outward velocity, the outward momentum flux $\dot{m}_o$
associated with it can be evaluated:

$$\dot{m}_o = \rho_o U_o^2 = a^2 \rho_o U_N^2 \qquad \text{III-9}$$

By applying a material balance, the gases leaving the
recirculation zone, $\rho_1 U_1$, must be equal to the gases
entering that zone:

$$\rho_o U_o = \rho_1 U_1 \qquad \text{III-10}$$

The inward momentum flux, $\dot{m}_1$, is then

$$\dot{m}_1 = \rho_1 U_1^2 = (\rho_o U_o^2) \, \rho_o/\rho_1 = a^2 \rho_o U_N^2 \, \rho_o/\rho_1 \qquad \text{III-11}$$

Hence the net momentum flux at the boundary is:

$$\Delta \dot{m} = a^2 \rho_o U_N^2 \left(\frac{\rho_o}{\rho_1} - 1 \right) \qquad \text{III-12}$$

and for two zones, the pressure difference between them may
be calculated, assuming there is negligible temperature
rise in the jet mainstream, by the equation;

$$P_a - P_b = a^2 \rho_N U_N^2 \left(\frac{T_a}{T_N} - \frac{T_b}{T_N} \right) \qquad \text{III-13}$$

Now by an energy balance:

$$\frac{T}{T_N} = \beta \left(\frac{T_{af}}{T_N} - 1 \right) + 1 \qquad \text{III-14}$$

Hence:

$$\Delta P_r^* = a^2 \left(\frac{T_{af}}{T_N} - 1 \right) (\beta_a - \beta_b) \qquad \text{III-15}$$

This equation, when compared with Equation III-2 is of identical form, i.e. the pressure difference is directly proportional to the burnedness difference.

Figure III-4 may be replotted using coordinates of $(V_a - V_b)/(V_a + V_b)$ and $\beta_a - \beta_b$, yielding a generalized expression of the relative performance of the two sides of the model. In this diagram all possible combinations of $V_a - V_b$ and $\beta_a - \beta_b$ must lie within the square bounded by the limits of $(V_a - V_b)/(V_a + V_b) = \pm 1$ and $\beta_a - \beta_b = \pm 1$. On this same diagram the response of the jet to a burnedness difference may also be plotted, this relation being obtained by a combination of Equations III-7 and III-15:

$$\frac{V_a - V_b}{V_a + V_b} = \left[a^2 \left(\frac{T_{af}}{T_N} - 1 \right) \frac{2wy_N^2}{V_a + V_b} F(L_r) \right] (\beta_a - \beta_b)$$

$$\text{III-16}$$

This plot of the relations embodied in Equations III-1 and III-3 has the advantage that all of the geometrical design variables are lumped into one coefficient, namely the slope of the line representing III-16. Inspection will verify that for a given value of the overall loading factor, $G/(V_a + V_b)P^n$, the relative performance of the two reactors of the model (branches I and II of Figure III-4) when plotted on these coordinates will yield the same curve,

independent of the shape of the chamber. Different curves
of branches I and II will be obtained for each value of
the loading factor chosen. However, from Equation III-16,
the response of the jet to the burnedness differences is
independent of the velocity (or loading factor). Hence,
in comparing the response of a given chamber, fed a given
fuel/air ratio and fuel type, to changes in the feed rate
a family of curves of branches I and II will be obtained
which intersect the one line representing Equation III-16.

Design variables such as chamber and nozzle shape, on
the other hand, are reflected only in the slope of the
line representing Equation III-16. These variables, together
with the volumetric expansion of the burned fuel/air mixture,
$(T_{af}/T_N) - 1$, determine the fractional volume change produced
by jet movement in response to a unit of burnedness difference
in the two sides. In Equation III-16 the variables affected
by chamber design are the constant a^2 which is related to
the jet spreading angle and the quantity $[(2wy_N^2)/(V_a + V_b)]F(L_r)$

which is related to the chamber geometry. Changes in the
feed composition and inlet temperature will affect both
branches I and II (since this will change the basic stirred
reactor relation shown in Figure III-3) and the jet
sensitivity through $(T_{af}/T_N) - 1$.

Using a diagram such as Figure III-4 in the generalized
form discussed above, both the response of the chamber to

changing feed rates and the stability characteristics of
the chamber may be investigated. Consider the chamber to
be burning initially in a stable, symmetrical pattern
(operation corresponding to the origin of Figure III-4).
If the total loading factor of the chamber is increased,
point "O" of Figure III-3 will move toward the β axis.
As it approaches the nose of the curve of Figure III-3,
branch II of Figure III-4 becomes smaller and thinner
(i.e. its slope at the origin becomes smaller and its
$\beta_a - \beta_b$ intercept approaches the origin). This change in
operating conditions will not affect the slope of the
curve representing jet position. When the loading factor
has increased sufficiently to make branch II become tangent
to the jet position curve at the origin (Figure III-5),
the origin becomes an unstable intersection of the jet
position line and the reactor operating lines. Hence
the only remaining stable solution is the intersection of
the jet position line with branch I of Figure III-5,
corresponding to one side burning stably and the other
blown out. This calls for a sudden deflection in the jet
to the new stable position of $V_a - V_b$. Further increase
in the feed rate will cause the disappearance of branch II,
and eventually branch I will become tangent to the line of
Equation III-16 (Figure III-6). This represents the condi-
tion for total blowout of the chamber, since at this point

$$\frac{V_a - V_b}{V_a + V_b} \text{ MAX}$$

$(V_a - V_b)/(V_a + V_b)$

I

STABLE
SOLUTION

EQ'N III-1

TANGENCY

II

$\beta_a - \beta_b$
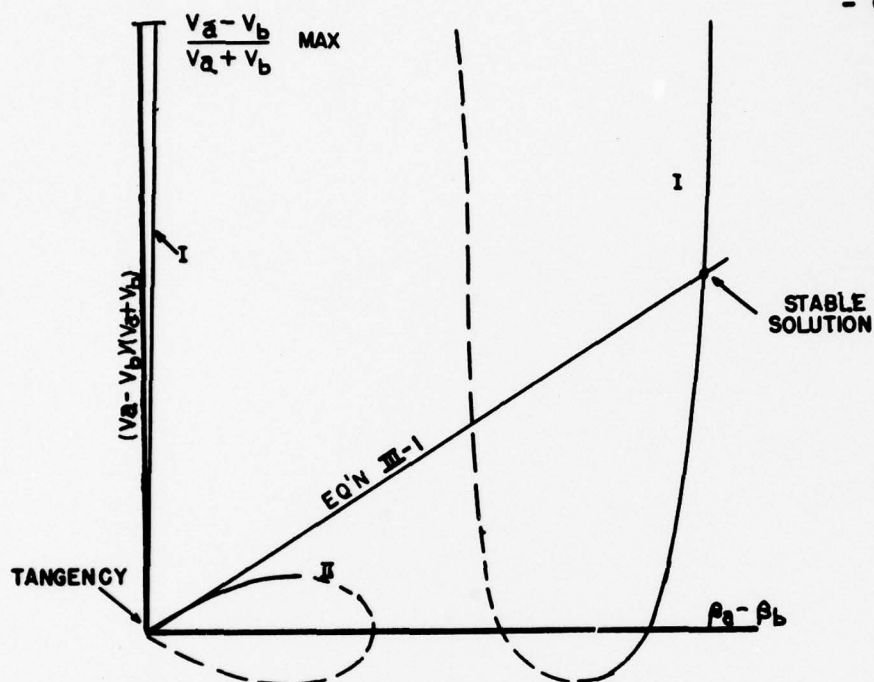
FIGURE III-5: ONE-SIDED BLOWOUT CONDITION IN THE
TWO-STABILITY-LIMIT MODEL

$$\frac{V_a - V_b}{V_a + V_b} \text{ MAX}$$

$\frac{V_a + V_b}{V_a + V_b}$

I

I

TANGENCY

EQ'N III-1

ONLY STABLE
SOLUTION

$\beta_a - \beta_b$
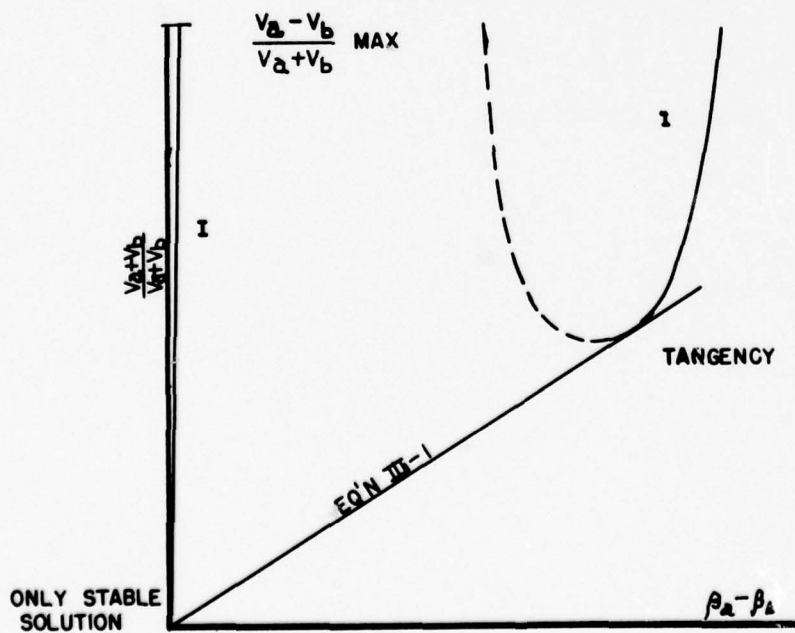
FIGURE III-6: FINAL STABILITY LIMIT FOR THE TWO-
STABILITY-LIMIT MODEL

and higher feed rates there are no stable intersections of branch I of Figure III-6 with the line of Equation III-16.

This model also has interesting implications concerning behavior at other chamber feed rates. Figures III-7a to III-7f represent six feed rates with six corresponding pairs of branches I and II, along with a common curve showing the jet stiffness independent of feed rate. Here only the stable portions in the first quadrant of Figure III-4 are shown. On each of these diagrams a horizontal dotted line is drawn tangent to the nose of branch II. This represents the blowout point of branch II, i.e. the maximum volume difference allowable for a given volume/ feed ratio if both zones are to be simultaneously stable. If $V_a - V_b$ exceeds this level the smaller side will be blown out, and if $V_a - V_b$ is below this limit, either the smaller side will burn stably, or if it is blown out it may be relighted by a sufficiently strong source.

Consider a chamber operating at a volume/feed ratio represented by Figure III-7b with both sides active, i.e. with operation at the origin of Figure III-7b. If a disturbance, $V_a - V_b$, is imposed on the jet, the jet will tend to return to its central position unless the $V_a - V_b$ imposed is greater than the blowout limit represented by the dotted line. If this limit is exceeded then one side will become cold, and a high $P_a - P_b$ will be developed.

7-C

7-B

7-A

7-F

7-E

7-D

$\beta_a - \beta_b$

$\beta_a - \beta_b$

$\beta_a - \beta_b$

ONE-SIDED
BLOWOUT

TWO-ACTIVE
ZONES

ΔV

$\dfrac{V_a - V_b}{V_a + V_b}$

$\dfrac{V_a - V_b}{V_a + V_b}$

DECREASING FEED RATE

DECREASING FEED RATE
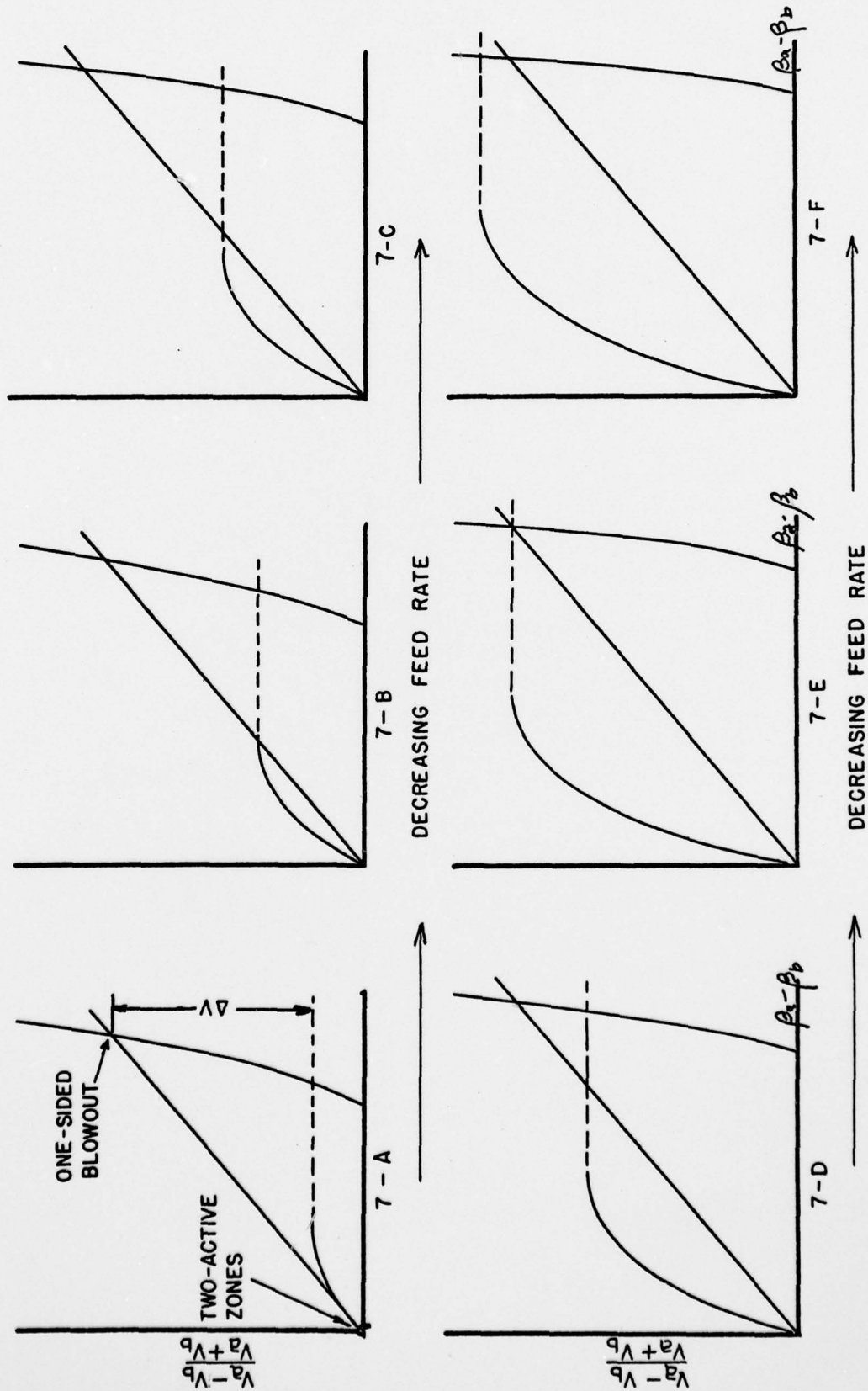
FIGURE III-7: EFFECT OF FEED RATE IN TWO-STABILITY-LIMIT MODEL.

The jet will consequently move to the one-sided blowout
position (the branch I intersection) instead of returning
to its central position. If the chamber is operating at
the one-sided blowout position when the disturbance is
imposed, then the reverse argument is applied; however,
in this case the problem of re-light must be considered.
Even if the disturbance is large enough to bring the small
side to a re-lightable position, the small side will not
relight if the ignition source is too weak; and the jet
will return to the one-sided blowout position. Since in
this case the disturbance required to reach the critical
level is much larger than in the first case, it would be
expected that the one-sided blowout position would be
the more stable one.

At a lower feed rate than in Figure III-7b, such as
represented by Figure III-7c, the blowout point of branch
II is about centrally located with respect to the two
stable jet positions. In a highly turbulent combustor in
which there are high transfer rates from active zones to
extinguished zones (conditions typical of many high-output
combustors) it is easy to imagine that if the volume/feed
ratio for any cold zone is above the minimum required for
stability by the well-stirred reactor kinetics, ignition
will occur. If simultaneously there is an equal liklihood
that a disturbance in $V_a - V_b$ from either stable jet

position will cross the critical blowout level, conditions
for a flickering flame exist.

At even lower feed rates, represented in Figure III-7d,
the situation is reversed from that represented by
Figure III-7b. In Figure III-7d the two-active-zone solution
is the relatively more stable since a smaller disturbance
is required to go from the one-sided blowout position to
the maximum relight level than in the opposite direction.

In the sixth diagram, Figure III-7f, the feed rate
is so low that the one-sided blowout solution is below the
critical blowout level of branch II. Thus, assuming that
relight will always occur if the opportunity exists, the
only stable solution at this rate is the origin (two active
zones).

This type of argument also leads to the conclusion
that a hysteresis effect exists in this combustion chamber
model. In reaching the transition from two-active zones
to the one-sided blowout from low feed rates, chamber
operation moves from a low feed rate condition represented
by Figure III-7f to that high flow rate condition repre-
sented by Figure III-7a, where the origin becomes an
unstable solution. Once the transition occurs, relight
can be caused only by reducing the feed rate to a point
where the one-sided blowout solution is below the blowout
point of branch II. The feed rate where this critical

level is reached is represented in Figure III-7
Thus, it may be concluded that this simple model of a com-
bustion chamber is useful not only for studying pressure
interactions of two or more zones but also for suggesting
mechanisms for other important chamber problems.

Model Showing Effect of Recirculation

Flow recirculation is another phenomenon of combustion
chambers which is characteristic of many systems. This
has been recognized by Spaulding (24) in a paper which
appeared after the present model had been developed.
Spaulding proposed a model of a recirculating system
similar to the model developed here, although the treat-
ment and conclusions are markedly different. In a chamber
fed by a jet of fuel/air mixture the region of the jet
near the base of the chamber aspirates burned gases from
the surrounding region. These gases are replaced by
reverse-flow from near the exit of the chamber.

In constructing a model of this behavior, Spaulding
suggested that the gases flow around this loop in plug-
flow. The central core serves only to mix the recirculated
gases with the fresh feed. A portion of this mixture is
discharged from the model as burned products, and the
remainder recirculates in a plug-flow combustion zone.
Spaulding has calculated two cases for this model; one

FIGURE III-8

EFFECT OF RECYCLE IN A COMBUSTION CHAMBER MODEL

BASIC RELATION
FROM WELL-STIRRED
REACTOR THEORY:

$$\beta = f\left(\frac{G}{V_\beta P^n}\right)$$

β = BURNEDNESS
G = FEED RATE
V = VOLUME
R = RECIRCULATION RATIO

P = PRESSURE

SOLUTION OF EXAMPLE

GIVEN: R=1, β_1=.75, V_2=2 V_1

FIND: $\dfrac{G}{(V_1+V_2)P^n}$

ASSUME β_2=.94
FROM MATERIAL BALANCE

$$\beta_1 = \beta_2 \frac{R}{1+R} = .47$$

AT β_1=.75, $\dfrac{V_1'}{GP^n}$ = 700
THEN:

$$\frac{V_1}{GP^n} = \frac{V_1'}{GP^n}(\frac{\beta_1 - \beta_2}{\beta_1})(1+R) = 522$$

$$\frac{V_2}{GP^n} = 2\frac{V_1}{GP^n} = 1044$$

$$\frac{V_2'}{GP^n} = \frac{V_2}{GP^n}(\frac{\beta_2}{\beta_2 - \beta_1})(1-\frac{1}{R}) = 4670$$

AT $\dfrac{V_2'}{GP^n}$ = 4670, β_2=.94

CHECK ASSUMED β_2 VALUE

BURNEDNESS
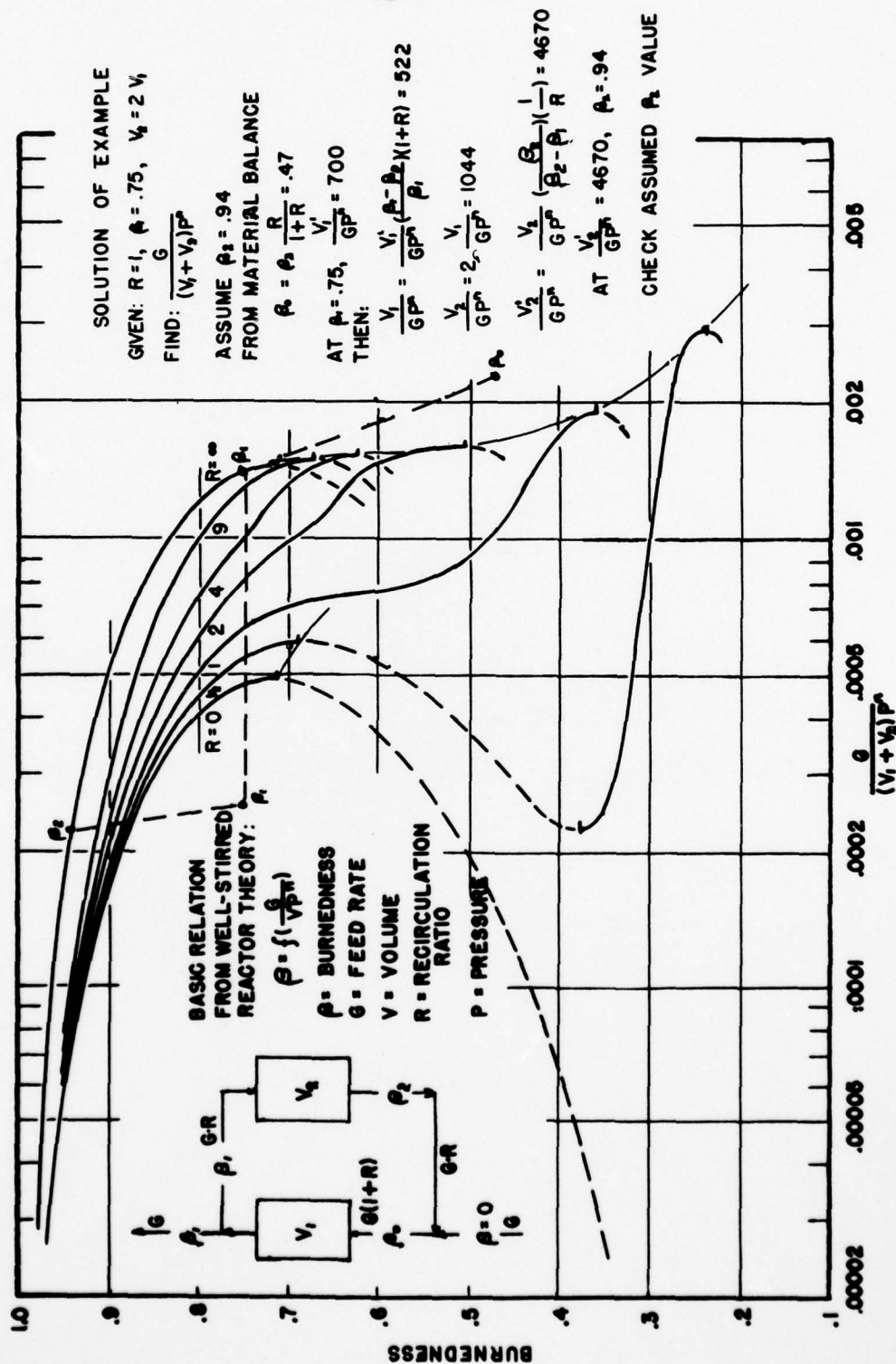
where there is no interchange between the jet mainstream
and the recirculation zone (all recirculated material
enters at the base of the jet) and a second case where
allowance is made for continuous aspiration of burned
gases from the recirculation zone along the length of
the jet. The first of these cases is directly comparable
to the results obtained here, and the behavior of this
model is shown in Figure II-9.

No allowance has been made in Spaulding's model for
combustion occurring in the central core of the jet. A
model in which such an allowance is made is probably in
better agreement with the actual situation. The con-
sequences of allowing for combustion in the central core
are illustrated by the model considered here. In this
model both the central core and the recirculation zone
have been treated as well-stirred reactors. Figure III-8
shows this model diagrammatically. Fresh feed enters
and is mixed instantaneously with recycled burned gases.
The mixed gases then enter zone V_1, representing the
central core of the jet. A portion of the partially burned
products leaving V_1 is recycled through the recirculation
zone V_2, where further combustion occurs, and then is
returned to V_1 again.

To find the feed rate to each of the zones, a
recirculation ratio is defined as:

$$R = \frac{\text{Molal recirculation rate to zone } V_2}{\text{Molal fresh feed to model}}$$

This definition is the same as that used by Spaulding. From a performance curve showing the relation between feed rate and burnedness (i.e. Figure III-3), the response of this system to feed rate changes may now be calculated for a given ratio of V_2/V_1 and recirculation ratio R.

This calculation has been carried out for a fixed value of $V_2/V_1 = 2.0$ and for various recirculation ratios. Burnedness, as a function of feed/total volume is shown in Figure III-8.

Several performance characteristics of this system should be noted. If the chamber is operating at a recirculation ratio of zero, the volume V_2 allowed for recirculation represents "dead" space, and the central core V_1 has only fresh, unburned gases entering it. The central core, therefore, operates as a simple well-stirred reactor without any additional assistance from the recirculated gases. The curve representing the behavior of zero recirculation may be found by multiplying the curve for the simple well-stirred reactor by the fraction of the volume in the model which represents the active central core, (i.e. by $V_1/(V_1 + V_2)$; curve $R = 0$ of Figure III-8).

If, on the other hand, the recirculation ratio is infinite, the composition of both zones is identical, and the performance becomes that of the well-stirred reactor performance used to generate all of the other curves.

(Curve $R = \infty$, Figure III-8).

For recirculation ratios neither zero nor infinite, significant interaction occurs between the central core and the recycle volume. This is illustrated by considering the relative contributions of each of the reactors to the total amount of combustion. Let the burnedness of the streams leaving reactors V_1 and V_2 be represented by β_1 and β_2 (the former also represents the burnedness of the gases entering V_2 and leaving the system); and let β_0 represent the burnedness of the gases fed to V_1, obtained by mixing gas of composition β_2 with fresh feed. The contribution to burnedness of each reactor may be expressed quantitatively as the flow rate through the reactor times the increase in burnedness in that reactor:

$$G \cdot \beta_1 = G(1+R) \cdot (\beta_1 - \beta_0) + (G \cdot R) \cdot (\beta_2 - \beta_1)$$

$$\begin{bmatrix} \text{fresh} \\ \text{feed} \\ \text{rate to} \\ \text{model} \end{bmatrix} \cdot \begin{bmatrix} \text{total} \\ \text{change} \\ \text{in burn-} \\ \text{edness} \\ \text{in model} \end{bmatrix} = \begin{bmatrix} \text{feed} \\ \text{rate} \\ \text{to } V_1 \end{bmatrix} \cdot \begin{bmatrix} \text{increase} \\ \text{in burn-} \\ \text{edness} \\ \text{in } V_1 \end{bmatrix} + \begin{bmatrix} \text{feed} \\ \text{rate} \\ \text{to } V_2 \end{bmatrix} \cdot \begin{bmatrix} \text{increase} \\ \text{in burn-} \\ \text{edness} \\ \text{in } V_2 \end{bmatrix}$$

By dividing through by the total burning rate of the system, $G \cdot \beta_1$, two terms are obtained representing the fractional contributions, J, of each reactor:

$$J_1 = \frac{\beta_1 - \beta_0}{\beta_1} (1 + R)$$

$$J_2 = \frac{\beta_2 - \beta_1}{\beta_1} (R)$$

Choose an operating point corresponding to a moderately low feed rate, and consider the response of a fixed-volume reactor pair to an increase in feed rate. Figure III-9 shows the behavior of various points in the model for a recirculation ratio of 1/2 and a V_2/V_1 of 2. Curve β_1 is the burnedness in the reactor V_1 and also the burnedness leaving the system (this curve is also $R = 1/2$ of Figure III-8). Curve β_2 is the burnedness in the recirculation zone; and curve β_0 is the burnedness of the feed to V_1 obtained by mixing fresh, unburned feed with recirculated products. At a low feed rate (represented by dotted line "A") the feed material to V_2, of composition β_1, has a high burnedness and there is very little burning remaining to be accomplished in reactor V_2. Under these conditions, the fractional utilization, J_2, of the recirculation zone is low, i.e. most of the burning occurs in V_1. At a higher feed rate, represented by line "C", the composition, when approached from low flow rates, corresponds to points 1, 3, and 5; and most of the burning still occurs in V_1. However, since the burnedness in V_1 has decreased slightly, J_2 increases correspondingly. As the feed rate increases further past line "D", the central core becomes chilled, and blowout occurs, after which only the recycle volume is active (i.e. a residual flame). At feed rates beyond line "D" combustion occurs only along
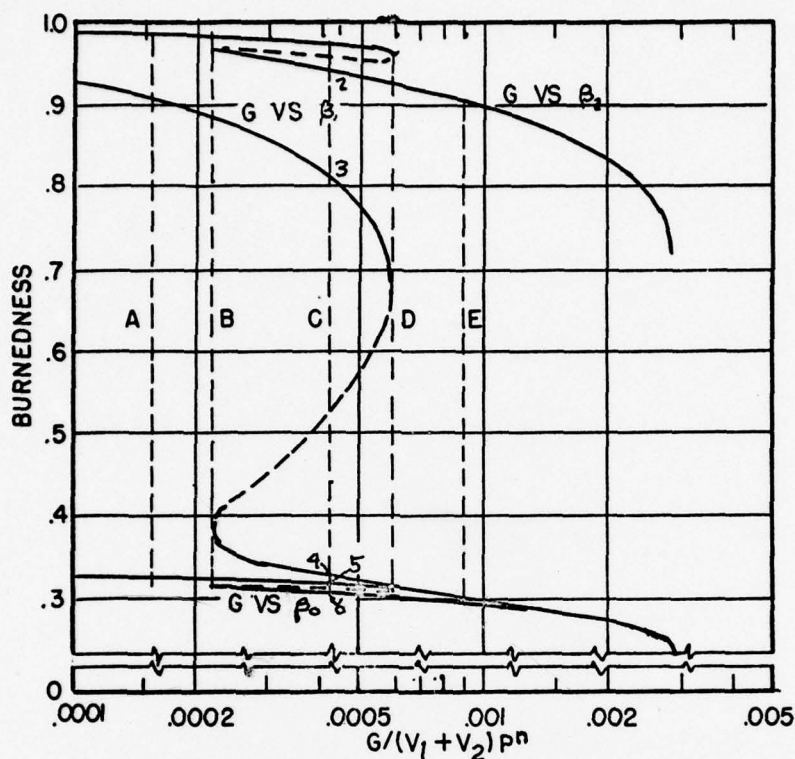
FIGURE III-9: β_0, β_1, & β_2 FOR RECIRCULATION MODEL
$R = \frac{1}{2}$, $V_1/V_2 = 2$, $\phi = 1.0$
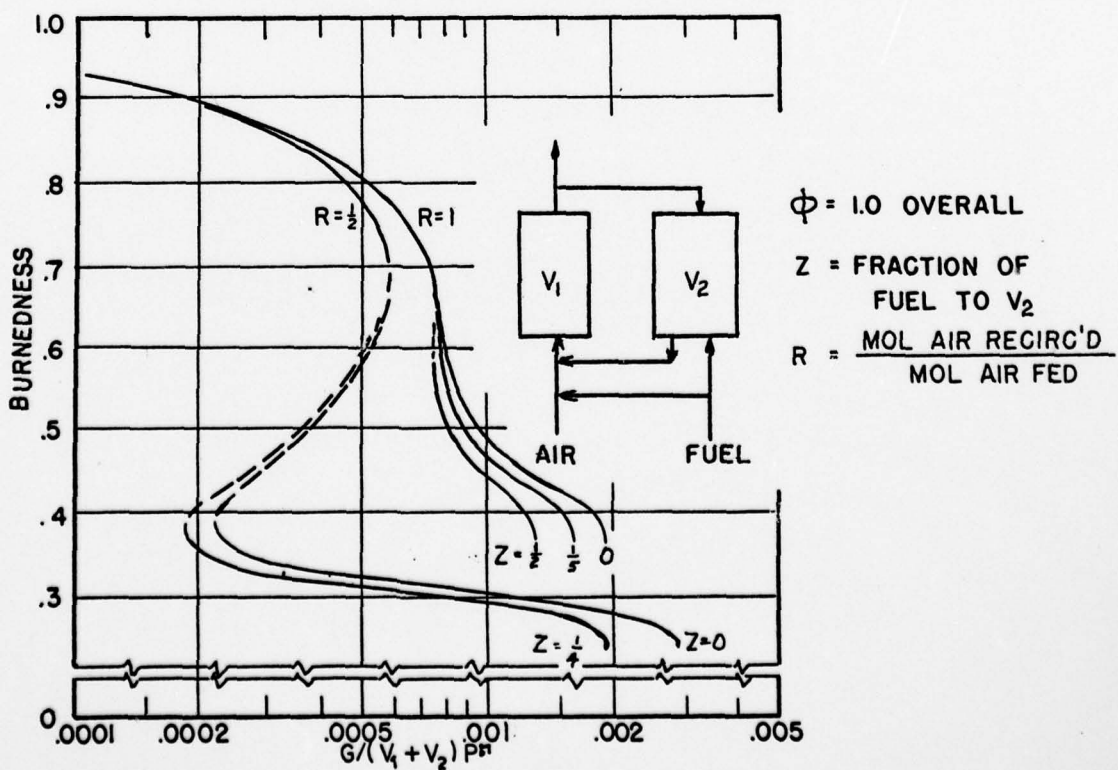
FIGURE III-10: EFFECT OF SPLIT FUEL FEED ON
RECIRCULATION MODEL

the lowest branch of the curve (corresponding to dotted line "C"). At these feed conditions practically no combustion occurs in the central core, and J_2 is nearly unity.

If the flow rate is now decreased from this high level, the central core stays cold past line "D" and at line "C" the compositions 2, 4, and 6 are reached. When line "B" is reached there is a sudden relighting of the central core. This hysteresis loop is the most interesting part of these models, since it is a potential source of a flickering flame. In this region the central core may light or blowout in response to small disturbances in operating conditions with very little change in the burnedness of V_2.

At higher recirculation ratios the behavior is similar but because of the "stirring" effect of higher recycle rates, the ratio of the fractional contributions of the two volumes, J_1/J_2, approaches unity for a wider range of feed rates. As Figure III-8 shows, the undercut of the curve β_1 disappears at higher recirculation ratios, and as the recycle is continually increased, the inflection in the curves becomes less pronounced until it also disappears.

Model Showing Effect of Non-Uniform Fuel/Air Ratio

Another problem of interest is that of allowing for
the effect of unequal fuel/air ratios in the various
chamber zones. Such a condition would arise in a combustor
where the fuel and air were injected separately into a
moderately well-mixed system. A possible model of such a
combustor is a variation of the above recirculation model,
in which only a portion of the fuel, but all of the air,
is fed into the central core and the remainder of the
fuel is fed into the recirculation zone. This produces
a richer mixture in the recycle volume than in the central
core. The one additional variable required may be thought
of as either the fraction of the original fuel introduced
into the central core or the fuel/air ratio of the
recirculation zone. The former has the advantage of
showing the limitations on the variation of the fuel/air
ratio of the recycle volume. The latter shows more
directly the effect of the split fuel feed. Since the
fuel/air ratio in the central volume is the same as
the overall fuel/air ratio, it will not be affected by
this split.

The results of calculations made on this recircula-
tion model are shown in Figure III-10 for an overall
fuel/air ratio which is stoichiometric for consistency
with the previous models. Because of this condition,

other fuel/air ratios in the recirculation zone can only
be a detriment to the overall heat release rate since the
recycle zone must operate on less than the optimum effi-
ciency curve. At low feed rates this effect is of little
consequence since the gases in the recirculation zone are
essentially completely burned in either case. However,
if the feed rate is increased sufficiently the burning
rate in the recirculation zone becomes significant, and
the consequence of operating this volume at other than
stoichiometric fuel/air ratio is apparent.

If the chamber were operating with a lean overall
fuel/air ratio and the fuel/air ratio in the recirculation
zone were stoichiometric the reverse situation would be
expected. In this case the recirculation zone would be
operating on a more favorable efficiency curve than the
central core. In those feed rate ranges where the per-
formance of the model for an overall lean fuel/air ratio
would be higher than for the case of feeding all the
fuel into the central core.

Models of More Complex Situations

Thus far, the models discussed have been restricted
to specific phenomena. In modeling practical situations,
however, one may wish to consider situations where two or
more phenomena are simultaneously significant. If models
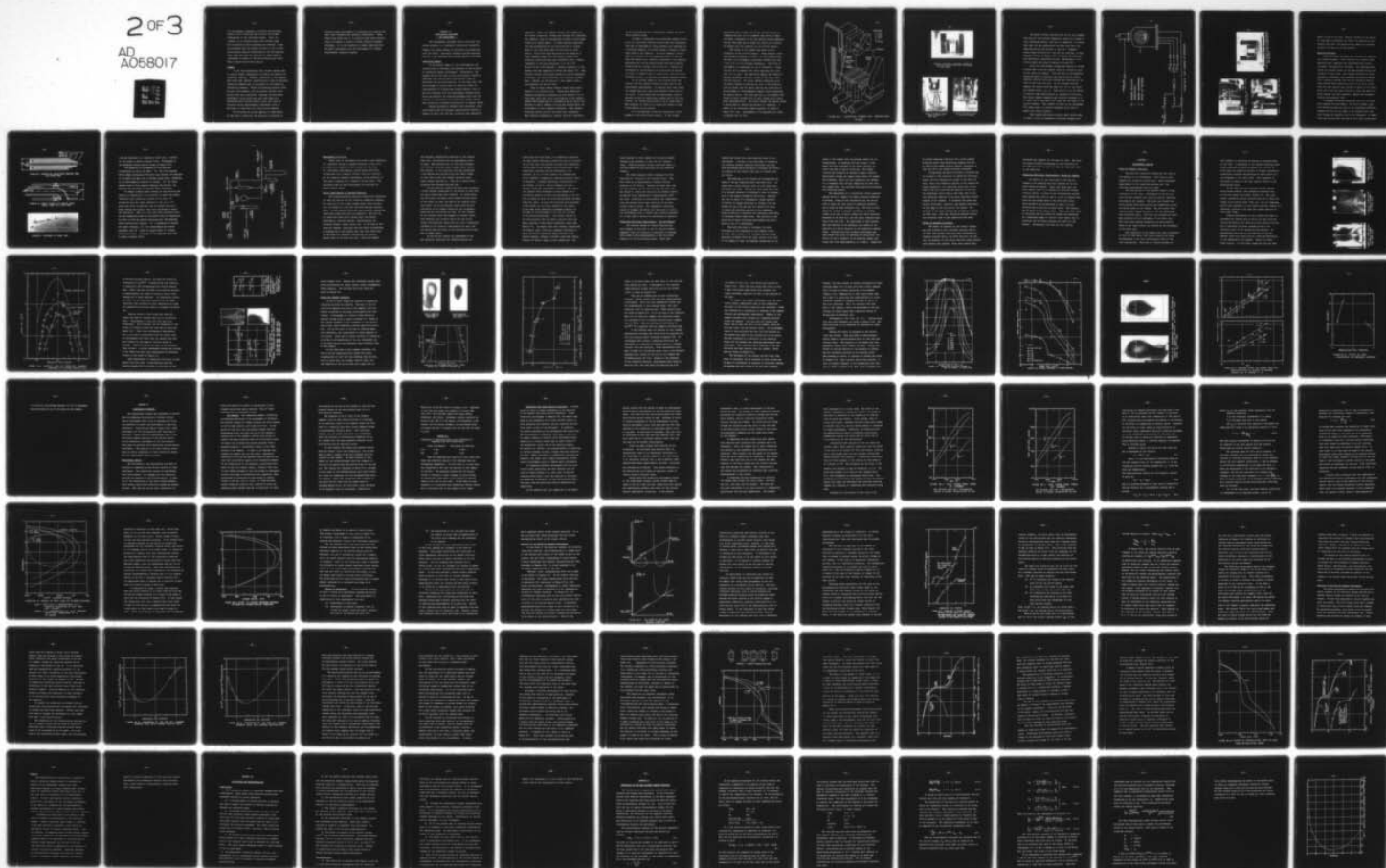
for the separate phenomena of interest are available,
models of such situations may be built from simple
combinations of the individual models. Thus, for
instance, in a situation where both residual flame
and two-stability-limit phenomena are observed, it may
be postulated that the chamber consists of two or more
recirculation zones as represented by the two-stability
limit model and that the structure of these zones is
represented by models of the recirculation type rather
than a simple well-stirred reactor.

Summary

It has been hypothesized that stirred reactors may
be used in simple combinations to predict the behavior of
combustion chambers. Examples considered in this chapter
have shown that behavior characteristics found in practical
combustion chambers may be duplicated by such models of
interacting elements. Models illustrating pressure inter-
actions, recirculation, and non-uniform fuel/air ratio
effects have been considered. Although the calculated
performance curves given here have been based on a
theoretical well-stirred reactor curve, one could in
principle use an experimentally determined curve of
efficiency vs feed rate for a well-stirred reactor.

The criterion of success applied to these models
is that only a relatively few variables be required to

specify a model performance in conformity with reality and that these variables have physical significance. These models have shown that it is possible under these restrictions to simulate a variety of known combustion chamber phenomena. It is now proposed to compare quantitatively the model performance with the performance of a simple experimental combustion chamber.

CHAPTER IV
EXPERIMENTAL EQUIPMENT
AND PROCEDURES

The experimental equipment used in this work con-
sisted primarily of a specially constructed combustion

chamber of a simple design to facilitate the comparison
with the theory. Ancillary equipment included metering
devices, a gas sampling train and gas analysis equipment.

Combustion Chamber

In the initial stages of this investigation the
objective was to determine the influence of recirculation
on combustion chamber performance. Consequently, the
chamber desired was one in which recirculation played an
important role, and in which some control could be
exercised over the recirculation. At the same time, care
was necessary to insure that the combustor chosen be
representative of conventional chamber design, since it
was felt desirable that the experimental program should
avoid the necessity of studying phenomena which were the
results of a peculiarity of a particular chamber rather
than principles of general applicability to chamber design.

Several alternative chambers were considered. Since
recirculation was the dominant characteristic desired, a
chamber in which the flow was circulatory was immediately

suggested. Three such chamber designs have appeared in
the recent literature. Schmidt and Schoppe (19) presented
two chambers, both for non-premixed systems in which gases
flowed in a spiral manner. In these chambers stabiliza-
tion was accomplished by the recirculation of burning
gases to the cold zones near the fuel and air inlet
points. Very little data was given on the behavior of
these chambers except that the authors claimed wide
stability limits and high heat liberation rates, roughly
comparable to can-type combustors (1 to 10 x 10^6
Btu/hr ft^3 at 1 atm pressure). Another combustor of this
general type was suggested by Hottel and Person (9). They
studied a vortex type system similar to the one suggested
by Schoppe, but with a different fuel injection arrange-
ment; however, as did Schoppe's, this chamber used a
non-premixed fuel and air feed.

None of these chamber designs seemed particularly
adapted to the present study. Person gave moderately
detailed information concerning the flow pattern, but he
found that there was little recirculation in his chamber.
Schmidt and Schoppe gave no information at all about flow
patterns in their chambers nor were any details about the
performance of their chambers presented. Other designs
involving forced cyclonic flow were also considered.
These various alternatives, however, were all considered

to be so non-typical of a conventional chamber as not to merit detailed study.

A simple, rectangular two-dimensional chamber fed by a jet of a pre-mixed fuel/air mixture was then considered. This had the advantage of being somewhat more analogous to a practical chamber, yet simple enough in design to permit easy study of its behavior. In such a chamber, recirculation is achieved by the aspirating effect of the jet. Near the chamber exit, material equivalent to the material aspirated must reverse direction and form recirculation zones around the central core of the jet. Control over the amount of recirculation can be achieved by varying the ratio of chamber width to nozzle with, and with quite different results, by varying the chamber dimension ratios.

In the initial stages of this problem there was concern over the possible effects of heat loss on the experimental measurements. To minimize wall heat losses the chamber was built with three parallel feed slots in its floor. It was hoped that the experiments could be carried out with no significant interaction of the jets; however, jet interactions proved to be so large that it was necessary to return to a single-jet design to study recirculation in this system.

It is interesting to note the similarity of this chamber to the well-stirred reactor. If the volume

associated with a single jet of the stirred reactor is
compared with the jet of a chamber into which a single
jet flows, similarity of the two systems becomes apparent.
One may then hope that a single-jet system will provide
an insight into the operation of the stirred reactor.

The design of the chamber was based on this
similarity to the stirred reactor. Three parallel slots,
each having an opening of 0.030" x 2" were placed along
the floor of a rectangular combustion chamber which was
3 1/2" x 3" x 2" in internal dimensions. (The floor of
the chamber is represented by the 3" dimension.) Along
the roof of the chamber were three opposing exit flues
1/2" x 2" in size. The combustion chamber was formed by
placing insulating firebrick inside of the frame which
held the nozzles. The inside chamber dimensions would
be readily altered by varying the size of the firebrick
used as lining, and the nozzle spacing was controlled by
an assortment of interchangeable spacer blocks separating
the nozzle bodies. The front and back of the chamber were
formed by Vycor windows held by steel frames and a sheet-
metal retaining piece. The entire chamber was placed inside
a vacuum tank to control the pressure of operation. A
sketch of the combustion chamber assembly is shown in
Figure IV-1, and   photographs of the apparatus are shown
in Figures IV-2 to IV-4.

DIMENSIONS:

3 " HIGH
3" WIDE
2" DEEP
D = 1"
d = 0.030"

FIREBRICK

WINDOW
FRAME

RETAINING
FRAME

NOZZLE
HEADS
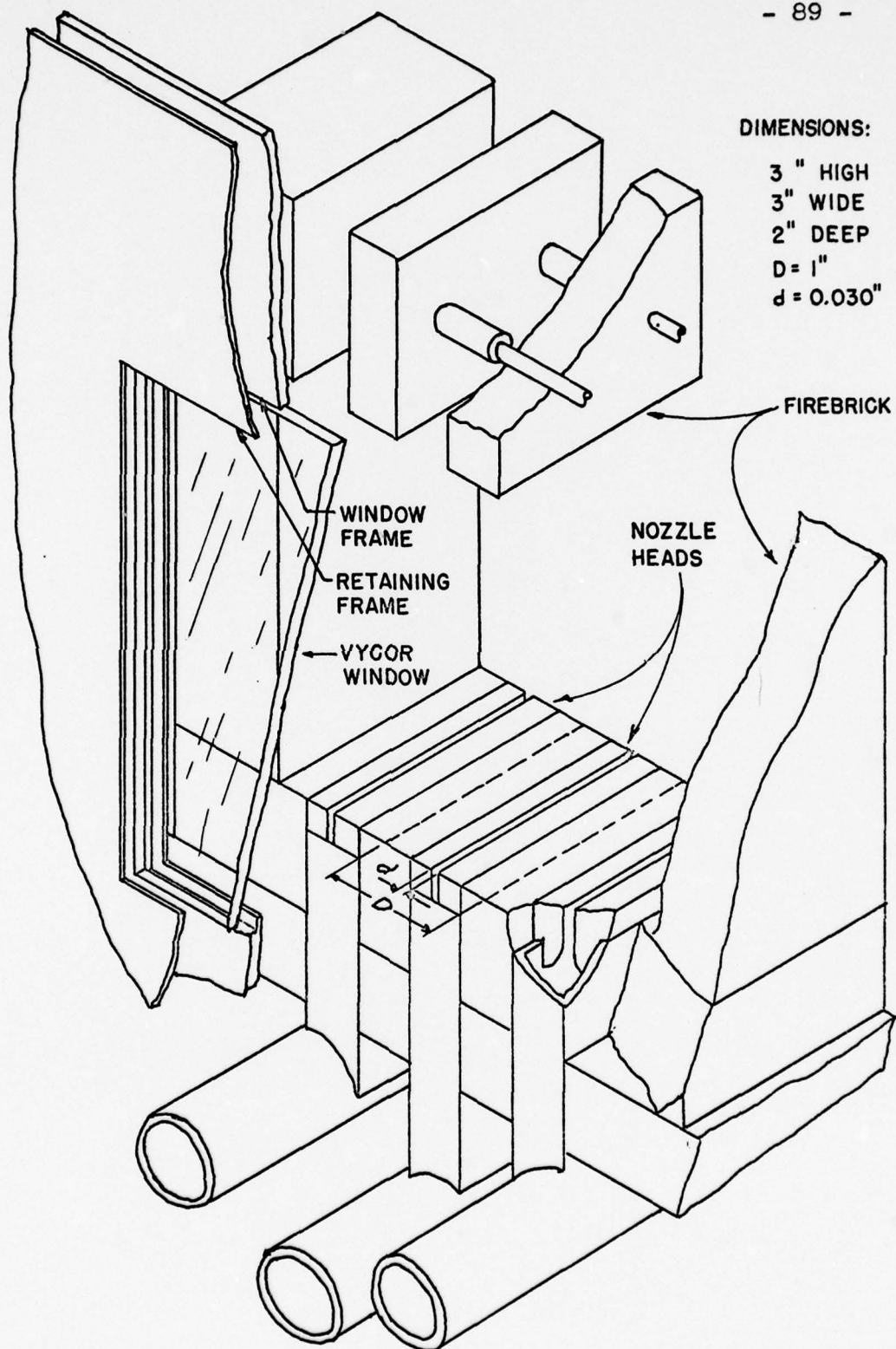
VYCOR
WINDOW

FIGURE IV-1:   COMBUSTION CHAMBER FOR   RECIRCULATION
STUDIES
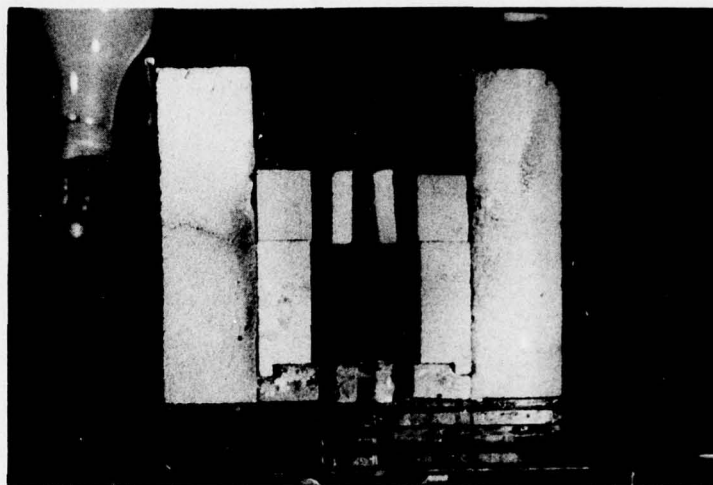
FIGURE IV-2: PHOTOGRAPH OF COMBUSTION CHAMBER WITH
THREE FEED JETS AND THREE FLUES. SIDE WINDOWS
OF VYCOR REMOVED.
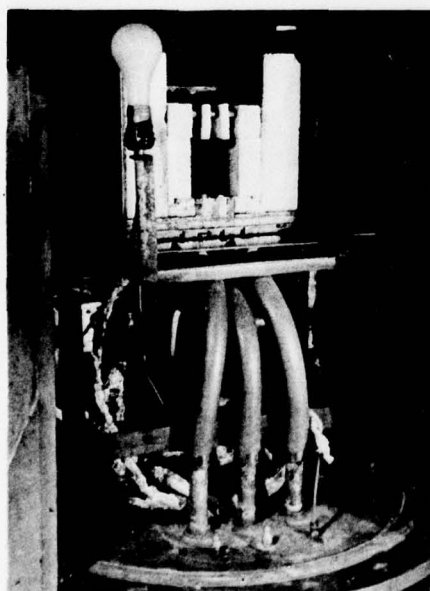
FIGURE IV - 3: PHOTOGRAPH OF ASSEMBLED
CHAMBER AND EQUIPMENT. SIDE
WINDOWS REMOVED
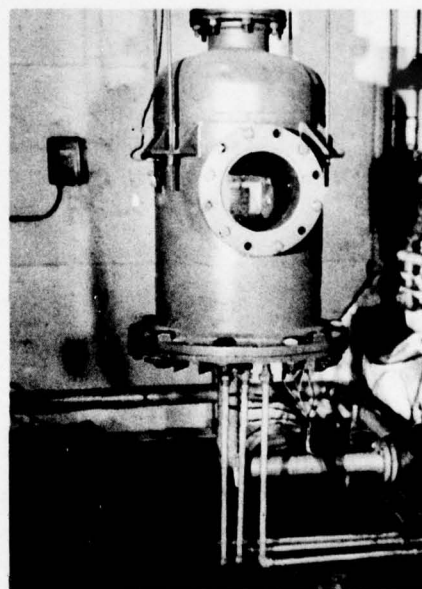
FIGURE IV-4: PHOTOGRAPH OF VACUUM
TANK READY FOR EXPERIMENT.

Pre-mixed fuel/air mixtures were fed to this chamber.
Fuel and air were metered separately, mixed in a length of
pipe containing baffles, and fed to a manifold. To insure
that each jet was operating at the same feed rate, the
manifold mixture was metered to each jet. Standard
square-edges orifices were used for all metering. A flow
diagram is shown in Figure IV-5, including the metering
and temperature measurement points. Photographs of the
control panel are shown in Figures IV-6 and IV-7.

After the experimental program was started it became
evident that a one-jet chamber should be studied as well
as the three-jet chamber. This was done in the apparatus
described above by replacing the side bricks so that a
narrower interior width was obtained and shutting off the
feed to the outer two jets. In the original one-jet
chamber the inside width was made just 1/3 of the three-
jet chamber width, i.e. 1". This proved to be too narrow
to achieve flame stabilization at reasonable feed rates.
The inside chamber dimension was therefore enlarged to a
2" width (by 2" deep and 3 1/2" high) for the study of the
one-jet chamber. This chamber is shown in the photograph
IV-8 (also shown is a mounted sampling probe used to
sample the interior gases).

This chamber was placed inside a small vacuum tank
so that it could be operated at pressures ranging from

QUENCH AIR

PR   PRESSURE REGULATOR

T   THERMOCOUPLE

P   PRESURE MEASUREMENT

┤├   ORIFICE, ΔP MEASURED
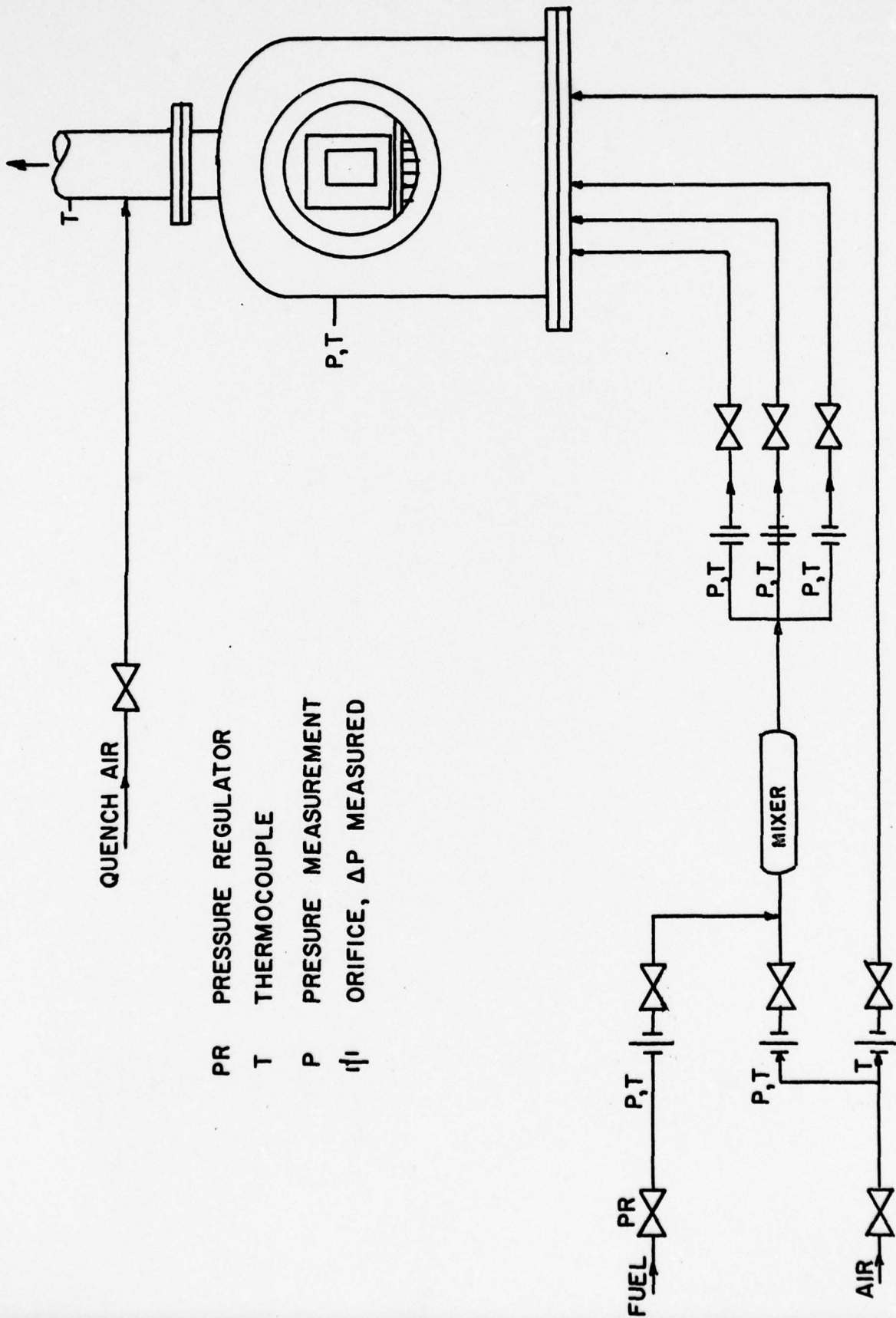
FIGURE IV-5: FLOW DIAGRAM OF APPARATUS

- 93 -

FIGURE IV-8: PHOTOGRAPH OF ONE-JET CHAMBER BRICKWORK. NOTE THE SAMPLING PROBE ENTERING FROM THE LEFT-HAND-SIDE.
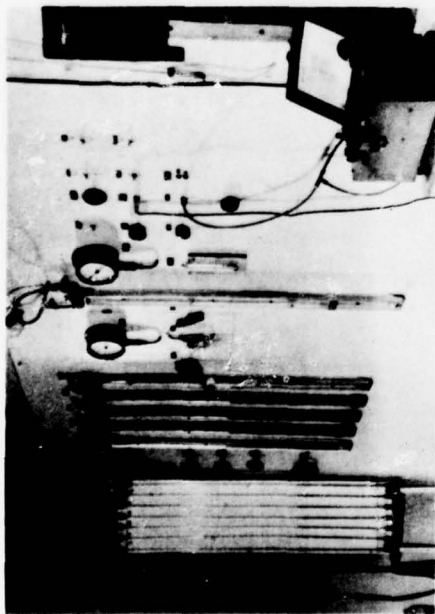
FIGURE IV-6: PHOTOGRAPH OF CONTROL PANEL SHOWING MANOMETERS AND MANOMETER BOARD.
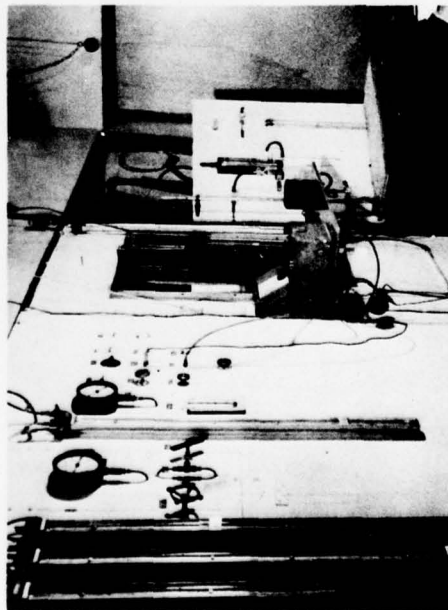
FIGURE IV-7: PHOTOGRAPH OF CONTROL PANEL SHOWING SAMPLING BOARD ASSEMBLY.

about 0.1 atm to 0.5 atm. However, except for one series
of runs made to determine the effect of pressure on the
blowout feed rate, the data were all taken at a pressure
of about 0.34 atm, or 10" Hg absolute.

Sampling Equipment

Some additional equipment was required for sampling
the combustion gases. This consisted of a water-cooled
sampling probe, sampling rate measurement and control
equipment, and analytical equipment. For sampling gases
inside the chamber probes of the same general design used
by Baker (3) were used. This design consisted of three
concentric hypodermic tubes assembled as shown in Figure
IV-9, forming a central tube and two concentric annuli.
High pressure water passed at a rate of 10 to 50 cc/min
down the inner annulus and returned to drain in the outer.
About 200 to 400 psi were required to send this amount of
water through the probe assembly. Sample was withdrawn
through the innermost tube.

A somewhat different design was used for the probe
which sampled the exit gases. For this a single, long
tube entered through one side of the supporting framework,
crossed the flue in the plane of the chamber roof, and
left through the opposite side of the framework. A sample
inlet was drilled into the side of this long cooling water
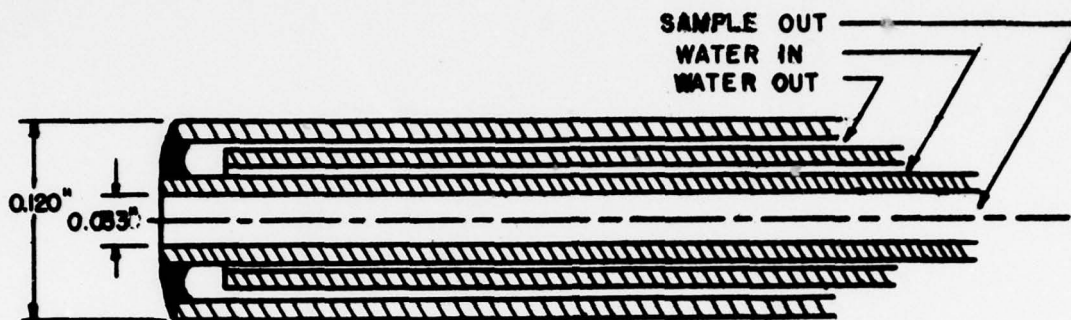
FIGURE IV-9: REVERSE-FLOW COOLING WATER SAMPLING PROBE
(10 x ACTUAL SIZE)
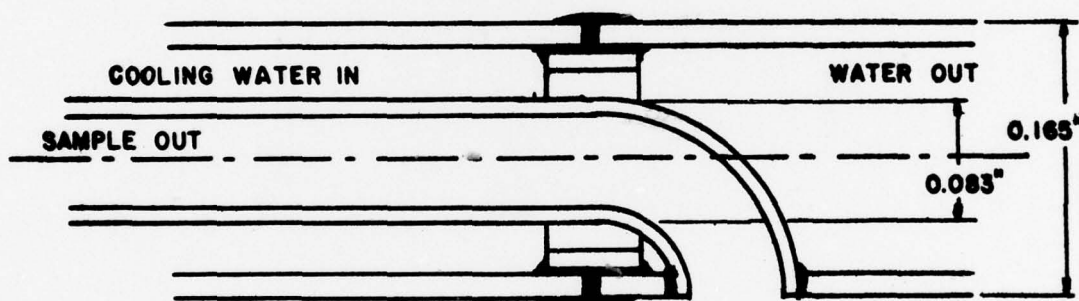
FIGURE IV-10: STRAIGHT-THROUGH FLOW COOLING WATER
SAMPLE PROBE (10 x ACTUAL SIZE)
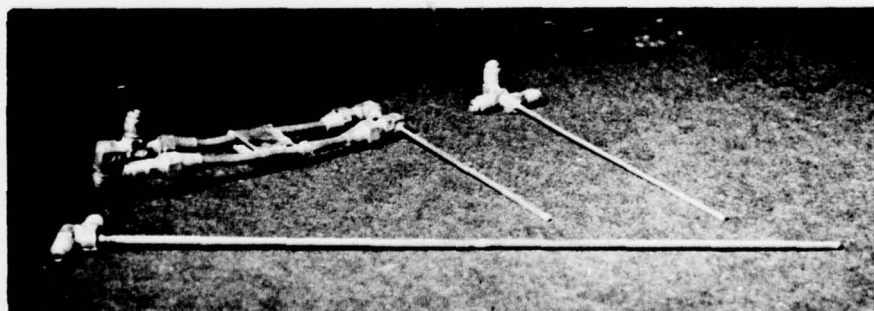
FIGURE IV-11: PHOTOGRAPH OF PROBES USED

tube and connected to a concentric inner tube. A sketch
of this probe is shown in Figure IV-10. Photographs of
the assembled probes used are shown in Figure IV-11.

The analysis of the samples in this work was
accomplished in one of two ways: (1) For those samples
where oxygen consumption efficiency was desired, the analysis
of the gases was made with a Beckman Oxygen Meter, operating
on the para-magnetic property of oxygen. (2) For those
samples where a more complete analysis was desired, the
analysis was performed by standard Orsat techniques.

To sample properly gases flowing at high velocity and
varying in composition it is desirable to match the stream
velocities just inside and outside of the tube. To
accomplish this the impact pressure at the tip of the
probe must first be measured, and the sample then with-
drawn through the probe at that rate calculated to match
the velocities. This is a trial and error procedure since
the gas temperature must be calculated from the composition
in order to find the desired sampling rate. The sampling
train required must include: (1) a manometer to measure
the impact pressure, (2) flow measurement and control
equipment, and (3) either an oxygen meter or a sample
collection bottle. A diagram of the sampling train used
is shown in Figure IV-12.
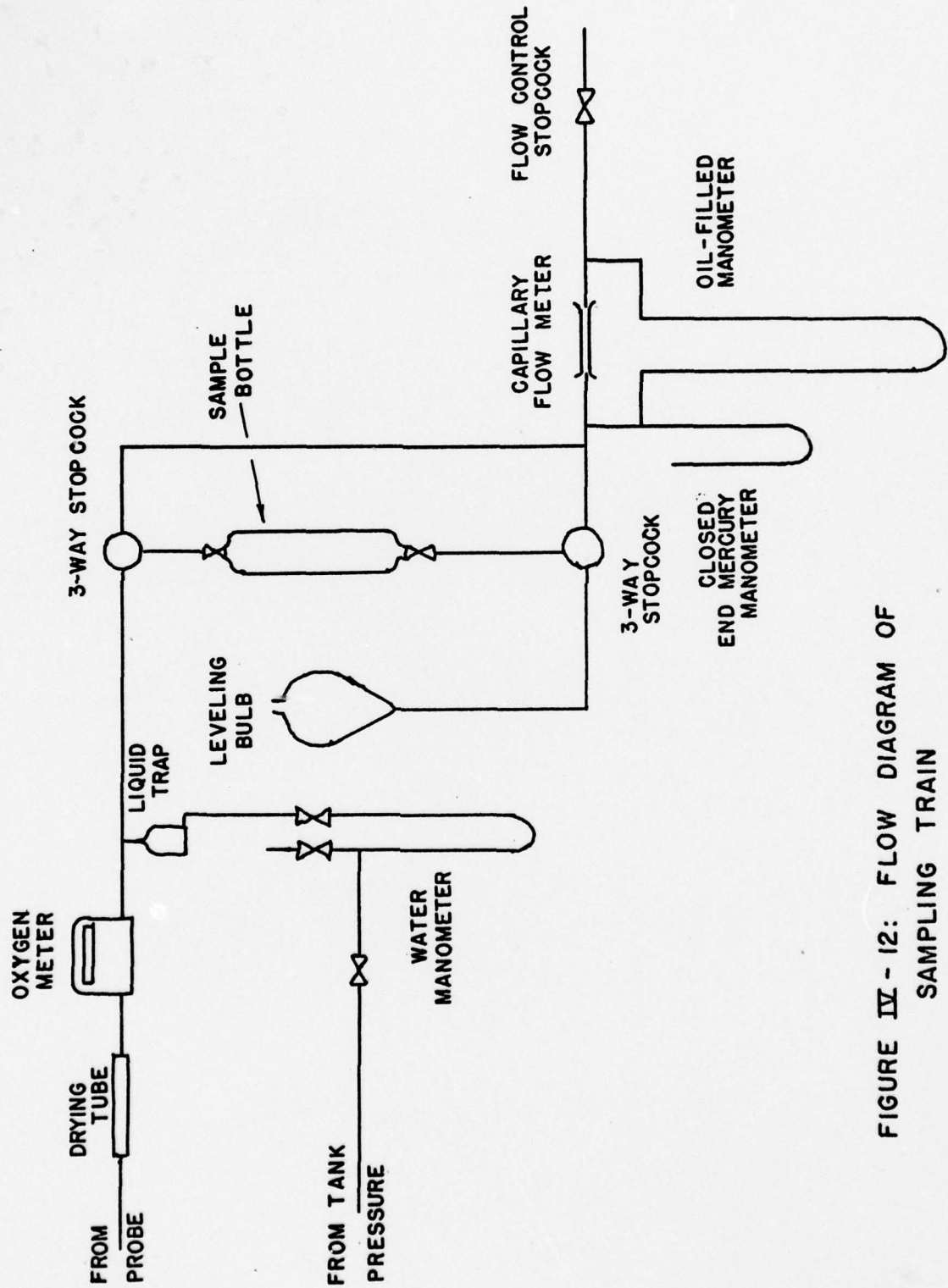
FIGURE IV - 12: FLOW DIAGRAM OF SAMPLING TRAIN

Experimental Procedures

Three types of experiments were made on this apparatus:
(1) stability limits at constant pressure, giving fuel/
air ratio as a function of the blowout air feed rate;
(2) efficiency measurements, giving oxygen efficiency
vs feed rate for a constant fuel/air ratio and pressure;
and (3) pressure exponent measurement, giving pressure vs
feed rate at blowout for a constant fuel/air ratio. The
procedures used in these experiments are described in
greater detail below.

Blowout Measurements at Constant Pressure

The constant-pressure stability limits were determined
for both the one-jet and the three-jet combustion chambers.
The flame was lit by a high-voltage spark above the exit
flue (or flues) at a very low feed rate and high fuel/air
ratio. If the fuel/air ratio was then carefully reduced the
flame would flash back into the combustor. The fuel and
air rates were then slowly raised until the desired
operating air rate was reached. Simultaneously the
brickwork became a bright cherry red. In the case of the
three-jet chamber, flash-back was more easily accomplished
by feeding one of the outside jets, and then, after that
jet had been lit, gradually introducing the fuel/air
mixture feed to the other two jets. After the chamber

had reached a steady-state operation at the desired
feed rate, the desired blow-out measurements could
be made. With pressure and air feed rate constant,
the fuel-air ratio was slowly changed until blowout
was reached. As the stability limit was approached,
a few minutes were allowed after each small change
in fuel rate so that the chamber operation could
reach thermal equilibrium. (The use of kaolin brick
minimized the necessary waiting time.)

In the three-jet chamber the three jets coalesced
a short distance downstream of the nozzles so that only
two major flame areas were observed. At sufficiently
low flow rates, two small zones trapped between pairs
of the three jets near the base of the chamber would
also light, but in the regions studied they did not
contribute to the chamber stability, and in general,
gases did not burn stably in them. In this chamber,
as the fuel/air ratio was changed two blowout limits
were observed, one in which one of the two active
(large recirculation) zones blew out, with a consequent
increase in the volume of remaining active zone, and
the second when the flame in the remaining active zone
was no longer stable.

In the one-jet chamber the phenomenon of the
two stability limits was not observed because the

flame would not burn stably in a symmetrical position. The only stable combustion pattern was the one in which the jet was bent over against one wall with combustion visible only in the enlarged recirculation zone. This undoubtedly resulted from the narrowness of the chambers, as in a 3" wide chamber (as compared with the 2" chamber) a symmetrical combustion pattern could be obtained. A second interesting characteristic of the blowout in the 2", one-jet chamber was that a residual flame was consistently observed. The combustion pattern which developed in this chamber had a circulatory pattern in which the mainstream of the jet went up along one wall and recirculating gases returned along the other. A small recirculation zone developed in the center of the vortex created by this motion. At low feed rates combustion proceeded primarily at the edge of the mainstream of the jet and the edge of the recirculating gases. The central portion of the recirculation zone was nearly inactive since the gases reaching it were almost completely burned (see Figure V-7). As higher rates were reached, approaching the blowout limit, there was a gradual transition in which the active combustion region shifted to the central regions, forming a residual flame near blowout (Figure V-8 shows a stage in this transition). The

data reported for this chamber are the gross chamber
loading rates necessary to blow out this residual
flame. Constant-pressure blowout data were taken in
the same manner as that described for the three-jet
chamber.

For these chambers blowout loading rates were
measured as a function of the fuel-air ratio. Data
were taken at an approximately constant absolute
pressure of 10" mercury. Several air rates were used
for each chamber, and at each air rate the fuel rate
was varied to obtain both lean and rich blowout limits.
An ambient inlet temperature of approximately 540°R
was used. Deviations in both pressure and temperature
from the desired values were corrected for by well-
stirred reactor theory. The temperature correction
charts of Longwell and Weiss (14) were used to correct
the experimental data to 540°R, and a pressure exponent
of 1.8 was used to correct for deviations in pressure.

Combustion Efficiency Measurements - One-Jet-Chamber

The observed change in visible flame pattern
with changes in feed rate to the 2", one-jet chamber
suggested that its variation of efficiency vs loading
rates might conform approximately to the calculated
behavior of the recirculation model. Hence this

chamber was chosen for a more detailed study of its
performance. A series of runs were made to determine
the relation between combustion efficiency and feed
rate and another group was made to determine the effect
of pressure on the blowout feed rate at several fuel-
air ratios.

The sampling of this chamber was accomplished by
means of the gas sampling probes described above. In
these runs a fixed fuel-air ratio of 1.35 times stoi-
chiometric was used. Various air feed rates were used
at a constant pressure to determine a curve of loading
rate vs the oxygen consumption efficiency. Analysis
was done by means of a paramagnetic oxygen analyzer.
A traverse of oxygen efficiency vs distance into the
chamber at one level was made for various air rates
to locate the position and size of the combustion
zones as well as to determine the combustion efficiency
of the gases within these zones. The position of the
probe tip in these traversing measurements was deter-
mined by use of a cathetometer.

Runs were also made to determine the gross
efficiency of the combustion at the chamber outlet.
In these runs a probe of the straight-through design
described in Figure IV-10 was used, buried in the roof
of the chamber so that the sampling opening was in the

plane of the chamber roof and pointed toward the on-
coming gases. In sampling this gas stream, a case
where the gases impinged on the sample opening, an
effort was made to match velocities. The stream
velocity was estimated by making an impact pressure
measurement through the sample probe before the sample
was withdrawn. Since the gas temperature was assumed
to be dependent only the gas composition as read from
the oxygen meter, the required trial-and-error procedure
was relatively simple.

The measurement of a satisfactory static pressure
against which to compare the impact pressure presented
a problem. Purge air was introduced into the vacuum
tank to sweep the tank clean of combustion products,
and to keep the tank internals cool. The flow of this
purge air created a pressure difference of several
tenths of an inch of water between the static pressure
measured at the tank wall and the impact pressure open-
ing at the exit flue. An improvement in this measure-
ment was achieved by an extension tube inside of the
tank wall to a point adjacent to the combustion chamber
frame. Although this poor pressure measurement may
have caused some error in matching the velocities, the
effect of such a mismatch on the measured oxygen effi-
ciency was found experimentally to be small. Comparison

of several sampling velocities for a given chamber
condition showed that mismatching ranging from 50%
to 120% of the stream velocity caused a variation of
less than 3% in the oxygen efficiency measured.

In measuring the gross efficiency, attention had
to be given to the variation of combustion efficiency
across the flue opening even though it was only 1/2"
wide. Since the combustion pattern in the chamber was
highly assymetric, the combustion efficiency on one
side of the flue reflected the behavior of the cold
jet mainstream, while that on the other side of the
flue reflected behavior in the more completely burned
regions of the chamber. To determine the gross com-
bustion efficiency, therefore, gas samples were taken
at each edge of the flue and at the center. The
position of the probe opening was determined visually
in these runs; this was considered adequate because
the variation found in gas composition was small.

Effect of Pressure on Blowout

The effect of pressure on the blowout loading
was also studied at four different fuel/air ratios.
In these runs several feed rates were established at
constant fuel/air ratio, and after each air rate was
set, the pressure in the vacuum tank was slowly reduced
until blowout was reached. After each blowout this

procedure was repeated for the next air rate. The fuel-air ratios studied corresponded to fuel fractions, F, of 0.600 and 0.575 on the rich side and 0.450 and 0.475 on the lean side.

Combustion Efficiency Measurements - Three-Jet Chamber

In addition to the above data on the one-jet chamber a few sampling data were obtained on the original three-jet chamber. These were taken near the rich blowout limit at a constant air rate and varying fuel-air ratios. A probe of the reversed-flow cooling water design was built so that it could be dropped down from the top through each of the three exit flues. Probe movement was accomplished by means of an air solenoid and an electric actuator motor. The analysis was by means of the oxygen meter. These data were taken to establish that the three-jet chamber was operating in a reasonable range of fuel/air ratio rather than to establish the efficiency-loading rate curve for the chamber. Consequently the data are very limited.

CHAPTER V

EXPERIMENTAL RESULTS

Three-Jet Chamber Operation

The three-jet combustion chamber was the first of
the chambers to be investigated. Data taken on this
chamber were primarily blowout data. Some photographic
measurements of the combustion pattern and a few
efficiency measurements were also made.

The flow pattern in this chamber showed a strong
interaction of the jets. Convergence of the two out-
side jets was observed both with and without combustion
occurring in the chamber. The three jets formed four
recirculation zones whose pattern was symmetrical around
the center plane of the chamber. The two inside recir-
culation zones trapped by pairs of the jet mainstreams
were relatively small. The outer two occupied the space
made available by the convergence of the three jets.
The outer zones behaved essentially as recirculation
zones to the large central jet created by the convergence
of the three jets.

When combustion in the chamber was first established
at very low flow rates, the flame occupied four zones,
corresponding to the four recirculation zones of the
cold flow pattern. There was no visible evidence in

this chamber of combustion occurring in the mainstreams
of the jets. A photograph of the chamber operating under
these conditions is shown in Figure V-1. It will be
noted that the combustion pattern is slightly assymetric,
indicating a possible mis-matching of nozzle sizes or a
mis-alignment of the nozzle axes. This assymetry is
discussed in detail in the next chapter (Errors in the
Experimental Work).

As the feed rate was increased the two smaller
zones became unstable, and combustion continued only
in the two larger outer zones, Figure V-2. The final
stable combustion pattern occurred when one of these two
larger recirculation zones "blew out", and the remaining
active zone expanded to a more stable position, Figure V-3.
Continued increase in the feed rate caused blow-out of
this final flame.

Blowout measurements on this chamber were made to
determine the loading rate at which the shift from the
two-active-zones to the one-active-zone pattern occurred,
and to determine the gross loading factor at the
stability limit of the one-active-zone pattern. No
measurements were made on the stability of the two
smaller zones since these did not contribute materially
to the operation of the chamber. Figure V-4 shows
these results. To facilitate comparison with the data
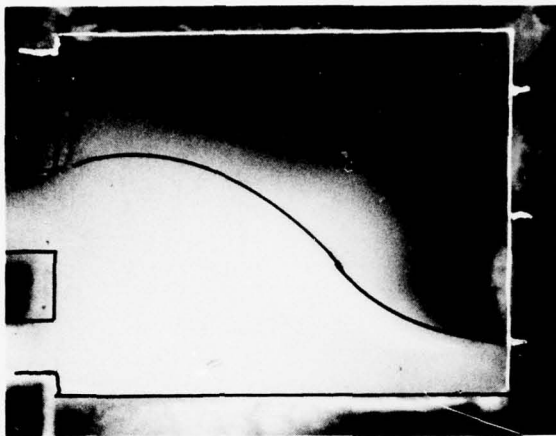
FIGURE X-3: FLAME PATTERN IN THREE-JET CHAMBER. ONE ZONE ACTIVE
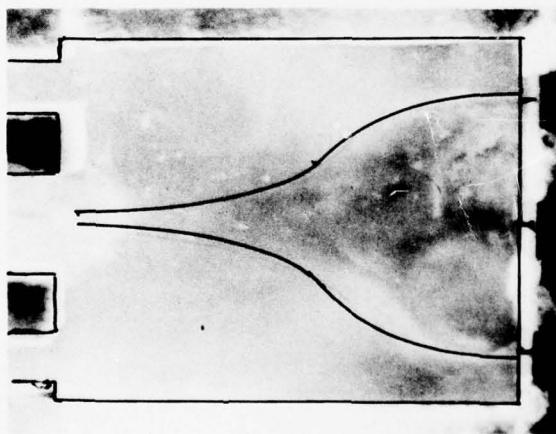
FIGURE X-2: FLAME PATTERN IN THREE-JET CHAMBER. TWO ZONES ACTIVE
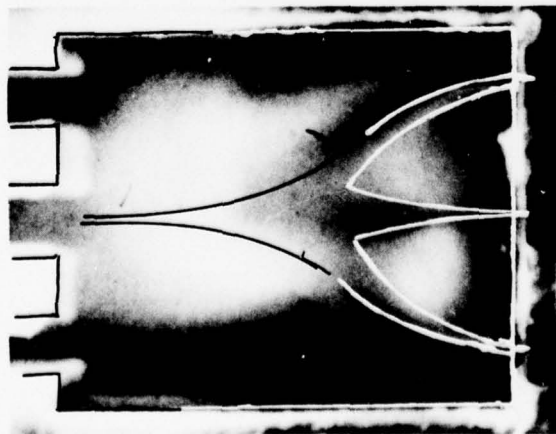
FIGURE X-1: FLAME PATTERN IN THREE-JET CHAMBER. FOUR ZONES ACTIVE.
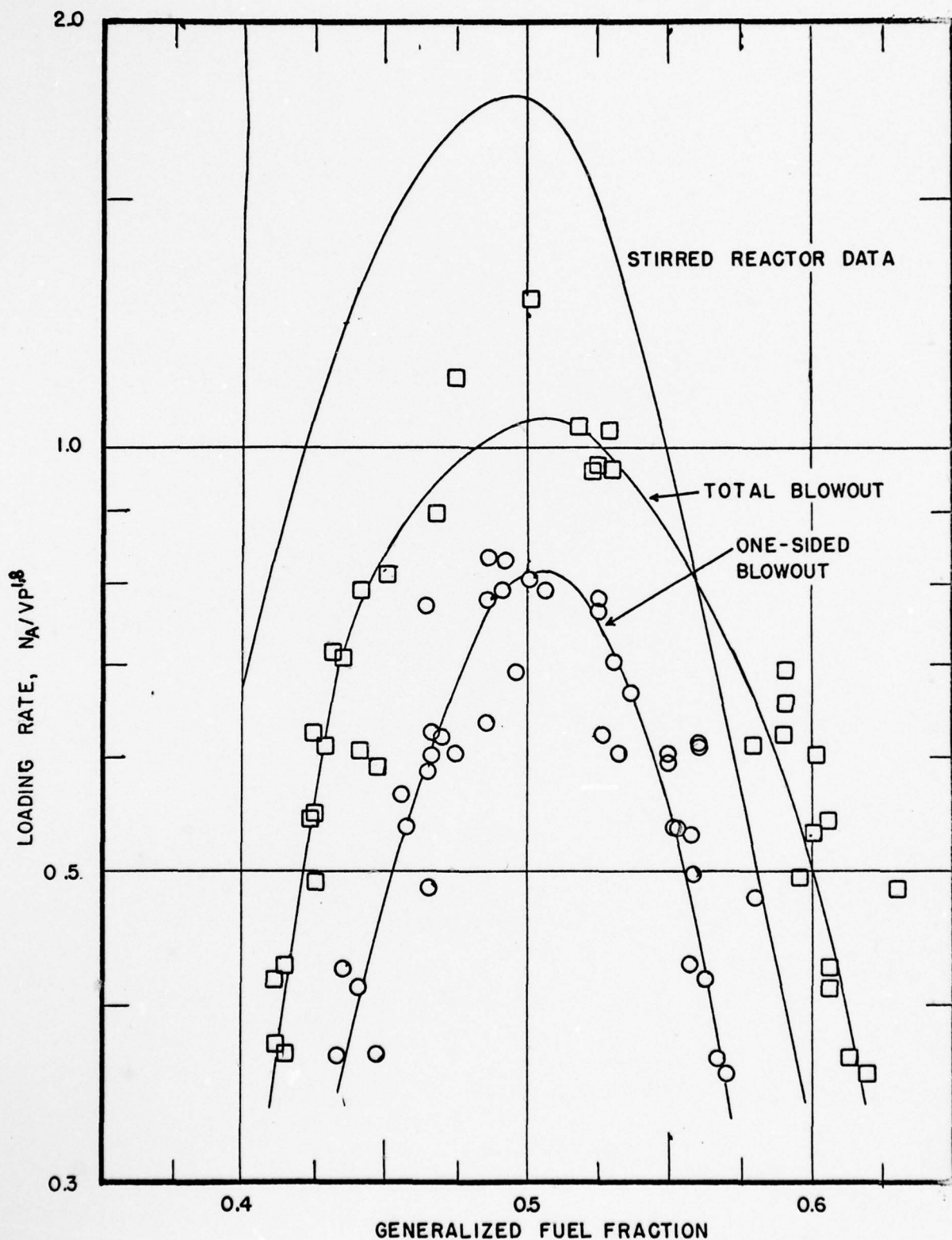
FIGURE V-4: BLOWOUT DATA OF THREE-JET CHAMBER COMPARED TO STIRRED REACTOR (14)

on the well-stirred reactor, the data are plotted on coordinates of $N_a/VP^{1.8}$ vs generalized fuel fraction, F, along with the corresponding well-stirred reactor data. These runs were all made at an absolute pressure of approximately ten inches of mercury, and an inlet temperature of 540°R (ambient). No temperature control was used, but the data were corrected for the small variations that occurred in inlet temperature by using the temperature-correction charts of Longwell and Weiss (14).

Another series of runs using this three-jet chamber was made to estimate the size of the various zones. Measurements of zone size were made from photographs. This technique for the estimation of the volume of combustion zones has been used by Simon and Wagner (22). Since these photographic measurements were to be used in conjunction with the blowout data, the photographs were taken with the chamber feed rate near blowout for the range of fuel/air ratios of interest. Figure V-5 gives the data on the estimated flame volumes. A typical photograph showing the outlines of the flame zone which were planimetered to determine volumes is also shown in Figure V-5.

Some measurements of combustion efficiency in this chamber were also made. A gas-sampling probe was inserted between the flue bricks to the level of the

FUEL FRACTION

FIGURE Ⅵ-6: THREE-JET CHAMBER EFFICIENCY. OXYGEN EFFICIENCY VS FUEL FRACTION AT $N_A/VP^b = 0239$

O LEFT-HAND FLUE
☐ CENTER FLUE
△ RIGHT-HAND FLUE
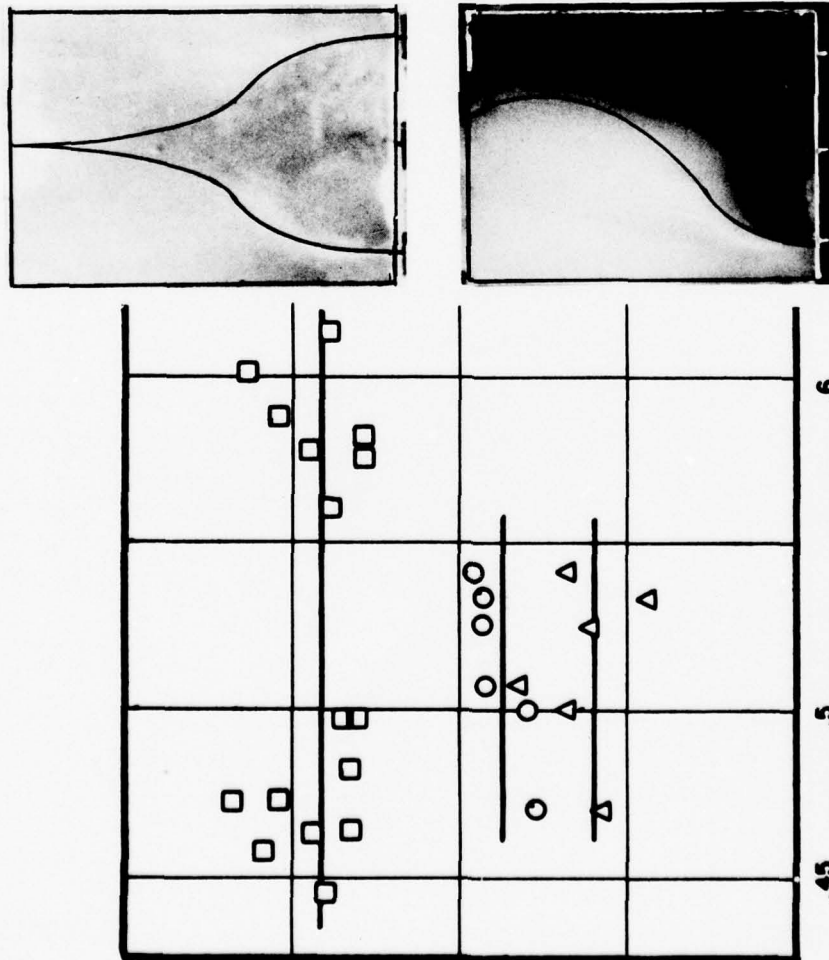
GENERALIZED FUEL FRACTION

FIGURE Ⅵ-5: COMBUSTION ZONE VOLUME DATA, THREE-JET CHAMBER. (PHOTOGRAPHS SHOW AREAS MEASURED)

O LEFT-HAND ZONE, TWO ZONES ACTIVE
△ RIGHT-HAND ZONE, TWO ZONES ACTIVE
☐ LEFT-HAND ZONE, ONE ZONE ACTIVE

inside chamber roof. Samples were withdrawn through this probe and analyzed for oxygen content using a paramagnetic oxygen analyzer. The few data which were taken are shown in Figure V-6.

Single-Jet Chamber Operation

In the 2" wide, single-jet chamber no symmetrical combustion pattern was observed. The axis of the jet curved over against one side of the chamber, with combustion occurring in the large recirculation zone thus created. A photograph of a typical flame pattern at moderate firing rates is shown in Figure V-7. Flame in this chamber appeared in the boundaries of the recirculation zone, where relatively unburned gases were available. But in the "eye" of the zone no unburned gases could penetrate, and consequently no flame appeared in this volume. There was no visible evidence of combustion occurring in the mainstream of the jet, presumably due to the high velocity and consequent short residence time of this region.

As the feed rate to this chamber increased, the zone of active combustion moved toward the center, occupying more of the "eye" and receding from the wall, until at rates near the ultimate blowout limit, all that remained of the active zone was a small ball of

FIGURE Ⅴ-7: FLAME PATTERN
ONE-JET CHAMBER. LOW
FLOW RATE, GASES IN EYE
NEARLY BURNED

FIGURE Ⅴ-8. FLAME PATTERN
ONE-JET CHAMBER. HIGH
FLOW RATE, RESIDUAL FLAME
PARTLY FORMED
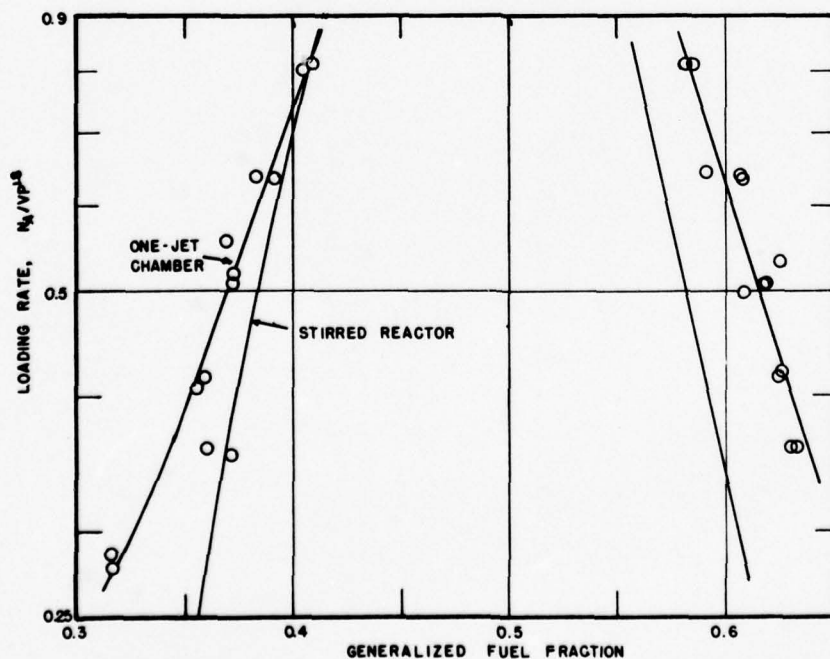
FIGURE Ⅴ-9: ONE-JET CHAMBER STABILITY DATA. STIRRED
REACTOR DATA INCLUDED FOR COMPARISON (14).
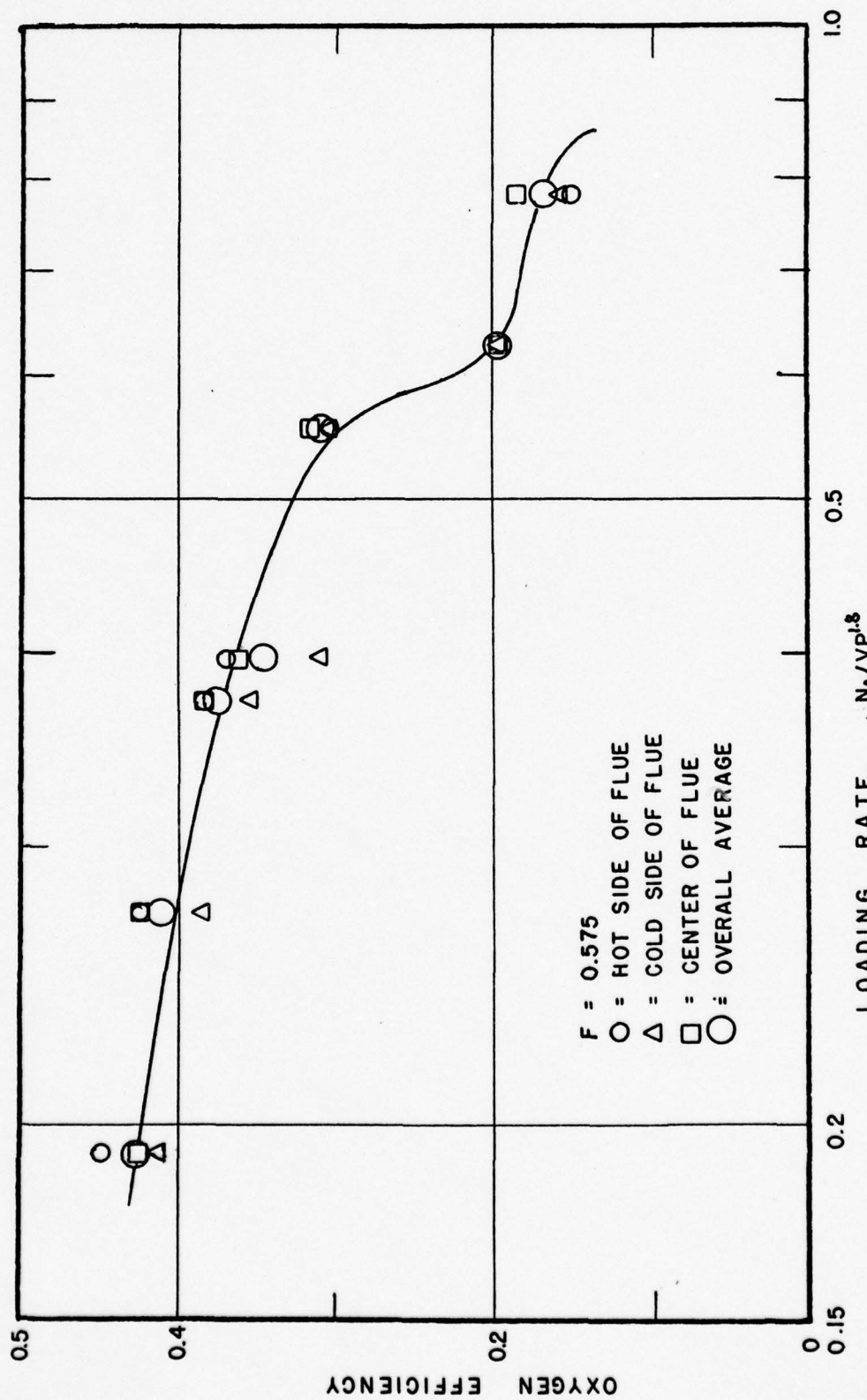
FIGURE VI-10: OVERALL COMBUSTION EFFICIENCY OF ONE-JET CHAMBER

flame in the place where the dark "eye" of the low-flow-rate pattern had been. A photograph of the residual flame partially formed (but still not at the blowout limit) is shown in Figure V-8.

This one-jet chamber was the most extensively studied. Blowout limits were the first characteristic investigated. Since the only unambiguous blowout was the disappearance of the residual flame, only this stability limit is reported here. These blowout data are shown in Figure V-9. As in the case of the stability data for the three-jet chamber these data were taken at a pressure of 10" of mercury absolute and a temperature of 540°R. They are plotted on coordinates of $N_a/VP^{1.8}$ vs F together with the Longwell and Weiss data.

It was observed that the behavior of this chamber qualitatively followed that which would be expected from the recirculation model discussed in Chapter III. To investigate this further, combustion efficiency was determined as a function of loading rate at a constant fuel-air ratio and pressure. These measurements were made by means of a horizontal probe, with a side-entrance sampling port, buried in the roof of the chamber and extending across the flue. Because of the assymetry of the combustion pattern, three samples were taken at each air rate, one from each flue edge and one from

the center of the flue. The results are plotted in
Figure V-10. Since this plot shows that there is only
a small difference among these three samples, the
simple arithmetic mean will be used in the analysis of
the data.

To compare the chamber performance with the theo-
retical model, quantitative data on the composition
and sizes of the various zones are also desirable. These
were obtained by a combination of sampling in the chamber
interior and photographic measurement. Samples of the
chamber contents were obtained by a sampling traverse
across the chamber. This was done for several feed
rates, but at only one level in the chamber, about 2"
from the floor, and one fuel/air ratio. One unfortunate
result of this procedure was that the flow pattern in
the chamber was upset by the introduction of the probe.
This was indicated by a reduction in the stability
limits for the chamber when sampling measurements were
being made. This reduction was a function of how far
the probe had been inserted into the chamber. These
data are shown in Figure V-11.

The existence of the central eye and outer ring
zones is indicated, and an estimate of zone volumes can
be made by considering the midpoint in efficiency between
the maximum and wall values to be the zone boundary.

However, the zone concept is better illustrated by cross-plotting Figure V-11 to give efficiency versus loading rate for each of several positions in the chamber (Figure V-12). Examination of that figure shows that the 2 and 3 cm. positions are characterized by a quite different response to loading from that of the 0, 1, and 4 cm. positions. The 5 cm. position (the cold wall of the chamber), where the mainstream of the non-burning jet passes shows some combustion because of mixing with the adjacent zone.

Photographs of the flame for t w o loading rates with the probe withdrawn are shown in Figure V-13. The probe positions in the sampling are indicated on these photographs.

Finally the effect of pressure on the blowout limit was studied. Runs were made by establishing a stable flame at a predetermined value of feed rate and fuel/air ratio. The pressure on the chamber was then gradually reduced until blowout occurred. During this series of runs the pattern of the approach to blowout was not noticeably affected by the pressure level. Data showing the effect of pressure on blowout are given in Figure V-14. Four fuel-air ratios were studied. A plot of pressure exponent vs the generalized fuel fraction is shown in Figure V-15. Also shown in Figure V-14
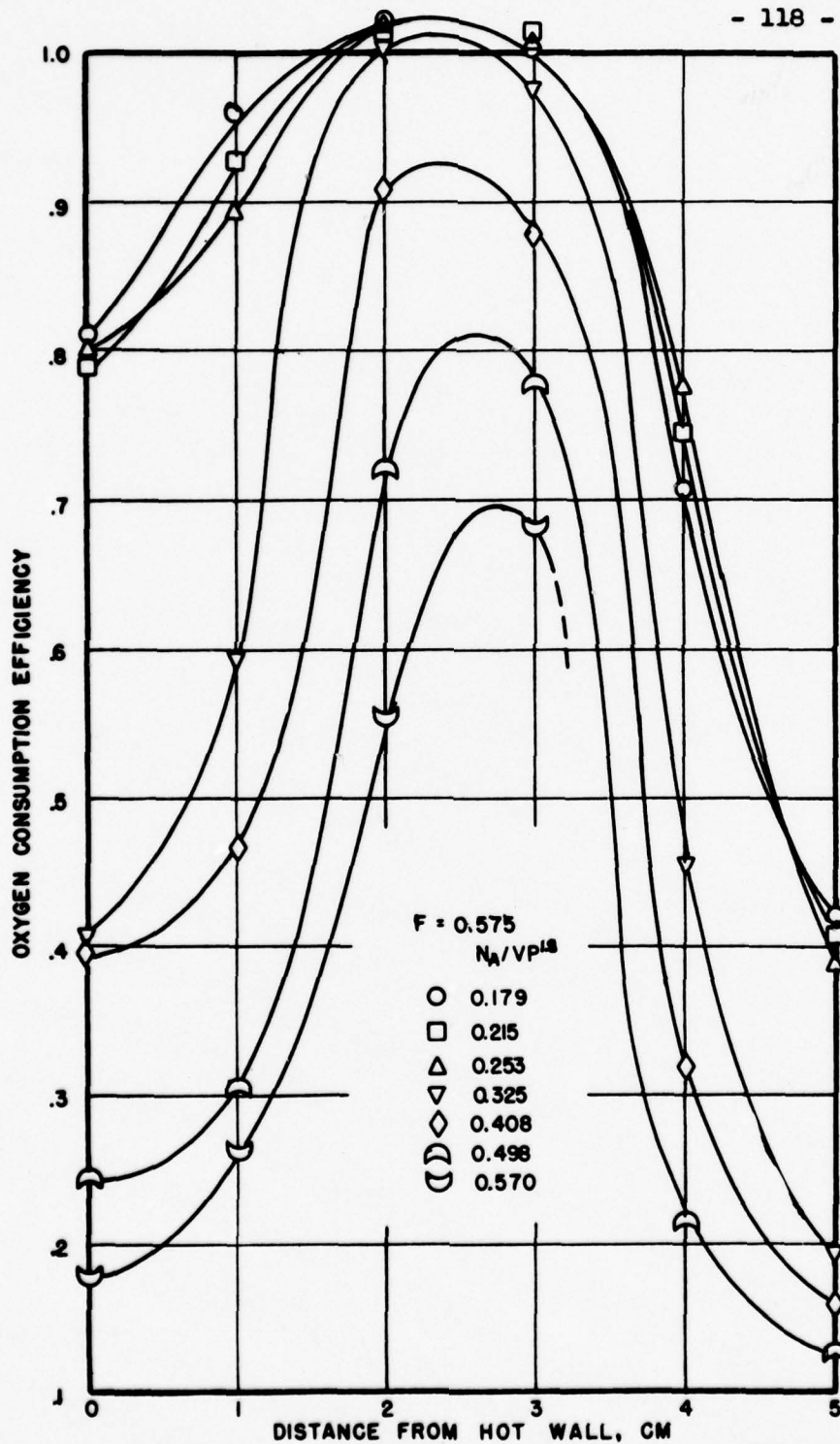
FIGURE V-11: COMBUSTION EFFICIENCY TRAVESES IN
ONE-JET CHAMBER (2" FROM FLOOR)
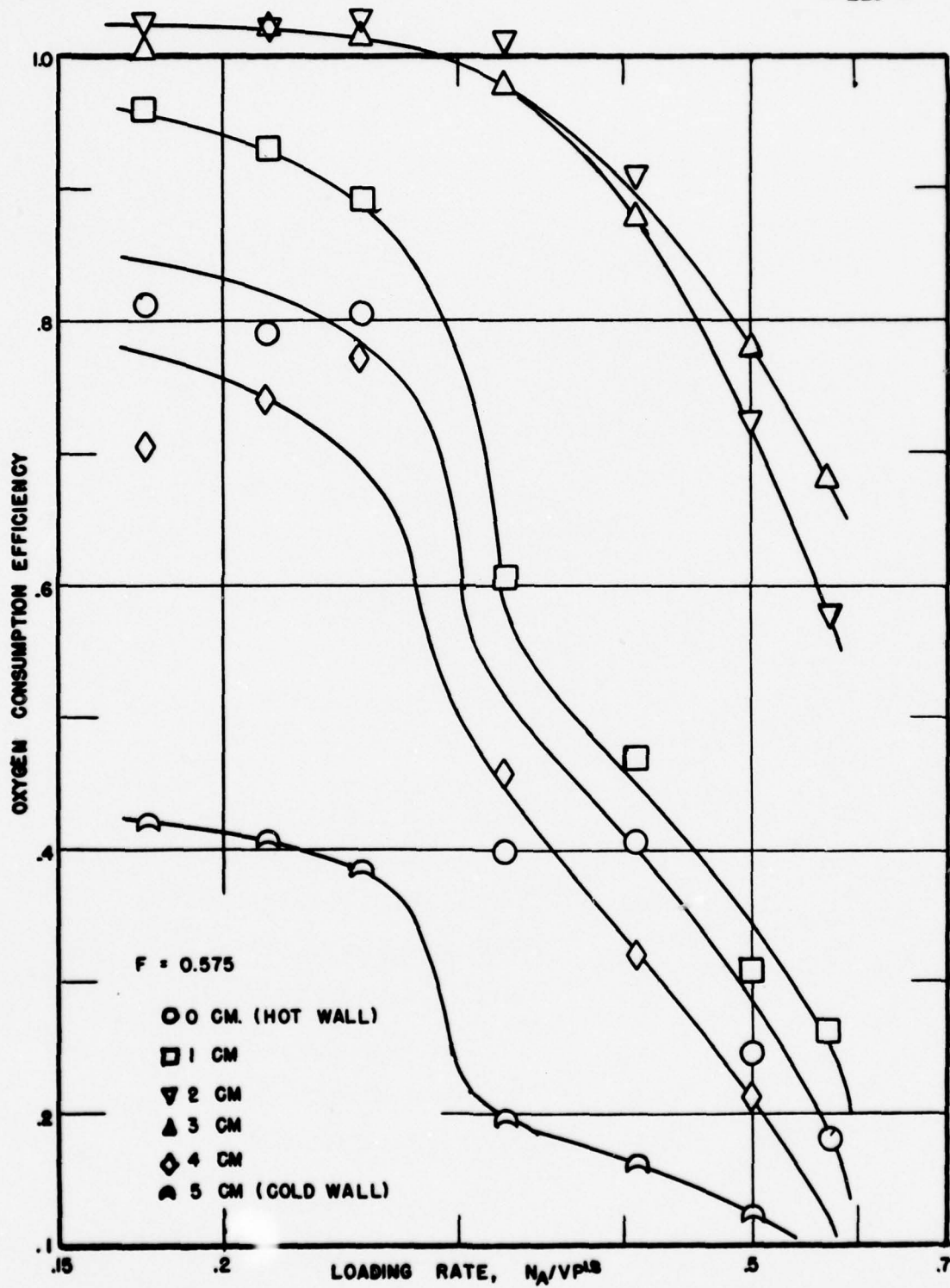
FIGURE X-12: CHAMBER BURNEDNESS AT VARIOUS POSITIONS

-120-
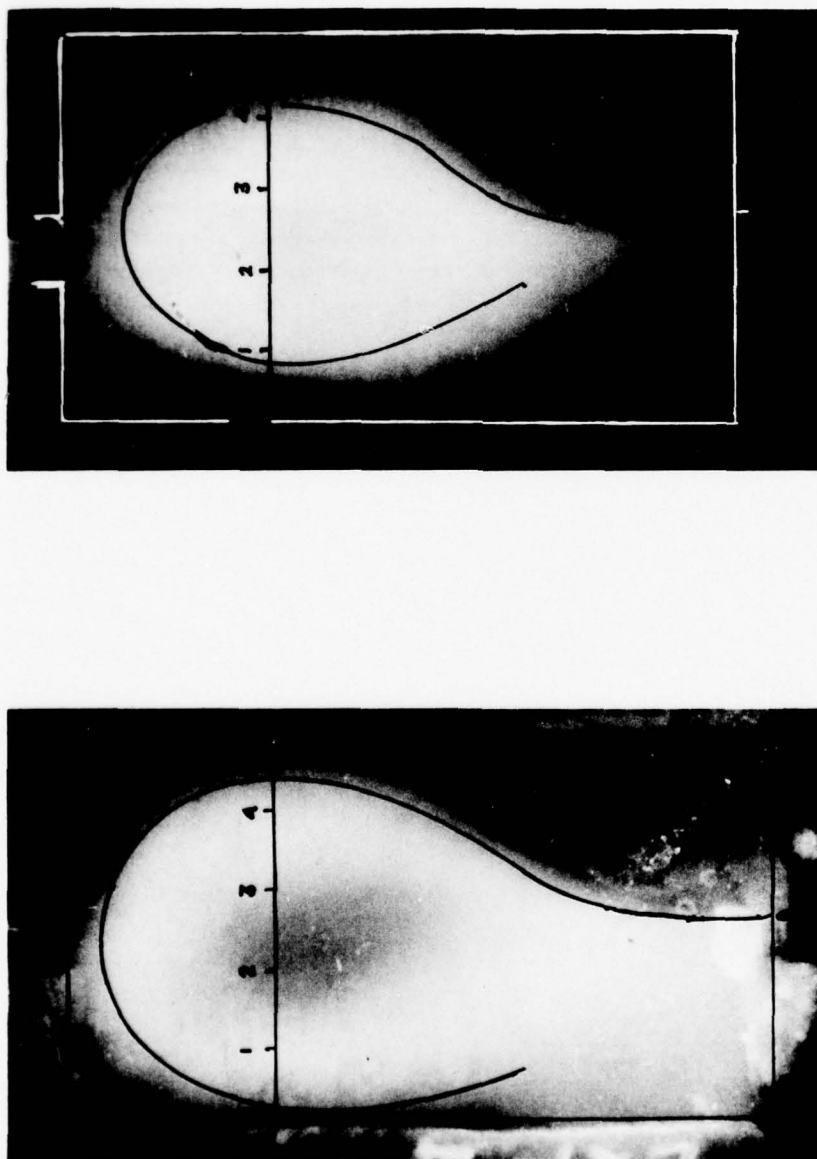
FIGURE Ⅴ-13: PHOTOGRAPHS SHOWING TRAVERSE STATIONS IN SAMPLING CHAMBER CONTENTS. LEFT, $N_A/VP^{1.8} = 0.215$; RIGHT, $N_A/VP^{1.8} = 0.498$.
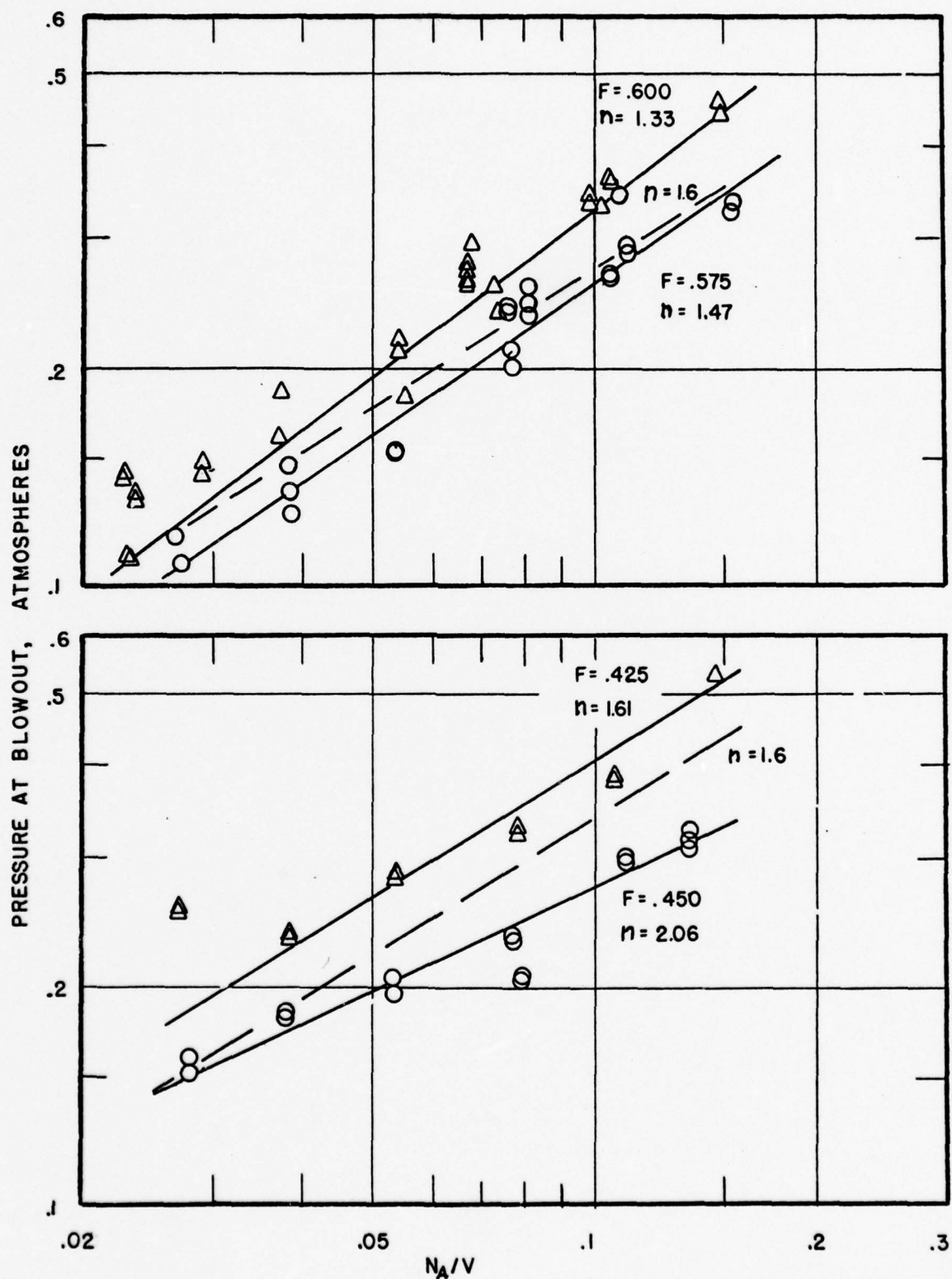
FIGURE Ⅴ-14: PRESSURE EFFECT ON BLOWOUT FEED RATE.
FEED/VOLUME RATIO AT BLOWOUT VS PRESSURE
(DASHED LINE IS AVERAGE $n = 1.6$)
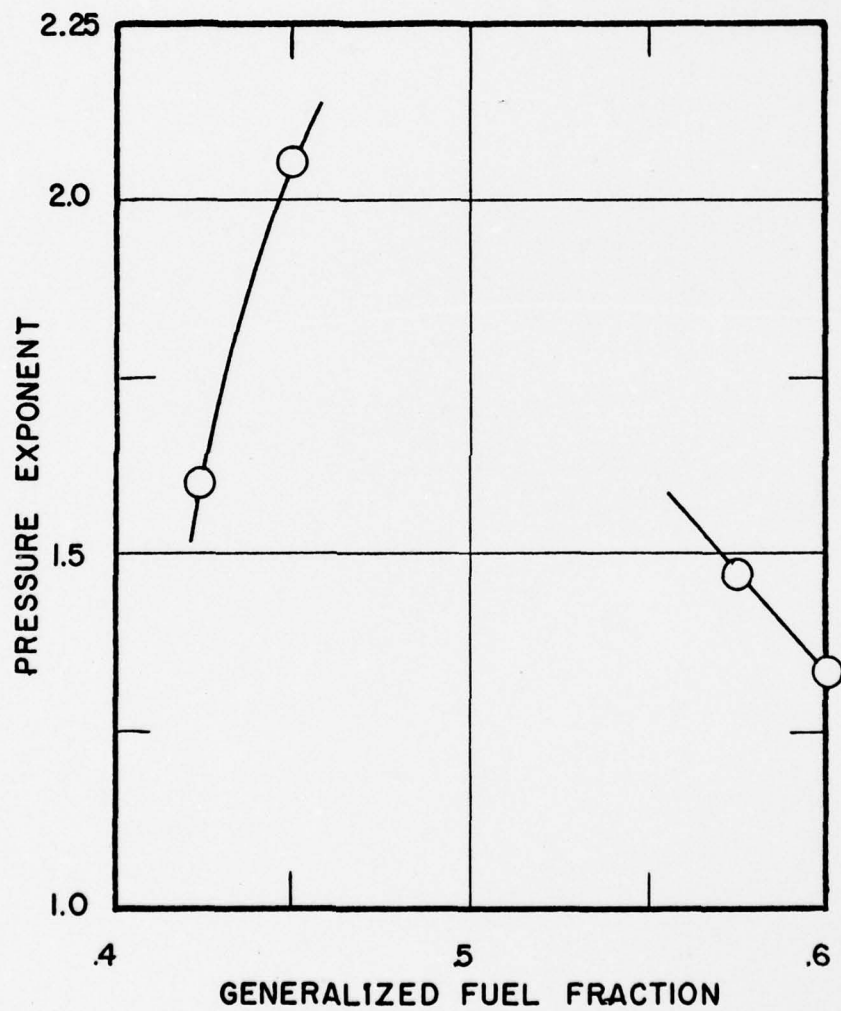
FIGURE V-15: EFFECT OF FEED
COMPOSITION ON PRESSURE EXPONENT

is a line for the average exponent "n" of 1.6 representing the results of all of the data on this chamber.

CHAPTER VI

DISCUSSION OF RESULTS

The experimental program was undertaken to provide
data for examining the question of whether stirred
reactor performance data could be combined with fluid
flow patterns to predict the performance of practical
combustors. Using stirred reactor blowout data, model
performance for the two-stability-limit model may be
predicted. Since sufficient experimental data on the
efficiency-loading relation for the stirred reactor
are not available, performance of the recirculation
model must be predicted from theoretical stirred-reactor
performance. The analysis of the data consists princi-
pally of direct comparison of these theoretical models
with the experimental reactor results.

Experimental Errors

The discussion of the experimental work must be
prefaced by commentary on the errors involved in these
experiments. Two significant sources of experimental
error were present; air leakage into the combustion
zone and non-ideality of the stirred reactor. A third
lay in the construction of the nozzle header assembly
which ideally should have perfectly aligned and matched
nozzles. This last was not as much a problem as the

first two because the effect of mis-matched or mis-
aligned nozzles was easily detected. Each of these
problems will be discussed in turn.

Air Leakage. The combustion chamber, consisting
as described previously of an arrangement of firebrick
and nozzles between two frames carrying the Vycor windows,
is fed by high velocity jets along its floor. In any
system of this sort the jets aspirate gases from the
surrounding fluid, and near the top of the chamber a
reverse flow of the chamber a reverse flow occurs to
replace the gases aspirated from the recirculation zone.
To create this reverse-flow pattern requires (from a
momentum balance) a low-pressure region in the lower
portion of the chamber. If there is an improper seal
between the chamber and its side walls, substantial
quantities of air can be aspirated from the ambient air
into this low pressure region of the combustion chamber.
In the construction of the apparatus, precautions were
taken to seal the chamber tightly. However, from time
to time thermal warpage of the side frames or improperly
fitted bricks made a satisfactory seal impossible. This
problem may be alleviated to some extent by careful
sizing of the exit flue or flues. If these are made
narrow enough the pressure drop required to force the
exhausted gases through them may be sufficient to raise

the pressure at the top of the chamber so that the low-pressure region in the recirculation zone is at or above ambient pressure.

The presence of an air leak in the chamber assembly could be most easily detected by a shifting of the stability limits of the chamber toward the rich side (i.e. stability data which lacked symmetry around a stoichiometric fuel/air ratio). This criterion, however, was not highly sensitive, as a substantial shift was required to differentiate assymetry due to air leakage from the small assymetry inherent in the well-stirred reactor stability curves.

To test whether the chamber was properly sealed when the blowout curves were symmetrical, one run was made in which a sample of gas was withdrawn from the interior of the chamber. An Orsat analysis of this sample for the carbon/nitrogen ratio was compared to the ratio calculated from the metered rates of fuel and air. The results are tabulated in Table VI-1. Included in this table is the hydrogen/carbon ratio which serves as a check by comparison with the hydrogen/carbon ratio for propane. Since only enough data were obtained to calculate the H/C ratio from the known ratio of nitrogen/oxygen in air (or visa-versa), only one check on the analysis could be calculated. Indicated in

Table VI-1 is the H/C ratio of propane, 2.67. Analyses
of the fuel have shown the propane to be about 96%
pure (10), the principal impurities being ethane,
propylene, and butane. Assuming a typical analysis as
given by Woo (30) of 0.8% ethane, 1.5% propylene, 1.5%
butane, and the balance propane, the calculated atoms
of carbon per mole of propane are 3.01 and the H/C ratio
is 2.66.

TABLE VI-1

Comparison of Carbon/Nitrogen ratio Determined by
Sampling with the Metered Ratio

	Value from Sample	Calculated by Metering
C/N	0.150	0.156
H/C	2.68	2.66

When the sampling data reported in this table were
taken the stability limits of the combustor were ap-
proximately symmetrical. In this table it is seen from
the comparison of H/C that the analysis of the sample
is reliable. The agreement between the C/N ratios,
though it indicates a small leakage, is close enough
to constitute a good check on the absence of serious
leaks at the time of this test. On the basis of this
analysis it is concluded that symmetrical blowout limits
are a sufficient test of the absence of air leaks.

Departure from ideal reactor conditions   A second
source of error in these experiments is the departure
of the chamber from ideal reactor operation.   In the
theoretical development of Chapter III, the models were
based on the assumption of an ideal stirred reactor in
which operation was adiabatic and the reaction rate was
first order in each of the reactants.   In principle,
the models discussed are not necessarily thus restricted.
Any relationship of combustion efficiency to feed rate
or blowout loading to fuel/air ratio determined experi-
mentally on a stirred reactor may be used in place of
the theoretical curves used in the previous chapter.
As pointed out, however, this generalization is restricted
to reaction schemes in which a single reaction controls
the rate.   Where successive or competitive reactions are
possible, one cannot use a single experimental stirred
reactor performance curve to compute model performance.

In comparing combustor performance with the theo-
retical model prediction, one need consider only the
first of these problems (i.e. heat loss) in the two-
stability-limit model, since the reactors of the model
are operating in parallel.   In the recirculation model,
both heat loss and multi-step reaction departures are
significant.

In the present work, the comparison of the experi-

mental results with the theory is based on experimental
stirred-reactor performance for the two-stability-limit
model. For work with the recirculation model the ideal-
ized stirred reactor theory is used. Although it would
be clearly preferable to use an experimental stirred
reactor performance curve, such data have not yet been
reported in the literature in sufficient detail to be
of use here. To the author's knowledge, only one curve
of efficiency vs feed rate has been reported (14), and
this curve was at a different fuel/air ratio than the
one used for the present investigation.

There are ample blowout data reported in the
literature. The available data indicate that for
hydrocarbons, there is no substantial difference in
the performance of various members of the same family
(i.e. saturates, olefins, etc.), and in general, most
hydrocarbons behave approximately the same. Acetylene
and hydrogen are different. This permits analysis of
the blowout data to be based on empirical curves of
blowout rates vs fuel/air ratio.

Using either the theoretical performance curves
or the experimental blowout curves, account must be
taken of the fact that the heat losses from this reactor
are significantly greater than those for the stirred
reactor experimental conditions. In the present

experimental work, no direct measurement of the heat losses was made. An estimate of their magnitude involved accounting for losses by radiation through and from the Vycor windows, and for conduction-convection losses directly through the windows. No correction for losses through the firebrick was made since it was felt that it was sufficiently thick to make losses in this direction negligible compared with the other heat losses in this chamber.

In computing the heat losses from this chamber both radiative and convective heat transfer had to be considered. Since the chamber was of small dimensions and operated at low pressures, gas radiation could be neglected. Heat transfer from the gases to the chamber walls and Vycor windows was by convection. Heat transferred to the walls and roof of the chamber was then radiated to the Vycor windows and the outside surroundings seen through the windows. Heat transferred to the windows was transferred by radiation and convection simultaneously to the outside.

In computing the heat transferred by radiation, the chamber was divided into three zones; the walls and roof, the floor and the windows. The walls and roof were considered to be a heat source at a temperature T_w (different from the gas temperature). The windows

were considered to be a heat sink. The floor of the chamber represented a refractory surface, returning as much heat by radiation to the chamber as it received from the walls and windows. Vycor windows, made of nearly pure quartz, transmit radiation whose wave length is shorter than 3.7μ, and are nearly opaque to radiation of longer wavelengths. Therefore, the absorptivities and emissivities of Vycor to radiation from various temperature sources (the walls and the floor) had to be accounted for in the calculations.

Calculations were carried out for the three-jet chamber using a heat transfer coefficient from the gases to the brick of 10 Btu/hr ft² °F at the blowout velocity, and it was assumed that the heat transfer coefficient varied linearly with velocity. A convection coefficient from the Vycor windows to the ambient air was taken to be 2 Btu/hr ft² °F. The brickwork and the floor of the chamber were assumed to have an emissivity of 1.0. The Vycor was assumed to be black at wave lengths above 3.7μ, and transparent at wavelengths below this. The reflectivity of the Vycor was ignored in this calculation. Figure VI-1 shows the resultant heat loss rate from the chamber as a function of temperature and relative firing rate.

Allowance for the effect of heat loss in the
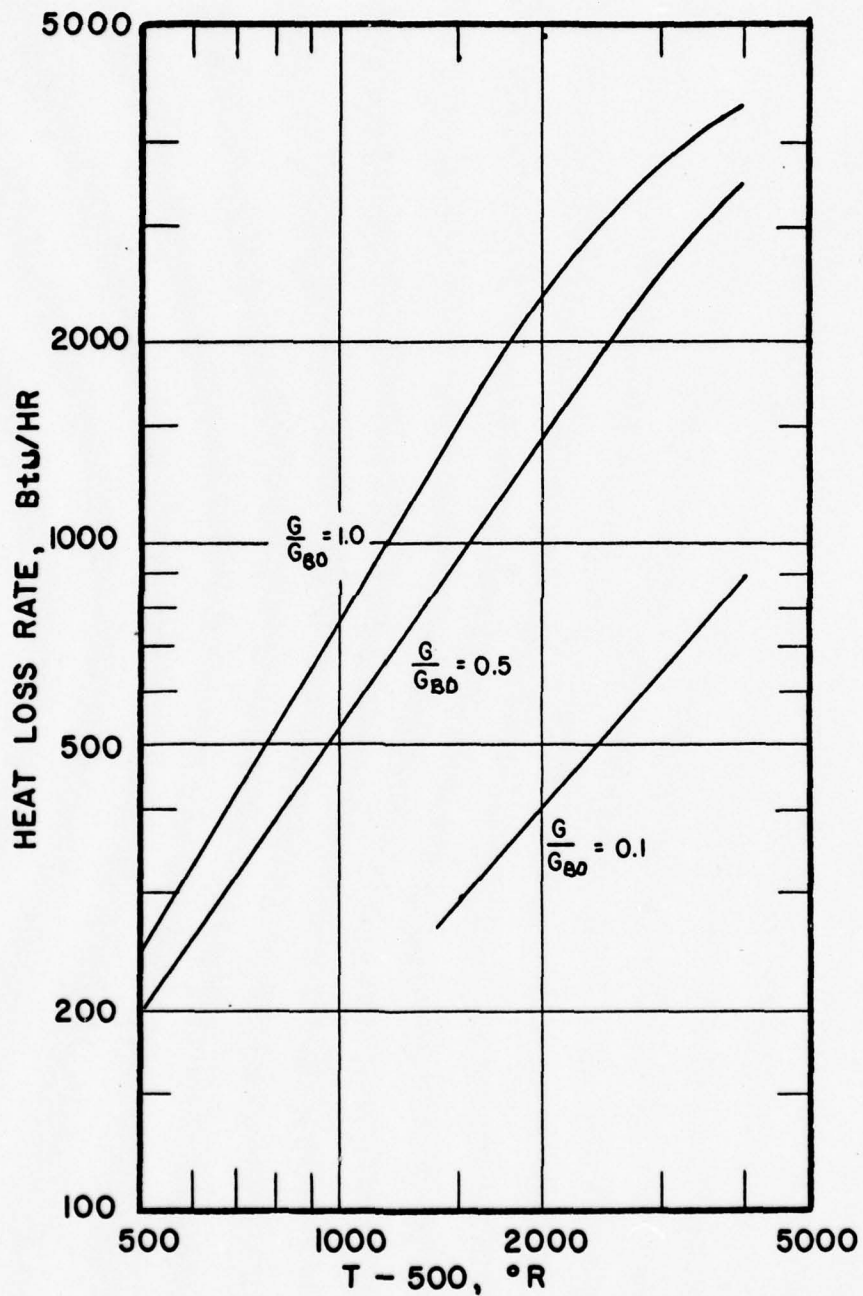
FIGURE VI-I: HEAT LOSSES FROM THREE-JET CHAMBER

HEAT RELEASE RATE FOR A STOICHIOMETRIC
MIXTURE AT BLOWOUT = 120,000 Btu/HR (β = 70%)
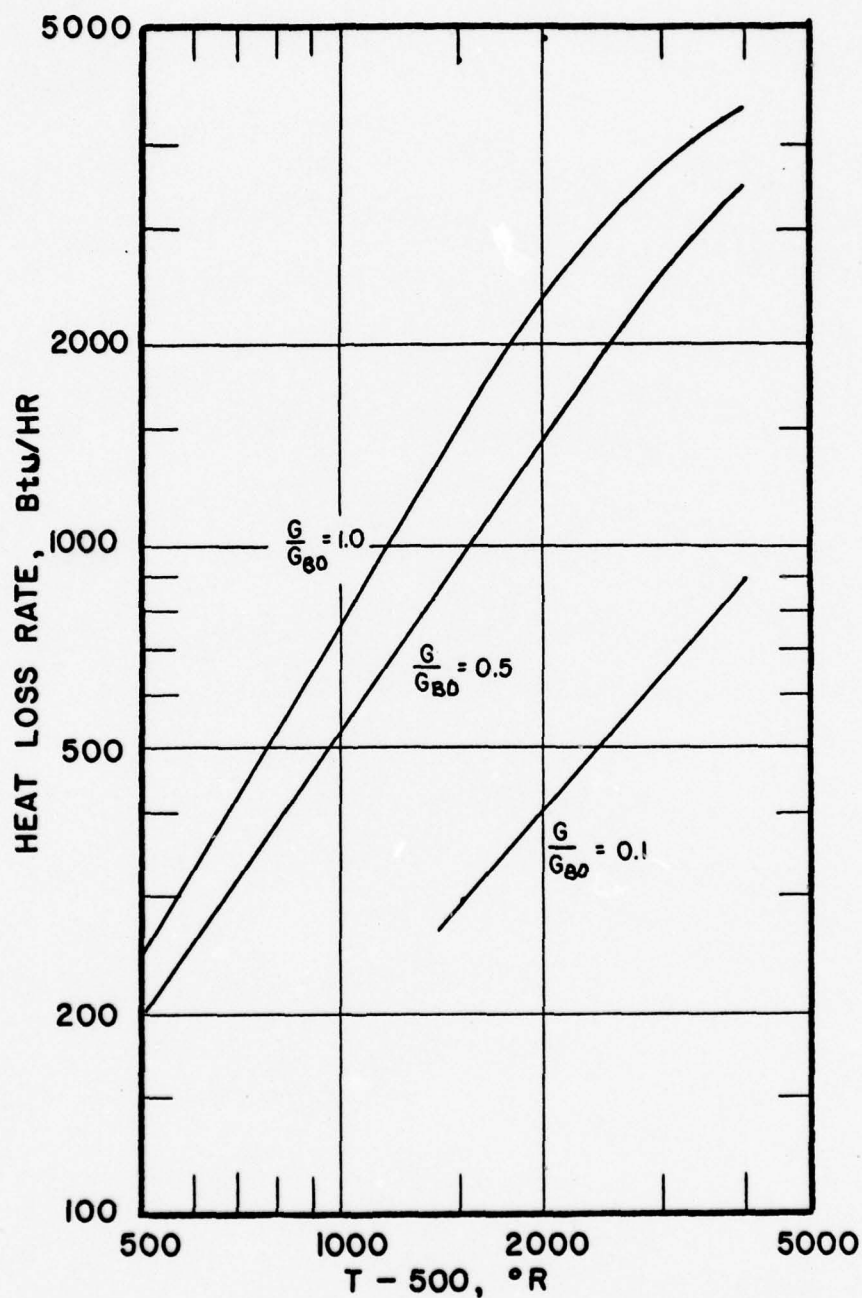
FIGURE VI-I: HEAT LOSSES FROM THREE-
JET CHAMBER

HEAT RELEASE RATE FOR A STOICHIOMETRIC
MIXTURE AT BLOWOUT = 120,000 Btu/HR (β = 70%)

calculation of chamber performance has been made in the past (3, 14) by assuming the heat losses to correspond to an effectively lower inlet temperature to the reactor. This technique has been applied principally to the problem of the effect of temperature on blowout limits. Allowance for the effect of heat losses by substitution of an artificial inlet temperature requires a previous knowledge of, or an independent calculation of, the heat loss. If the heat loss is known as a function of temperature and/or Reynolds number, a modified approach is suggested. This is outlined below.

Consider a reactor for which the heat loss rate may be expressed by the relation:

$$q = UA(t - t_o) \qquad\qquad \text{VI-1}$$

where U is the heat transfer coefficient based on the heat transfer area, A, the temperature, t, of the burning gas and the ambient temperature, t_o, (also the inlet gas temperature).
The simplified heat balance for the adiabatic reactor is given by:

$$t_a = t_o + \Delta_{af}\, \beta \qquad\qquad \text{VI-2}$$

and by a process analogous to that used to obtain VI-2, the heat balance for a non-adiabatic reactor may be written:

$$G\, c_p\, (t - t_o) + UA\, (t - t_o) = \Delta_{af}\, \beta \qquad \text{VI-3}$$

where Δ_{af} is the adiabatic flame temperature rise for
complete combustion

β is the fractional burnedness of the gases

G is the molal feed rate to the chamber

and c_p is the molal heat capacity of the gases fed.

Rewriting VI-3 leads to an expression parallel to VI-2;

$$t = t_0 + \frac{\Delta_{af}}{1 + \frac{UA}{G c_p}} \beta \qquad \qquad \text{VI-4}$$

The heat balance represented by Equation VI-4 may now
be combined in the usual manner with the equation
describing the stirred reactor behavior.

Two limiting cases for VI-4 are of interest. If
the heat transfer rate is controlled by forced con-
vection or turbulent diffusion, then to a first approxi-
mation the heat transfer coefficient, U, may be assumed
to be directly proportional to the mass feed rate, G.
Then the denominator of the fraction in IV-4 becomes a
constant, and the heat loss rate is a constant per-
centage of the total heat released, i.e. $t = t_0 + \frac{\Delta_{af}}{1 + \alpha} \beta$.
This is nearly equivalent to an adiabatic reactor operating
on a fuel-air mixture diluted with additional inert gas
such as nitrogen.

If, on the other hand, the heat transfer coefficient
is independent of the Reynolds number, such as in

radiation or conduction, and if U may be treated as a
constant over substantial ranges of temperature, then
Equation VI-4 assumes the form:

$$t = t_o + \frac{\Delta_{af}}{1 + \frac{\gamma}{G}} \beta \qquad\qquad VI-5$$

In radiant heat transfer the assumption of linear varia-
tion of heat loss with temperature over substantial
temperature ranges is not good, but it is justified
here by the simplicity thus introduced. Efficiency
vs burnedness curves for a stirred reactor operating
with heat losses corresponding to the two limiting
heat loss cases above are shown in Figure VI-2. In
this figure it is seen that the shape of the reactor
performance curves near blowout is not greatly affected.
At lower feed rates, however, the heat loss in the con-
stant U case correspond to marked cooling of the gases
and results in quenching the reaction. Thus significant
departure from the adiabatic stirred reactor curve is
predicted.

A second error introduced into the comparison of
the experimental reactor performance with the theoretical
stirred reactor lies in the departure of the stirred
reactor from the simple bimolecular kinetic mechanism.
There seems to be general agreement in the literature
that the apparent overall order of high-temperature
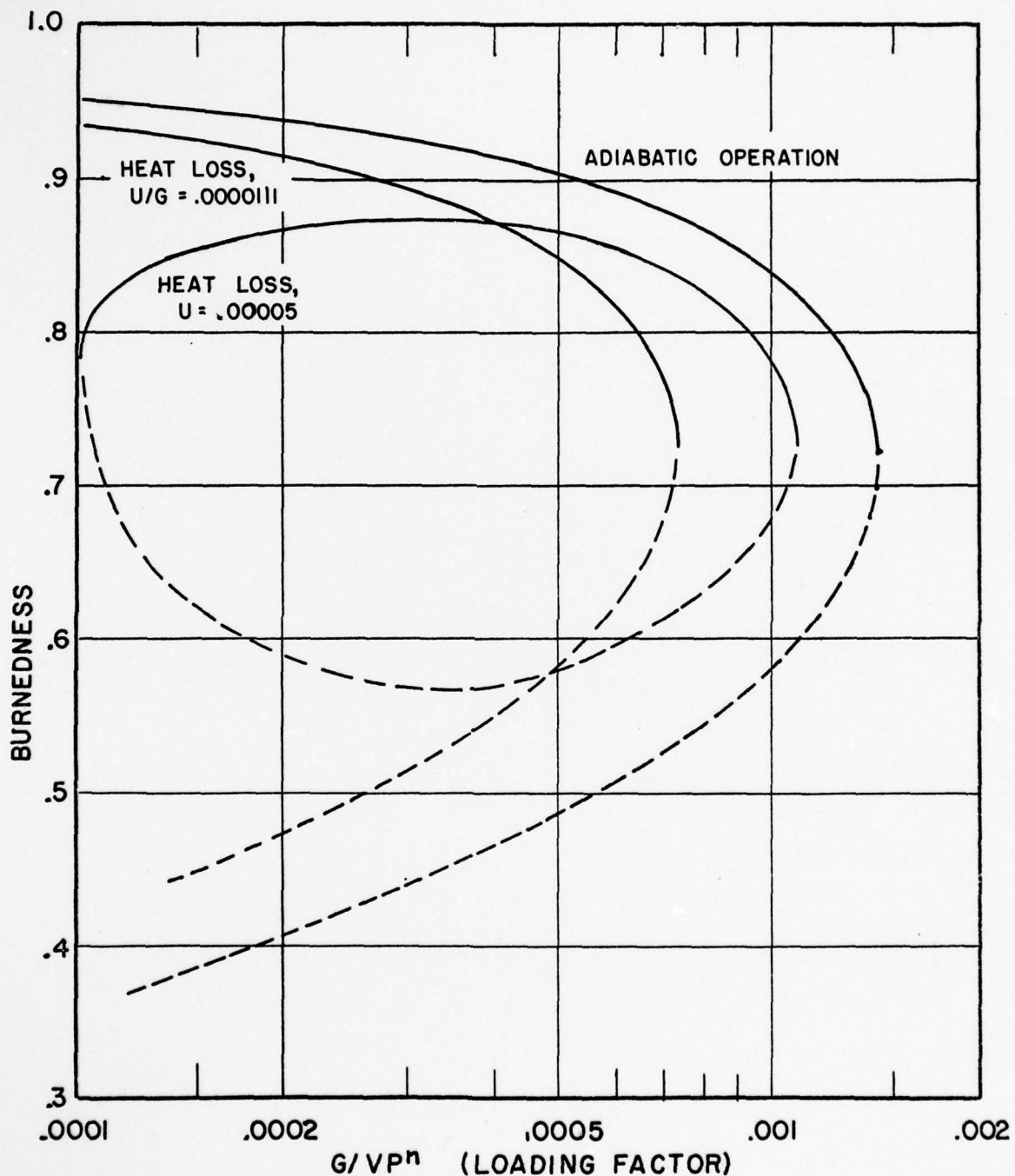
FIGURE VI - 2: EFFECT OF HEAT LOSS ON STIRRED REACTORS

CASE I: RATIO U/G = C, CORRESPONDING TO A
CONSTANT PERCENTAGE OF HEAT LOSS
(U/G = .0000III)

CASE II: U = C, CORRESPONDING TO HEAT TRANSFER
COEFFICIENT INDEPENDENT OF G.
(U = .00005)

reaction in combustion is less than two. Values from
about 1.3 to 2.0 have been reported, with no general
agreement on the exact value. Values between 1.6 and
1.8 are the most generally accepted. In the present work
the pressure exponent of the reactor at blowout was
determined for four different fuel/air ratios, and values
of "n" ranging from 1.3 to 2.0 were found. It should be
pointed out, however, that this variation may involve
the simultaneous effect of the variation of reaction
rate with composition and variation of mixing rate with
Reynolds number, since the experiments were not run at
a constant Reynolds number. Even when experiments are
restricted to a single feed composition, the variation in
results illustrated due to pressure may be to an unknown
degree due as well to Reynolds number variation with
its associated effect on mixing and to variation in heat
loss with velocity change in feed rate.

A consequence of using a second order equation
when the actual equation is of lower order but with the
activation energy unchanged is a change in the shape of
the curve as illustrated in Figure VI-3. In this figure
the theoretical curve for a reaction rate first order
in each of fuel and air is compared with the curve for
a rate which is first order in air and 0.8 order in
fuel. These latter values for exponents were recommended
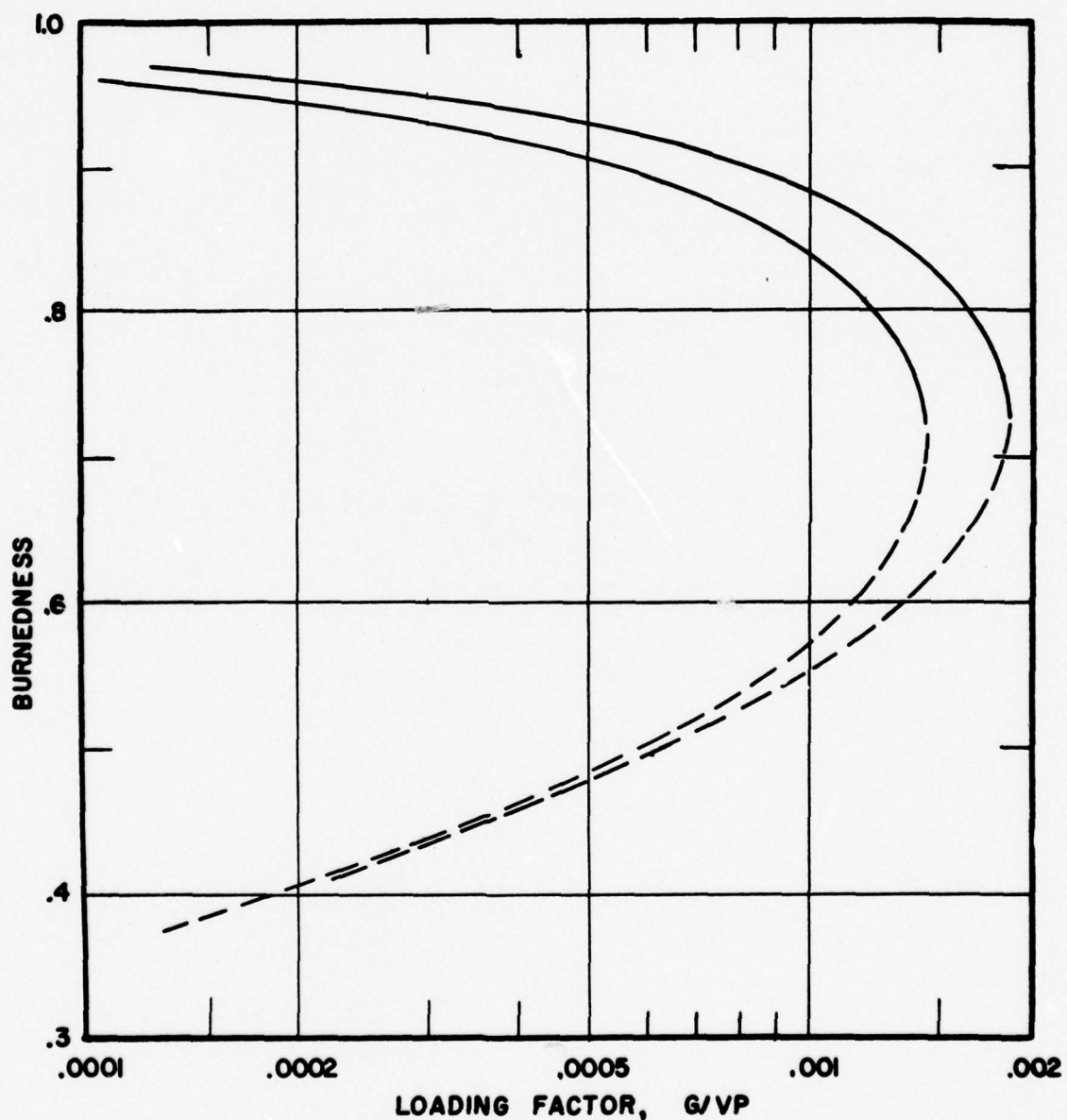
FIGURE VI-3: EFFECT OF CHANGING PRESSURE EXPONENT
ON PREDICTED STIRRED REACTOR OPERATION

by Longwell and Weiss on the basis of their studies.
(The lateral displacement of the curve in Figure VI-3
is irrelevant, and is simply a consequence of not
changing the numerical value of the "collision constant".)

For the present work it has been concluded that
although accurate experimental data on the loading rate-
efficiency behavior of the stirred reactor would be
desirable, the use of theoretical curves for a compari-
son of the model behavior with the experimental behavior
is necessary. Since in the firing rate range of interest
the difference in shape between idealized stirred reactor
curves of β vs G and reactor performance corrected for
heat loss and order of reaction are not great, it does
not appear justifiable to include these corrections.
The corrections are not known sufficiently well to attach
greater certainty to a corrected curve than to an
uncorrected one.

Errors in Measurement   A third general category
of error to which this experimental program was subject
is that of errors in measurement. The measurements of
significance in this experimental work are:

(1) measurement of flow rates

(2) measurement of chamber dimension. This in-
cluded the height, width and depth, location
and size of the nozzles and exit flue

(3)   the parallelism of the jets when the three
jet chamber is being used, and parallelism of
the nozzle block assembly and the sidewalls
of the chamber.

By far the most critical measurements were those
on the size, spacing and alignment of the feed-jet
assembly. Even slight errors here were sufficient to
cause substantial reductions in the chamber stability.
Every effort was made to obtain uniformity in the jet
assembly. The slot openings were measured with a
feeler gauge, and the jet alignment was checked by means
of a scale with 1/100" graduations read with a magnifying
glass. In the final analysis, however blowout measure-
ments provided the best test of accurate assembly.
Although it is believed that errors of this type do not
significantly effect the blowout and efficiency studies,
it is difficult to demonstrate this conclusively.

Errors in the measurement of flow rate and of
brickwork dimensions are relatively unimportant in this
work. Experience with calibrating and metering with
standard square-edge orifices indicates that the error
in metering was approximately 1% in mass flow. Errors
of the dimension were kept as small as possible with the
loose, friable type of refractory used. However, brick-
work dimension errors which were known to be substantial

had no apparent effect on the chamber stability; so it
was concluded that errors resulting from this source
had negligible effect on the overall result.

Analysis of the Three-Jet Chamber Performance

In the study of the three-jet chamber, two stability
limits were observed, one corresponding to a sudden shift
in flow pattern with blowout of the flame in part of the
chamber, and the other corresponding to total blowout.
A theory explaining this behavior qualitatively has been
discussed in Chapter III. It is now proposed to fit
the theory quantitatively to the data.

Consider, first, approximations which can be made
to the theory of Chapter III. As the blowout condition
is approached, (the figure representing this condition
is reproduced for conveniency in Figure VI-4), the
stable intersections, corresponding to stable combustion,
approaches the noses of Branches I or II, depending on
the mode of chamber operation. In doing this, the
corresponding operating point on the well-stirred reactor
curve for the zone in question also approaches the blow-
out point of the stirred reactor curve. A reasonable
approximation which can be made to this situation is to
say that the blowout of a stable zone will occur when
that zone has reached the blowout loading rate calculated
on the basis of the stirred reactor. Since it was
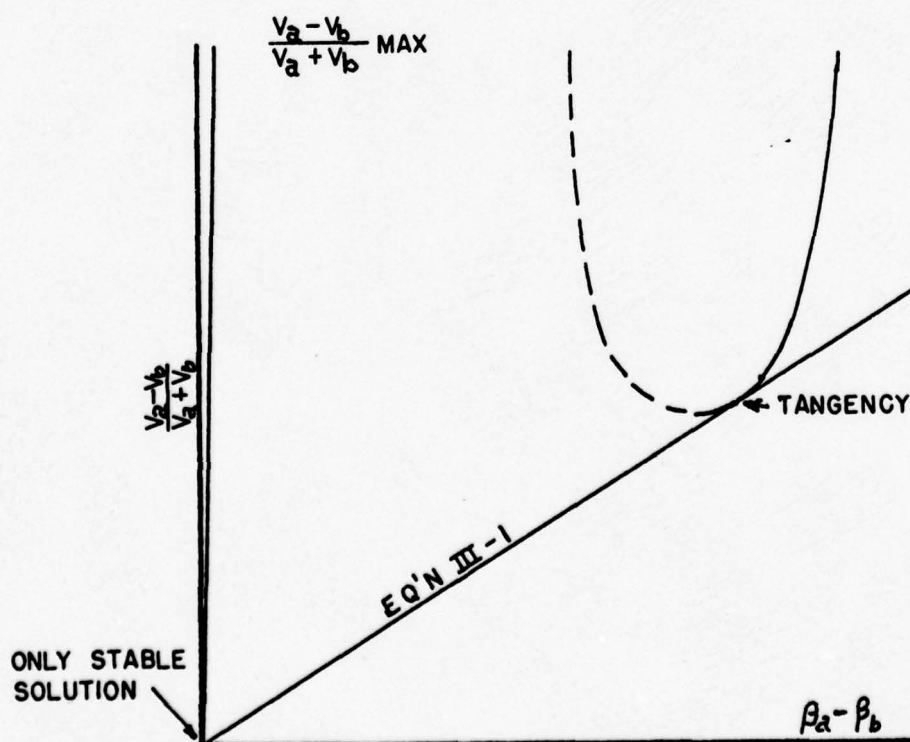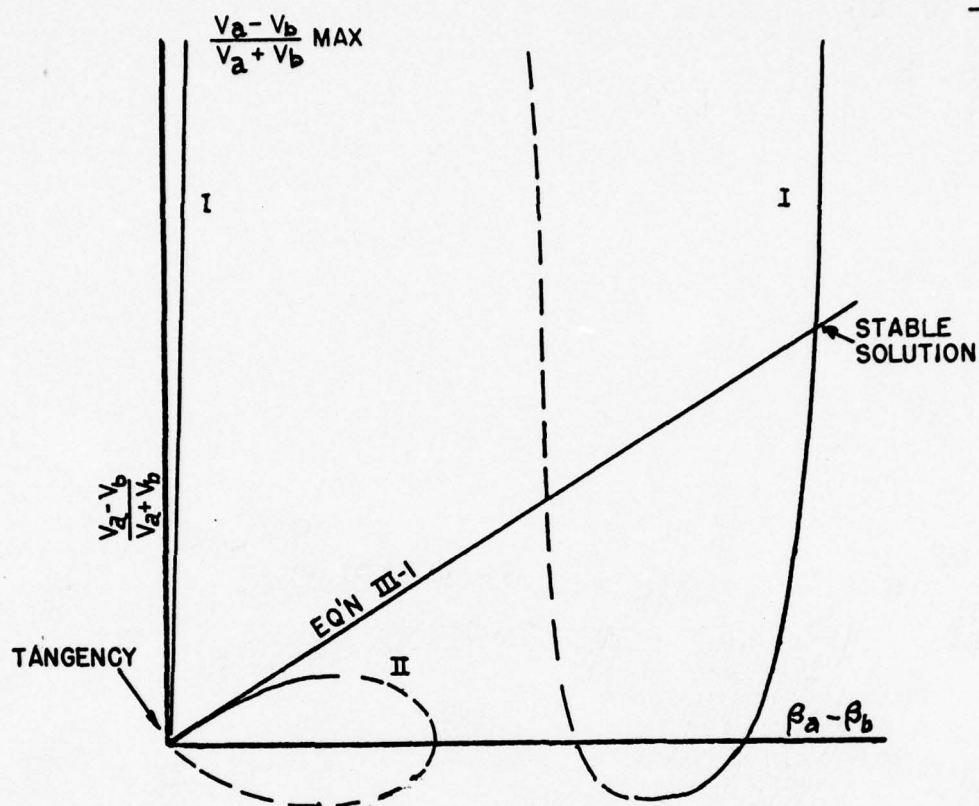
FIGURE VI-4: TWO-STABILITY-LIMIT MODEL
BLOWOUT CONDITIONS

theoretically predicted that blowout occurred in this model at a somewhat higher burnedness than that corresponding to stirred reactor blowout, this assumption is not rigorously valid. However, in this range of loading rates, burnedness changes very rapidly with loading, so that only a small error in blowout flow rate is introduced by this assumption. If knowledge of the volumes and feed rates of the two zones in this chamber is postulated, it is possible to predict whether the chamber will burn stably in the two-zone or one-zone configuration, or be completely blowout at a given feed rate.

The measurement of combustion zone volume in a turbulent bunsen cone has been accomplished by Simon and Wagner (22) using flame photographs of the blue luminosity of a pre-mixed fuel/air mixture. The theoretical validity of this method is uncertain, since some combustion reactions, such as carbon monoxide and hydrogen oxidation produce nearly non-luminous flames, whereas reactions involved in the initial stages of hydrocarbon combustion, generally involving C-H or C-C bond fracture, give rise to the characteristic color of normal flames. If the hypothesis is that the initial stages of combustion are rate-controlling, then the measurement of the luminous zone will give a reasonable

approximation to the volume of combustion. If carbon monoxide oxidation is postulated to be the rate-controlling step, then this measurement may be grossly misleading.

The feed rate to each half of the chamber is postulated to be a constant fraction of the total feed and in addition, a constant fraction of the fresh feed is assumed to grossly bypass the active volumes in the chamber. In the case of a symmetrical combustion pattern, this is a reasonable assumption. For assymetrical combustion patterns it is assumed that this is still valid (i.e. when the combustion pattern changes due to a blowout of one side of the chamber, no change in the fraction of the fresh feed reaching the remaining active zone occurs).

Combining these assumptions with the data on the photographically measured flame volumes leads to the conclusion that both blowout curves for the three-jet chamber should be displaced from the well-stirred reactor curve by a constant multiplying factor, and that the two blowout curves for the three-jet chamber should be displaced from each other by a constant predicted from the difference in zone volumes only. Since Figure V-6 shows the zone volumes to be independent of fuel/air ratio, if the three-jet chamber were composed of stirred
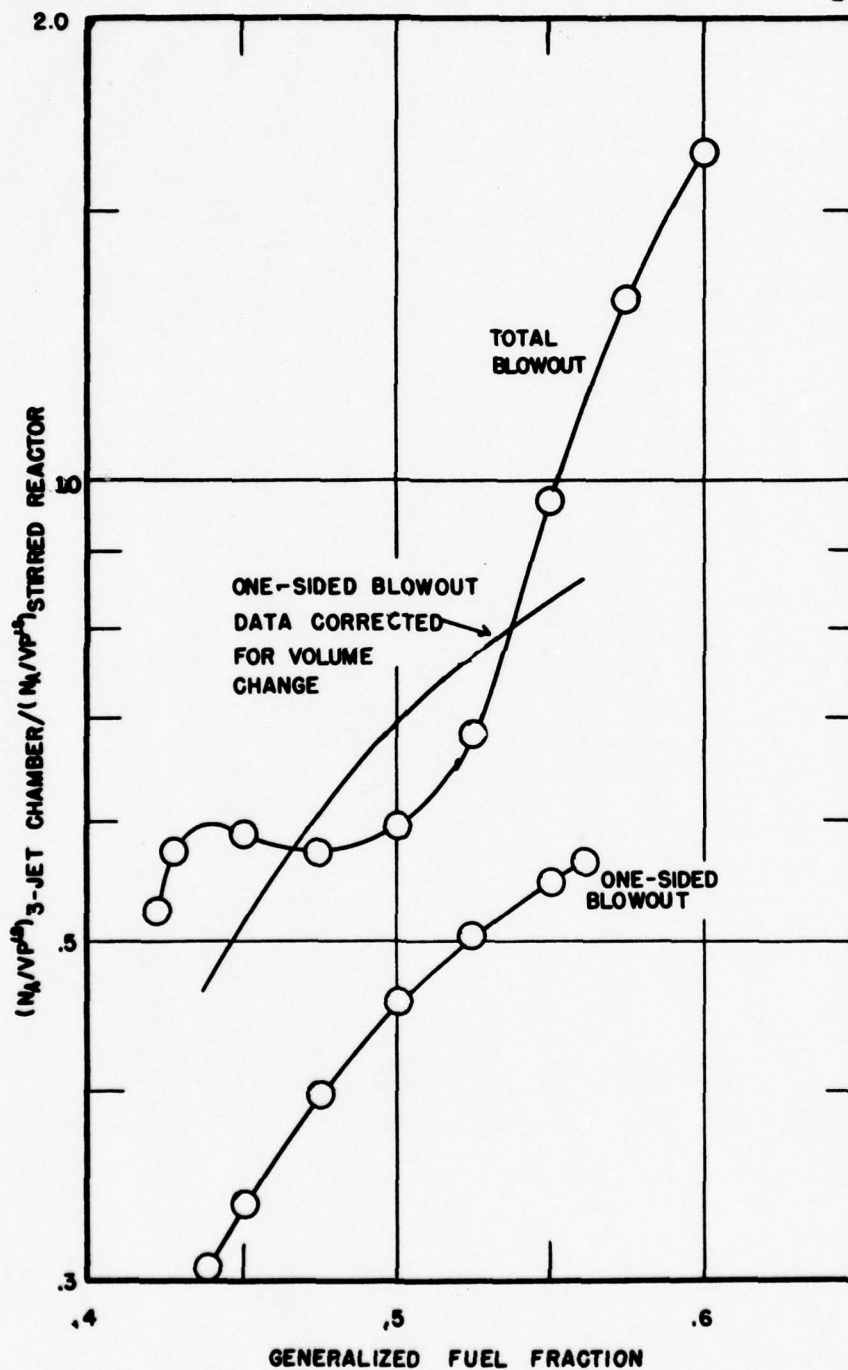
FIGURE VI-5: COMPARISON OF STIRRED REACTOR
BLOWOUT DATA AND THREE-JET CHAMBER DATA.

ONE-SIDED BLOWOUT DATA HAVE BEEN CORRECTED
BY THE RATIO OF ZONE VOLUME AT ONE-SIDED
BLOWOUT TO ZONE VOLUME AT TOTAL BLOWOUT.

reactor elements, one would expect that the performance curves of the well-stirred and the three-jet combustors should be displaced from each other by a constant which is independent of fuel/air ratio. This is not observed, as may be seen in Figure VI-5. This deviation from the expected behavior may result from the inadequacy of the assumptions above or it may reflect the inability of the stirred reactor to describe operation in the active zones.

The model also predicts that the two curve for the three-jet chamber should be separated from each other by a constant which may be derived from the zone-volume data. This may be argued formally:

(1) If V_1 represents the volume of the smaller zone (of the two active zones),

(2) V_2 represents the volume of the large zone when there is only one active zone, and

(3) If Y represents the fraction of the feed reaching each zone which is the same for each active zone and independent of flow rate and zone volume,

then, $V_1/GY = L_1$, the loading factor for active zone 1 and $V_2/GY = L_2$, the loading factor for active zone 2.

When an active zone blows out, it is postulated that it is at the critical loading factor, L_{BO}, of the

stirred reactor at blowout. Hence $L_{BO_1} = L_{BO_2}$, or

$$\frac{YG_{BO_1}}{YG_{BO_2}} = \frac{V_1}{V_2} = \frac{G_{BO_1}}{G_{BO_2}}$$

In Figure VI-5, the stirred reactor curve has been compared to the three-jet chamber stability curves by plotting an ordinate of $(N_A/VP^{1.8})_{3jc}/(N_A/VP^{1.8})_{wsr}$ vs generalized fuel fraction. It is immediately apparent that the three-jet chamber does not follow the expected performance based on that of the well stirred reactor. However, the two curves representing the blowout limits of the three-jet chamber are approximately displaced from each other by the expected amount. The significance of the unexpected relative performance is not clear. It might be argued that this resulted from air leakage into the chamber. This argument is countered, however, with the evidence discussed at the outset of this chapter that the data are essentially free from air leakage errors. A second possible reason for this behavior is that the difference in the combustion characteristics of propane (used here) and octane (used by Longwell) is sufficient to cause this behavior. This argument is not supported by any evidence. Recent work done at M. I. T. (5) as yet unpublished) using pure propane as

the fuel in a well-stirred reactor gave the results
indicated in Figure II-8, showing no difference in
stirred reactor performance which could account for
the observed difference in the three-jet chamber and
the stirred reactor performance characteristics.
Therefore, one is led to the conclusion that the ob-
served difference represents a characteristic of the
operation of the active zones not accounted for by
the stirred reactor performance.

The efficiency measurements made on this chamber,
though not extensive enough to fit to any model, are
useful for showing that the chamber operates at a
reasonable efficiency level. From these measurements
it is also possible to estimate the quantity of gross
bypassing of the combustion zones. If one takes a
value of β of 90% for the burnedness of each of the
zones (an average figure representative of the
efficiency data reported by Longwell (14)), then for
the gross efficiency to be about 70% leaving the three-
jet chamber requires approximately 22% of the total
feed to the chamber to bypass completely the combustion
zones. The balance (78% of the total feed) enters the
combustion zones and burns to a 90% efficiency. Were
the ratio of gross loading factor for the three-jet
chamber at blowout to the well-stirred reactor at

blowout known with certainty, it would be possible to calculate the fraction of volume in each recirculation zone which was active and that fraction which was inactive. However, because of the behavior of the ratio (Figure VI-5) no constant value for volume ratio is consistent with the rest of the theory.

In addition to the results reported here, an attempt was made to use Schlieren photography to gain an insight into the mechanism of chamber behavior. These efforts, unfortunately, were unsuccessful, due particularly to extraneous patterns caused by the hot glass and by the warm turbulent air ambient to the chamber in the vacuum vessel which were in the optical path.

Analysis of the One-Jet Chamber Performance

The theory developed to explain the two-stability limits observed in the three-jet chamber implied that a similar behavior should be observed in the one-jet chamber. To test this hypothesis a one-jet chamber was built and tested. The first design tried was a chamber of width 1/3rd that of the original three-jet chamber. As mentioned previously, this proved to be too narrow since its stability limt was unreasonably low. Stable operation was achieved by making the chamber 2" wide

rather than the original 1" width, still narrower,
however, than the original 3" wide three-jet chamber.
Stable combustion was easily established in the one-
jet chamber, though the combustion pattern was not
symmetrical (see Figure V-7 and 8). It is postulated
that this asymmetrical combustion pattern is a con-
sequence of a basic instability of the cold flow pattern
in which there is no stable symmetrical flow pattern
regardless of how slowly the chamber is fed. Because
no symmetrical combustion pattern existed, there was no
possibility of the dual stability limit found in the
three-jet chamber. From the behavior of the combustion
pattern as blowout was approached, a model analogous
to the recirculation model discussed in Chapter III
was suggested.

To compare the narrow one-jet chamber with the
theoretical recirculation model of Chapter III, efficiency
vs loading rate data were required. Blowout data were
also taken to compare the performance of this chamber
with that of the stirred reactor.

The comparison of the stirred reactor data and the
one-jet chamber blowout data is shown in Figure VI-6.
These data show a deviation from the stirred reactor
which is not accounted for by the model. As in the
case of the two-stability-limit model, the recirculation
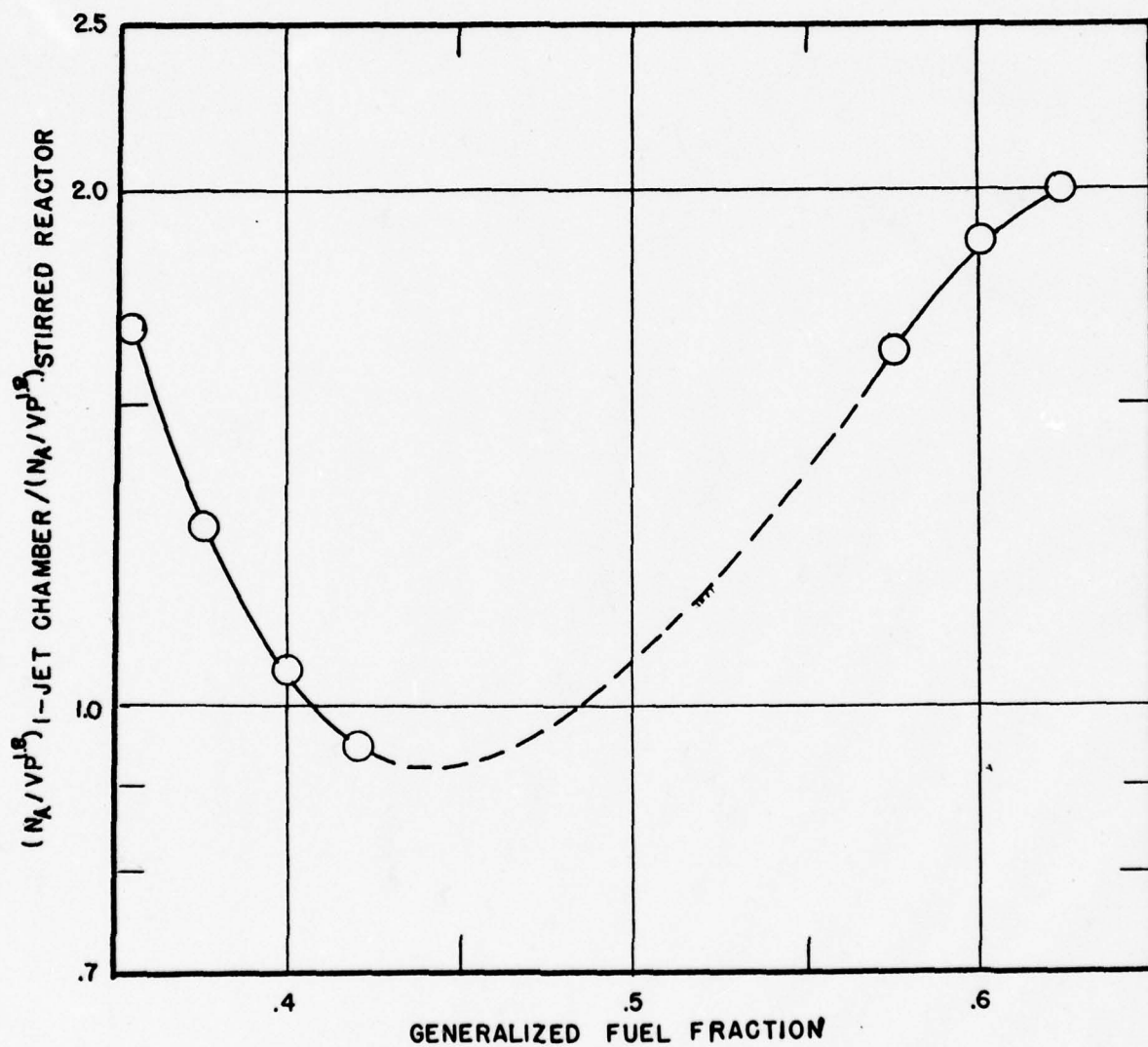
FIGURE VI-6: COMPARISON OF THE ONE-JET CHAMBER
BLOWOUT DATA WITH STIRRED REACTOR DATA
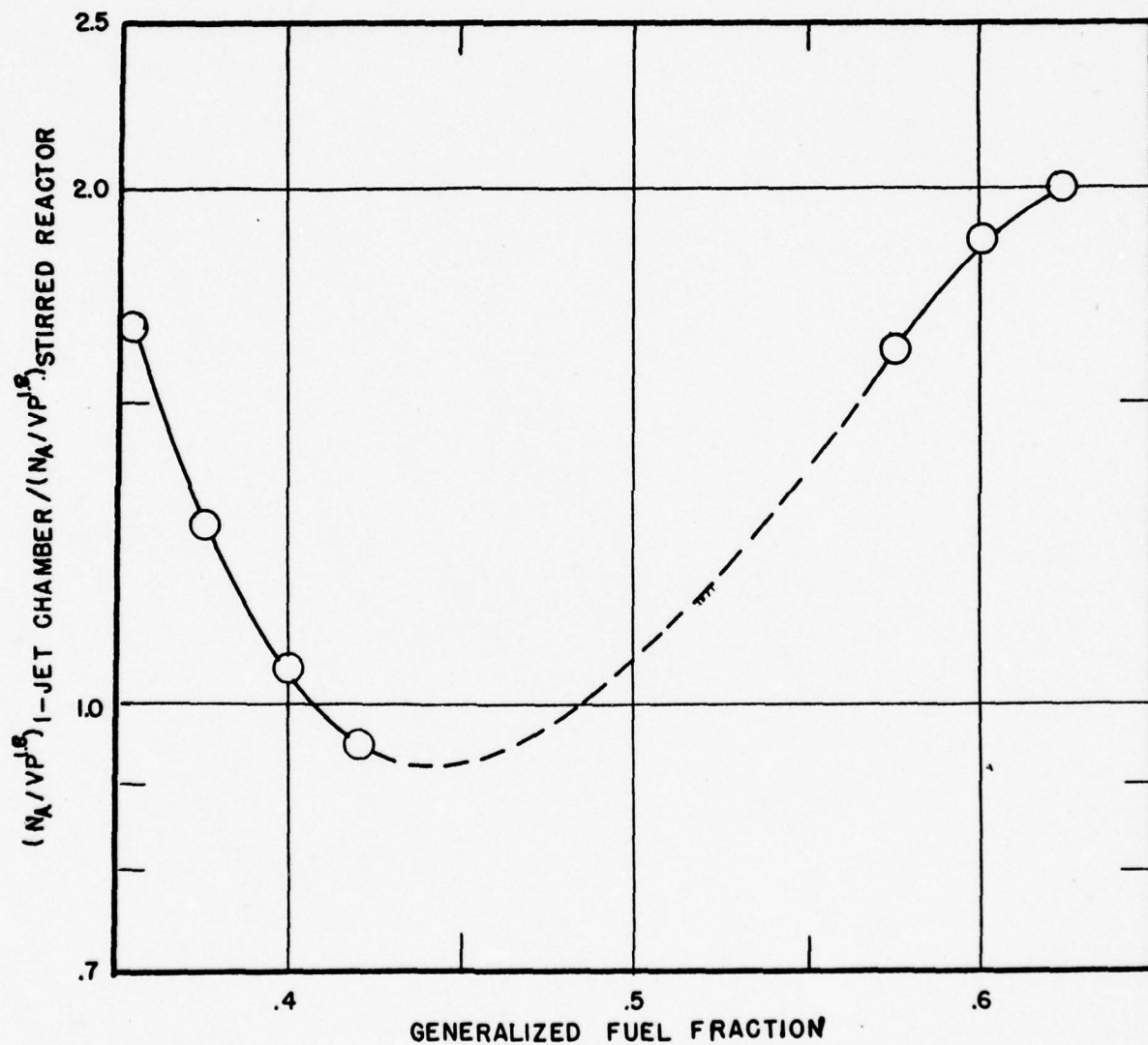
FIGURE VI-6: COMPARISON OF THE ONE-JET CHAMBER
BLOWOUT DATA WITH STIRRED REACTOR DATA

model also predicts that there should be a constant
difference between the stirred reactor blowout and
the experimental chamber blowout. The trend observed
here may reflect the departure of the stirred reactor
from the assumed simple kinetic picture.

The recirculation models and the actual performance
of a combustor are compared by the efficiency vs loading
rate curve. Given this information about a combustor's
performance, a value of R, the recirculation ratio, and
V_2/V_1 may be chosen so that the theoretical behavior
will match the model behavior. Both the position of the
curve (blowout loading rate) and the chamber outlet
efficiency are adjusted in these models by the use of
gross bypassing and of inactive volumes. These two
variables do not affect the basic shape of the efficiency
loading rate curve. In addition, data on the size and
composition of the individual zones will make correlation
between theory and experiment more meaningful since
fewer constants are then to be determined from the data.
Such data were obtained by the use of sampling traversed
across the chamber and by photographic measurements. The
behavior of the combustor pattern as the flow approached
the blowout limit suggests that the bright zone of
Figure V-7 be taken as the central core (of volume V_1),
and the dark eye of the pattern be taken as the

recirculation zone (of volume V_2). This results in such
a small V_2/V_1 ratio, however, that a model calculated
on this basis does not give a reasonable model
performance.

In the recirculation models discussed in Chapter
III, the performance of a combustion chamber was simu-
lated by using only two zones whose relative volumes
could be varied. In a real chamber, however, the
postulation of only two zones and the consequent large
and abrupt change in composition between them is in-
consistent with reality. It is not surprising that a
model incorporating this assumption might fail to
provide a basis for correlating the data. As may be
seen from the traverses of composition within the chamber,
the change in burnedness in moving between the various
zones in the chamber is gradual, and a model allowing
for a more nearly continuous change would probably be
in better agreement with the observed data.

If one considers a circulatory flow pattern in
which gases may enter and leave at the circumference,
the inner zone (or zones), further removed from the
circumference of the combustion pattern, receive a
smaller fraction of the fresh, combustible gases, and
consequently, are less "heavily loaded" than those
outer zones nearer to the circumference. In such a

combustor as the feed rate is increased, the outer zones
will blow out first because of their heavier loading
rate, and the inner zones will consequently receive a
less well-burned feed since the outer, shielding zones
now contain more unburned gases. In a conceptual model
such as this, as the feed rate is increased the region
of most intense burning rate will gradually recede
from the circumference of the combustion pattern to
the center until the inner-most zone of the model blows
out, causing total extinction of the flame.

Although a two-zone approximation to this behavior
has already been seen to be unsatisfactory, treatment
of this model by integration of the performance of
differential elements would be a formidable task. A
satisfactory approximation considers recirculation models
involving a small number of identical elements, each
successive recirculation zone being fed by its
immediate predecessor , and receiving recirculated
gases from its immediate successor. Burned gases from
a typical zone are split in two, one portion feeding
the recirculation zone which is its immediate predecessor
and the other feeding the zone which is its immediate
successor. A diagram of such a model is shown in
Figure VI-7. Since this extended recirculation model
is an approximation to the circumferentially-fed

recirculation model described above, the recirculation
ratios and relative zone volumes at each stage of the
model are   independent of previous model stations.
The volumes (comparable to finite-difference intervals
in a conventional finite-difference solution) are
taken equal to each other (or in the case of cylindrical
coordinates, for example, may be proportional to the
distance from the origin) and the recirculation ratios
representing the diffusional transport of matter in
the chamber, are equal (or again may be proportional to
the distance from the inner zone).

For prediction of combustor performance using
this model only variable, the recirculation, is in
principle required to find the behavior of the
circumferentially-fed recirculation model. A character-
istic recirculation ratio having been chosen, a model
with a sufficient number of volumes is calculated to
make its behavior practically the same as the infinite-
number-of-zones case. In practice, the calculation of
a model containing more than four or five zones is too
laborious to consider by hand calculation techniques,
and for models containing this small number of zones,
the behavior of the model is strongly dependent on the
number of zones in the model. This is shown in Figure
VI-8, where three cases are calculated for three
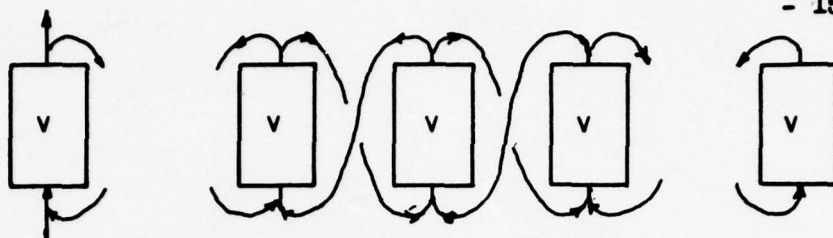
FIGURE VI-7: EXTENDED RECIRCULATION MODEL

2 ZONES
R = 0.65

3 ZONES
R = 1.0

4 ZONES
R = 1.4

BURNEDNESS

FIGURE VI-8: EFFECT OF NUMBER
OF ZONES IN EXTENDED RECIR-
CULATION MODEL

G/VP^n
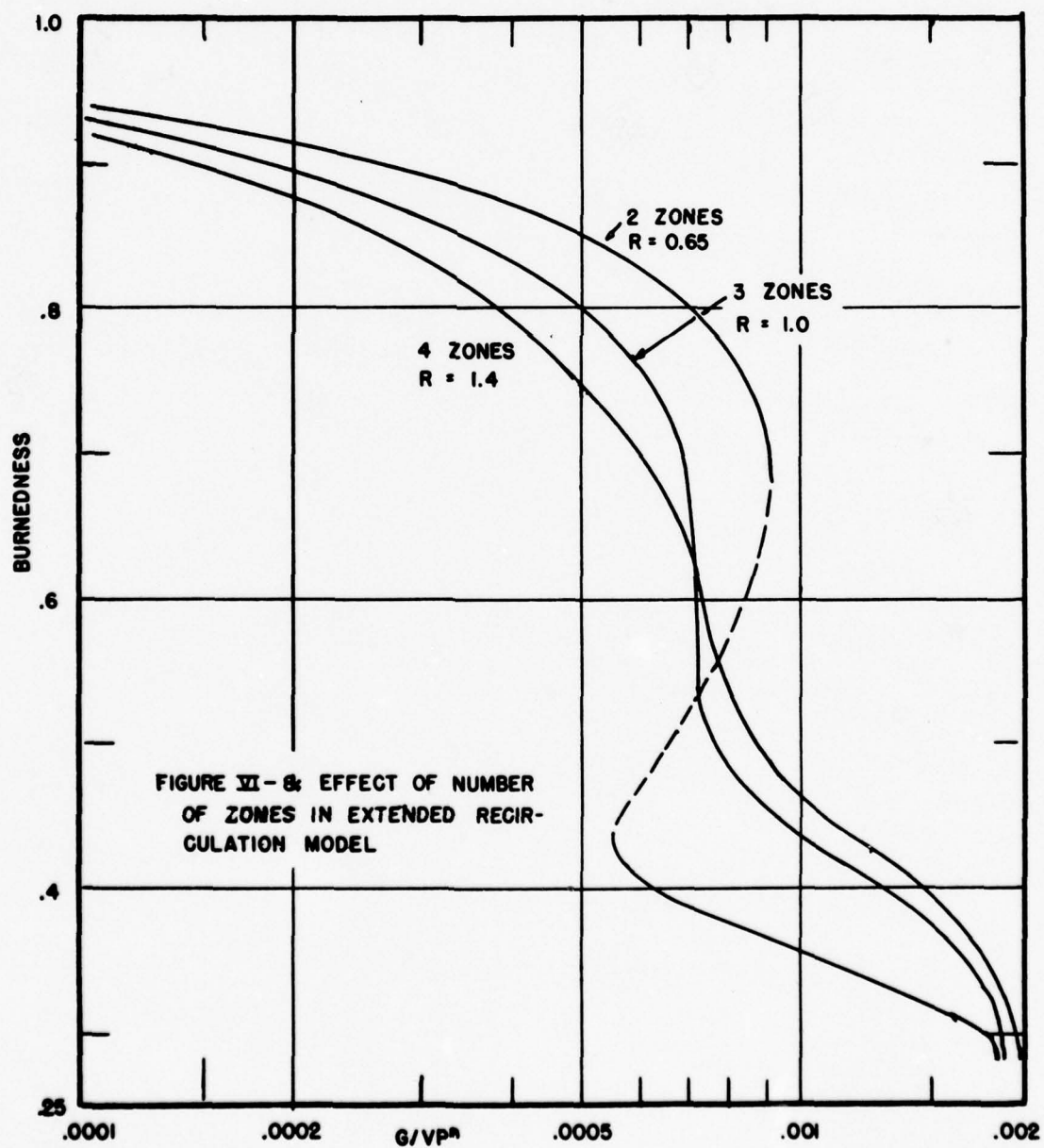
different models. (for this calculation, R in each
case was so chosen to bring the blowouts to about the
same burnedness.) In these calculations both the volume
sizes and the recirculation ratios have been taken to
be independent of position in the model.

The effect of the number of volume units, p, in
a model is better shown by comparison of the models on
a basis of (total feed)/(first volume) ratio. Since
at high burnedness the recirculation zones contribute
little to the performance of a chamber, performance
curves for models of different p's will coincide when
plotted on this basis. Using this basis the behavior
of a model of constant recirculation ratio and initial
volume but of varying number of zones is shown in
Figure VI-9.

When the calculated performance curves are plotted
in this manner, two interesting observations emerge:
(1) additional zones do not cause corresponding addi-
tional humps in the performance curve (as did the first
recirculation zone), and (2) increasing the number of
zones of the model increases the stability of the
residual flame, but does not affect the stability of
the first zone significantly. This suggests that if a
residual flame zone exists in a combustor, there will
be a sudden change in combustion efficiency as the
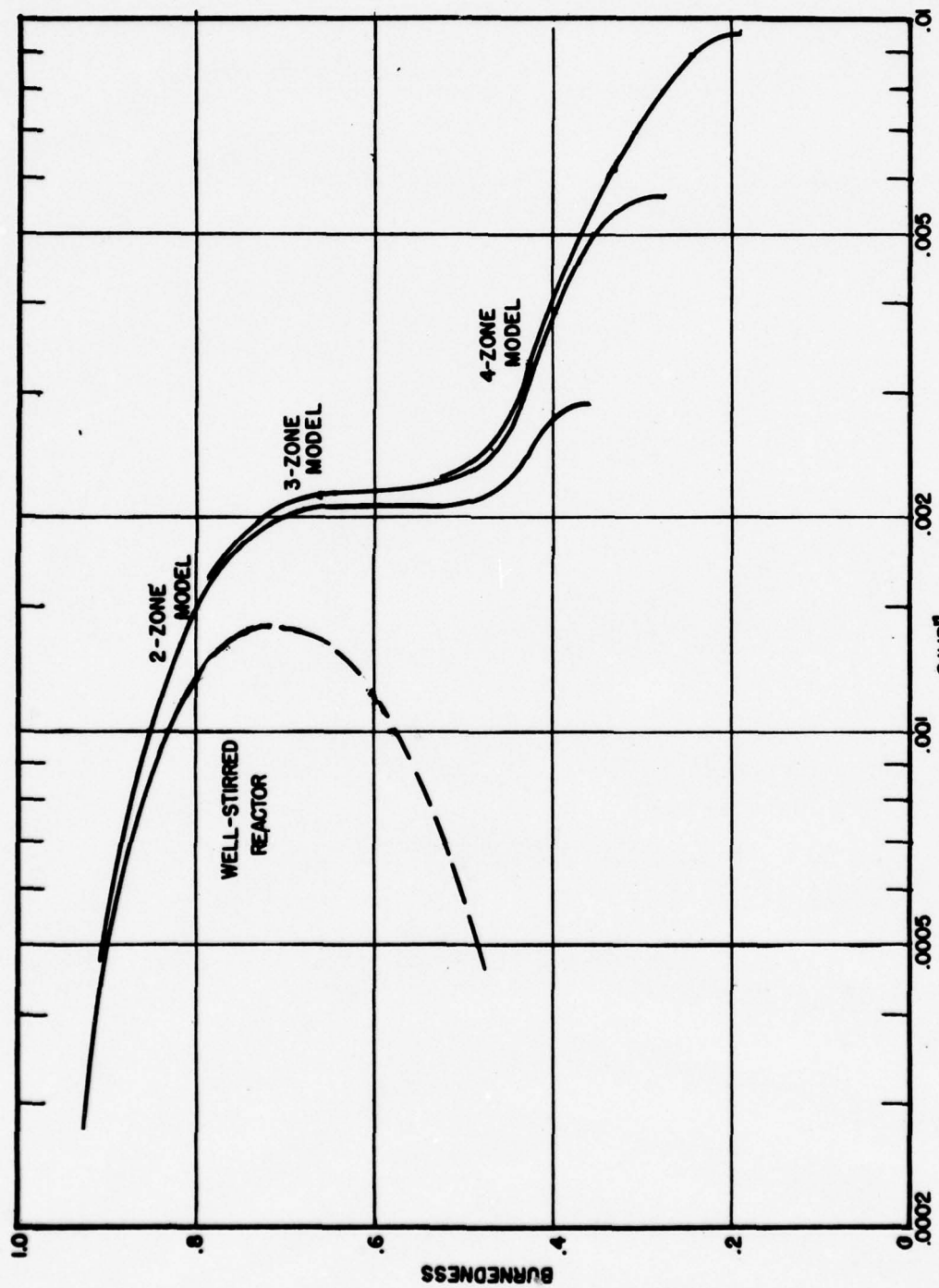
FIGURE XI-9: EXTENDED RECIRCULATION MODEL, FIRST ZONE VOLUME AS BASIS, R = 1.0

main combustion zone blows out, leaving the residual
flame, but further increases in flow rate will only
cause the residual flame to recede gradually from the
main combustion zone. No additional partial blowout
of zones within the residual flame are to be expected.

The possibility of designing combustors of much
improved stability is also suggested. By deliberately
allowing for a zone which is sufficiently sheltered
and which is deep enough to allow the residual flame
to recede into it, a substantial distance, a chamber
equivalent to a high-p model is obtained, having a
high ratio of ultimate blowout loading to initial
blowout loading.

The use of this extended recirculation model will
now permit a fitting of the experimental data obtained
in the present experiments. There are two variables
in the model, namely, the recirculation ratio and the
number of recirculation zones. In addition, allowance
must be made for "dead" or inactive zones in the chamber
and for gross bypassing of the combustion zones.

Only the variables of recirculation ratio and
number of zones will affect the shape of the performance
curve. Increasing recirculation ratio will cause a
change in the sharpness of the first blowout limit
without causing much change in the ratio of the two

blowout limits (Figure VI-10). An increase in the number
of zones will increase the relative stability of the
recirculation zone (Figure VI-9).

A change in gross bypassing of gases around the
combustion zones affects both the outlet burnedness
(by dilution) and the relative stability with respect
to the stirred reactor. It does not, however, affect
the shape of the curve at all. The addition of "dead"
space to the combustion chamber model permits the
apparent volumetric heat liberation rate to be adjusted
so that the model prediction is in conformity with the
stirred reactor data. The effectiveness of this type
of model in correlating the data on chamber efficiency
is demonstrated in Figure VI-11, where the experimental
data are compared with a model having a recirculation
ratio of   one, two or three recirculation zones plus
bypassing and dead space. By plotting these data on
log-log coordinates, movements corresponding to
addition of dead space or bypassing correspond to
either a simple lateral and/or vertical displacement
of the two curves. (The raw data have been shifted
by a constant factor of 3×10^{-3} to facilitate plotting
on this graph.)
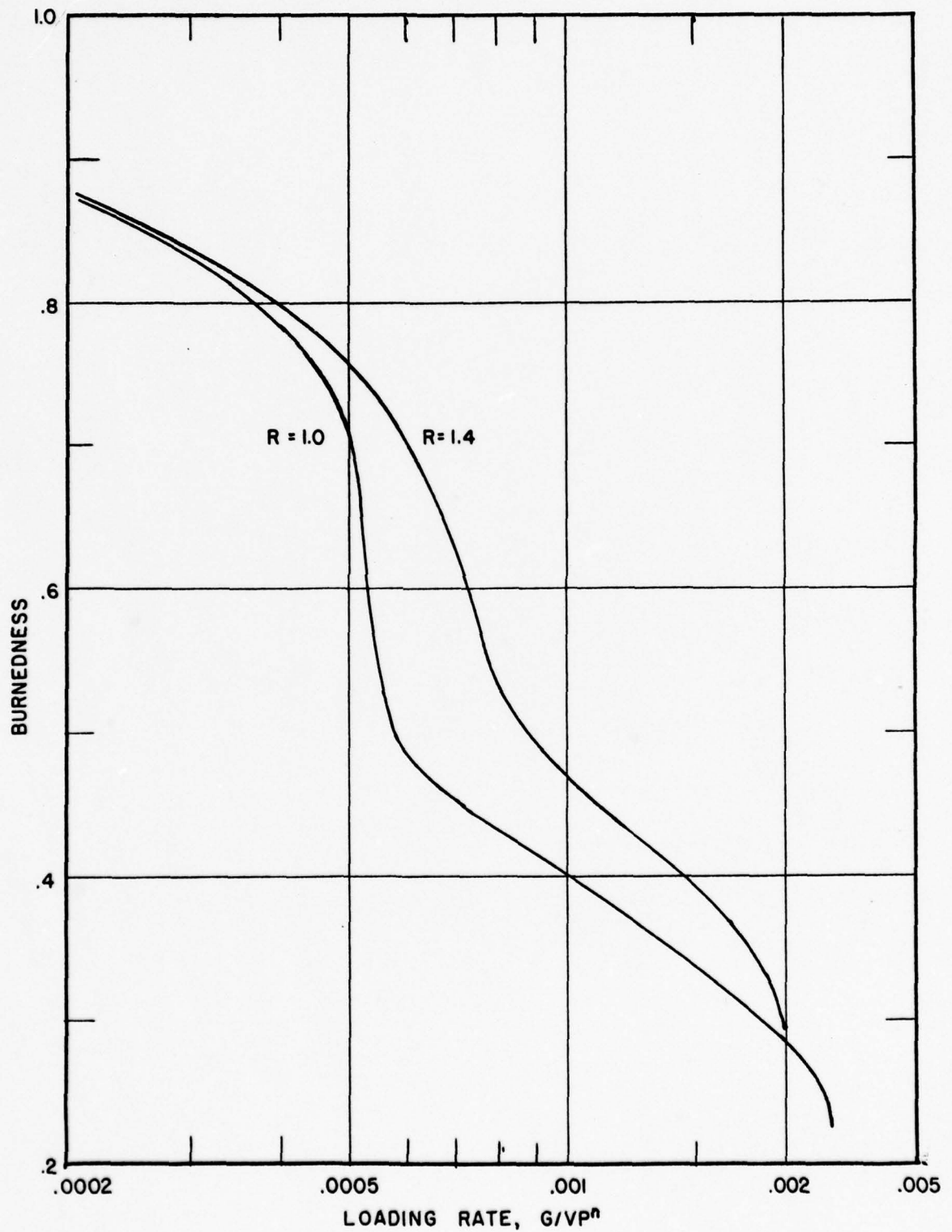
FIGURE VI-10: EFFECT OF RECIRCULATION RATIO IN FOUR-
ZONE RECIRCULATION MODEL
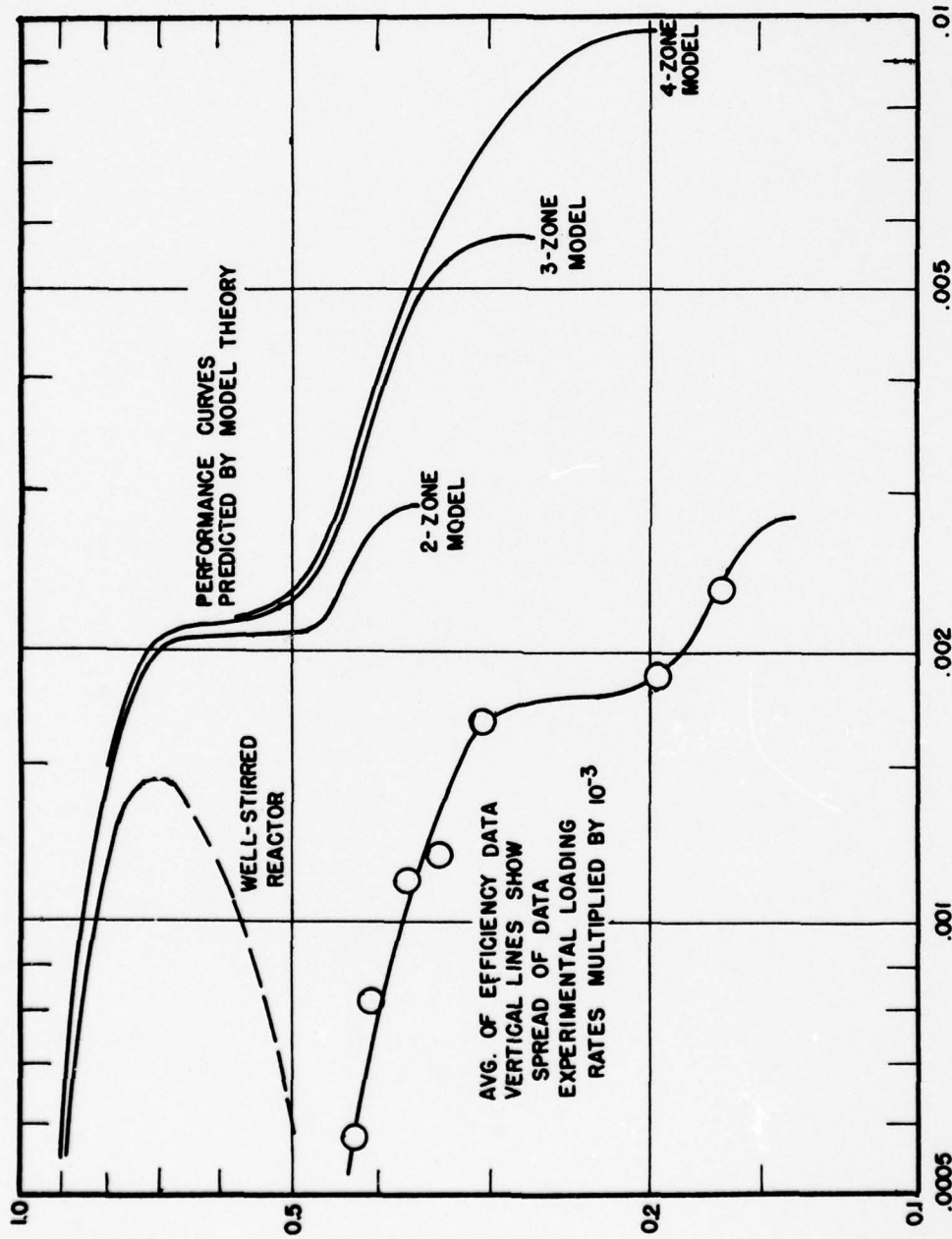
FIGURE XI-11: COMPARISON OF MODEL THEORY WITH EXPERIMENTAL COMBUSTOR PERFORMANCE.

Summary

The demonstration of the ability of simple theoretical combustion chamber models to reproduce the behavior of an experimental chamber in a semiquantitative manner is of great significance. Previous models of combustion chamber performance have not, as yet, been used in conjunction with an experimental program. In this investigation several theoretical models were considered, and the calculated performance of the models was compared with the experimentally measured performance of a simple chamber which demonstrated characteristics common in many practical chambers.

Ultimately one would hope to use models of this nature to predict the performance of any combustion chamber. Using a relatively small number of variables it has been possible to generate a wide variety of performance curves for various combustor models. Thus, for instance, in moderately well-stirred systems, typical of can-type combustors, the extended recirculation model suggested seems to be applicable to the prediction of residual flame phenomena, and the use of the two-stability-limit model is suggested for the analysis of pressure interaction phenomena. Hopefully extension of these modeling techniques will lead to a general method of combustion chamber analysis, and possibly

permit an a-priori prediction of the combustion chamber
performance from fundamental physical data involving
only a small number of characteristic zones and their
flow interactions.

CHAPTER VII

CONCLUSIONS AND RECOMMENDATIONS

Conclusions

1. The theoretical models of combustion chambers have been investigated. These models have predicted qualitatively phenomena observed in actual combustors.

   a) A two-zone model of stirred reactors in parallel was used to predict the effects of pressure interaction between two combustion zones.

   b) A two-zone recirculation model in which one zone was fed only partially burned products produced in the first and the first zone received a mixture of fresh gases and burned products from the second zone was used to investigate recirculation phenomena. This model showed the conditions for residual flame, hysteresis, and flickering flame phenomena.

   c) An extended recirculation model was investigated which allowed for a more continuous variation in composition in the combustor than could be obtained in a two-zone model. This model showed phenomena similar to those observed in the two-zone model.

2. An experimental combustion chamber, fed by a two-dimensional jet of a pre-mixed fuel/air mixture was built and operated to test the models of combustion chambers quantitatively.

a) All the models predicted that stirred reactor blow-out and combustion chamber loading rates should be displaced from each other by a constant factor. This was not observed. This deviation was postulated to result from the breakdown of certain assumptions and from departure of the reaction kinetics from a mechanism controlled by a single reaction.

b) The two-stability-limit model predicted the displacement of the two stability limits of the experimental reactor to a reasonable approximation.

c) The overall combustion efficiency of the chamber was measured by gas sampling. These data were correlatable by the extended recirculation model.

d) The combustion efficiency of the chamber contents was determined by gas sampling. These data showed a qualitative behavior in agreement with the models. No attempt was made to fit the data quantitatively.

e) The effect of pressure on the blowout loading, $G/VP^{1.8}$ was determined experimentally. An average pressure exponent, "n" of 1.6 was found which compares well with reported literature values of 1.6 to 1.8. A trend of "n" was observed with variation in fuel/air ratio. However, no significance was attached to this trend because of unequal Reynolds numbers between experiments.

Recommendations

(1) The prediction of combustor performance by the use of these models requires experimental data on combustion

efficiency vs loading rate for the well-stirred reactor. There is not yet available an adequate amount of these performance data for the stirred reactor. It is recommended that an experimental program be undertaken to determine these data and to determine whether they are in agreement with the performance predicted from the stirred reactor theory.

(2) Although the experimental program undertaken gives some support to the theories, unexplained phenomena still exist. It is recommended that further experimental work be undertaken to establish methods for fitting the combustion chamber phenomena to the theory. Investigation of certain special phenomena, is also recommended:

a) To fit the present data to existing stirred reactor data it is necessary to postulate substantial bypassing of the combustion zones. An experimental verification of the extent of this bypassing is recommended.

b) The theory has only been fitted at one fuel/air ratio to experimental performance data. It is recommended that other fuel/air ratios be investigated and that particularly, the prediction of the effects of fuel/air ratio changes by the theoretical models be studied.

3. Data on the stirred reactor has indicated some lack of complete mixing. An investigation of the stirred reactor is recommended to determine what the consequences of this lack of mixing are, and to determine which zones in a combustion

chamber are comparable to a unit volume of both "perfectly" stirred reactor and experimental stirred reactor.

APPENDIX A

DERIVATION OF THE WELL-STIRRED REACTOR EQUATION

The derivation of a generalized well-stirred reactor equation has already been discussed. In the literature several more detailed discussions of the exact algebraic form of the equations have been given for specific postulated stoichiometric schemes (3, 14). Since it was felt that the use of complex stoichiometric schemes did not yield a justifiable increase in accuracy of the model predictions, the derivation of the algebraic relation between burnedness and loading rate used in this thesis was restricted to the simplest possible case in which no intermediate products are postulated.

The stoichiometric equation of the reaction representing the overall combustion reaction was written for propane,

$$C_3H_8 + 5 O_2 \longrightarrow 3 CO_2 + 4 H_2O \qquad \text{A-1}$$
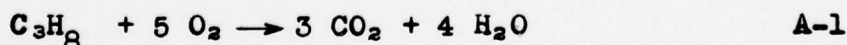
The heat of reaction was assumed to be sufficient to give a 2270°K temperature rise for a stoichiometric mixture, and the heat capacities of the reactants and products were assumed to be equal and independent of temperature so that the fraction of fuel consumed, β, was related to temperature for a stoichiometric mixture by:

$$\beta = \frac{T - T_o}{2270} \qquad \text{A-2}$$

In the simplest description of the stirred reactor the identifiable components of the mixture at any stage of completion of combustion are burned products plus fuel and oxygen; therefore only a single variable, β, is necessary to specify the composition of the mixture. If the fraction φ of the stoichiometrically required fuel is used, then for each 5 moles of oxygen the moles of each component are given as follows:

C_3H_8	$\varphi(1-\beta)$
O_2	$5(1-\varphi\beta)$
N_2	18.8
H_2O and CO_2	$7\varphi\beta$
Total mols	$23.8 + \varphi(1+\beta)$

If a rich fuel-air mixture is used, there should be no unburned fuel appearing at completion of combustion (as would be called for by the above stoichiometry for $\varphi > 1$). Thus for rich mixtures the stoichiometric equation A-1 is altered to give:

$$\varphi\, C_3H_8 + 5\, O_2 \longrightarrow \varphi\left[3(CO + CO_2) + 4(H_2 + H_2O)\right]$$

$$\text{A-3}$$
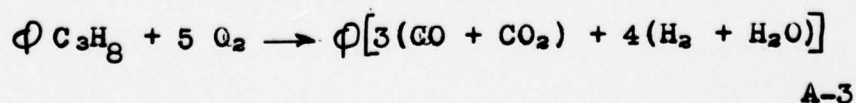
In this equation the summation of oxygen atoms on the right-hand side of the equation must be equal to 10. Longwell and Weiss (24) and Baker (3) have both used this assumption to fit data on the rich side, and in both cases

the authors assumed that the water-gas equilibrium could be used to calculate the composition of the products. The present calculations were simplified by assuming that the heat of reaction contributed by the water-gas reaction was negligible compared to the heat released by the initial combustion step. With this assumption it is not necessary to specify the composition of the mixture to calculate the temperature. The stoichiometry of reaction A-3 yields the following species (basis - 5 moles oxygen):

C_3H_8	$\phi(1-\beta)$
O_2	$5(1-\beta)$
N_2	18.8
products	$7\phi\beta$
total	$23.8 + \phi + (6\phi-5)\beta$

For fuel-air mixtures other than stoichiometric the heat balance equation, A-2, relating temperature and burnedness, must be modified. In principle an enthalpy balance should be made to account for dissociation products and water-gas equilibrium, especially for rich mixtures. However, calculations may be greatly speeded by the simplifying assumptions of (1) a constant heat capacity of the gases and (2) ignoring the energy of the water gas reaction and dissociation products. For the present calculations the following temperature-burnedness relations were used:

$$\frac{500,000 \, \phi}{30 \, \phi + 190} \qquad \beta = T - T_o \text{ (lean)} \qquad\qquad \text{A-4.1}$$

$$\frac{500,000}{30 \, \phi + 190} \qquad \beta = T - T_o \text{ (rich)} \qquad\qquad \text{A-4.2}$$

It should be noted that for a stoichiometric fuel-air mixture both rich and lean schemes are identical.

The composition of the gases in a stirred reactor in which this combustion occurs is a function of the firing rate to the reactor. This function is derived from the reaction rate equation applicable to this reaction. For this case here, only a single equation is required, and this is assumed to be an equation of first order in each of the reactants. The temperature dependence of the rate is indicated by the conventional exponential term:

$$-\frac{dN_F}{Vdt} = \sqrt{T} \, k' \, e^{-E/RT} \cdot C_{O_2} \cdot C_F \qquad\qquad \text{A-5}$$

From the stoichiometry discussed the concentrations of the fuel and oxygen, C_{O_2} and C_F, may be found as the respective mole fraction terms times the molar density of the gas determined from the perfect gas law;

$$C_{O_2} = \frac{5 (1 - \phi\beta)}{23.8 + \phi(\beta + 1)} \quad \frac{P}{RT}$$

$$C_F = \frac{\phi(1 - \beta)}{23.8 + \phi(\beta + 1)} \quad \frac{P}{RT} \Bigg\} \quad \text{lean} \qquad \text{A-6.1}$$

$$C_{O_2} = \frac{5 (1 - \beta)}{23.8 + \phi + (6\phi - 5)\beta} \quad \frac{P}{RT}$$

$$C_F = \frac{\phi(1 - \beta)}{23.8 + \phi + (6\phi - 5)\beta} \quad \frac{P}{RT} \Bigg\} \quad \text{rich} \qquad \text{A-6.2}$$

Since the rate of fuel consumption is given by $G \cdot \beta$;

$$\frac{G}{VP^2} = \frac{k'e^{-E/RT}}{T^{3/2}} \frac{5\phi(1 - \phi\beta)(1-\beta)}{\beta[23.8 + \phi(1+\beta)]^2} \quad \text{lean} \quad \text{A-7.1}$$

$$\frac{G}{VP^2} = \frac{k'e^{-E/RT}}{T^{3/2}} 5 \frac{(1 - \beta)^2}{23.8 + \phi + (6\phi - 5)\beta} \quad \text{rich} \quad \text{A-7.2}$$

For calculational purposes it is desirable to normalize equations A-7 so that those changes in operating variables which counteract each other will be evident. At the same time it is desirable that each of the groups chosen be independent i.e. so that a change in a factor in one group will not affect the values of the other groups.

In an experiment to determine the reaction rate constants k' and E, the rate constant of the reaction, $k = k'e^{-E/RT}$, will be found at some high temperature, and by varying the temperature k' and E may be found separately. Since this

experiment must be carried out in a temperature region where the reaction proceeds with a reasonable velocity, knowledge of k' at room temperature will be very uncertain. This suggests that an appropriate normalization factor would be the rate constant, k, determined at some high temperature designated as the key temperature, T_K. Temperatures would also be normalized by T_K. This normalization procedure yields the reduced equation;

$$\frac{G}{VP^2} \frac{R^2 T_K^{3/2}}{k' e^{-E/RT_K}} = \frac{e^{-E/RT_K[(1/T_r)-1]}}{T_r^{3/2}} \frac{5\phi(1-\beta\phi)(1-\beta)}{[23.8+(1-\beta)]^2 \beta}$$

A-8

For this investigation a basic stirred reactor curve calculated from A-8 was used to compare the performance curves of the various models. This curve is based on the following constants:

$$\phi \quad = \quad 1.0$$
$$T_K \quad = \quad 2000\,°K$$
$$T_o \quad = \quad 500\,°K$$
$$T_{af} \quad = \quad 2772\,°K$$
$$E/RT_K \quad = \quad 10$$

A plot of $(G/VP^2)(R^2 T_K/k' e^{-E/RT_K})$ vs β is shown in Figure A-1 for these constants. This curve (plotted elsewhere in this thesis as G/VP^2 or G/VP^n vs β is used to generate all of the other model performance curves calculated.

In the model investigating the effect of non-uniform fuel-air ratio on combustor performance curves for stirred reactors being fed a rich fuel-air mixture were required. For this purpose Equation A-7.2 was normalized and curves calculated for a ϕ of 1.2 and 1.5 using all other constants shown above the same.
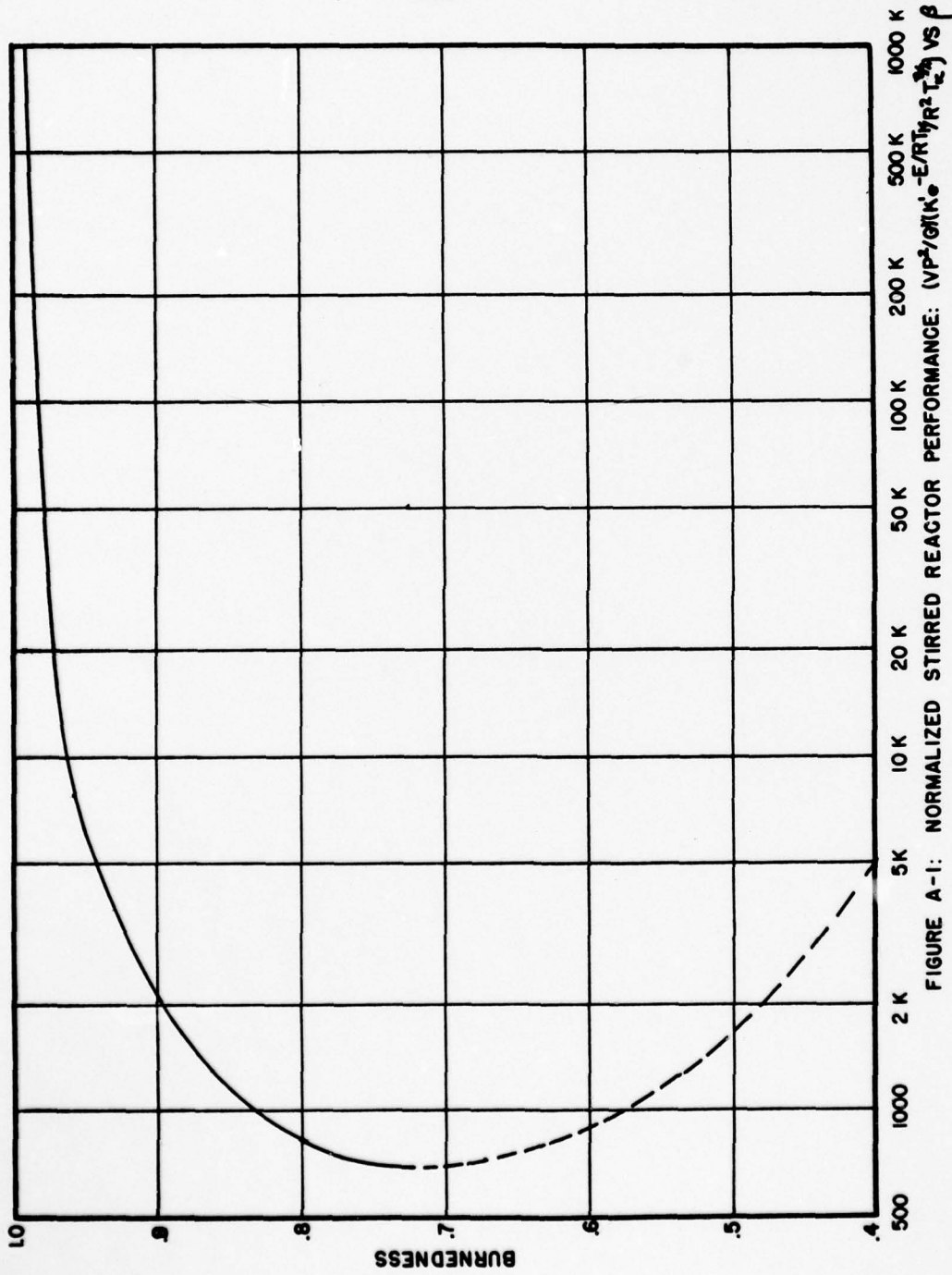
FIGURE A-1: NORMALIZED STIRRED REACTOR PERFORMANCE: $(VP^2/G \cdot (k'_e{}^{-E/RT}/\rho_R{}^2 T_e^{3/2}))$ vs β

APPENDIX B

MULTI-STEP KINETIC SCHEMES

Calculational techniques discussed in the main body
of this thesis have assumed that the reaction rate of
burning gases is limited by a single chemical reaction
throughout the composition range of interest. It must be
recognized that this is an assumption justified only by
the resulting simplifications in the theory and the hope
that it will introduce only a small error in the predicted
model performance. In fact it is possible to make rigorous
allowance for multi-step reaction although for more than
two or three steps the calculational work becomes prohibitive.

Calculations of multi-step cases are greatly simplified
by the use of graphical techniques to solve the stirred
reactor equations. To illustrate the use of such techniques
a typical two-step mechanism will be considered. The two
steps postulated are:

$$C_3H_8 + 7/2\ O_2 \longrightarrow 3\ CO + 4\ H_2O \qquad\qquad \text{B-1}$$
$$3\ CO + 3/2\ O_2 \longrightarrow 3\ CO_2 \qquad\qquad \text{B-2}$$
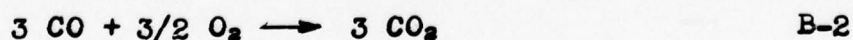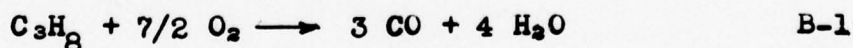
For this postulated mechanism two variables are required to
specify the composition, representing respectively the
progress of reactions B-1 and B-2. It is assumed that
operation is adiabatic so that the temperature is fixed
by the composition and initial temperature of the unreacted

expression.

$$-\frac{dN_{C_3H_8}}{Vdt} = \sqrt{T} \ k_1' \ e^{-E_1/RT} \ C_{C_3H_8} \qquad \text{B-3}$$

$$\frac{dN_{CO}}{Vdt} = 3 \ \sqrt{T}k_1' \ e^{-E_1/RT} \ C_{C_3H_8}$$
$$\text{B-4}$$
$$- \sqrt{T} \ k_2' \ e^{-E_2/RT} \ C_{CO} \cdot C_{O_2}$$

Substitution for appropriate concentration terms yields:

$$(G/V)d\beta = \sqrt{T} \ k_1 \ e^{-E_1/RT} \ \frac{(1-\beta)}{\xi} \ \frac{P}{RT} \qquad \text{B-5}$$

$$\frac{3G}{V}d(\beta-\gamma) = 3 \ T \ k' \ e^{-E_1/RT} \ \frac{1-\beta}{\xi} \ \frac{P}{RT}$$
$$\text{B-6}$$
$$- T \ k' \ e^{-E_2/RT} \ \frac{3(5/\varphi -7/2\beta-3/2\gamma)(\beta-\gamma)}{\xi^2} \ \frac{P}{RT}$$

Relative reaction rate constants of reactions B-1 and B-2 as well as a reduced feed rate are now defined:

$$\text{Relative Reaction Rate,} \ \xi = \frac{RT_K \ k_1 \ e^{-E_1/RT_K}}{p \ k_2 \ e^{-E_2/RT_K}}$$

$$\text{and} \quad G_r = \frac{G}{VP^2} \left[\frac{R^2 \ T_K^{3/2}}{k_2 \ e^{-E_2/RT_K}} \right]$$

Equation B-5 thus becomes:

$$G_r d\beta = \xi \ \frac{e^{-(E_1/RT_K)(1/T_r -1)}}{T_r^{1/2}} \ \frac{1-\beta}{\xi} \qquad \text{B-7}$$

fuel-air mixture. It will be assumed that the oxygen is from air, and consequently specification of composition and temperature requires that allowance be made for the presence of nitrogen. Let the two composition variables, β and γ be defined as:

β = fraction of C_3H_8 consumed by B-1

γ = fraction of CO equivalent to C_3H_8 consumed by B-2.

The composition of the gas corresponding to any pair of β, γ values may now be calculated (let φ times the stoichiometrically required fuel be used):

Component	mol pr mo C_3H_8
C_3H_8	$1 - \beta$
O_2	$5(1/\varphi) - 7/2\beta - 3/2\gamma$
N_2	$18.8(1/\varphi)$
H_2O	4β
CO	$3(\beta-\gamma), \ (\beta < \gamma)$
CO_2	3γ
Total	$\xi = 1 + 23.8(1/\varphi) + 5/2\beta - 3/2\gamma$
Temperature	$T = T_o + \dfrac{\Delta H_1}{Cp}\beta + \dfrac{\Delta H_2}{Cp}\gamma$

For each reaction postulated there is a corresponding reaction rate expression. For the present case assume that the initial cracking of propane is the rate-limiting step in reaction B-1 and that the combustion of carbon monoxide may be represented by a simple second-order reaction rate

and substituting B-5 into B-6 yields:

$$G_r d\gamma = \frac{e^{-(E_2/RT_K)(1/T_R-1)}}{T_r^{3/2}} \frac{(5/\phi - 7/2\beta - 3/2\gamma)(\beta-\gamma)}{\epsilon^2} \qquad \text{B-8}$$

The calculation of temperature for substitution into B-7 and B-8 is simplified by the relation:

$$T_r = T_r + \Delta_{1_r}\beta + \Delta_{2_r}\gamma \qquad \text{B-9}$$

where Δ_{1_r} and Δ_{2_r} represent the corresponding reduced adiabatic flame temperature rises resulting from complete reaction of reactions B-1 and B-2 at the prevailing fuel-air ratio.

In calculations based on B-7 and B-8, two cases may be distinguished; (1) where it is desired to investigate a single stirred reactor with varying values of ξ, and (2) where it is desired to investigate staged reactors in each member of which the relative reaction rate parameter is the same.

Case I: Single stirred reactor. ξ varying. If a single stirred reactor is considered, then $Gd\beta$ and $Gd\gamma$ may be replaced by $G\beta$ and $G\gamma$ respectively. Corresponding division of each equation by β and γ yields the equations:

$$G_r = \frac{e^{-(E_1/RT_K)(1/T_r - 1)}}{T_r^{1/2}} \frac{1-\beta}{\beta\xi} \qquad \text{B-10}$$

$$G_r = \frac{e^{-E_2/RT_K(1/T_r-1)}}{T_r^{3/2}} \frac{(5/\phi - 7/2\beta - 3/2\gamma)(\beta-\gamma)}{\gamma\xi^2} \qquad \text{B-11}$$

Each of these equations may be represented graphically as G_r vs β for constant values of γ (or visa-versa). B-10 is plotted for a ξ value of 1.0. Superposition of the two graphs permits solutions for the values of β and γ corresponding to any given G_r. If these two figures are plotted on a coordinate of log G_r then changes in ξ are represented by translation of the graphs with respect to each other along the G_r axis, and for any position desired a set of β, γ values may be found. Figures B-1 and B-2 show such a graphical representation of equations B-10 and B-11 for the following constants:

$$E_1/RT_K = 5$$
$$E_2/RT_K = 10$$
$$\varphi = 1.0$$
$$\Delta_{1_r} = 0.674$$
$$\Delta_{2_r} = 0.462$$
$$T_{o_r} = 0.25$$
$$T_K = 2000°K$$

Three typical sets of solutions for ξ of 1.0, 0.3 and 0.1 are given in Figure B-3. Since the absolute magnitudes of the values of G_r in Figure B-3 reflect the normalization procedure they are of no significance in comparing these curves with experimental stirred reactor data. The choice of ξ or relative reaction rate, in this two-step mechanism must be based on the relative performances of the stirred

reactor with respect to some key point (such as the rate
at the firing rate giving the key temperature). The correct
ξ having been chosen, the absolute values of the reaction
rate constants are then found.

Case II: Multi-stage reactors, fixed ξ. In consider-
ing a multi-stage reactor system it is necessary to predict
the effect of feeding a stirred reactor with a partially
burned feed when the burning rate is significantly affected
by two (or more) reactions. So long as both reactions are
significant in determining combustion rate the relative
rates of change of β and γ differ at each point along the
single-stage stirred reactor curve. Hence for each postu-
lated degree of combustion of the feed a new stirred reactor
curve must be drawn. In the general case, a graphical
relation between inlet and outlet composition of a stirred
reactor being fed a feed composition β_o, γ_o is desired.

Since the rate of change of β and γ are specified
uniquely by β and γ (i.e. independent of reactor inlet
conditions), one may plot lines of constant $d\beta/d\gamma$ on a
graph of β vs γ. On such a plot the locus of all possible
reactor outlet conditions for any given β,γ combination
(or visa-versa) may be represented. For any combination of
β,γ represent reactor outlet conditions the $(\beta-\beta_o)/(\gamma-\gamma_o)$
ratio across the reactor must be equal to $d\beta/d\gamma$. From this,
loci of reactor outlet conditions from any given $\beta_o\gamma_o$
combination may be constructed. Similarly loci of plug-flow

reactor conditions may be found.

Given reactor inlet and outlet conditions (found from
Figure B-4) the feed/volume ratio is easily found from
either Figures B-1 or B-2. Since these figures were plotted
as $f_1(\beta,\gamma)/\beta$ and $f_2(\beta,\gamma)/\gamma$, a correction must be made for
the ratio $\beta/(\beta-\beta_o)$ or $\gamma/(\gamma-\gamma_o)$.
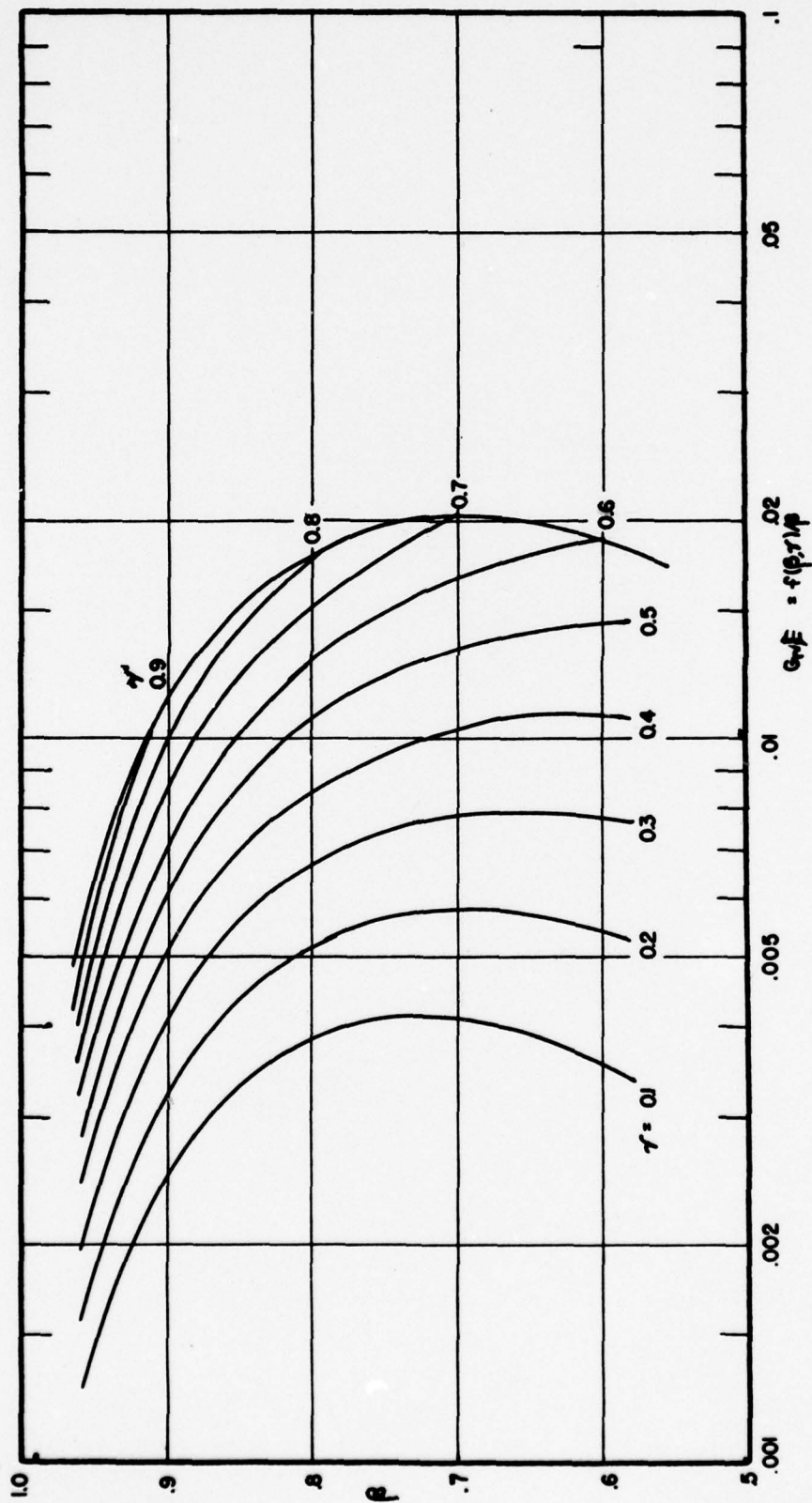
FIGURE B-I: PERFORMANCE OF TWO-STEP REACTION IN A WELL-STIRRED REACTOR: STEP I

- 184 -
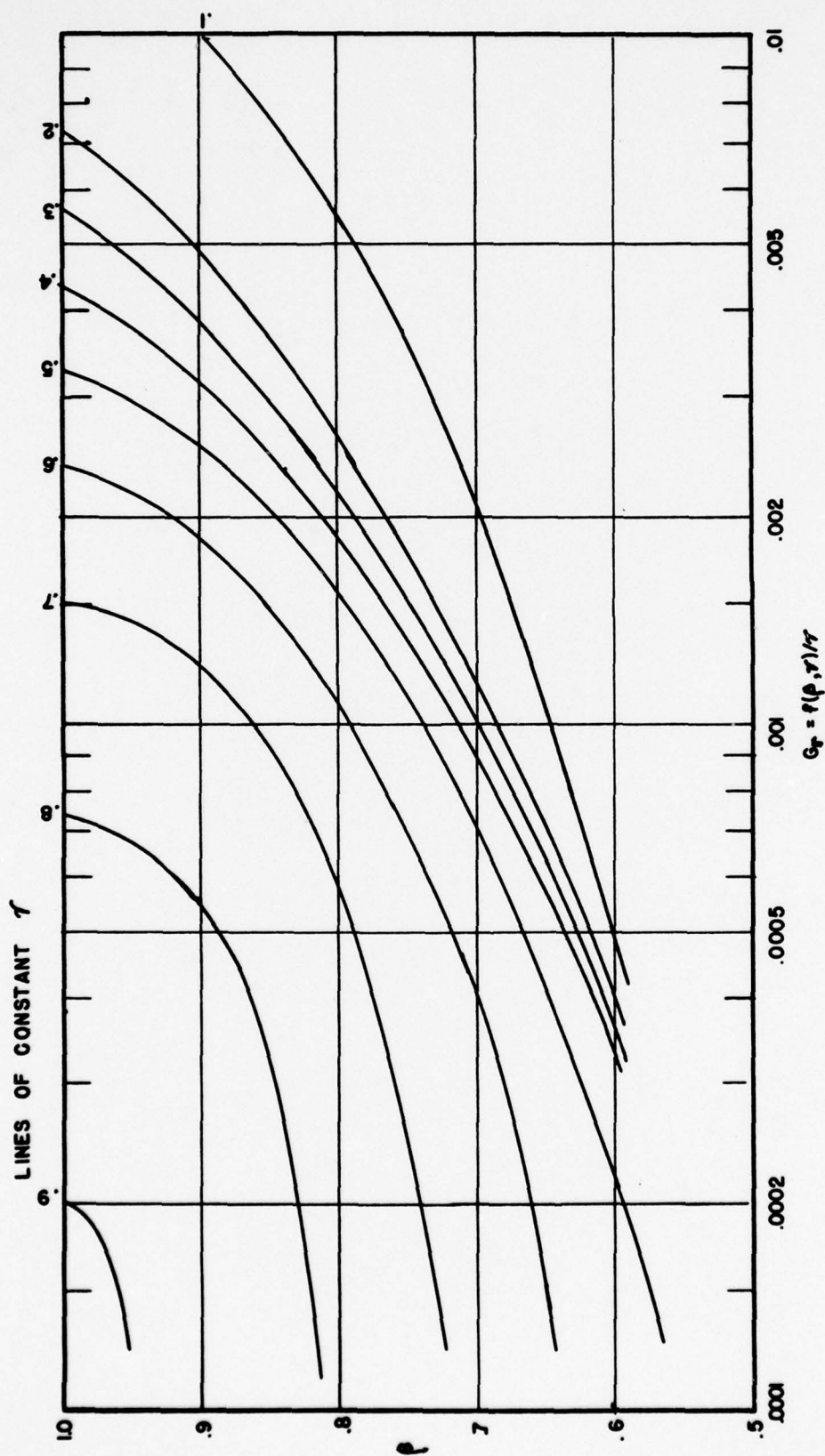
FIGURE B-2: PERFORMANCE OF TWO-STEP REACTION IN A WELL-STIRRED REACTOR: STEP 2

- 185 -
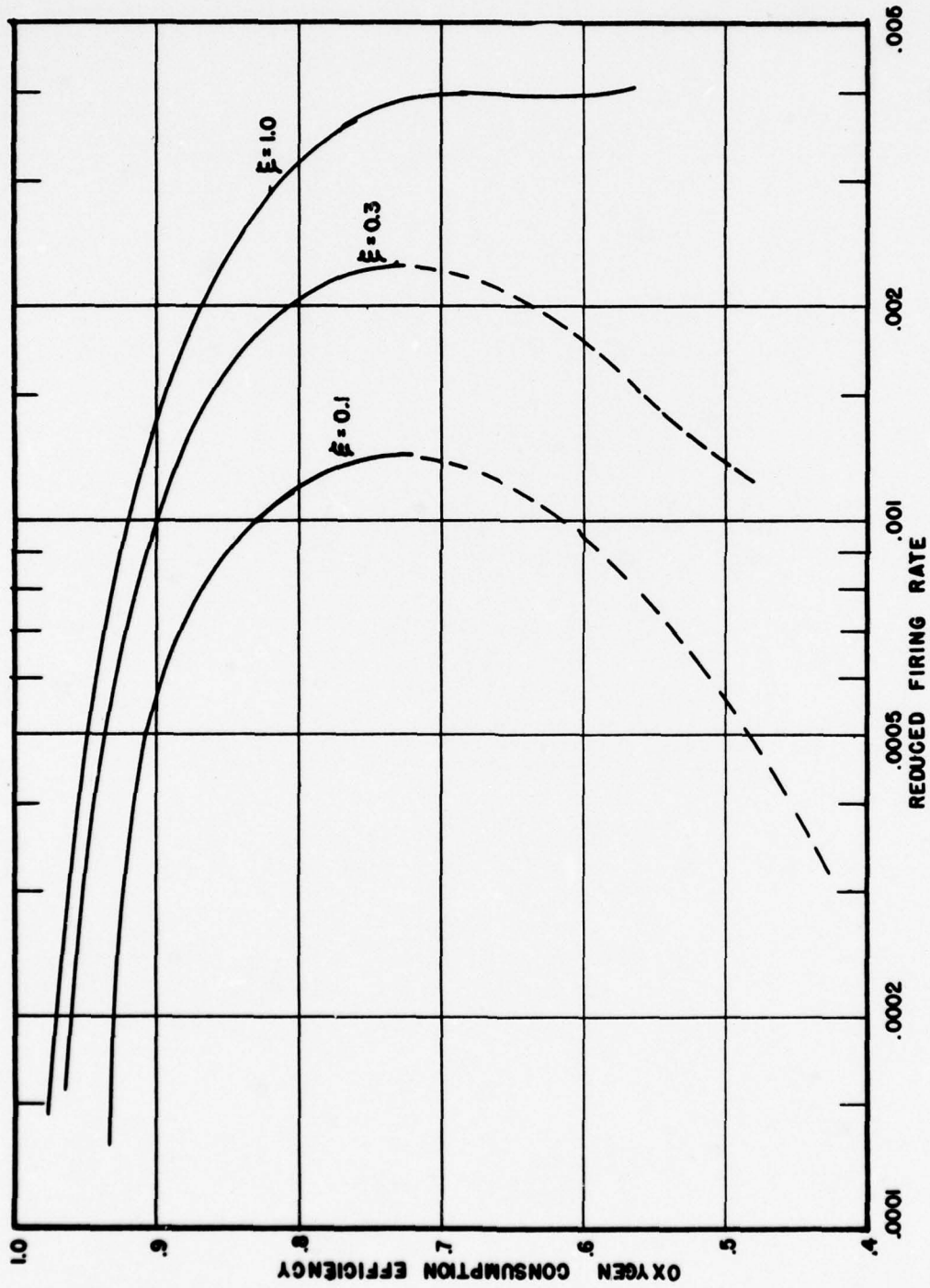
FIGURE B-3: PERFORMANCE OF TWO-STEP REACTION IN A STIRRED REACTOR: COMBINED RESULTS
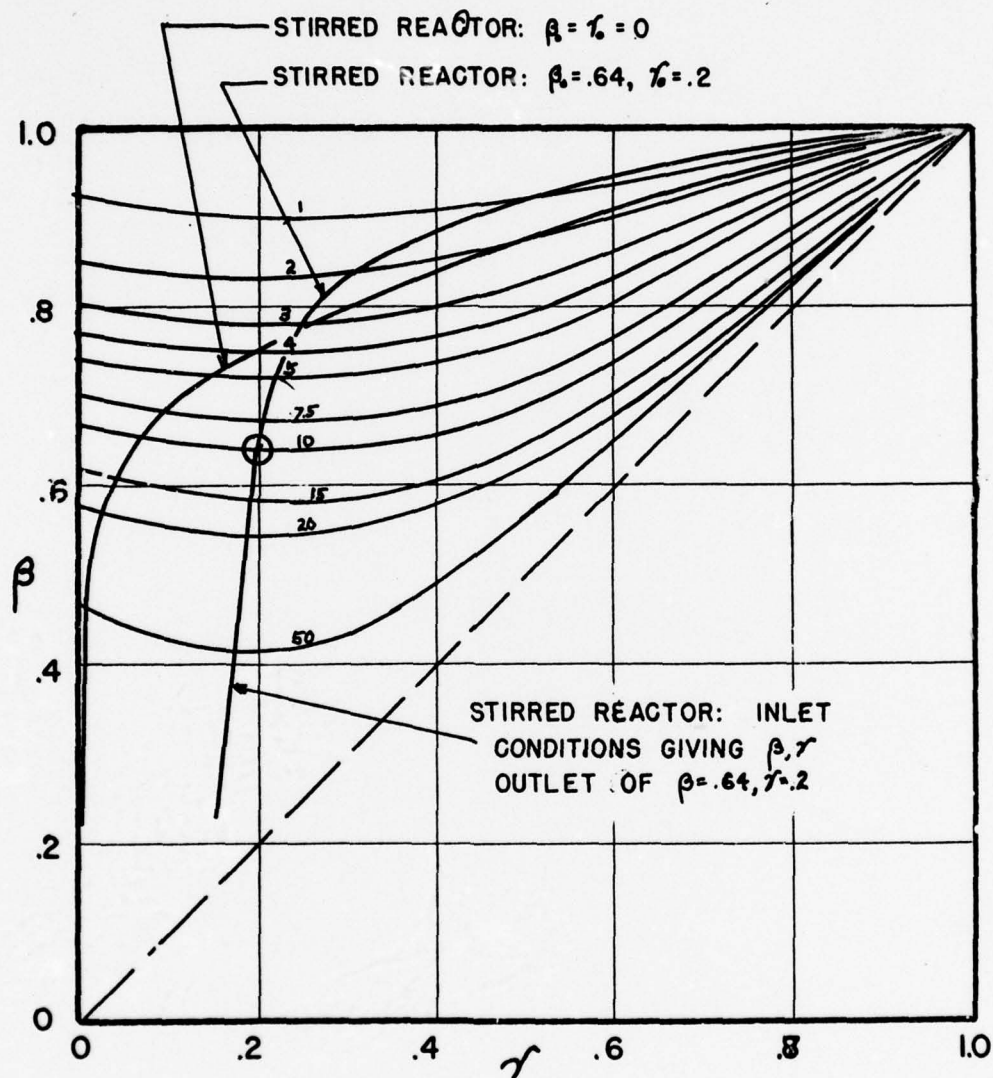
FIGURE B-4: PERFORMANCE OF TWO-STEP REACTION: LINES OF CONSTANT $\frac{d\beta}{d\gamma}$ ON COMPOSITION DIAGRAM. $E=1$

APPENDIX C

ESTIMATED HEAT LOSS FROM THREE-JET CHAMBER

Heat losses from the experimental chambers were known to be substantial because of the high surface-volume ratio and because of the opportunity for radiant heat transmission through and from the Vycor windows. Experimental estimation of this heat loss would be very difficult because of the multiple paths (radiation, conduction, convection) by which heat was lost. Heat loss rates were therefore estimated by calculation. The calculations were based on the geometry of the three-jet combustion chamber.

In calculating heat losses from this chamber several parallel mechanism must be considered:

(1) Convection to the firebrick and Vycor walls followed by:

      (a) direct or indirect radiation from the firebrick to the ambient gas

      (b) transfer by convection and radiation from the Vycor walls to the ambient

      (c) conduction through the firebrick from an inside face to an outside face followed by radiation-conduction transfer to the ambient.

(2) Gas radiation from the burning gases to the firebrick and Vycor walls followed by a, b, and/or c above.

In addition to these possible multiple-mechanisms, the problem

is complicated by the existence of strong temperature gradients in the firebrick and presumably also in the Vycor, especially when the gases are burning unevenly.

Because the precise accounting for all of these losses is unjustifiably complex, simplifying assumptions to the problem were sought. These are enumerated as follows:

A. Because of the short gas path-lengths and low pressure operation, all heat transfer by gas radiation is neglected.

B. Because of the strong temperature gradients in the firebrick simplifications in the radiation from and convection to the brick are necessary. About 2/3 of each side wall and the entire roof (consisting of flues and spacer bricks) normally glowed visibly -- a bright cherry red. Radiation from the floor and lower portions of the side-walls appeared to be much colder, presumably due to colder gases and/or lower gas velocities in this region. Calculations were simplified by assuming:

(1) uniform gas temperature,

(2) side-walls and roof of uniform temperature, receiving heat by convection from the gas and radiating to the floor, Vycor, and ambient,

(3) the roof has a heat-transfer area equal to an equivalent plane (holes for the flues were ignored),

(4) radiation from the roof and walls is black,

(5) the floor receives and looses heat only by radiation and is black,

(6) heat loss by conduction through the firebrick is

negligible because of the low thermal conductivity of kaolin brick.

C.   In the temperature range of interest, Vycor (nearly pure silica) is partly transparent and a partial reflector. The following assumptions were made:

(1)   Vycor is transparent to radiation of wave-length shorter than 3.7μ and black to radiation of longer wave-length.   Hence its absorptivity (or emissivity) is found from the Stefan-Bolzman equation as a function of the temperature of the source (or Vycor). Since all emmissors in the chamber were postulated to be black, complications arising from multiple reflections are avoided.

(2)   Since the reflectivity of Vycor is low (10%) it is neglected.

(3)   Thermal conduction through the Vycor is assumed to be rapid.

D.   Heat transfer by convection has been studied in various geometries, but no data specifically adapted to this geometry is reported in the literature.   Hence assumed values are necessary.   Since most transfer coefficients across gas films are in the range of 1 to 10 Btu/hr ft^2 °F (17), and are approximately proportional to gas velocity (16), the following relation is assumed for convection from the burning gas to the firebrick and Vycor;

$$h_g = 10 \ G/G_{BO} \ (\text{Btu/hr ft}^2 \ {}^\circ F)$$

where G is the firing rate and G_{BO} is the firing rate at blowout. The transfer coefficient from the Vycor to the ambient air was assumed to be $h_c = 2$ Btu/hr ft^2 $^\circ$F.

E. All back radiation from the surroundings to the chamber is neglected.

With these assumed conditions the heat loss from the burning gas to the ambient air may now be calculated. Radiative heat transfer is calculated by the method of Hottel (16). For any given gas temperature and firing rate all independent parameters are fixed and the heat loss is uniquely determined. However because of the temperature dependence of the Vycor emissivity and absorptivity (assumption C-1 above) it is necessary to evaluate the temperatures of the firebrick, Vycor, and floor. These are found by a heat balance on those respective areas.

A. Heat balance on walls and roof;

$$h_g A_w (T_g - T_w) = A_w F_{wv} \sigma (T_w^4 - \epsilon_v T_v^4) + A_w F_{wf} \sigma (T_w^4 - T_f^4)$$

$$\text{C-1}$$

B. Heat balance on floor

$$\sigma A_w F_{wf} (T_w^4 - T_f^4) = \sigma A_f F_{fv} (T_f^4 - \epsilon_v T_v^4) \qquad \text{C-2}$$

C. Heat balance on Vycor

$$h_g A_v (T_g - T_v) + A_f F_{fv} \sigma (\alpha_{vf} T_f^4 - \epsilon_v T_v^4)$$
$$+ A_w F_{wv} \sigma (\alpha_{vw} T_w^4 - \epsilon_v T_v^4) \qquad \text{C-3}$$
$$= A \sigma \epsilon_v T_v^4 + h_a A_v (T_v - T_a)$$

where:

α_v = absorptivity of Vycor for radiation as a function
of source temperature. Subscript vw refers to wall
radiation, vf refers to floor radiation.

ϵ_v = emissivity of the vycor, a function of Vycor temperature.

F = direct view factor, fraction of radiation leaving
source arriving at sink. First subscript refers
to source, (on whose area the view factor is based)
and second subscript refers to sink.

h_g = convection heat transfer coefficient from burning
gas to walls and Vycor.

h_c = convection heat transfer coefficient from Vycor
to ambient air.

Simultaneous solution of equations C-1 to C-3 for each gas
temperature and firing rate permits evaluation of T_w and T_v.
Heat loss from the chamber is then found by the equation:

$$q = h_g A_w (T_g - T_w) + h_g A_v (T_g - T_v) \qquad \text{C-4}$$

Figure C-1 gives α_v or ϵ_v of Vycor as a function of Vycor
or source temperature based on the assumptions given in C above.
This plot must be used in conjunction with a trial and error
solution of Equations C-1 to C-3. The heat losses calculated
from these equations are shown as functions of gas temperature
and firing rate in Figure C-2.
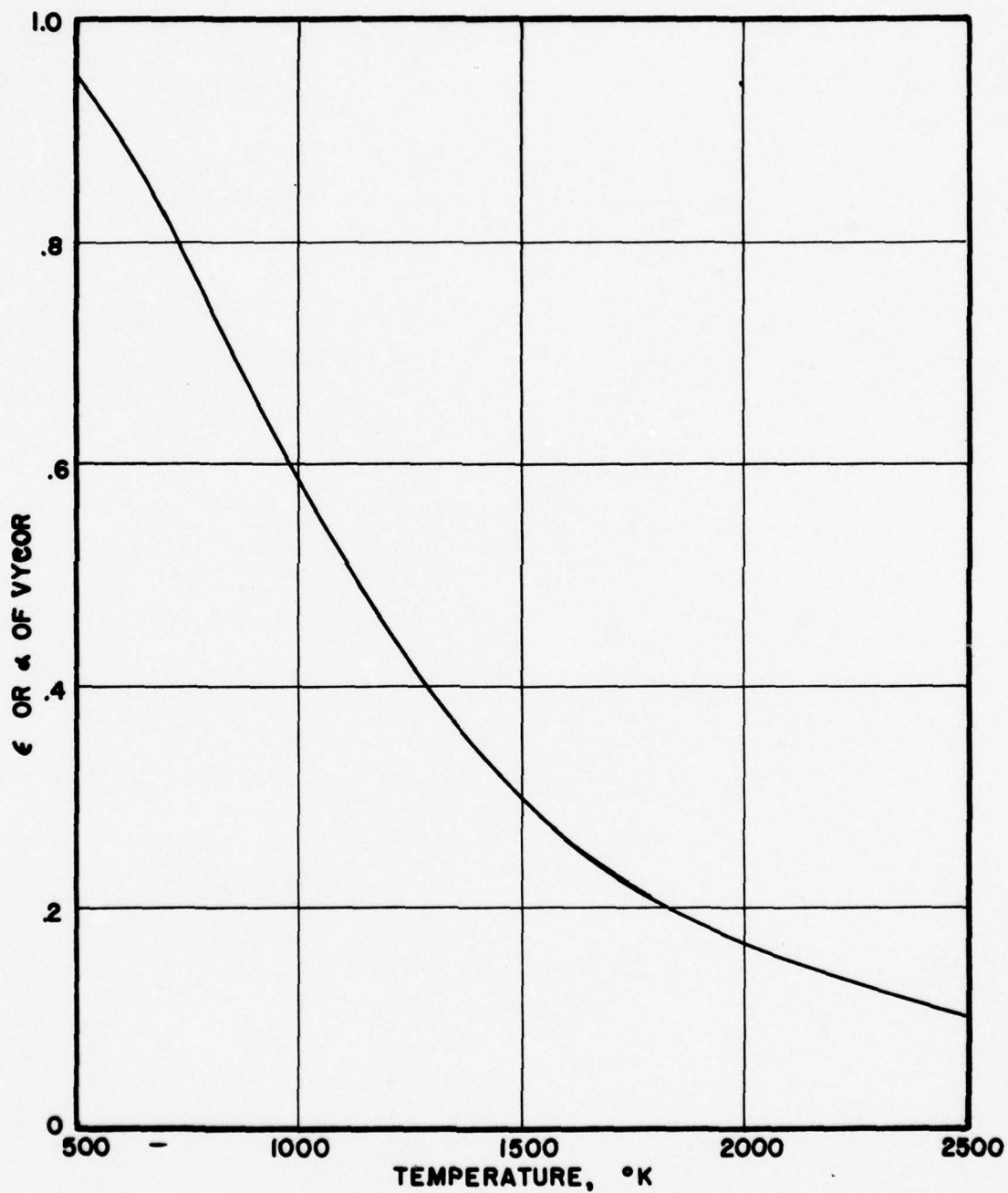
FIGURE C-1: EMMISSIVITY OR ABSORPTIVITY OF VYCOR
(% OF RADIANT ENERGY ABOVE $\lambda = 3.7\mu$)
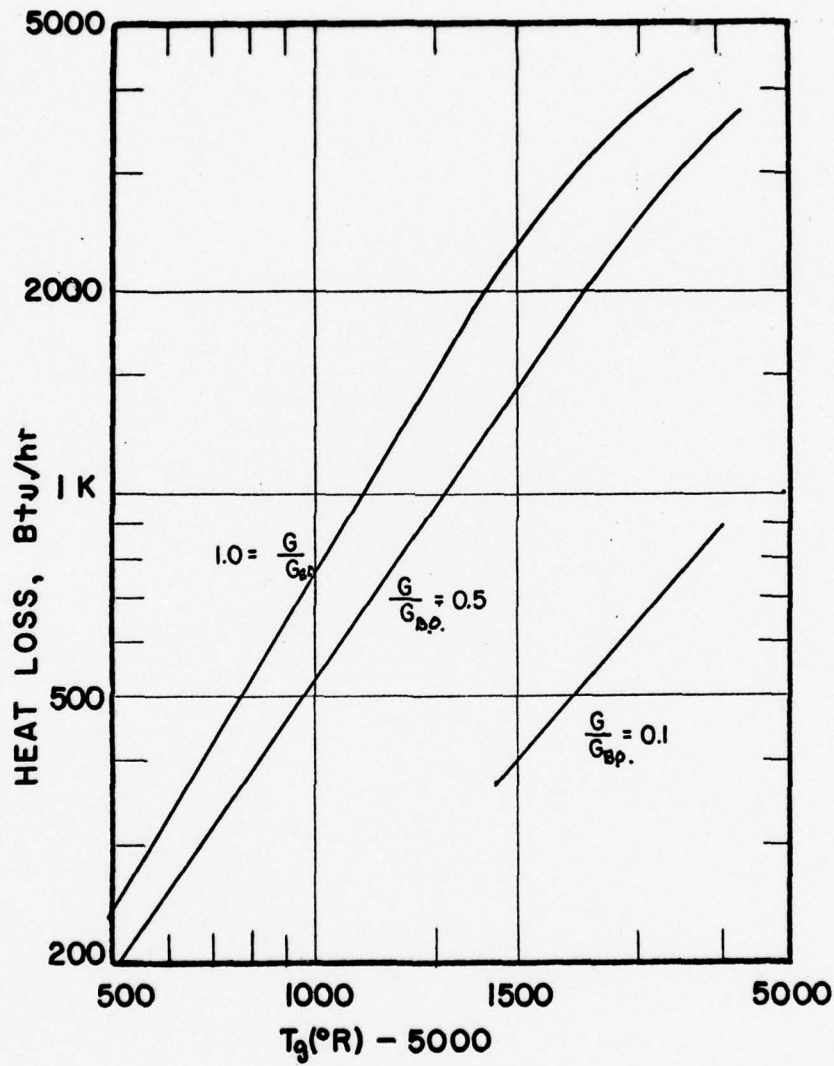
FIGURE C-2: HEAT LOSS OF 3-JET
CHAMBER, $Q = f(T_g, G)$.

APPENDIX D

DETAILS OF EQUIPMENT AND APPARATUS

The combustion chamber used in this work consisted of
three parallel two-dimensional jets mounted in a framework
holding a firebrick lining. The front and back of the frame
were closed with Vycor windows to permit ease of observation.
In this chamber recirculation was created by the aspirating
effect of the jets. This recirculation could be controlled,
if desired, by varying the spacing of the jets; however,
in these experiments only one jet spacing was used. Sketches
showing the dimensions of the chamber and nozzles are given in
Figures D-1 and D-2. (An isometric sketch of the assembly
has been given in the main body of this thesis Figure IV-1).

The feed to this chamber was a pre-mixed fuel-air mixture.
Fuel and air were metered separately and mixed. This mixture
was then manifolded and the manifold mixture to each jet was
metered to insure equal distribution of feed. The orifices
used in the primary air, fuel and manifold mixture lines were
standard square-edge orifices and were calibrated to insure
accuracy of metering. Calibration was done with air against
a standard orifice set. Corrections were made to the cali-
bration curve for fuel to account for the compressibility and
higher molecular weight of propane. A similar correction
should have been made to the calibration curves for the manifold

mixture orifices (addition of propane changed the molecular weight but did not affect compressibility); however this correction was small, and since it entered into all three equally, it was not necessary to achieve the desired distribution of feed. A flow diagram showing the orifice designations is given in Figure D-3. Calibration curves for each of the orifices are given in Figures D-4 to D-9. Compressibility factor for propane is given in Figure D-10. (Calculated from data reported by Stearns and George (25)).

A sampling train was constructed to facilitate sampling of the chamber gases. (A flow diagram of this train is given in Figure IV-12). In sampling gases where the gases impinge directly on the probe opening, the velocity of the gases at the probe should be matched to the sampling velocity. To do this it is necessary to meter the sampling rate. This metering was accomplished by means of a capillary flow meter. The metering element was a short piece (about 4") of hypodermic tubing of i.d. 0.049". This was calibrated against a wet-test meter. The calibration curve is given in Figure D-11.

0.030"

5-40 MACH. SCREW
SILVER SOLDERED
INTO NOZZLE HEAD,
TWO EACH SIDE.

0.200"
0.450"

4"

$\frac{3}{4}$ ", SCHED 40
PIPE
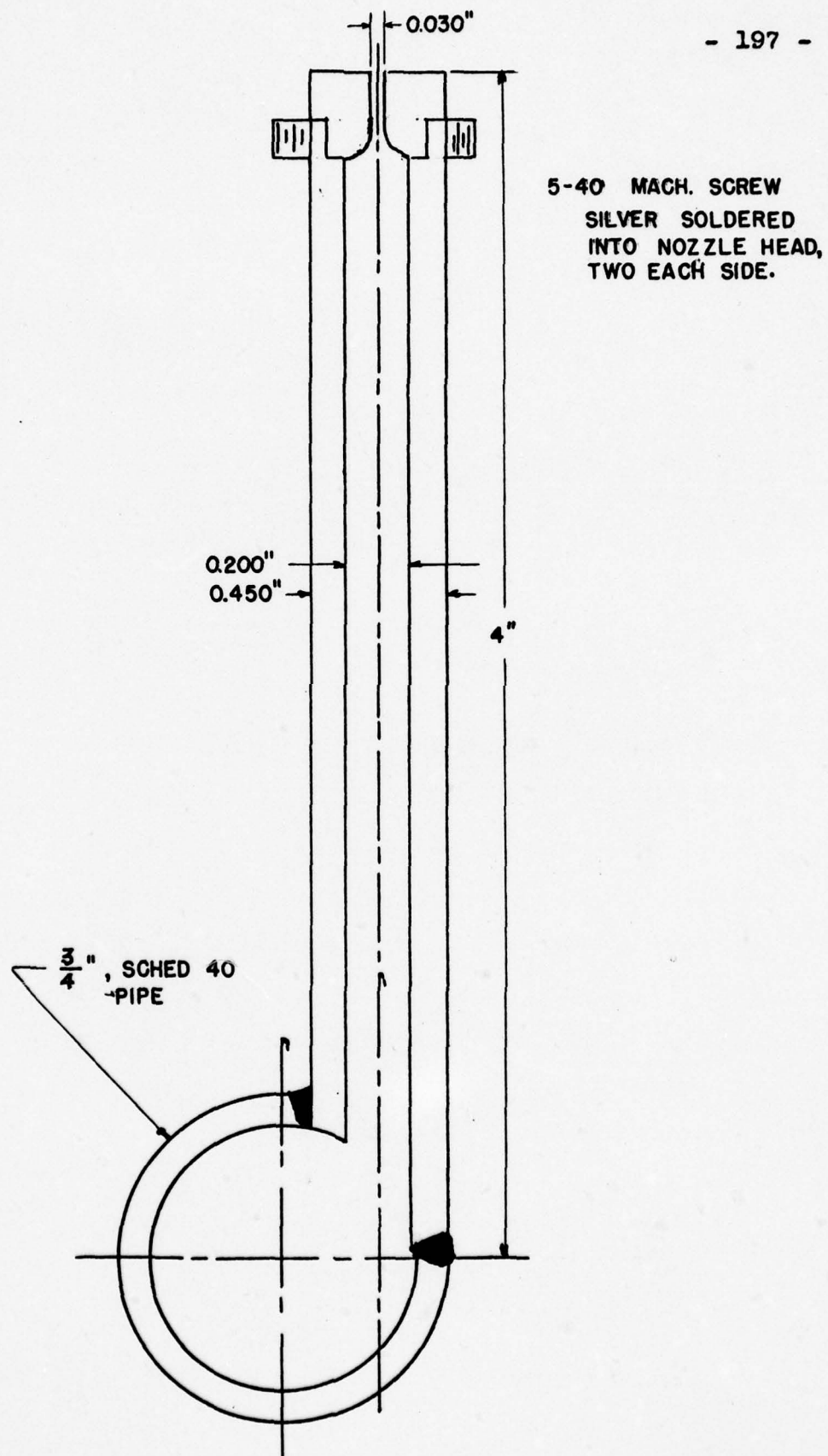
FIGURE D-1: ENLARGED DETAIL OF NOZZLE.   SCALE: 2"= 1"
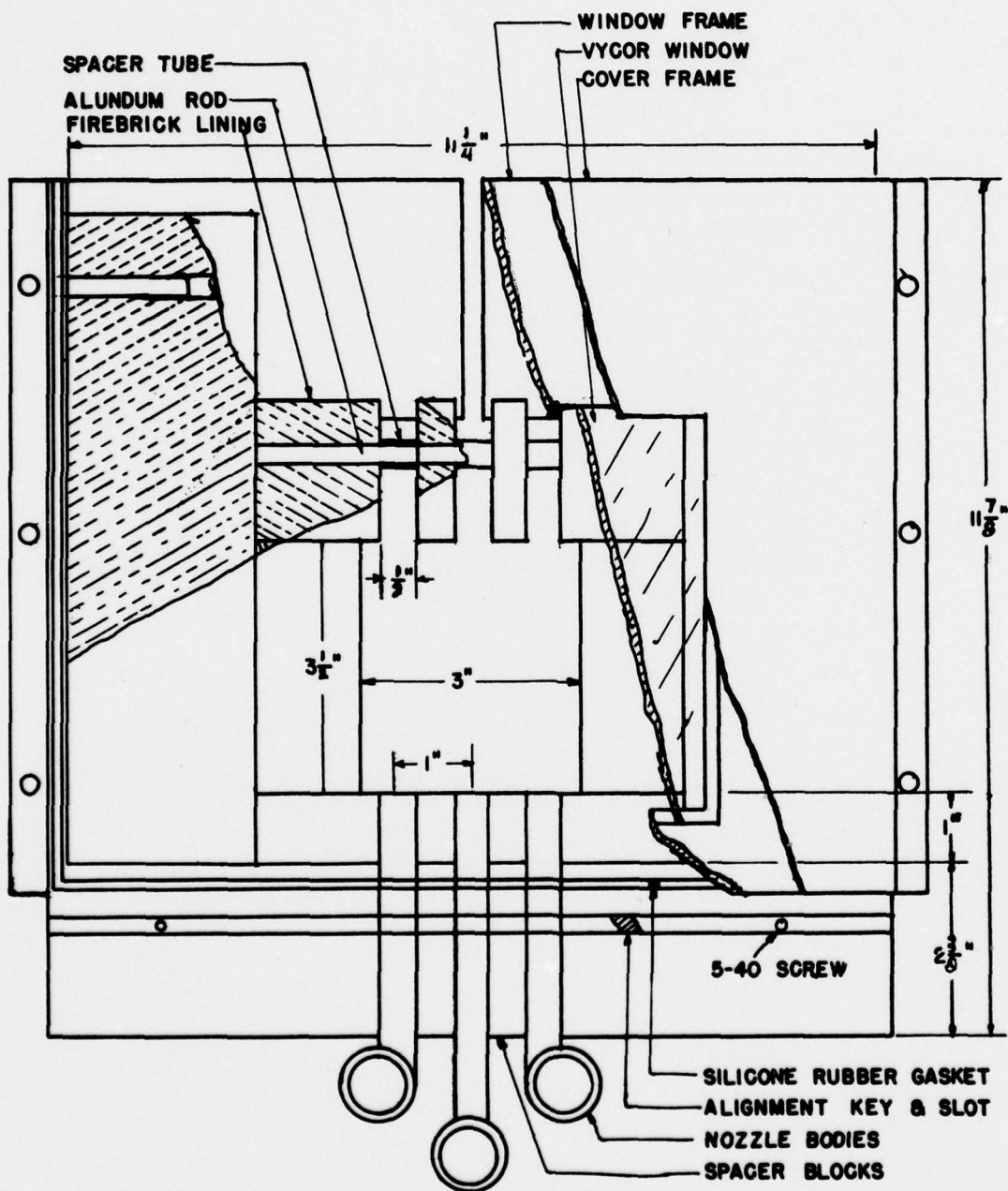
FIGURE D-2: COMBUSTION CHAMBER ASSEMBLY
SCALE: $\frac{1}{2}" = 1"$
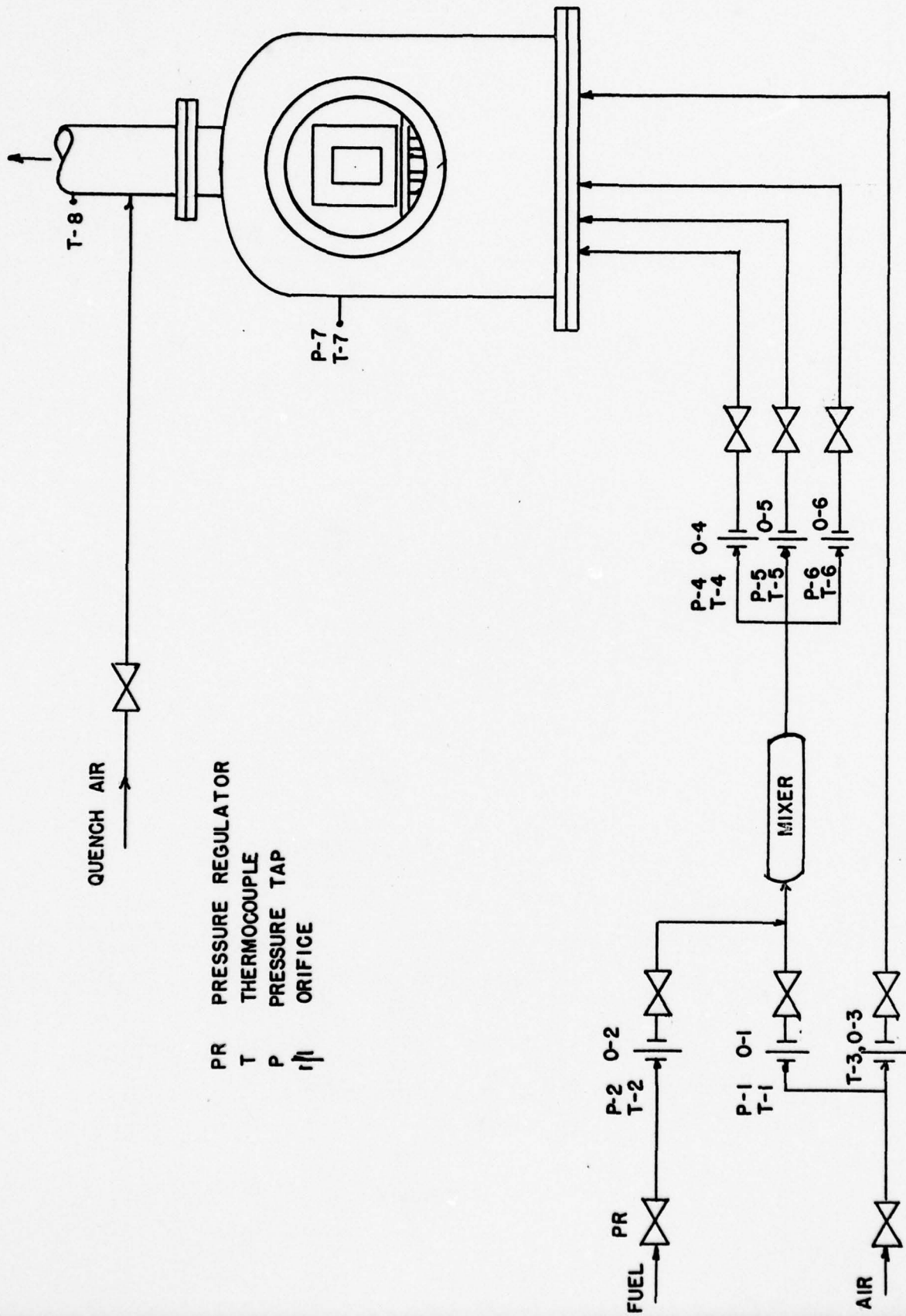
FIGURE D-3: ORIFICE LOCATIONS
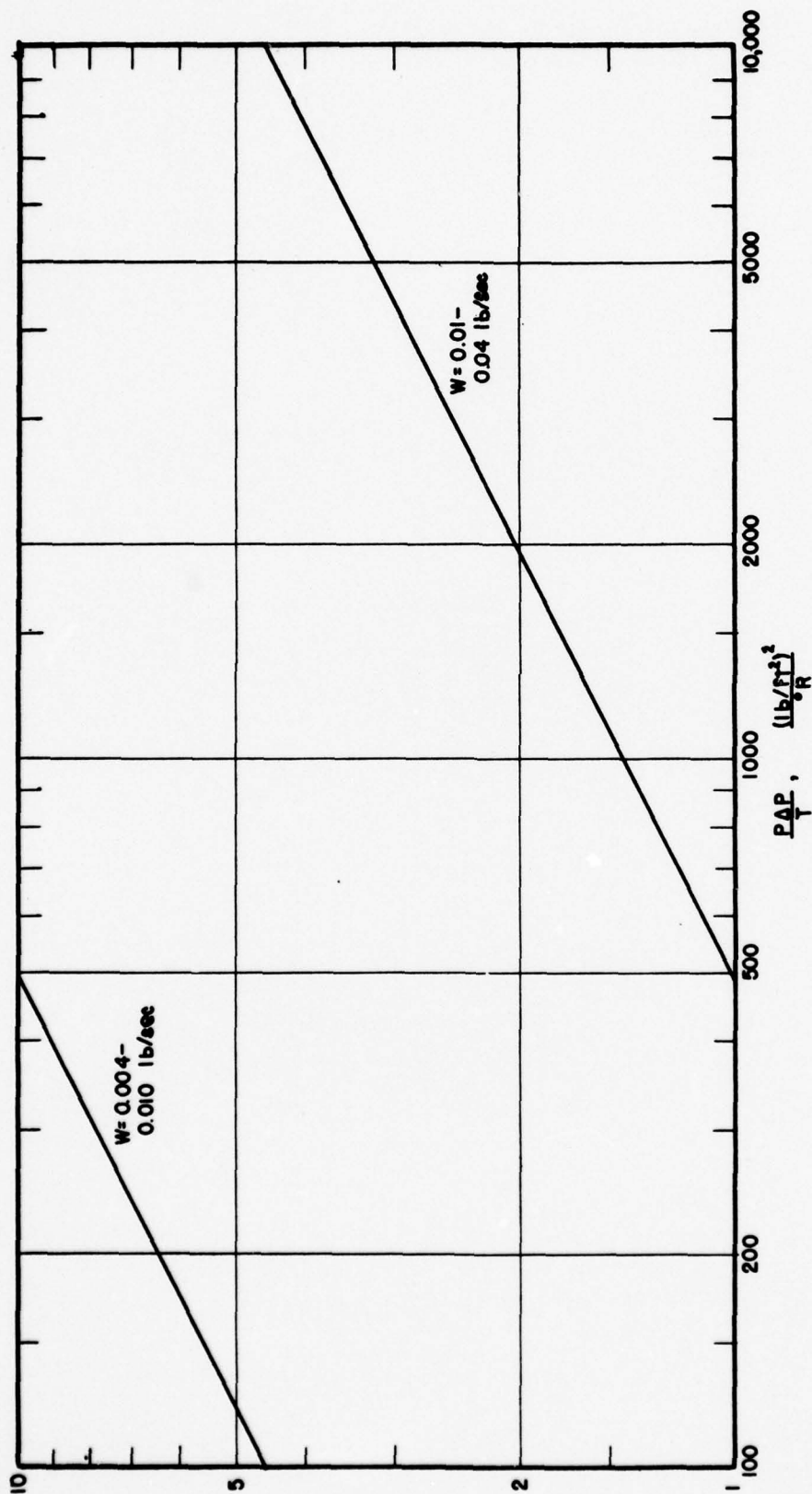
FIGURE D-4: CALIBRATION CURVE, ORIFICE O-1 LOW RANGE

ORIFICE: 0.348" IN 1$\frac{1}{2}$" PIPE

FLUID: AIR

$\frac{P \Delta P}{T}$, $\left(\frac{lb}{ft^2}\right)^2 \frac{1}{R}$

W = 0.01 – 0.04 lb/sec

W = 0.004 – 0.010 lb/sec
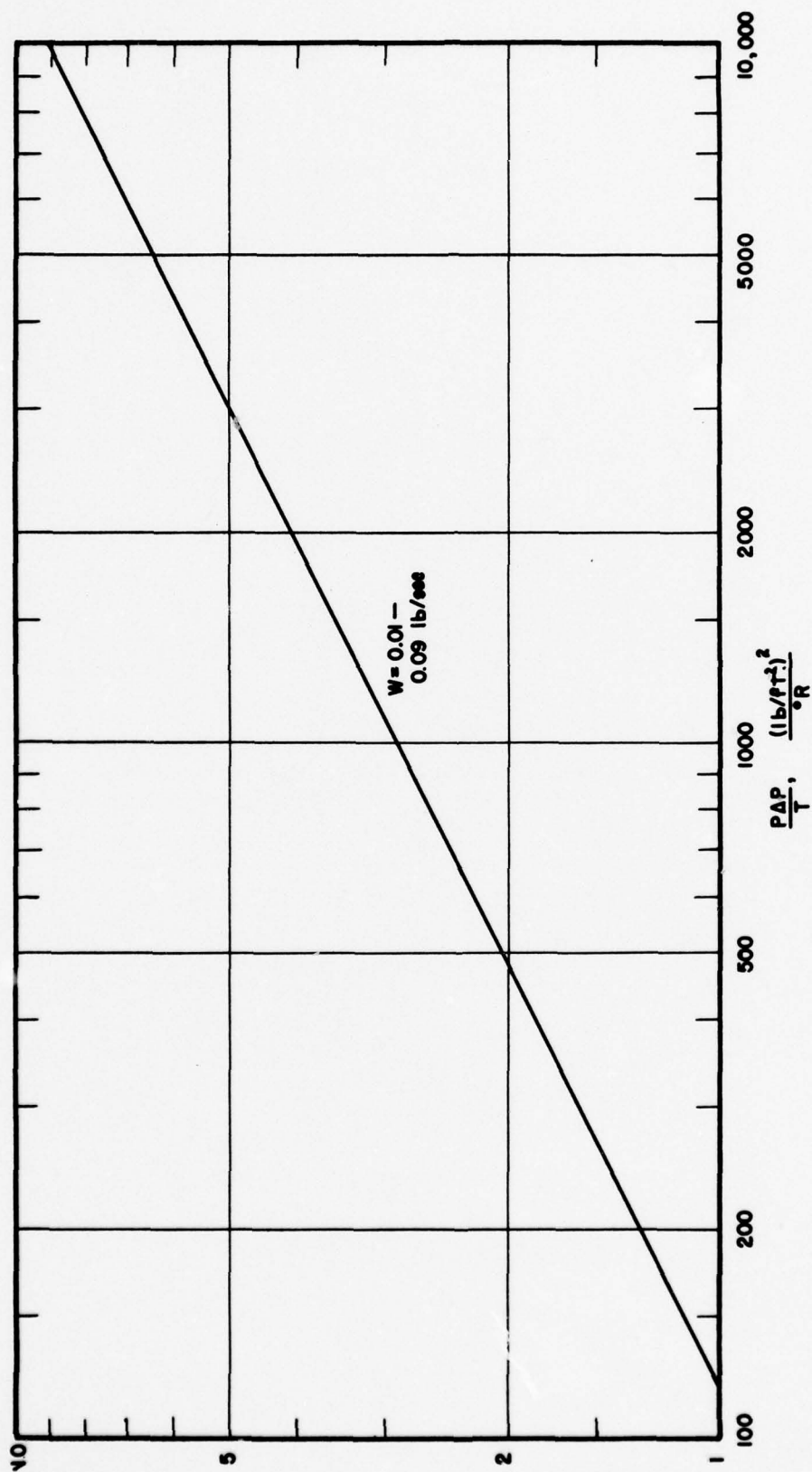
FIGURE D-5: CALIBRATION CURVE, ORIFICE O-1 MED. RANGE

ORIFICE: 0.500" IN $1\frac{1}{2}$" PIPE

FLUID: AIR

$\frac{P\Delta P}{T}, \quad \frac{(lb/ft^2)^2}{^\circ R}$

W = 0.01 — 0.09 lb/sec
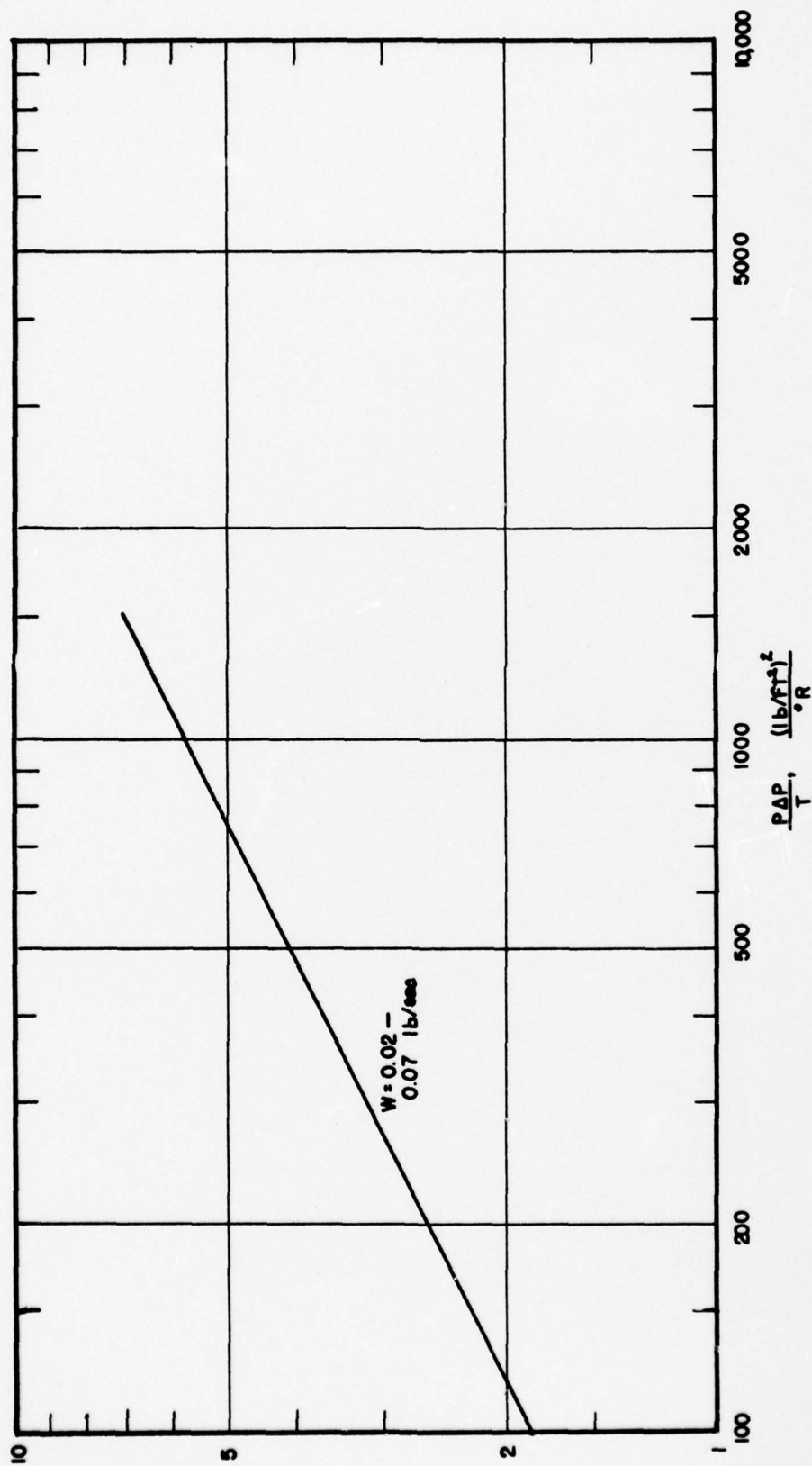
FIGURE D-6: CALIBRATION CURVE, ORIFICE O-1 HIGH RANGE
ORIFICE: 0.706" IN $1\frac{1}{2}$" PIPE
FLUID: AIR

W = 0.02 –
0.07 lb/sec

$\frac{P\Delta P}{T}$, $\frac{(lb/ft^2)^2}{°R}$
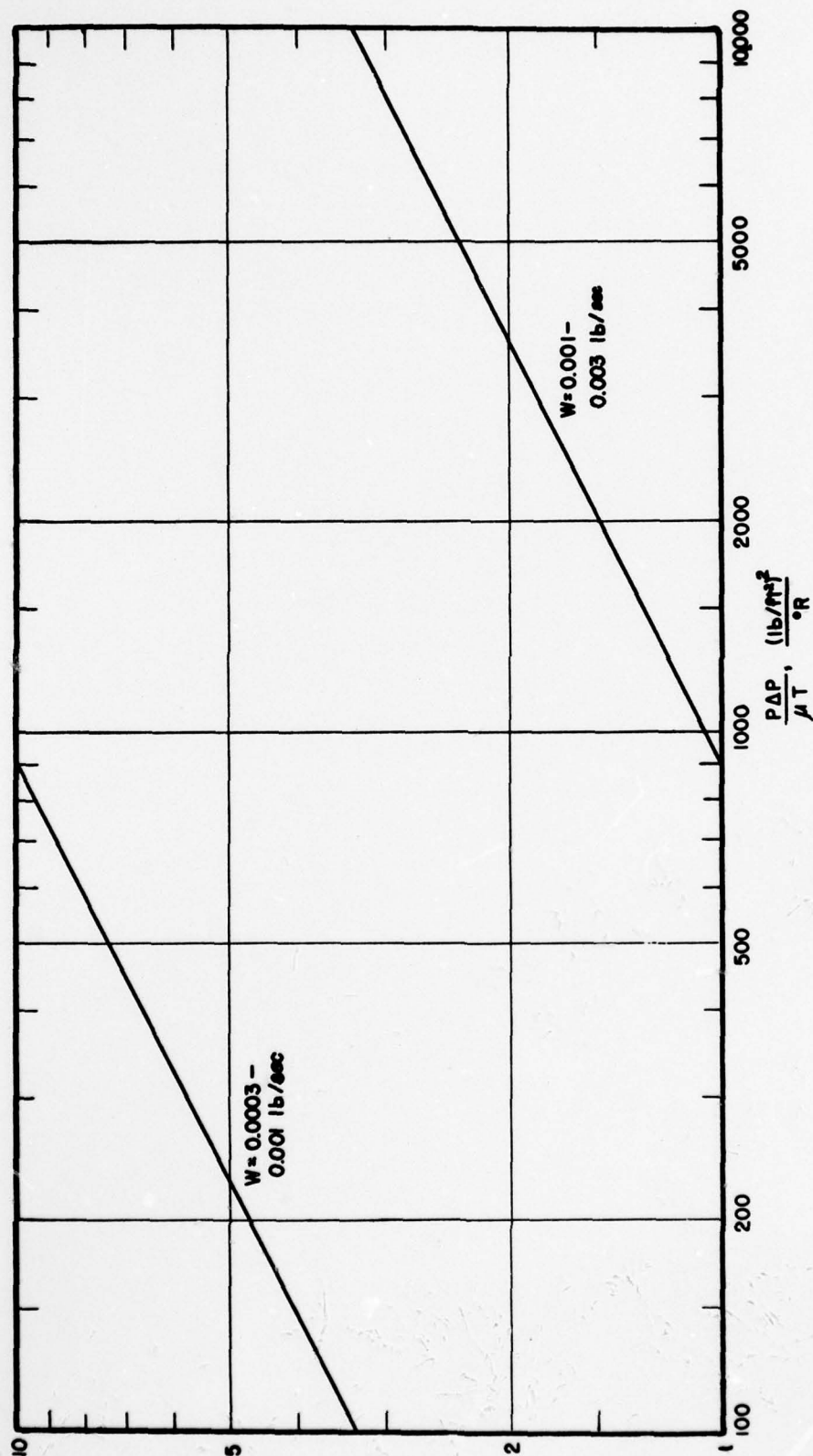
FIGURE D-7: ORIFICE CALIBRATION CURVE, ORIFICE O-2 LOW RANGE
ORIFICE: 0.082" IN 2" PIPE
FLUID: PROPANE
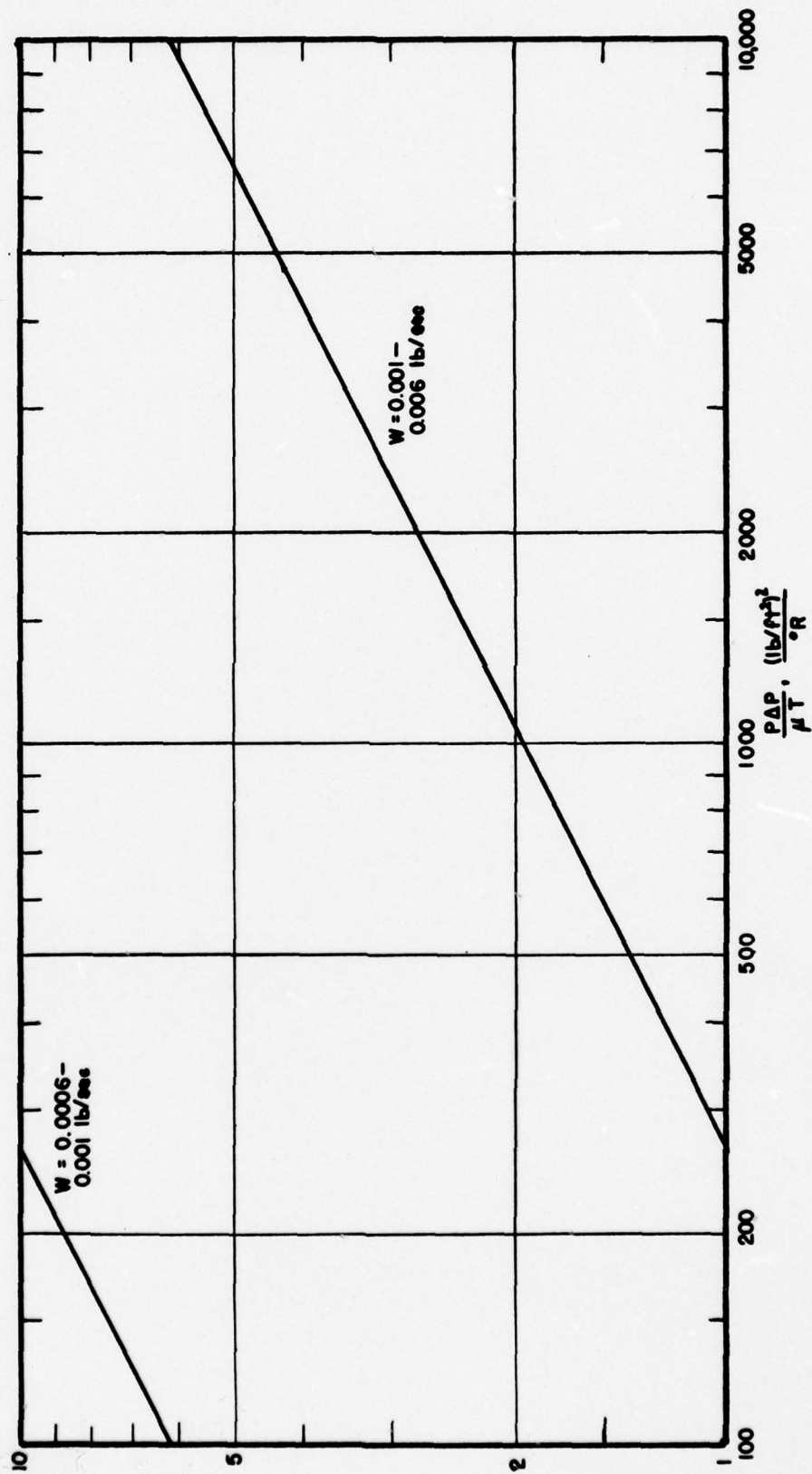
FIGURE D-8: CALIBRATION CURVE, ORIFICE O-2 HIGH RANGE
ORIFICE: 0.1163" IN 2" PIPE
FLUID: PROPANE

- 204 -
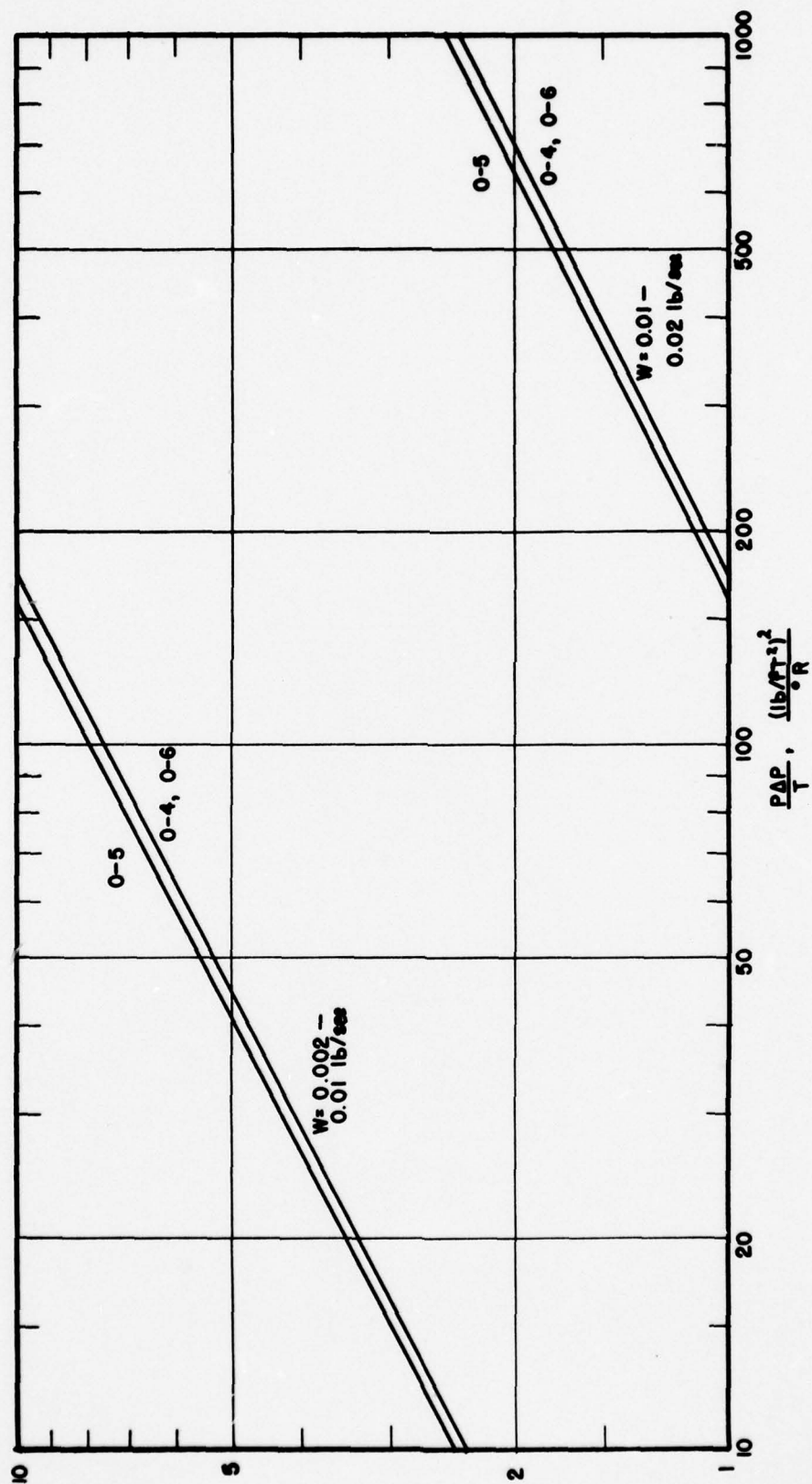
FIGURE D-9: CALIBRATION CURVES: ORIFICES O-4 TO O-6

ORIFICES: 0.4375" IN $\frac{3}{4}$" PIPE

FLUID AIR
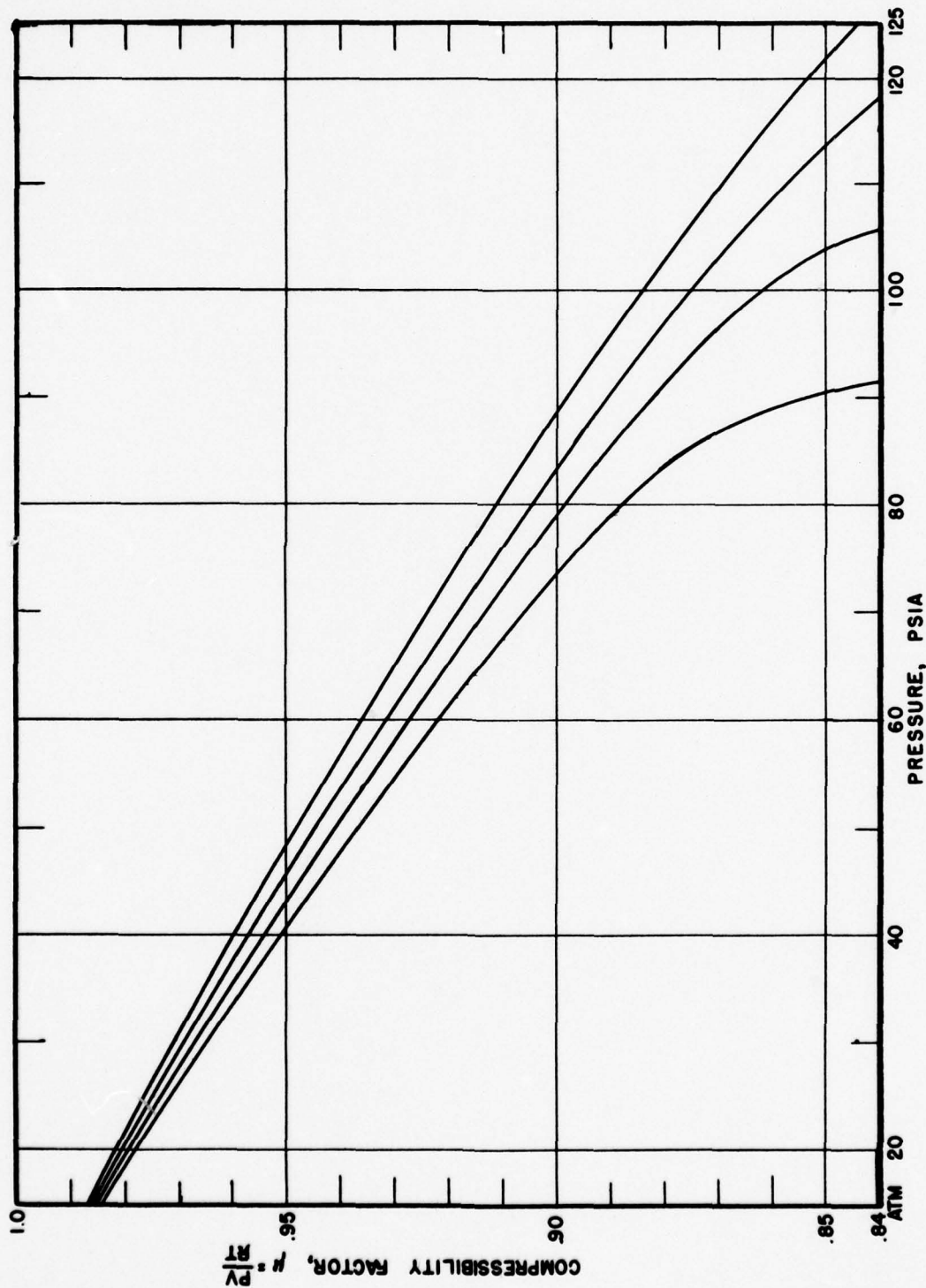
FIGURE D-10: COMPRESSIBILITY OF PROPANE (25)
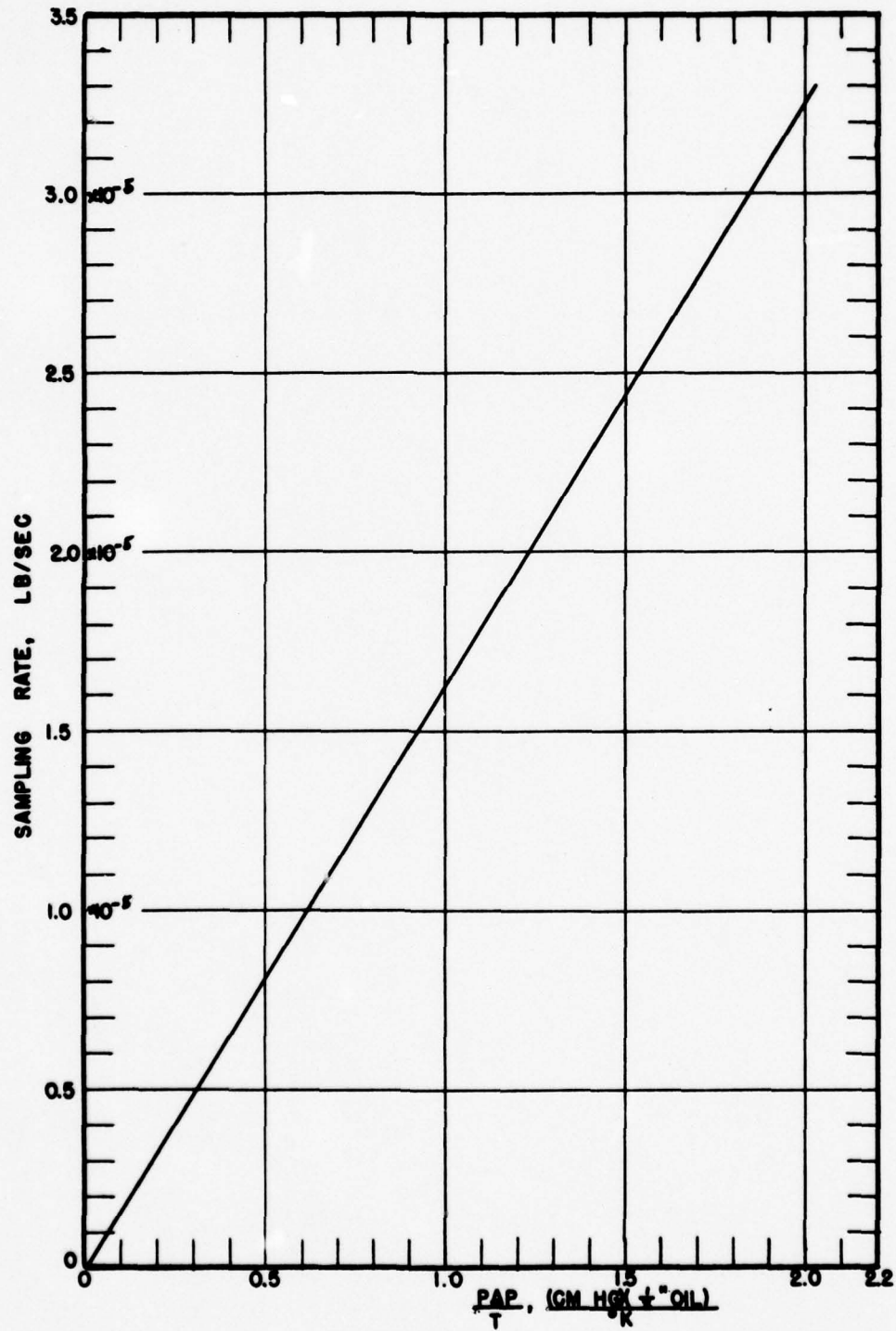
FIGURE D-11: CALIBRATION CURVE FOR CAPILLARY FLOW
METER IN SAMPLING TRAIN. FLUID-AIR.

APPENDIX E

SAMPLE CALCULATIONS

A. Calculation of blowout or loading rates (example, Run 4B)

TABLE E-1

DATA OBTAINED IN A TYPICAL RUN

Station	P	ΔP	T	
0-1	24.2 psig	9.22" H_2O	525°R	(0.706" orifice)
0-2	34.8	30.35	513	(0.1163" orifice)
0-4	-4.21"Hg*	17.14	527	
0-5	-4.23"*	17.00	527	
0-6	-4.26"*	16.15	527	
P-7	19.40"*			
atm	30.06"			

  * Pressure measured in inches of mercury vacuum.
  Negative pressure indicates pressure above atmospheric.

From these data flow rates, w, in lb/sec of gas are calculated.
Since the calibration charts for the various orifices are given
in (PΔP)/T units of $(lb/ft^2)^2/°R$, a conversion factor must be
used to account for the units of the measurements. The flow
rates calculated from the data of Table E-1 are given in
Table E-2. It should be noted from the flow diagram, Figure
D-3, that the sum of the flow rates through orifices 0-1 and
0-2 should equal the flow through orifices 0-4 to 0-6. Loading
rates, fuel-air ratio and other calculated quantities are also
indicated in Table E-2.

TABLE E-2

CALCULATED QUANTITIES

	P	ΔP	T	μ	$\dfrac{P\Delta P}{T}$	conv.	$\dfrac{P\Delta P}{T} \times C$	w	Figure
0-1	39.0 psia	9.22" H$_2$O	525°R		0.6849	748.8	512.9	0.0429	D-6
0-2	49.6	30.35	513	0.939	3.125	748.8	2340	0.00298	D-8
0-4	33.49" Hg	17.14	527		1.089	367.7	400.5	0.0149	D-9
0-5	33.51"	17.00	527		1.081	367.7	397.5	0.0149	D-9
0-6	33.54"	16.15	527		1.027	367.7	377.6	0.0145	D-9
P-7	10.61"								

Fuel-air ratio = $(w_F/w_A)(1/15.68)$ = .1096; $F = \dfrac{\phi}{\phi+1}$ = .524

Loading Rate:

$\quad$ Loading = $N_A/Vp^{1.8}$

$\quad\quad N_A/V = w_A/.3524$ $\quad\quad$ (Volume of chamber = 0.01215 ft^3)

$\quad\quad p^{1.8} = 0.1545$ $\quad\quad$ (Figure E-1)

$\quad\quad$ Loading rate = 0.761

$\quad\quad$ Temperature correction = 1/0.973 $\quad$ (Figure E-2)

$\quad\quad$ Loading rate corrected to 5400°R = 0.782

TABLE E-2

CALCULATED QUANTITIES

	P	ΔP	T	μ	$\frac{P\Delta P}{T}$	conv.	$\frac{P\Delta P}{T}$×C	w	Figure
0-1	39.0 psia	9.22" H$_2$O	525°R		0.6849	748.8	512.9	0.0429	D-6
0-2	49.6	30.35	513	0.939	3.125	748.8	2340	0.00298	D-8
0-4	33.49" Hg	17.14	527		1.089	367.7	400.5	0.0149	D-9
0-5	33.51"	17.00	527		1.081	367.7	397.5	0.0149	D-9
0-6	33.54"	16.15	527		1.027	367.7	377.6	0.0145	D-9
P-7	10.61"								

Fuel-air ratio = $(w_F/w_A)(1/15.68) = 1.096$; $F = \frac{\phi}{\phi + 1} = .524$

Loading Rate:

Loading = $N_A/VP^{1.8}$

$N_A/V = w_A/.3524$ (Volume of chamber = 0.01215 ft^3)

$P^{1.8} = 0.1545$ (Figure E-1)

Loading rate = 0.761

Temperature correction = 1/0.973   (Figure E-2)

Loading rate corrected to 540°R = 0.782

FIGURE E-1: PRESSURE VS $P^{1.8}$
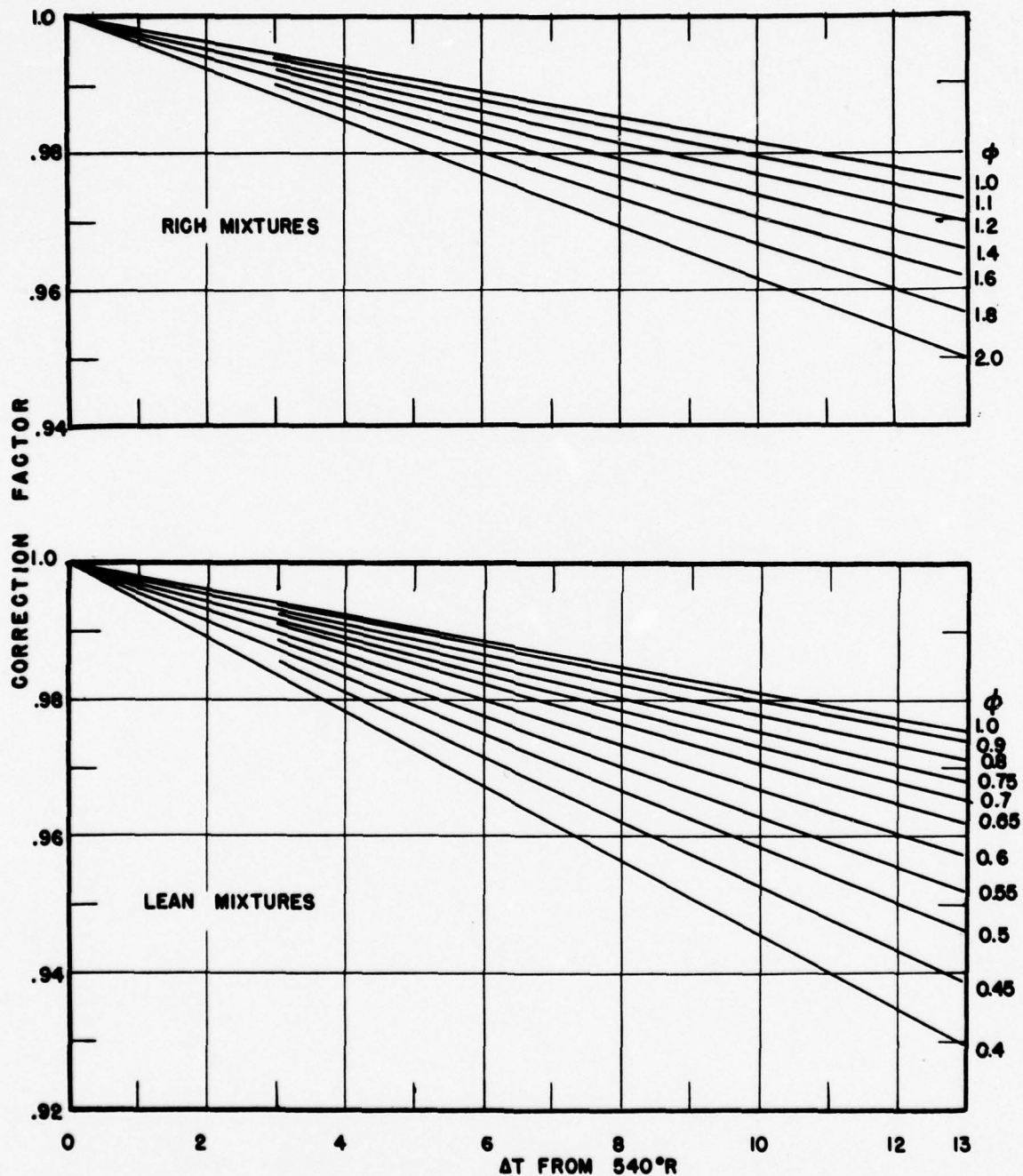
FIGURE E-2: TEMPERATURE CORRECTION FACTORS (14). FOR TEMPERATURE ABOVE 540.°R MULTIPLY BY FACTOR. FOR TEMPERATURE BELOW 540°R DIVIDE BY FACTOR.

B. Calculation of combustion efficiency (example Run 86A)

TABLE E-3

DATA OBTAINED IN A TYPICAL RUN

a) Loading rate

	P	ΔP	T	
O-1	56.3 psig	22.26" H_2O	537°R	(0.348" orifice)
O-2	29.7 psig	14.22""	531°	(0.1163" orifice)
O-5			537°	
O-7	20.04" Hg vac			
O-9	30.23" Hg			

b) sampling data -- probe position, cold side of flue

	P	--- rate data --- ΔP	T	P_{O_2}
Impact	10.19" Hg	4.9" H_2O		
Sample	20.10 mm Hg	33.1 ½" oil	297°K	32.8 mm Hg

From the above data the following quantities are calculated:

a) Loading rate (calculated as in previous example);

$N_A/VP^{1.8})_{540}$ = 0.620, F = 0.575, A/F = 11.58 lb/lb

b) Sampling rate;

$P\Delta P/T$ = (20.10)(33.1)/(297) = 0.044

w = 3.67 x 10^{-5} lb/sec   (Figure E-3)

c) Composition;

N_2 correction* = 0.7 mm   (Figure E-3)

$\frac{\text{Mol dry products}}{\text{Mol wet products}}$ = 0.856   (Figure E-4)

---

* A correction to magnetic oxygen meters must be made to correct
for the magnetic properties of other gases present. It is assumed
for this work that the background gas is only N_2. Only a small
error is introduced by this assumption.

c) Composition -- continued

Moles O_2/ 100 mols wet products =

(33.5)(.856)(100)/(20.10) = 14.26

O_2 req'd/100 mol wet prod. = 17.74   (Figure E-5)

= 1 - (O_2 remaining)/(O_2 req'd) = 19.7%

d) Estimated gas temperature;

Adiabatic flame temperature = 3755°R   (Figure E-6)

(T_{af} - 530) + 530 = 1145°R

e) Sample rate required by impact measurement;

$P\Delta P/T$ = (10.19)(4.9)/(1145) = 0.044   (Figure E-7)

w = 5.79 x 10^{-5} (Figure E-7)

w required = (.856)(5.79 x 10^{-5}) = 4.9 x 10^{-5}

(to be compared with 3.67 x 10^{-5} used)

C. Pressure exponent calculation   (example Run 76A)

TABLE E-5

DATA OBTAINED IN A TYPICAL RUN

	P	ΔP	T	
0-1	57.0 psig	2.02" H_2O	544°R	(0.348" orifice)
0-2	43.3 psig	6.20"	536°	(0.1163" orifice)
0-5			540°	
P-7	23.90" Hg vac			
atm	30.08" Hg			

From these data the following quantites are calculated as in

example A above:

w of air = 0.0129 lb/sec

Fuel fraction F = 0.599

C.   Pressure exponent calculation -- continued

   $N_A/V = w_A \times 4.26 = 0.0549$

   Temp = $540°R$ Temp. Correction = 1.00

   F   = .599   F correction = 0.993

      F correction calculated from relative blowout rates

   of actual fuel-air mixture and the fuel-air mixture desired.

   On the rich side this is F corr = $e^{7(F-F^*)}$ and on

   the lean side this is F corr = $e^{15(F^*-F)}$.

   $N_A/V)_{540.} {}_{.600} = 0.0545$

   P = 6.18" Hg = 0.207 atm

   A series of these points are taken for a given fuel/air

ratio and plotted on log-log paper.   The slope of the resulting

line is determined.
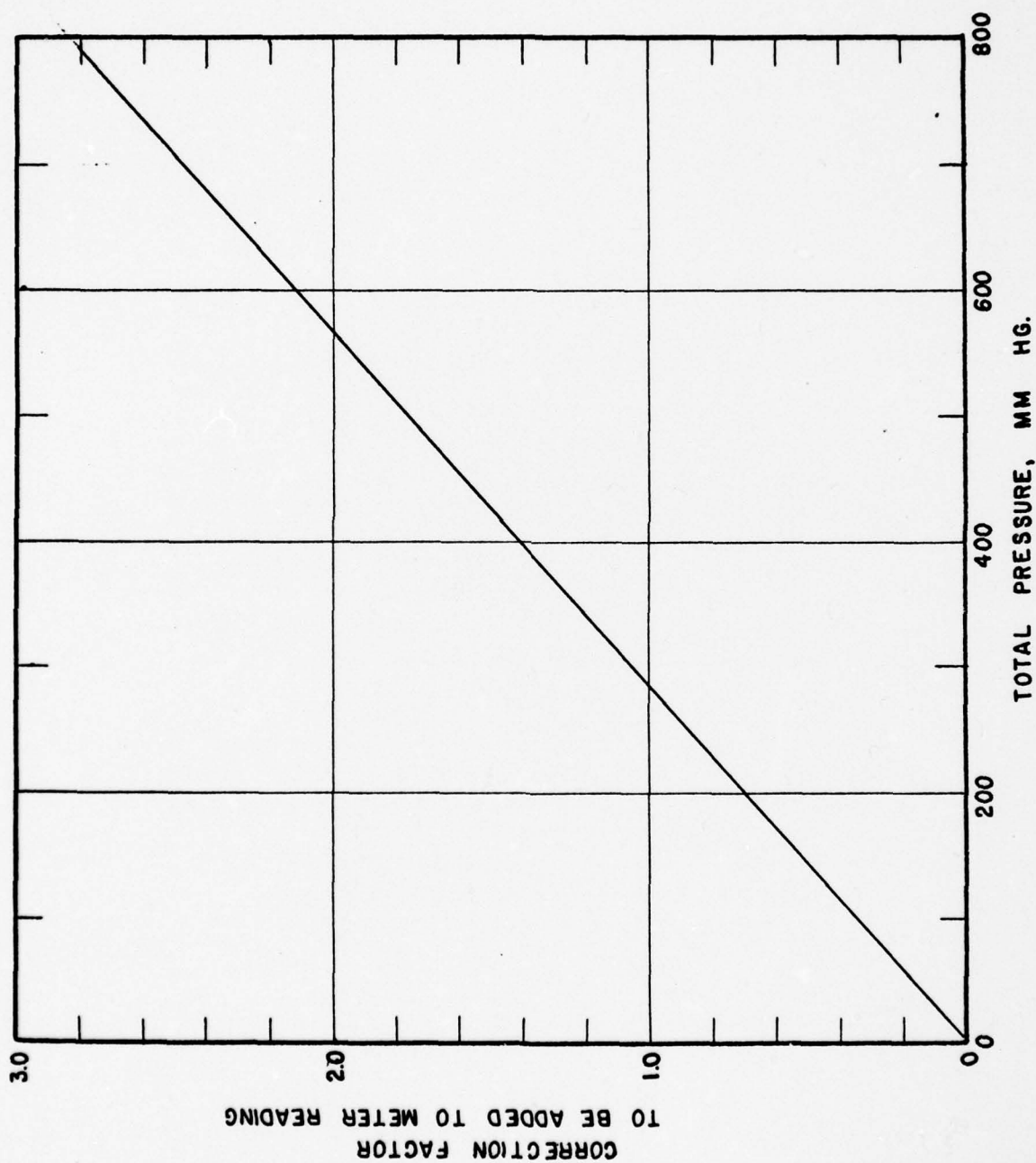
FIGURE E-3: BACKGROUND GAS CORRECTION FACTOR (26)
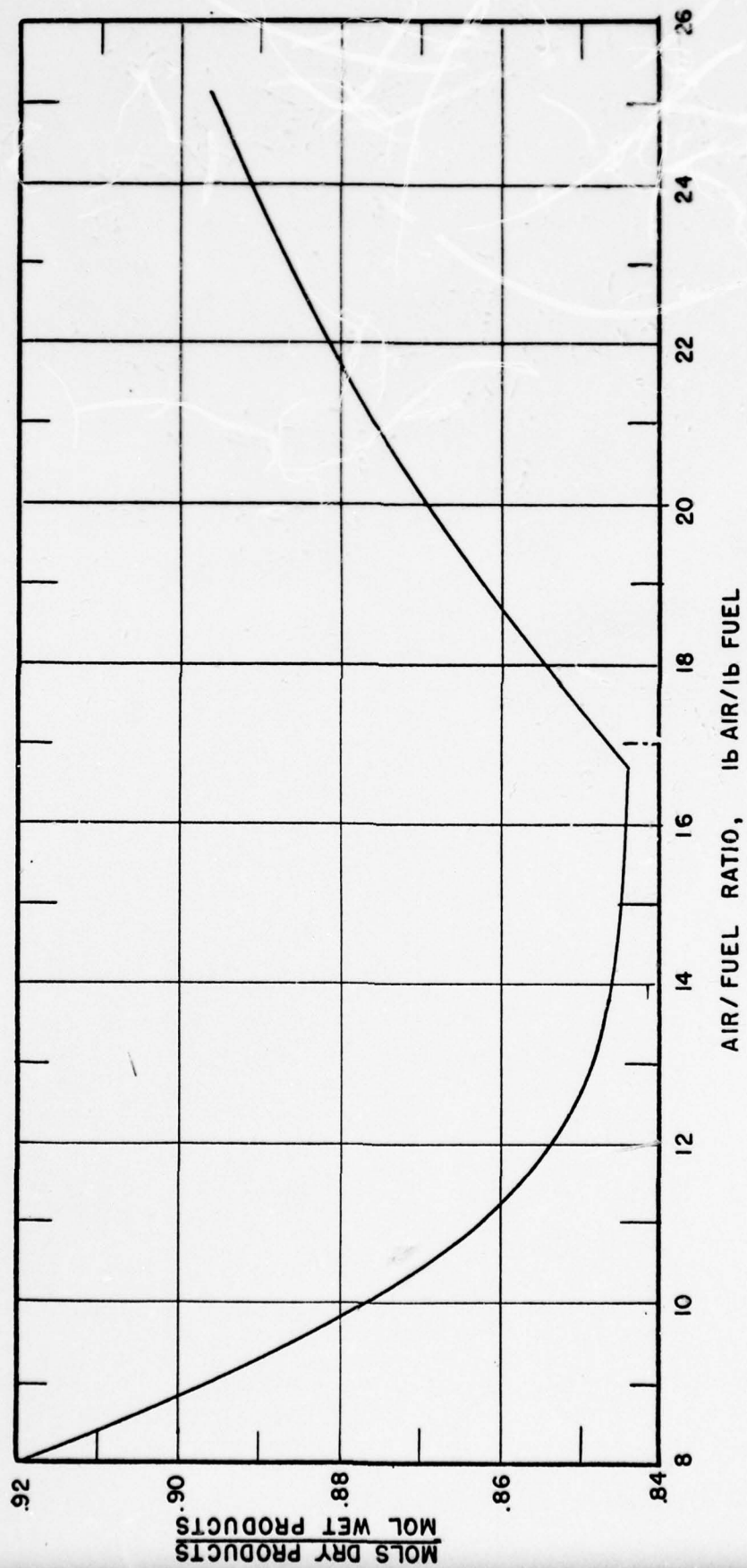
FIGURE E-4: MOLES OF DRY COMBUSTION PRODUCTS PER MOL OF WET PRODUCTS (26)
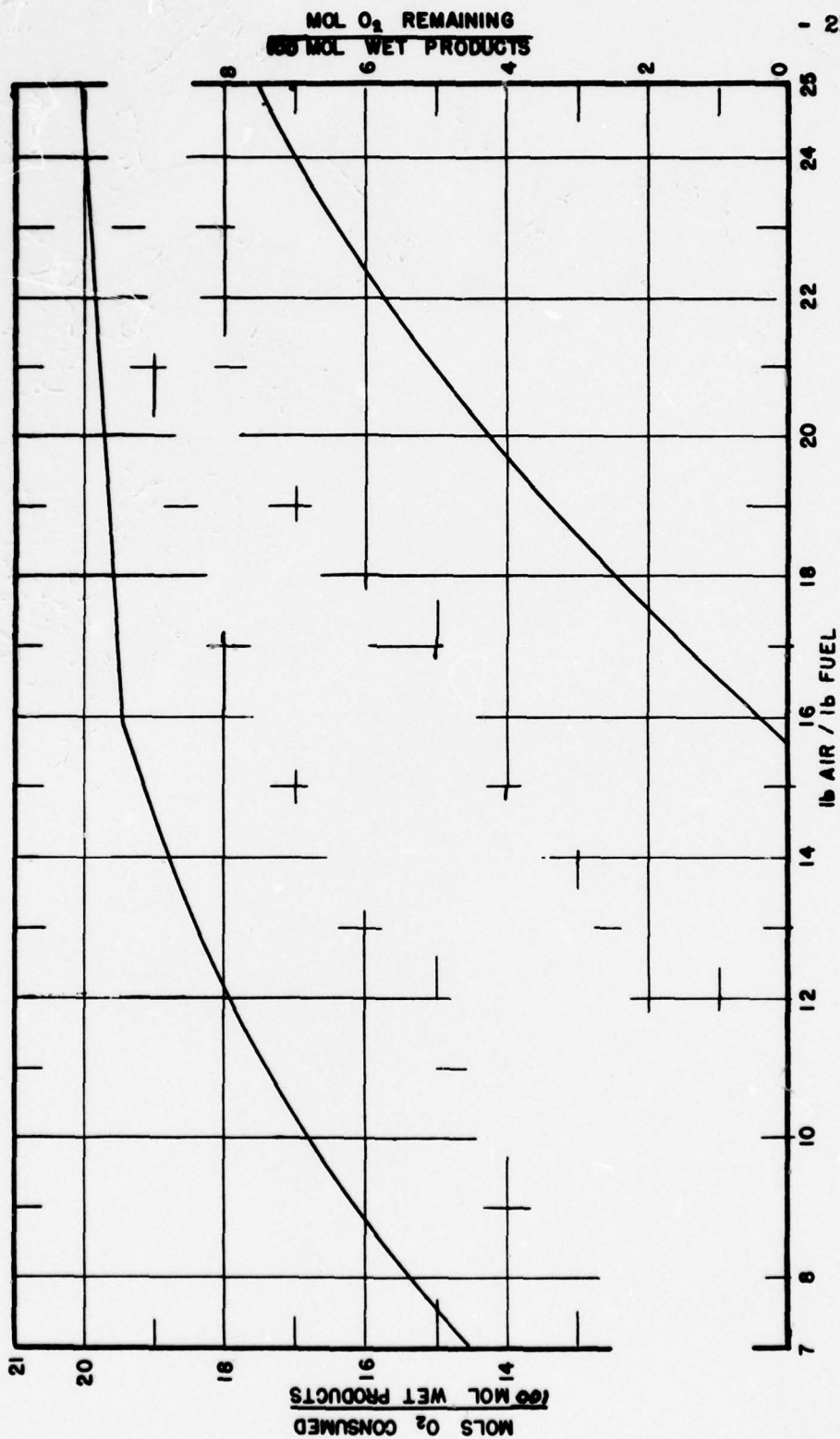
FIGURE E-5: MOLES OF OXYGEN CONSUMED AND REMAINING AT COMPLETE COMBUSTION (26)
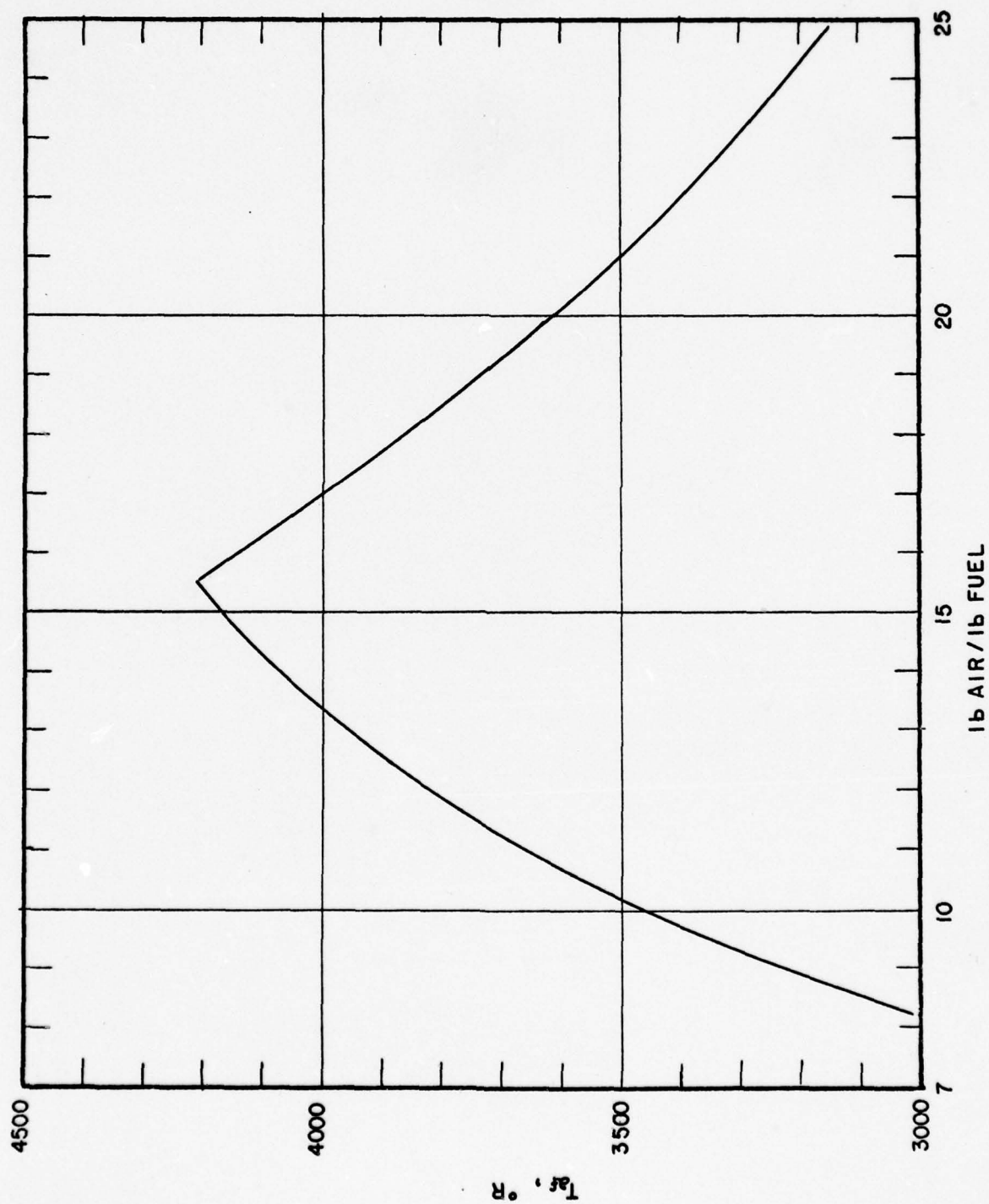
FIGURE E-6: ADIABATIC FLAME TEMPERATURE, $T_o = 70°F$ (26)
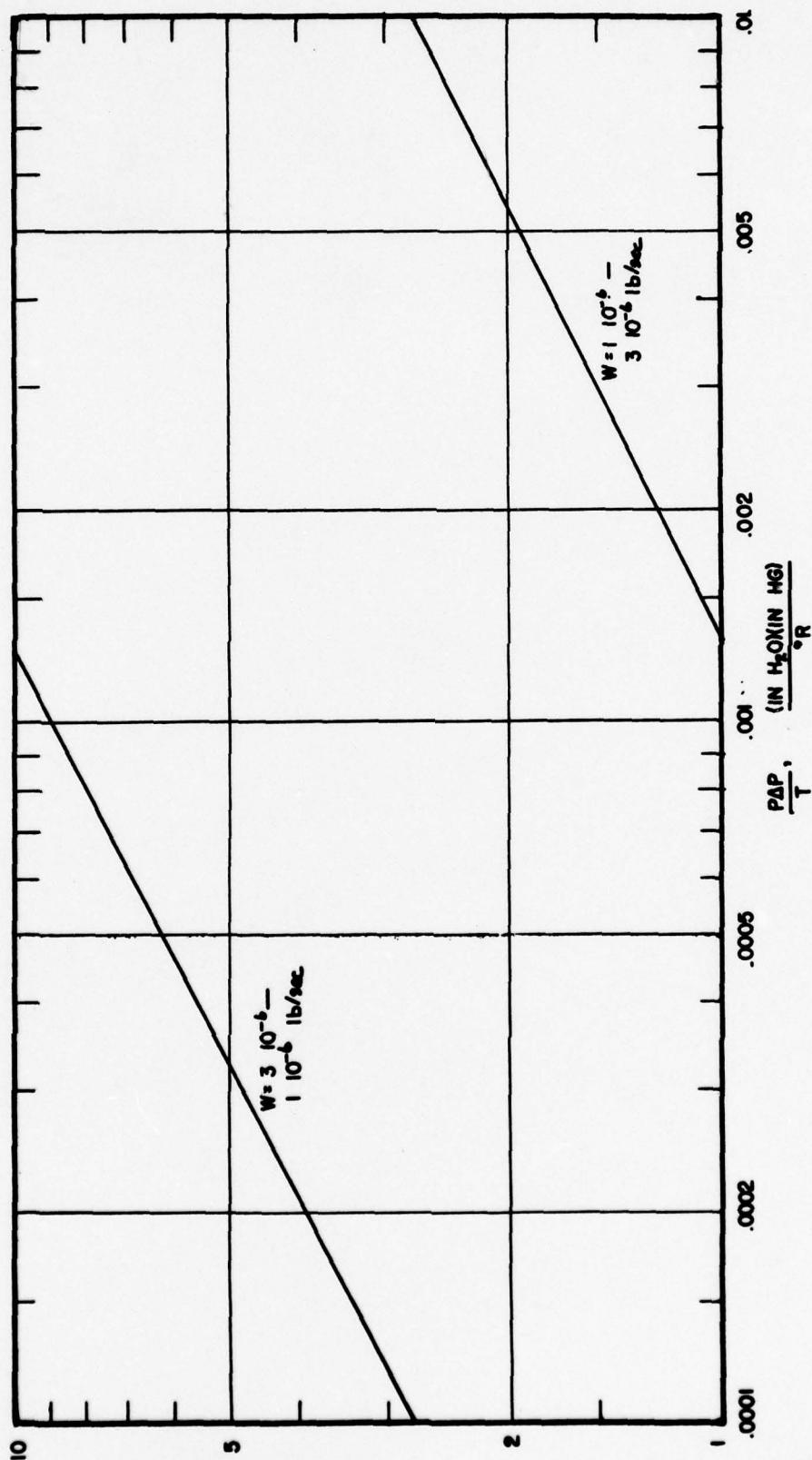
FIGURE E-7: SAMPLING RATE REQUIRED FROM IMPACT PRESSURE MEASURED. CALCULATED FROM IDEAL PITOT TUBE.

APPENDIX F

SUMMARY OF CALCULATED VALUES

TABLE-F-1

BLOWOUT MEASUREMENTS, THREE-JET CHAMBER

Run	Air rate lb/sec	Pres. in Hg	Temp $^\circ R$	Loading, lb mol/sec raw	$N_A/VP^{1.8}$ ft^3 atm$^{1.8}$ corr'd	Gen'l fuel fr'n	Zones blown out
4B	0.0424	10.61	527	0.761	0.782	0.524	1
4C	0.0431	10.62	527	0.722	0.791	0.493	1
4D	0.0445	10.64	527	0.792	0.815	0.445	2
4E	0.0420	10.66	525	0.741	0.765	0.525	1
4F	0.0420	10.66	525	0.741	0.765	0.529	2
4G	0.0420	10.65	522	0.741	0.770	0.469	1
4H	0.0417	10.64	525	0.763	0.790	0.442	2
4I	0.0445	10.71	524	0.803	0.832	0.488	1
4J	0.0473	10.69	524	0.857	0.893	0.470	2
5A	0.0278	10.46	536	0.525	0.530	0.558	1
5B	0.0278	10.48	537	0.524	0.529	0.569	2
6A	0.0264	10.06	538	0.533	0.536	0.554	1
6B	0.0263	9.95	540	0.542	0.542	0.607	2
6C	0.0272	10.14	542	0.541	0.537	0.457	1
6D	0.0272	10.07	542	0.547	0.545	0.428	2
6E	0.0268	10.14	540	0.534	0.534	0.552	1
6F	0.0268	10.11	541	0.534	0.532	0.602	2
6G	0.0270	10.10	542	0.539	0.537	0.460	1
6H	0.0270	10.07	542	0.545	0.542	0.424	2
6I	0.01865	10.28	542	0.361	0.359	0.570	1
6J	0.01865	10.27	542	0.361	0.360	0.619	2
6K	0.01880	10.18	542	0.372	0.370	0.433	1
6L	0.01880	10.18	542	0.372	0.370	0.415	2
6M	0.01900	10.26	542	0.371	0.369	0.506	1
6N	0.01900	10.21	542	0.372	0.370	0.616	2
6O	0.01900	10.23	542	0.372	0.370	0.447	1
6P	0.1900	10.21	542	0.376	0.374	0.413	2
7A	0.0222	10.31	538	0.428	0.430	0.557	1
7B	0.0221	10.29	540	0.428	0.428	0.620	2
7C	0.0220	10.32	540	0.424	0.424	0.485	1

TABLE F-1 continued

Run	Air rate lb/sec	Pres. in Hg	Temp °R	Loading, $N_A/VP^{1.8}$ lb mol/sec raw	ft³ atm$^{1.8}$ corr'd	Gen'l fuel fr'n	Zones blown out
7D	0.0221	10.29	540	0.428	0.428	0.417	2
7F	0.0219	10.35	541	0.420	0.419	0.560	1
7G	0.0216	10.31	541	0.416	0.415	0.607	2
7H	0.0214	10.36	540	0.411	0.411	0.442	1
7I	0.0215	10.30	540	0.417	0.417	0.411	2
7J	0.0314	10.31	540	0.605	0.605	0.535	1
7K	0.0308	10.19	(540)	0.606	0.606	0.596	2
7L	0.0323	10.33	541	0.623	0.622	0.528	1
7M	0.0323	10.24	543	0.633	0.629	0.590	2
7N	0.0328	10.44	540	0.620	0.620	0.470	1
7O	0.0328	10.36	542	0.629	0.626	0.427	2
7P	0.0329	10.44	538	0.623	0.626	0.471	1
7Q	0.0328	10.42	538	0.623	0.626	0.427	2
*32A	0.0411	10.26	526	0.803	0.828	0.495	1
*32B	0.0450	9.78	523	0.889	0.919	0.456	2
*34A	0.0279	10.56	533	0.511	0.523	0.626	2
*34B	0.0315	10.60	530	0.580	0.600	0.633	2
*34C	0.0276	10.63	533	0.504	0.516	0.648	2
*34D	0.0246	10.69	534	0.445	0.455	0.657	2
*35B	0.0296	10.49	532	0.490	0.502	0.620	1
*35C	0.01735	10.34	532	0.332	0.341	0.655	1
36A	0.0291	10.34	534	0.558	0.568	0.410	1
36B	0.0387	10.36	534	0.738	0.750	0.414	1
36C	0.0487	10.42	531	0.918	0.937	0.431	1
37A	0.0413	9.38	530	0.944	0.965	0.534	2
37B	0.0440	9.37	528	1.009	1.034	0.532	2
37C	0.0418	9.42	530	0.951	0.970	0.531	2
37D	0.0430	9.40	528	0.982	1.000	0.507	2
37E	0.0446	9.48	529	1.001	1.025	0.532	2
37F	0.0424	9.47	529	0.944	0.966	0.533	2
*38	0.0349	9.13	533	0.839	0.854	0.557	2
*39A	0.0403	8.93	534	1.003	1.018	0.561	2
*39B	0.0402	8.95	532	1.001	1.023	0.571	2
*39C	0.0396	8.88	531	1.000	1.023	0.437	2
*39D	0.0395	8.89	531	0.996	1.017	0.694	2
*39E	0.0386	8.96	531	0.956	0.980	0.592	2
*39F	0.0386	9.05	530	0.940	0.967	0.598	2
*39G	0.0385	8.95	530	0.959	0.986	0.434	2
*39I	0.0470	8.96	530	1.177	1.202	0.469	2
*39J	0.0468	8.92	528	1.173	1.222	0.484	2

* These data were disregarded in plotting as they were unreasonable compared to the rest of the data. These values reflect probably the consequences of air leakage and poorly fitting firebricks.

TABLE F-1 continued

Run	Air rate lb/sec	Pres. in Hg	Temp °R	Loading, lb mol/sec raw	$N_A/VP^{1.8}$ ft³ atm¹·⁸ corr'd	Gen'l fuel fr'n	Zones blown out
40A	0.0367	10.47	533	0.690	0.700	0.609	1
40B	0.0364	10.48	533	0.681	0.690	0.498	1
40C	0.0364	10.34	531	0.688	0.703	0.434	2
40D	0.0309	10.50	531	0.579	0.591	0.605	1
40E	0.0312	10.60	531	0.574	0.585	0.467	1
40F	0.0312	10.50	531	0.578	0.590	0.447	2
41A	0.0330	10.65	533	0.606	0.617	0.561	1
41B	0.0329	10.69	532	0.593	0.603	0.474	1
41C	0.0329	10.61	531	0.429	0.593	0.607	2
41D	0.0335	10.75	531	0.598	0.612	0.559	1
41E	0.0330	10.75	531	0.590	0.601	0.467	1
41F	0.0330	10.70	531	0.592	0.605	0.442	2
41G	0.0270	10.48	530	0.476	0.487	0.582	1
41H	0.0270	10.87	530	0.469	0.485	0.432	2
41I	0.0268	10.80	530	0.474	0.485	0.465	1
41J	0.0268	10.78	530	0.476	0.488	0.428	2
42A	0.0327	9.23	532	0.768	0.780	0.487	1
42B	0.0336	9.23	532	0.787	0.798	0.506	1
42C	0.0336	9.24	534	0.790	0.800	0.598	1
*43A	0.0317	10.13	529	0.631	0.648	0.454	2
*43B	0.0297	9.88	530	0.560	0.579	0.610	2
*43C	0.0463	10.00	530	0.935	0.952	0.469	2
*43D	0.0304	9.88	528	0.632	0.655	0.629	2
44A	0.0377	10.84	525	0.683	0.691	0.590	2
44B	0.0602	10.70	524	1.085	1.120	0.475	2
*45A	0.0385	10.30	524	0.742	0.785	0.629	2
*45B	0.0480	9.45	522	1.090	1.150	0.603	2
*45C	0.0482	9.48	523	1.070	1.125	0.593	2
*45D	0.0438	9.52	523	0.972	1.020	0.612	2
*48A	0.0248	10.17	529	0.498	0.515	0.590	1
*48B	0.0248	10.19	528	0.498	0.517	0.629	2
*48C	0.0417	8.46	525	1.166	1.203	0.540	1
*48D	0.0410	8.46	528	1.100	1.147	0.533	2
49A	0.0255	10.25	540	0.498	0.498	0.561	1
49B	0.0253	10.30	540	0.490	0.490	0.597	2
49C	0.0289	10.27	537	0.560	0.561	0.459	1
49D	0.0302	10.27	536	0.587	0.592	0.448	2
49E	0.0311	10.35	537	0.597	0.603	0.555	1
49F	0.0311	10.27	536	0.605	0.610	0.597	2
49G	0.0332	10.39	538	0.633	0.636	0.462	1

* These data were disregarded in plotting as they were unreasonable compared to the rest of the data. These values reflect probably the consequences of air leakage and poorly fitting firebricks.

TABLE F-1 concluded

Run	Air rate lb/sec	Pres. in Hg	Temp ^{O}R	Loading, $N_A/VP^{1.8}$ lb mol/sec ft^3 atm$^{1.8}$ raw	corr'd	Gen'l fuel fr'n	Zones blown out
49H	0.0368	10.34	536	0.704	0.711	0.434	2
49I	0.0347	10.39	535	0.662	0.670	0.540	1
49J	0.0347	10.48	536	0.650	0.657	0.596	2
*51	0.0238	10.18	532	0.468	0.481	0.532	2
52A	0.0317	11.12	535	0.527	0.534	0.634	2
52B	0.0378	11.22	535	0.626	0.635	0.622	2
52C	0.0350	11.20	533	0.580	0.593	0.640	2
52D	0.0367	11.21	533	0.608	0.617	0.535	2
52E	0.0590	11.26	529	9.973	0.995	0.520	2
52F	0.0311	11.22	529	0.515	0.531	0.593	2
*53A							
*53A	0.0340	10.49	531	0.634	0.656	0.636	2
*53B	0.0402	10.61	533	0.737	0.752	0.637	2
*53C	0.0648	10.99	534	1.205	1.22	0.504	2
*53D	0.0402	9.48	535	0.902	0.913	0.604	2
*53E	0.0560	9.52	537	1.245	1.25	0.545	2
*54F	0.0500	9.62	537	1.099	1.095	0.569	2

* These data were disregarded in plotting as they were unreasonable compared to the rest of the data. These values reflect probably the consequences of air leakage and poorly fitting firbricks.

TABLE F-2

SUMMARY OF FLAME VOLUME DATA IN THREE-JET CHAMBER

Run	Air rate lb/sec	Pres. in Hg	Temp °R	Loading, $N_A/Vp^{1.8}$ lb mol/sec ft³ atm$^{1.8}$ raw	corr'd	Gen'l fuel fr'n	Vol fr'n of right-hand side	Vol fr'n of left-hand side
18B	0.0233	10.60	531	0.433	0.442	0.469	0.308	0.356
18C	0.0368	10.66	530	0.675	0.690	0.542	0.335	0.389
19A	0.0291	10.37	530	0.556	0.568	0.533	0.294	0.382
19C	0.0332	11.41	532	0.531	0.539	0.499	0.336	0.359
19D	0.0331	11.44	531	0.528	0.538	0.525	0.321	0.382
19E	0.0359	11.45	531	0.572	0.583	0.506	0.362	0.383
19F	0.01925	10.45	535	0.365	0.370	0.613		0.476
19G	0.0228	11.46	537	0.364	0.367	0.600		0.526
19H	0.0269	11.44	535	0.508	0.525	0.586		0.505
19I	0.0302	10.48	535	0.568	0.575	0.582		0.455
19J	0.0331	10.52	534	0.616	0.626	0.578		0.489
19K	0.0355	10.54	533	0.657	0.669	0.576		0.454
19L	0.0383	10.53	533	0.705	0.718	0.561		0.475
20A	0.0230	10.88	529	0.392	0.400	0.497		0.461
20B	0.0275	10.92	528	0.479	0.492	0.445		0.462
20C	0.0309	10.95	528	0.531	0.540	0.474		0.540
20D	0.0339	10.98	528	0.583	0.589	0.463		0.488
20E	0.0368	11.01	529	0.621	0.636	0.459		0.515
20F	0.0391	11.02	528	0.673	0.689	0.474		0.502
20G	0.0407	11.05	528	0.696	0.713	0.481		0.465
20H	0.0437	11.05	528	0.748	0.765	0.497		0.467

TABLE F-3

COMBUSTION EFFICIENCY, THREE-JET CHAMBER

$w = 0.0239 \pm 0.0005$ #/sec, $P = 10.5 \pm 0.4$"H_g, $T = 531^\circ \pm 2^\circ R$

Loading rate, $N_A/VP^{1.8})_{540} = 0.467$ lb mol/sec ft^3 atm$^{1.8}$

Run	Gen'l fuel fr'n	Left flue	Cntr flue	Right flue
28	0.549	68.7%	62.1%	70.0%
29A	0.566	72.1	64.3	76.8
29B	0.581	69.6	60.8	72.9
29C	0.547	72.6	60.4	76.7
29D	0.534	72.6	62.8	77.8

TABLE F-4

BLOWOUT MEASUREMENTS, ONE-JET CHAMBER

Run	Air rate lb/sec	Pres. in Hg	Temp $^\circ R$	Loading, $N_A/VP^{1.8}$ lb mol/sec ft^3 atm$^{1.8}$ raw	corr'd	Gen'l fuel fr'n
60A	0.00934	10.18	530	0.276	0.287	0.661
60B	0.00929	10.19	530	0.274	0.285	0.661
60C	0.00923	10.18	530	0.276	0.286	0.651
60D	0.00924	10.17	531	0.274	0.286	0.316
60E	0.00907	10.25	531	0.266	0.277	0.316
60F	0.01180	10.26	531	0.346	0.356	0.630
60G	0.01175	10.20	532	0.347	0.356	0.633
60H	0.01175	10.28	532	0.343	0.353	0.371
60I	0.0118	10.24	532	0.347	0.357	0.359
60J	0.0138	10.25	532	0.405	0.415	0.624
60K	0.0139	10.23	532	0.410	0.420	0.625
60L	0.0138	10.27	532	0.403	0.415	0.359
60M	0.0138	10.39	531	0.395	0.409	0.356
60N	0.01685	10.27	531	0.493	0.507	0.618
60O	0.01680	10.34	532	0.485	0.496	0.608
60P	0.01685	10.27	532	0.493	0.505	0.617
60Q	0.01685	10.30	532	0.491	0.503	0.371
60R	0.01685	10.20	532	0.499	0.531	0.371
61A	0.01505	9.30	535	0.524	0.530	0.625
61B	0.01495	9.19	536	0.533	0.540	0.368
61C	0.01840	9.44	536	0.626	0.633	0.607
61D	0.01840	9.32	538	0.639	0.641	0.590
61E	0.01835	9.33	538	0.637	0.640	0.606
61F	0.01840	9.37	538	0.633	0.636	0.392
61G	0.01840	9.37	538	0.634	0.637	0.383
61H	0.0225	9.18	538	0.805	0.809	0.581
61I	0.0226	9.18	538	0.808	0.809	0.585
61J	0.0226	9.21	538	0.802	0.807	0.410
61K	0.0225	9.26	538	0.794	0.799	0.405

TABLE F-5

COMBUSTION EFFICIENCY, ONE-JET CHAMBER

Run	Air rate lb/sec	Pres. in Hg	Temp °R	Gen'l fuel fr'n	Loading, $N_A/VP^{1.8}$ ft³ atm¹·⁸ raw	corr'd*	Oxygen consumption efficiency cm from left-hand wall (hot side) 0	1	2	3	4	5
80A	0.00640	10.50	542	0.575	0.180	0.179	81.0	95.9	102.4	100.2	70.4	41.9
80B	0.00760	10.50	542	0.576	0.213	0.215	78.9	92.8	101.9	101.8	74.2	40.5
80C	0.00906	10.62	542	0.576	0.250	0.253	80.2	89.1	102.1	101.7	77.2	38.7
80D	0.01080	10.65	544	0.582	0.296	0.325	39.7	59.3	101.1	97.4	45.4	19.3
81A	0.0128	9.65	543	0.574	0.418	0.408	40.4	46.5	90.8	87.7	31.8	15.9
81B	0.0152	9.76	543	0.577	0.488	0.498	24.2	30.4	72.0	77.8	21.2	12.4
81C	0.0181	9.62	543	0.575	0.565	0.570	17.6	26.1	55.1	67.9	**	**

Run	Air rate lb/sec	Pres. in Hg	Temp °R	Gen'l fuel fr'n	Loading, $N_A/VP^{1.8}$ ft³ atm¹·⁸ raw	corr'd*	Overall efficiency LHS (hot)	Cntr	RHS (cold)	avg
85A	0.00640	10.13	541	0.575	0.192	0.191	44.9	42.3	41.2	42.8
85B	0.00905	10.18	541	0.576	0.269	0.272	42.2	42.2	38.6	41.0
85C	0.01285	10.30	541	0.575	0.373	0.372	38.3	38.3	35.4	37.3
85D	0.0179	10.11	541	0.577	0.538	0.554	30.4	31.7	30.5	30.9
85E	0.0259	10.10	541	0.576	0.774	0.782	15.4	18.5	15.8	16.6
86A	0.0215	10.29	537	0.575	0.625	0.620	19.5	19.9	19.7	19.7
86B	0.0157	10.29	538	0.567	0.457	0.396	36.8	36.1	31.1	34.7

* Loading data are corrected for deviations in temperature and fuel-air ratio. The data are corrected to an inlet temperature of 540°R and an inlet F of 0.575

** At this high firing rate the flame is not stable when the probe is inserted across the interior of the chamber this distance.

TABLE F-6

PRESSURE EXPONENT DATA, ONE-JET CHAMBER

Run	Air rate lb/sec	Temp °R	Gen'l fuel fr'n	Loading, N_A/V lb mol/sec ft3 raw	corr'd*	Corr'd fuel fr'n	Pressure at blowout atmospheres				
72A	0.01685	538	0.596	0.0718	0.0728	0.600	0.291				
72B	0.00885	538	0.598	0.0377	0.0367	0.600	0.157				
72D	0.0259	542	0.574	0.110	0.108	0.575	0.340				
72E	0.0131	542	0.575	0.0558	0.0556	0.575	0.184				
72F	0.00882	543	0.600	0.0376	0.0373	0.600	0.183				
73A	0.00514	543	0.600	0.0224	0.0228	0.600	0.140	0.143			
73B	0.00664	535	0.599	0.0290	0.0292	0.600	0.146	0.141			
73D	0.0191	536	0.573	0.0833	0.0817	0.575	0.235	0.244	0.258	0.258	
73E	0.0280	538	0.598	0.122	0.126	0.600	0.413	0.492	0.539	0.570	
74	0.0168	542	0.596	0.0715	0.0723	0.600	0.268	0.273			0.176
75A	0.00913	(540)	0.452	0.0389	0.0380	0.450	0.151	0.157	0.170	0.177	
75B	0.00913	541	0.427	0.0389	0.0383	0.425	0.210	0.218	0.253	0.235	
75C	0.0144	(540)	0.449	0.0613	0.0616	0.450	0.156	0.186	0.188		
75D	0.00565	541	0.599	0.0241	0.0238	0.600	0.119	0.130	0.134		
75E	0.00618	541	0.577	0.0263	0.0275	0.575	0.116	0.116			
75F	0.00618	541	0.456	0.0263	0.0245	0.450	0.158	0.152	0.171		
75G	0.0144	540	0.419	0.0613	0.0622	0.425	0.234	0.291	0.302	0.277	
75H	0.0251	535	0.597	0.107	0.102	0.600	0.330	0.330			
76A	0.0129	540	0.599	0.549	0.545	0.600	0.207	0.215			
76B	0.0183	540	0.590	0.0780	0.0725	0.600	0.262	0.258			
76C	0.0183	540	0.574	0.0780	0.0785	0.575	0.227	0.240	0.241		
76D	0.0183	540	0.448	0.0780	0.0796	0.450	0.203	0.206			
76E	0.0183	539	0.423	0.0780	0.0799	0.425	0.267	0.277			
76G	0.0259	538	0.597	0.1103	0.1076	0.600	0.356	0.360			
76H	0.0258	541	0.576	0.1099	0.112	0.575	0.290	0.288			

* Data corrected to an inlet temperature of 540°R and a fuel fraction indicated.

TABLE F-6 concluded

Run	Air rate lb/sec	Temp °R	Gen'l fuel fr'n	Loading, N_A/V lb mol/sec ft³ raw	corr'd*	Corr'd fuel frn	Pressure at blowout atmospheres		
77A	0.00555	537	0.598	0.0236	0.0231	0.600	0.109	0.110	
77B	0.00640	538	0.575	0.0272	0.0274	0.575	0.107	0.107	
77C	0.00904	538	0.597	0.0385	0.0369	0.600	0.140	0.142	
77D	0.00904	540	0.575	0.0385	0.0385	0.575	0.125	0.146	0.134
77E	0.0128	540	0.574	0.0545	0.0536	0.0575	0.154	0.152	
77F	0.0128	540	0.601	0.0545	0.0554	0.600	0.182	0.182	
77G	0.0181	540	0.575	0.0771	0.0771	0.575	0.198	0.210	
77H	0.0181	540	0.597	0.0771	0.0736	0.600	0.232	0.257	
78A	0.0258	540	0.573	0.1099	0.1066	0.575	0.264	0.267	
78B	0.0258	541	0.593	0.1099	0.983	0.600	0.338	0.336	
78C	0.0363	541	0.575	0.1546	0.1540	0.575	0.331	0.324	
78D	0.0363	547	0.599	0.1546	0.1494	0.600	0.458	0.442	
78E	0.0363	542	0.461	0.1546	0.1347	0.450	0.308	0.324	0.318
78F	0.0363	541	0.425	0.1546	0.1540	0.425	0.530	0.530	
78G	0.0258	541	0.428	0.1099	0.1058	0.425	0.384	0.386	
78H	0.0258	540	0.449	0.1099	0.111	0.450	0.295	0.297	
79A	0.00636	538	0.424	0.0271	0.0275	0.425	0.161	0.247	0.252
79B	0.00637	537	0.451	0.0271	0.0270	0.450	0.150	0.158	
79C	0.00904	537	0.425	0.0385	0.0388	0.425	0.235	0.232	
79D	0.00904	538	0.451	0.0385	0.0382	0.450	0.180	0.185	
79E	0.0128	538	0.426	0.0545	0.0541	0.425	0.285	0.283	
79F	0.0128	537	0.452	0.0545	0.0536	0.450	0.203	0.195	
79G	0.0181	537	0.424	0.0771	0.0786	0.425	0.324	0.328	
79H	0.0181	537	0.450	0.0771	0.0776	0.450	0.232	0.237	

* Data corrected to an inlet temperature of 540°R and the fuel fraction indicated.

APPENDIX G

SCHLIEREN PHOTOGRAPHY OF THE THREE-JET CHAMBER

In developing conceptual models of combustion chambers
knowledge of the flow pattern as well as of the combustion
efficiency pattern is useful in defining regions which may be
considered as one zone. Since Schlieren photography permits
visualization of density gradients in a gas it was hoped that
either still or motion pictures taken via a Schlieren apparatus
might help in defining appropriate zones. Still pictures would
help show hot and cold regions and motion pictures would help
in visualizing flow patterns.

The principles of Schlieren photography have been widely
discussed in the literature. A summary has been given by
Shipman (20) in discussing the design and operation of a small
Schlieren apparatus for the M. I. T. Fuels Research Laboratory.
This unit has two 6" diameter, 42" focal-length mirrors as the
principal optics. These are mounted on a heavy steel frame to
maintain their alignment. The frame was designed to permit
assembly around moderate size apparatus. The vacuum tank used
in this work was fitted with two opposing windows.

Photographs were taken using a xenon discharge tube
supplied through the courtesy of Dr. H. E. Edgerton (7). This
tube gave a flash duration of 2 to 3 msec of sufficient intensity
to easily expose a panchromatic film with an ASA rating of
100.

The presence of the turbulence found with these short-duration-flash pictures suggested that the regions which were considered as well-stirred zones were in fact somewhat inhomogeneous. The presence of this inhomogeniety also suggested that a single parcel of gas could be identified adequately to permit one to follow its movement over a short timed interval. It was proposed to follow this movement by means of a double-flash picture. This was achieved with a special flash control circuit supplied by Dr. Edgerton. The flash was a spark discharge of about 0.1 sec duration with intervals ranging between flashes of 5 to 100 secs. The intensity of this flash was low enough that special developer was required on high-speed panchromatic film to achieve an effective film speed of 600 to 800 ASA. These pictures did not show the turbulence with sufficient definition to follow a single gas parcel ; however, the shorter flash durations did give substantially clearer resolution of the Schlieren patterns.

Finally high-speed motion pictures (2-3000 frames per sec) were taken of the flame using an Eastman High Speed camera equipped with a synchronizing device to time a strobe-light discharge with each frame exposed, again supplied through the courtesy of Dr. Edgerton. These pictures showed a substantial gas movement; however the movement suggested that it was hot gases external to the combustion zone which were being observed rather than flow pattern within the chamber itself. Typical

photographs of the combustion chamber with a Schlieren apparatus
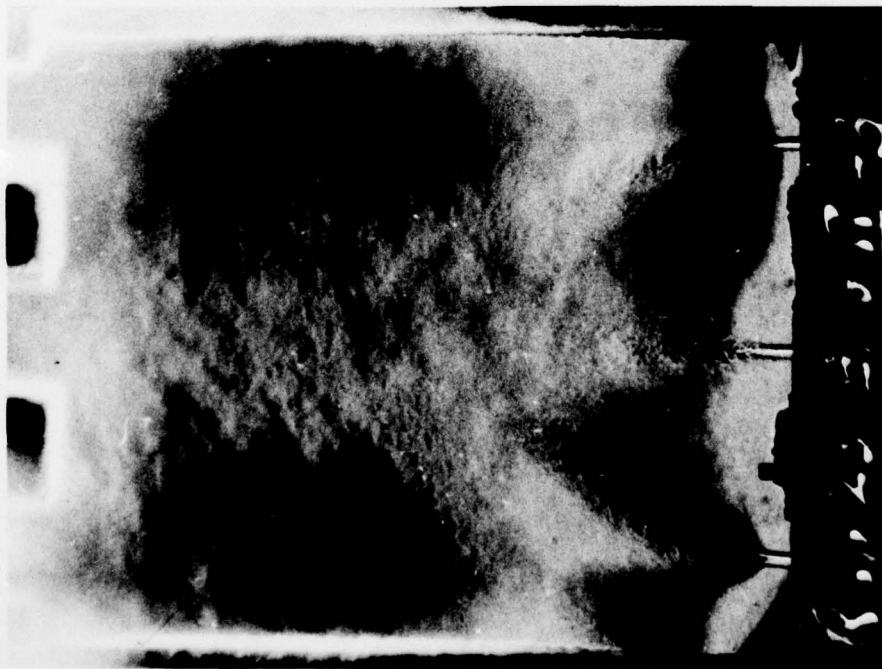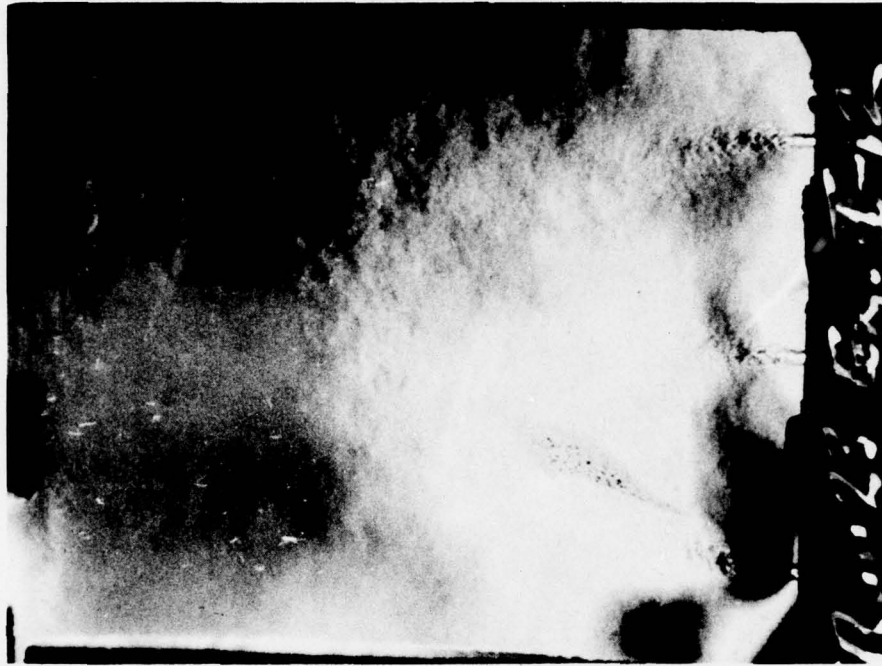are shown in Figure G-1.

FIGURE G-I: TYPICAL SCHLIEREN PHOTOGRAPHS. LEFT, TWO ZONES ACTIVE; RIGHT, ONE ZONE ACTIVE. FLASH DURATION 0.1 μSEC.

APPENDIX H

LITERATURE CITATIONS

(1) A.S.M.E. Research Publication: "Fluid Meters, Their Theory and Applications" 4th edition, (1937).

(2) Avery, W. H., and Hart, R. W., Ind. Eng. Chem. 45, 1634-7 (1953).

(3) Baker, M. L., "Combustion in an Intensely Stirred Reactor", Sc. D. Thesis, M. I. T., June (1956).

(4) Berl, W. G., Rice, J. L., and Rosen, P., Jet Propulsion, 25, 341 (1956).

(5) Blichner, O., private communication, June (1958).

(6) DeZubay, E. A., Jet Propulsion 26, 77, February (1956).

(7) Edgerton, H. A., private communication, November (1956).

(8) Edgerton, A. C., Saunders, O. A., and Spaulding, D. B., ASME-IME Joint Conference on Combustion, M. I. T., June (1955).

(9) Hottel, H. C., and Person, R. A., Fourth Symposium on Combustion (International), p. 781, Williams and Wilkins Co., Baltimore (1953).

(10) Jensen, W. P., private communication, March (1958).

(11) Koucky, R. W., "Mixing of Enclosed Liquid Jets", Sc.D. Thesis, M. I. T., June (1956).

(12) Landis, F., "Turbulent Mixing of Coaxial Jets", Sc. D. Thesis, M. I. T. (1950).

(13) Longwell, J. P., Frost, E. E., and Weiss, M. A., Ind. Eng. Chem., 45, 1629 (1953).

(14) Longwell, J. P., and Weiss, M. A., Ind. Eng. Chem., 47, 1634 (1955).

(15) McAdams, W. H., "Heat Transmission", 3rd Edition, Chapter IV, McGraw-Hill Book Co., New York (1954).

(16) McAdams, W. H., "Heat Transmission" 3rd edition, Chapter IX, McGraw-Hill Book Co., New York (1954).

(17) Perry, J. H. (editor), "Handbook for Chemical Engineers", 3rd Edition p 467-75, McGraw-Hill Book Co., New York (1950).

(18) Rosen, P., and Hart, R. W., Jl. of Aeronautical Science, 20, 549 (1953).

(19) Schmidt, E. H. W., and Schoppe, F., Fifth Symposium on Combustion (International), p 343, Reinhold Publishing Co., New York (1955).

(20) Shipman, C. W., "Flame Stabilization", Sc. D. Thesis, Appendix 5, M. I. T., (1952).

(21) Shuler, K. E., Fifth Symposium on Combustion (International), p 56, Reinhold Publishing Co., New York, (1955).

(22) Simon, D. M., and Wagner, P., Ind. Eng. Chem., 48, p 129 (1956).

(23) Spaulding, D. B., "An Analogue for High-Intensity, Steady-Flow Combustion Phenomenon", I.M.E. Preprint, January (1957).

(24) Spaulding, D. B., "Theoretical Relationships Between Combustion Intensity and Pressure Drop for One Stream Combustion Chambers", Report 10,181 , C.F. 393, Aeronautical Research Council, Great Britain (1957).

(25) Stearns, W. V., and George, E. J., Ind. Eng. Chem., 35, p 602 (1943).

(26) Tobey, A. C., Personal communication, April (1958).

(27) Ubbleholde, A. R., Fifth Symposium on Combustion (International), p 74, Reinhold Publishing Co., New York (1955).

(28) vonElbe, G., Fifth Symposium on Combustion (International) p 79, Reinhold Publishing Co., New York (1955).

(29) Weynand, E.E., "Investigation of Mixing of Confined Streams" Sc. D. Thesis, M. I. T., (1953).

(30) Woo, P. T., "Boundary Layer Effects on Bluff Body Stabilizer", Sc. D. Thesis, M. I. T. (1955).

APPENDIX I

TABLE OF NOMENCLATURE

a   Proportionality constant, Equation III-8.

C   Concentration, moles per unit volume. C_F, fuel concentration C_{O_2}, oxygen concentration.

E   Effective activation energy of overall reaction, stirred reactor equations, Ch. II and III.

F   Generalized fuel fraction, $F = \emptyset/(1 + \emptyset)$. Appendix C; F is direct view factor in radiation calculations.

G   Firing rate to stirred reactor or combustion chamber, moles of fuel per unit time.

h   Heat transfer coefficient, Appendix D; h_g, gas film coefficient from burning gas to Vycor and walls; h_c convection coefficient from Vycor walls to ambient air.

J   Fractional contribution of a reactor unit in combustor model to overall combustion rate.

k   Proportionality constants, k_1 and k_2 in equations III-1 and 2 respectively.

k'   Pseudo collision factor in overall reaction. Well-stirred reactor equations, Ch. II and III.

L   Length of combustor, Equation III-4, ff.

$\dot{m}$ Momentum flux, Equation III-11, ff.

n   Overall order of reaction, well-stirred reactor relations.

N_A Air firing rate to well-stirred reactor and experimental chamber, lb moles/sec.

p   Number of zones in extended recirculation model.

P   Pressure, atmospheres.

$\bar{R}$ Gas constant. Recirculation ratio in recirculation models.

T   Temperature, degrees rankine. T_{af}, temperature of an adiabatic flame at complete combustion, T_N,

nozzle temperature, T_o, inlet temperature of fuel/air mixture, T_K, key temperature in normalization of well-stirred reactor equation, Appendix A.

U   Velocity, Chapter III, U_i inward velocity (toward jet axis), U_o, outward velocity (away from jet axis), U_N, nozzle velocity of jet. Chapter VI; overall heat transfer coefficient, defined by Equation VI-1.

V   Volume, cubic feet.

x   Distance coordinate parallel to jet axis.

y   Distance coordinate perpendicular to jet axis.

Y   Fraction of fresh fuel/air mixture reaching a combustion zone.

Z   Fraction of fuel fed to recirculation zone in split-fuel feed model.

α Reaction order exponent on fuel, well-stirred reactor equations.

β Burnedness, fractional fuel consumption.

γ Variables describing the composition of a burning mixture.

δ Variables describing the composition of a burning mixture.

ϵ Emissivity in radiation calculations, Appendix D.

η Oxygen consumption efficiency.

ξ Relative reaction rates, defined by equation D- , App. D.

ρ Density.

σ Stefan-Bolzman Constant, 0.171×10^{-8} .

Σ Summation of moles present per mole of fuel.

$\emptyset$ Fuel/air ratio; fraction of stoichiometric fuel.

APPENDIX J

BIOGRAPHICAL NOTE

The author was born in Elizabeth, New Jersey and received his elementary and high school education in the public school system of Westfield, New Jersey.

He attended Albion College in Albion, Michigan from 1949 to 1951, and then the University of Michigan in Ann Arbor from 1951 to 1953. He was awarded a B. S. E. in chemical engineering from the University in August 1953.

He entered the Graduate School of M. I. T. in September 1953. While he was at M. I. T. he served as a Research Assistant, Teaching Assistand and Instructor in the Department of Chemical Engineering. He also held a General Motors Fellowship from February 1955 to February 1956, and received several grants from the Teagle Foundation.

The author now holds the position of Assistant Professor of Chemical Engineering at M. I. T. and is director of the Parlin Field Station of the School of Chemical Engineering Practice.